

**DEPOSITIONAL ENVIRONMENTS AND PROCESSES
WITHIN MUDFLATS AND MANGROVES ALONG
CENTRAL WEST COAST OF INDIA**



Ph.D. THESIS

BY

ANANT PANDE, M.Sc.

December, 2013

**Depositional environments and processes within mudflats and
mangroves along central west coast of India**



THESIS

**SUBMITTED TO THE GOA UNIVERSITY
FOR THE DEGREE OF DOCTOR OF PHILOSOPHY
IN MARINE SCIENCE**

BY

ANANT PANDE, M.Sc.

UNDER THE GUIDANCE OF

**Dr. G. N. NAYAK
Professor and Head,
Department of Marine Sciences,
Goa University,
Taleigao Plateau,
Goa - India
DECEMBER, 2013**

**DEDICATED
TO
MY PARENTS**

STATEMENT

As required under the University ordinance OB.9.9 (iv), I state that the present thesis entitled “***Depositional environments and processes within mudflats and mangroves along central west coast of India***” is my original contribution and the same has not been submitted on any previous occasion. To the best of my knowledge, the present study is the first comprehensive work of its kind from the area mentioned.

The literature related to the problem investigated has been cited. Due acknowledgements have been made wherever facilities and suggestions have been availed of.

Place: Goa, India

Date:

Anant Pande

CERTIFICATE

This is to certify that the thesis entitled “DEPOSITIONAL ENVIRONMENTS AND PROCESSES WITHIN MUDFLATS AND MANGROVES ALONG CENTRAL WEST COAST OF INDIA” submitted by **MR. ANANT PANDE** for the award of the Degree of Doctor of Philosophy in Marine Science is based on his original studies carried out by him under my supervision. The thesis or any part thereof has not been previously submitted for any other degree or diploma in any universities or institutions.

Place: Goa University

Date:

Dr. G. N. Nayak

(Research Guide)

Professor of Marine Sciences

Head, Department of Marine Sciences

Goa University

Goa - India.

CONTENTS

		Page No.
CONTENTS		i
LIST OF TABLES		v
LIST OF FIGURES		viii
ABSTRACT		xiii
CHAPTER 1	INTRODUCTION	1-22
1.1	Introduction	2
1.2	Literature review	7
1.3	Objectives	16
1.4	Study area	17
	1.4.1 Background of the study area	17
	1.4.2 Dharamtar creek	18
	1.4.3 Kundalika estuary	19
	1.4.4 Rajapuri creek	20
	1.4.5 Savitri estuary	21
	1.4.6 Vashishti estuary	21
CHAPTER 2	METHODOLOGY	23-34
2.1	Introduction	24
2.2	Field studies and sampling	24
	2.2.1 Location of sampling area	25
	2.2.2 Collection of sediment cores	26
2.3	Laboratory procedures and analysis	27
	2.3.1 pH	28
	2.3.2 Sediment components	28
	2.3.3 Clay mineralogy	29
	2.3.4 Total organic carbon (TOC)	30
	2.3.5 Total nitrogen (TN)	31

	2.3.6 Total phosphorous (TP)	31
	2.3.7 Digestion of sediments	32
	2.3.8 Metal analysis	32
	2.3.9 Diatoms	33
2.4	Data processing	34
CHAPTER 3	RESULT AND DISCUSSION	35-153
3.1	Dharamtar creek	36
	3.1.1 Collection of sediment cores	36
	3.1.2 Colour	36
	3.1.3 Sediment grain size	36
	3.1.4 Nutrients (TOC, TN and TP)	40
	3.1.5 C/N ratio	41
	3.1.6 pH	42
	3.1.7 Major elements (Fe, Mn and Al)	42
	3.1.8 Trace elements (Ni, Cr, Co, Zn and Pb)	44
	3.1.9 Diatoms	46
	3.1.10 Paired t-test analysis	47
	3.1.11 Correlation	48
	3.1.12 Enrichment factor (EF) and index of geoaccumulation (I _{geo})	50
	3.1.13 Factor analysis	51
	3.1.14 Isocon	53
	3.1.15 Conclusion	53
3.2	Kundalika estuary	55
	3.2A Mudflats	55
	3.2A.1 Collection of sediment cores	55
	3.2A.2 Colour	55
	3.2A.3 Sediment grain size	55
	3.2A.4 Nutrients (TOC, TN and TP)	59
	3.2A.5 C/N ratio	61
	3.2A.6 Major elements (Fe, Mn and Al)	61

	3.2A.7 Trace elements (Ni, Cr, Co, Zn and Pb)	63
	3.2A.8 Paired t-test analysis	65
	3.2A.9 Correlation	65
	3.2A.10 Enrichment factor (EF) and index of geoaccumulation (Igeo)	67
	3.2A.11 Factor analysis	68
	3.2B Mangroves	70
	3.2B.1 Collection of sediment cores	70
	3.2B.2 Colour	70
	3.2B.3 Sediment grain size	70
	3.2B.4 Nutrients (TOC and TN)	73
	3.2B.5 C/N ratio	75
	3.2B.6 pH	75
	3.2B.7 Major elements (Fe, Mn and Al)	76
	3.2B.8 Trace elements (Ni, Cr, Co, Zn and Pb)	77
	3.2B.9 Paired t-test analysis	78
	3.2B.10 Correlation	79
	3.2B.11 Factor analysis	81
	3.2B.12 Isocon	82
	3.2B.13 Conclusion	83
3.3	Rajapuri creek	84
	3.3A Mudflats	84
	3.3A.1 Collection of sediment cores	84
	3.3A.2 Colour	84
	3.3A.3 Sediment grain size	84
	3.3A.4 Nutrients (TOC and TN)	87
	3.3A.5 C/N ratio	88
	3.3A.6 pH	89
	3.3A.7 Major elements (Fe, Mn and Al)	89
	3.3A.8 Trace elements (Ni, Cr, Co, Zn and Pb)	90

	3.3A.9 Diatoms	91
	3.3A.10 Correlation	93
	3.3A.11 Principal component analysis (PCA)	95
	3.3A.12 Factor analysis	95
	Sub channel (core S-61)	96
	Sediment sources	96
	Sediment geochemistry	98
	Main channel (core S-60)	99
	Sediment sources	99
	Sediment Geochemistry	101
	Sub channel Vs Main channel	102
	3.3B Mangroves	104
	Conclusion	105
3.4	Savitri estuary	106
	3.4A Mudflats	106
	3.4A.1 Collection of sediment cores	106
	3.4A.2 Colour	106
	3.4A.3 Sediment grain size	106
	3.4A.4 Nutrients (TOC, TN and TP)	109
	3.4A.5 C/N ratio	110
	3.4A.6 pH	111
	3.4A.7 Major elements (Fe, Mn and Al)	112
	3.4A.8 Trace elements (Ni, Cr, Co, Zn and Pb)	113
	3.4A.9 Clay minerals	114
	3.4A.10 Diatoms	115
	3.4A.11 Paired t-test analysis	117
	3.4A.12 Correlation	117
	3.4A.13 Factor analysis	119
	3.4A.14 Enrichment factor (EF) and index of geoaccumulation (Igeo)	119
	3.4A.15 Isocon	121
	3.4B Mangroves	121

	Conclusion	122
3.5	Vashishti estuary	123
	3.5A Mudflats	123
	3.5A.1 Collection of sediment cores	123
	3.5A.2 Colour	123
	3.5A.3 Sediment grain size	123
	3.5A.4 Nutrients (TOC, TN and TP)	126
	3.5A.5 C/N ratio	127
	3.5A.6 pH	127
	3.5A.7 Major elements (Fe, Mn and Al)	128
	3.5A.8 Trace elements (Ni, Cr, Co, Zn and Pb)	128
	3.5A.9 Correlation	129
	3.5A.10 Factor analysis	129
	3.5B Mangroves	130
	3.5B.1 Collection of sediment cores	130
	3.5B.2 Colour	130
	3.5B.3 Sediment grain size	130
	3.5B.4 Nutrients (TOC)	132
	3.5B.5 Metals (Fe, Mn, Al, Ni, Cr, Co, Zn and Pb)	133
	3.5B.6 Correlation	134
	3.5B.7 Factor analysis	135
	3.5B.8 Isocon and enrichment factor (EF)	136
3.6	Comparison of different estuaries (mudflats) along central west coast of India	137
	3.6.1 Rivers and catchment area	137
	3.6.2 Sediment grain size	137
	3.6.3 Nutrients (TN, TP and TOC)	139
	3.6.4 C/N ratio	141
	3.6.5 Diatoms	143
	3.6.6 Major elements (Fe, Mn and Al)	147
	3.6.7 Trace elements (Ni, Cr, Co, Zn and Pb)	147

	3.6.8 Normalization	148
	3.6.9 Correlation	150
	3.6.10 Factor analysis	151
	3.6.11 Index of geoaccumulation (I _{geo}) and enrichment factor (EF)	152
CHAPTER 4	SUMMARY AND CONCLUSION	154- 160
REFERENCES		161- 187

List of Tables		
		Page No.
Table 1.1	Literature review of studies carried out in recent years	7
Table 2.1	Details of sampling with field observation	26
Table 2.2	Time schedule used for pipette analysis	29
Table 3.1	Mean and standard deviation (values in parenthesis) of different parameters in each zone for core S-2, S-3 and S-1. The p-value denote results of one-way ANOVA statistically significant at $p < 0.05$. n =number of samples	37
Table 3.1.1	Summary of paired sample t-test comparing core S-2 and S-3 ($p < 0.05$)	48
Table 3.1.2	Pearson correlation coefficient for core S-2	49
Table 3.1.3	Pearson correlation coefficient for core S-3	49
Table 3.1.4	R-mode factor analysis for core S-2	52
Table 3.1.5	R-mode factor analysis for core S-3	52
Table 3.2a	Mean and standard deviation (values in parenthesis) of different parameters in each zone for core S-62, S-45 and S-63. The p-value denote results of one-way ANOVA statistically significant at $p < 0.05$. n =number of samples	56
Table 3.2a.1	Summary of paired sample t-test ($p < 0.05$)	65
Table 3.2a.2	Pearson correlation coefficient for core S-62	66
Table 3.2a.3	Pearson correlation coefficient for core S-45	66
Table 3.2a.4	R-mode factor analysis for core S-62	69
Table 3.2a.5	R-mode factor analysis for core S-45	69
Table 3.2b	Mean and standard deviation (values in parenthesis) of different parameters in each zone for core S-47, S-40 and S-42. The p-value denote results of one-way ANOVA	71

	statistically significant at $p < 0.05$. n=number of samples	
Table 3.2b.1	Summary of paired sample t-test ($p < 0.05$) comparing core S-47 and S-40	79
Table 3.2b.2	Pearson correlation coefficient for core S-47	80
Table 3.2b.3	Pearson correlation coefficient for core S-40	80
Table 3.2b.4	R-mode factor analysis for core S-47	82
Table 3.2b.5	R-mode factor analysis for core S-40	82
Table 3.3	Mean and standard deviation (values in parenthesis) of different parameters in each zone for core S-61 and S-60. The p-value denote results of one-way ANOVA statistically significant at $p < 0.05$. n=number of samples	85
Table 3.3a.1	Pearson correlation coefficient for core S-61	94
Table 3.3a.2	Pearson correlation coefficient for core S-60	94
Table 3.3a.3	R-mode factor analysis for core S-61	96
Table 3.3a.4	R-mode factor analysis for core S-60	96
Table 3.3a.5	Range and average of index of geo-accumulation (I _{geo}) in zone 1 and zone 2 for core S-61 (A) and S-60 (B)	99
Table 3.3a.6	Paired t-test analysis comparing core S-61 and S-60 ($p < 0.05$)	103
Table 3.4	Mean and standard deviation (values in parenthesis) of different parameters in each zone for core S-18 and S-41. The p-value denote results of one-way ANOVA statistically significant at $p < 0.05$. n=number of samples	107
Table 3.4a.1	Summary of paired t-test comparing core S-18 and S-41 ($p < 0.05$)	117
Table 3.4a.2	Pearson correlation coefficient for core S-18	118
Table 3.4a.3	Pearson correlation coefficient for core S-41	118
Table 3.4a.4	Varimax R-mode factor analysis for core S-18 (A) and S-41 (B)	119

Table 3.4a.5	Mean and standard deviation of enrichment factor (EF) and index of geo-accumulation (I _{geo}) in zone 1, 2 and 3 for core S-18 (A) and S-41 (B)	120
Table 3.5a	Mean and standard deviation (values in parenthesis) of different parameters in each zone for core S-7, S-10 and S-16. The p-value denote results of one-way ANOVA statistically significant at p<0.05. n=number of samples	124
Table 3.5a.1	Pearson correlation coefficient for core S-10	129
Table 3.5a.2	R-mode factor analysis for core S-10	129
Table 3.5b	Mean and standard deviation (values in parenthesis) of different parameters in each zone for core S-20 and S-15. The p-value denote results of one-way ANOVA statistically significant at p<0.05. n=number of samples	131
Table 3.5b.1	Pearson correlation coefficient for core S-20	134
Table 3.5b.2	R-mode factor analysis for core S-20	135
Table 3.5b.3	Mean value of EF for core S-10 and S-20	136
Table 3.6	Major estuaries along central west coast of India between 18° and 17°N latitude	137
Table 3.6.1	Mean and standard deviation of sediment grain size for lower (A) and middle (B) estuary	138
Table 3.6.2	Mean and standard deviation of nutrients (TN, TP and TOC) for lower (A) and middle (B) estuary	140
Table 3.6.3	Relationship between nutrients (TN, TP and TOC) and fine sediments for lower (A) and middle (B) estuary	140
Table 3.6.4	Mean and standard deviation of carbon/nitrogen ratio for lower (A) and middle (B) estuary	142
Table 3.6.5	Mean diatom assemblage for lower (A) and	144

	middle (B) estuary	
Table 3.6.6	Mean and standard deviation of metals for lower (A) and middle (B) estuary	147
Table 3.6.7	Pearson's correlation coefficient between trace metals and sediment grain size, nutrients & major elements for lower (A) and middle (B) estuary	151
Table 3.6.8	Varimax R-mode factor analysis for cores collected from lower (A) and middle (B) estuary	152
Table 3.6.9	Mean and standard deviation of index of geoaccumulation (Igeo) for lower (A) and middle (B) estuary	153
Table 3.6.10	Mean and standard deviation of Enrichment factor (EF) for lower (A) and middle (B) estuary	153

List of Figures		
		Page No.
Figure 1.1	Study area map	18
Figure 2.1	Sampling and sample processing techniques	24
Figure 2.2	Study area map with sampling locations	25
Figure 2.3	Photographs depicting field work and sampling	27
Figure 2.4	Procedure followed for diatom analysis after Batterbee (1986)	33
Figure 3.1	Study area map with core location for Dharamtar creek	36
Figure 3.1.1	Down-core variation of sediment grain size for core S-2	38
Figure 3.1.2	Down-core variation of sediment grain size for core S-3	38
Figure 3.1.3	Down-core variation of sediment grain size for core S-1	38
Figure 3.1.4	Ternary diagram for classification of hydrodynamic conditions for core S-2 (A), S-3 (B) and S-1 (C)	39
Figure 3.1.5	Down-core variation of total organic carbon (TOC), total nitrogen (TN) and total phosphorous (TP) for core S-2	40
Figure 3.1.6	Down-core variation of total organic carbon (TOC), total nitrogen (TN) and total phosphorous (TP) for core S-3	40
Figure 3.1.7	Down-core variation of total organic carbon (TOC) for core S-1	40
Figure 3.1.8	Down-core variation of carbon/nitrogen ratio (C/N) for core S-2 (A) and S-3 (B)	42
Figure 3.1.9	Down-core variation of pH for core S-2 (A), S-3 (B) and S-1 (C)	42
Figure 3.1.10	Down-core variation of major elements (Fe, Mn	43

	and Al) for core S-2	
Figure 3.1.11	Down-core variation of major elements (Fe, Mn and Al) for core S-3	43
Figure 3.1.12	Down-core variation of trace elements (Ni, Cr, Co, Zn and Pb) for core S-2	45
Figure 3.1.13	Down-core variation of trace elements (Ni, Cr, Co, Zn and Pb) for core S-3	45
Figure 3.1.14	Down-core variation of diatoms for core S-2	46
Figure 3.1.15	Down-core variation of enrichment factor (EF) for core S-2	50
Figure 3.1.16	Down-core variation of enrichment factor (EF) for core S-3	50
Figure 3.1.17	Box and whisker plot of index of geo-accumulation (I _{geo}) for core S-2	51
Figure 3.1.18	Box and whisker plot of index of geo-accumulation (I _{geo}) for core S-3	51
Figure 3.1.19	Isocon diagram	53
Figure 3.2	Location of core collection from Kundalika estuary	55
Figure 3.2a.1	Down-core variation of sediment grain size for core S-62	57
Figure 3.2a.2	Down-core variation of sediment grain size for core S-63	57
Figure 3.2a.3	Down-core variation of sediment grain size for core S-45	57
Figure 3.2a.4	Ternary diagram for classification of hydrodynamic conditions for core S-62 (A), S-63 (B) and S-45 (C)	58
Figure 3.2a.5	Down-core variation of total organic carbon (TOC) and total nitrogen (TN) for core S-62	59
Figure 3.2a.6	Down-core variation of total organic carbon	59

	(TOC) and total phosphorous (TP) for core S-45	
Figure 3.2a.7	Down-core variation of total organic carbon (TOC) for core S-63	59
Figure 3.2a.8	Down-core variation of carbon/nitrogen ratio (C/N) for core S-62	60
Figure 3.2a.9	Down-core variation of major elements (Fe, Mn and Al) for core S-62	62
Figure 3.2a.10	Down-core variation of major elements (Fe, Mn and Al) for core S-45	62
Figure 3.2a.11	Down-core variation of trace elements (Ni, Cr, Co, Zn and Pb) for core S-62	63
Figure 3.2a.12	Down-core variation of trace elements (Ni, Cr, Co, Zn and Pb) for core S-45	63
Figure 3.2a.13	Down-core variation of enrichment factor (EF) for core S-62	67
Figure 3.2a.14	Down-core variation of enrichment factor (EF) for core S-45	67
Figure 3.2a.15	Box and whisker plot of index of geo-accumulation (I _{geo}) for core S-62	67
Figure 3.2a.16	Box and whisker plot of index of geo-accumulation (I _{geo}) for core S-45	67
Figure 3.2b.1	Down-core variation of sediment grain size for core S-47	72
Figure 3.2b.2	Down-core variation of sediment grain size for core S-42	72
Figure 3.2b.3	Down-core variation of sediment grain size for core S-40	72
Figure 3.2b.4	Ternary diagram for classification of hydrodynamic conditions for core S-47 (A), S-42 (B) and S-40 (C)	73
Figure 3.2b.5	Down-core variation of total organic carbon	74

	(TOC) and total nitrogen (TN) for core S-47	
Figure 3.2b.6	Down-core variation of total organic carbon (TOC) for core S-42	74
Figure 3.2b.7	Down-core variation of total organic carbon (TOC) for core S-40	74
Figure 3.2b.8	Down-core variation of carbon/nitrogen ratio (C/N) for core S-47	75
Figure 3.2b.9	Down-core variation of pH for core S-47 (A), S-42 (B) and S-40 (C)	75
Figure 3.2b.10	Down-core variation of major elements (Fe, Mn and Al) for core S-47	76
Figure 3.2b.11	Down-core variation of major elements (Fe, Mn and Al) for core S-40	76
Figure 3.2b.12	Down-core variation of trace elements (Ni, Cr, Co, Zn and Pb) for core S-47	78
Figure 3.2b.13	Down-core variation of trace elements (Ni, Cr, Co, Zn and Pb) for core S-40	78
Figure 3.2b.14	Isocon diagram comparing mangroves (S-47 and S-40)	82
Figure 3.2b.15	Isocon diagram comparing mudflat (S-62) and mangroves (S-47) of lower estuary	83
Figure 3.2b.16	Isocon diagram comparing mudflat (S-45) and mangroves (S-40) of middle estuary	83
Figure 3.3	Study area map with core location for Rajapuri creek	84
Figure 3.3a.1	Down-core variation of sediment grain size for core S-61 (A) and S-60 (B)	86
Figure 3.3a.2	Ternary diagram for classification of hydrodynamic conditions for core S-60 (A) and S-61 (B)	87
Figure 3.3a.3	Down-core variation of total organic carbon (TOC) and total nitrogen (TN) for core S-61	87

Figure 3.3a.4	Down-core variation of total organic carbon (TOC) and total nitrogen (TN) for core S-60	87
Figure 3.3a.5	Down-core variation of carbon/nitrogen ratio (C/N) for core S-61 (A) and S-60 (B)	88
Figure 3.3a.6	Down-core variation of pH for core S-61 (A) and S-60 (B)	88
Figure 3.3a.7	Down-core variation of major elements (Fe, Mn and Al) for core S-61 (A) and S-60 (B)	89
Figure 3.3a.8	Down-core variation of trace elements (Ni, Cr, Co, Zn and Pb) for core S-61 (A) and S-60 (B)	90
Figure 3.3a.9	Down-core variation of diatoms for core S-61	92
Figure 3.3a.10	Down-core variation of diatoms for core S-60	93
Figure 3.3a.11	Statistical relationship between diatoms and environment variables	95
Figure 3.3a.12	Rainfall data of last 100 years for station Mahad in Raigad district	97
Figure 3.3b.1	Down-core variation of sediment grain size, total organic carbon (TOC) and pH for core S-65	105
Figure 3.3b.2	Ternary diagram for classification of hydrodynamic conditions for core S-65	105
Figure 3.4	Study area map with core location for Savitri estuary	106
Figure 3.4a.1	Down-core variation of sediment grain size for core S-18 (A) and S-41 (B)	108
Figure 3.4a.2	Ternary diagram for classification of hydrodynamic conditions for core S-18 (A) and S-41 (B)	109
Figure 3.4a.3	Down-core variation of total organic carbon (TOC), total nitrogen (TN) and total phosphorous (TP) for core S-18 (A) and S-41 (B)	110
Figure 3.4a.4	Down-core variation of carbon/nitrogen ratio	111

	(C/N) for core S-18 (A) and S-41 (B)	
Figure 3.4a.5	Down-core variation of pH for core S-18 (A) and S-41 (B)	111
Figure 3.4a.6	Down-core variation of major elements (Fe, Mn and Al) for core S-18 (A) and S-41 (B)	112
Figure 3.4a.7	Down-core variation of trace elements (Ni, Cr, Co, Zn and Pb) for core S-18 (A) and S-41 (B)	114
Figure 3.4a.8	Down-core variation of clay minerals for core S-18 (A) and S-41 (B)	114
Figure 3.4a.9	Down-core variation of diatoms for core S-18	116
Figure 3.4a.10	Down-core variation of diatoms for core S-41	117
Figure 3.4a.11	Isocon diagram comparing core S-18 and S-41	121
Figure 3.4b.1	Down-core variation of sediment grain size for core S-21	122
Figure 3.4b.2	Ternary diagram for core S-21	122
Figure 3.5	Location of core location from Vashishti estuary	123
Figure 3.5a.1	Down-core variation of sediment grain size for core S-7 (A), S-10 (B) and S-16 (C)	125
Figure 3.5a.2	Ternary diagram for classification of hydrodynamic conditions for core S-7 (A), S-10 (B) and S-16 (C)	125
Figure 3.5a.3	Down-core variation of total organic carbon (TOC), total nitrogen (TN) and total phosphorous (TP) for core S-7 (A), S-10 (B) and S-16 (C)	126
Figure 3.5a.4	Down-core variation of carbon/nitrogen ratio (C/N) for core S-10	127
Figure 3.5a.5	Down-core variation of pH for core S-7 (A), S-10 (B) and S-16 (C)	127
Figure 3.5a.6	Down-core variation of major elements (Fe, Mn and Al) and trace elements (Ni, Cr, Co, Zn and Pb) for core S-10	128
Figure 3.5b.1	Down-core variation of sediment grain size for	131

	core S-20 (A) and S-15 (B)	
Figure 3.5b.2	Ternary diagram for classification of hydrodynamic conditions for core S-20 (A) and S-15 (B)	132
Figure 3.5b.3	Down-core variation of total organic carbon (TOC) for core S-20 (A) and S-15 (B)	133
Figure 3.5b.4	Down-core variation of major elements (Fe, Mn and Al) and trace elements (Ni, Cr, Co, Zn and Pb) for core S-20	134
Figure 3.5b.5	Isocon diagram comparing core S-10 and S-20	136
Figure 3.6	Ternary diagram for the classification of hydrodynamic condition after Pejrup (1988) for lower (A) and middle (B) estuary	139
Figure 3.6.1	Down-core variation of C/N ratio for lower (A) and middle (B) estuary	141
Figure 3.6.2	Scatter plot of C Vs N for lower (A) and middle (B) estuary	143
Figure 3.6.3	Down-core variation of diatoms for lower (A) and middle (B) estuary	143
Figure 3.6.4	Diatom photographs from studied estuaries along central west coast of India	145,146
Figure 3.6.5	Down-core variation of metal/Al for Dharamtar creek	149
Figure 3.6.6	Down-core variation of metal/Al for Kundalika estuary	149
Figure 3.6.7	Down-core variation of metal/Al for Rajapuri creek	149
Figure 3.6.8	Down-core variation of metal/Al for Savitri estuary	149
Figure 3.6.9	Down-core variation of metal/Al for Vashishti estuary	149

Abstract

Coastal areas in general and estuaries in particular, around the globe are receiving greater importance in the recent years owing to vast majority of human population and greater agricultural and industrial activities leaving them vulnerable to the transformation and destruction of natural habitats, over-fishing and pollution. Estuaries being ultimate sink for organic pollutants and metals are therefore most affected.

Sediments are important carriers of metals in aquatic environment. Sediments within estuarine regions are composed of different sedimentological and geochemical phase that acts as binding sites for metals entering the estuarine environment. Mudflats and mangroves are adjacent sub-environments along intertidal part of estuary in tropical region. Mudflats cover large unvegetated areas that are exposed during low tide and submerged during high tide. Mangroves, on the other hand, are salt tolerant shrubs and trees associated with a unique horizontal root network. They primarily consist of fine sediment deposits (<63 μm) and are influenced by tides, waves and fluvial processes. These fine cohesive sediments favour the accumulation of metals. Metals have great ecological significance because of their toxicity, persistence and bioaccumulation capacity. Metals cannot be biologically or chemically degraded. Understanding abundance and distribution of metals in mudflats and mangroves sediments is therefore important as they are key habitats for a number of macrofaunal species and act as important food sources or nursery grounds for fish communities and also has potential to harm human health via the food chain.

Mudflats and mangroves are extensive along central west coast of India. The Dharamtar, Amba, Kundalika, Rajapuri, Savitri and Vashishti are the major estuaries of Raigad and Ratnagiri district in Maharashtra along central west coast of India and form the study area. The present study reveals first information regarding concentration and distribution of selected metals (Al, Fe, Mn, Zn, Cr, Co, Ni, Pb), sediment components, total organic carbon (TOC), total nitrogen (TN), total phosphorous (TP), pH and diatoms with space and time along this coast. The objectives of the thesis are 1) to study

the distribution and abundance of sediment components, organic carbon, clay minerals and selected elements in sediments with space and time, along the coast between Mumbai and Ratnagiri 2) to understand the depositional environment and post depositional processes and 3) to investigate the past climate from the study of fossil diatoms.

To achieve the objectives of the thesis, total 20 sediment cores varying from 46 cm to 106 cm in length were collected from Vashishti, Savitri, Rajapuri, Kundalika, Dharamtar and Amba estuaries along central west coast of India. The sediment cores were studied for pH, sediment grain size, TOC, TN, TP, C/N ratio, selected metals (Fe, Mn, Al, Ni, Cr, Co, Zn and Pb), clay minerals and diatoms.

Two sediment cores collected from intertidal mudflats of Dharamtar creek, one near the mouth and the other from the middle region of Amba River were analyzed for sediment components, TOC and selected metals (Al, Fe, Mn, Ni, Co, Cr, Zn and Pb). The sediments are mainly composed of silt and clay contributing greater than 90% in both the cores, indicating calm environment prevailed during deposition of sediments. However, between the two cores, sediments in the middle estuarine region were deposited in relatively violent hydrodynamic environment compared to that near the mouth of the creek. TOC is slightly higher near the mouth. The distribution of metals is largely controlled by sediment components, organic carbon and Fe-Mn oxyhydroxides at both the locations. When the average values are considered, Mn and Co shows higher concentration in the middle estuarine region whereas, Fe along with Al shows higher concentrations near the mouth. Enrichment factor calculated indicates minor enrichment of Mn, Fe and Zn and moderately to moderately severe enrichment with respect to Ni, Co, Cr and Pb in the creek. Index of geo-accumulation (I_{geo}) computed indicated that Dharamtar creek is moderately polluted with respect to Pb and Co, unpolluted to moderately polluted with Ni, Cr and Fe and practically unpolluted with Zn and Mn.

The sediment grain size distribution across the mudflats and mangroves of Kundalika estuary is controlled by factors such as wave and tide. Sand, silt,

clay and TOC showed band type distribution along the estuary. Silt and clay forms the major component in lower and middle estuarine region respectively. The sediment deposition over the years took place under varying hydrodynamic conditions in lower and middle estuarine regions. In the lower estuary, sediment texture of mangroves corresponds to textural class mud while the mudflats facilitated the deposition of slightly sandy mud. Almost all the elements showed relatively higher average concentration in mudflats when compared to mangroves which is attributed to wave attenuation along with frequency of tidal inundation rate. In mangroves of the lower estuary Fe and Mn played a major role in the distribution of trace metals (Ni, Cr and Zn). Correlation results indicated the importance of clay and TOC in the process of removal and trapping of metals at lower and middle estuary respectively. In mudflats of middle estuary TOC played a major role in trace metals distribution. Factor analysis indicated that trace metal distribution is largely controlled by Fe-Mn oxyhydroxides and TOC. However, in mudflats of lower estuary Ni, Cr and Co showed no significant association with Fe, Mn or Al which probably suggests a different source. The significant association among Ni, Cr and Co as indicated by factor analysis suggests a common source, possibly anthropogenic, such as industrial and agricultural activities while mudflats of middle estuary showed a mainly lithogenic source. When the EF values are considered, nearly all elements (except Mn) show anthropogenic enrichment in the Kundalika estuary.

From Rajapuri creek, two mudflat sediment cores collected from a sub channel and the main channel were analyzed for sediment grain size, TOC, TN, C/N ratio, selected metals, pH and diatoms. The sub channel represents river environment which opens into main channel which represents marine environment being close to the sea. A transition from river dominated to marine dominated depositional environment is observed. The relatively higher sand percentage together with elevated C/N ratio and predominance of freshwater diatoms suggested greater river runoff in the past while marine influence is supported by sudden increase in sand percentage, decrease in C/N ratio and increase dominance of marine diatoms in the recent years. In

the main channel, distribution of metals is regulated by organic matter (TN and TOC) while in the sub-channel, Fe-Mn oxyhydroxides played a significant role in trace metal distribution. The highest numbers of diatoms are recorded in the sub channel which is also characterized by higher TN concentration. The Igeo value of Pb, Cr and Co suggests that sub channel is moderately polluted while main channel is unpolluted to moderately polluted with respect to these trace metals.

From Savitri estuary two mudflat cores collected from lower and middle estuary were analyzed for sediment grain size, TOC, TN, TP, pH, clay minerals, selected metals and diatoms. Silt and clay are the major sediment components in lower and middle estuary respectively. Sand content is higher in lower estuary while clay and nutrients (TOC, TN and TP) are relatively higher in middle estuary. Smectite is the dominant clay mineral and relatively higher in middle estuary. Marine diatoms showed higher relative dominance in lower estuary while in the middle estuary freshwater diatoms are predominant. The trace metal distribution is mainly controlled by Fe-Mn oxyhydroxides. However, in the lower estuary pH also regulated distribution of some of the trace metals (Ni, Cr and Co). Index of geo-accumulation (Igeo) computed indicated that Savitri estuary is unpolluted to moderately polluted with respect to Fe, Mn, Ni, Cr, Zn and Pb and moderately polluted with respect to Co. Enrichment factor (EF) calculated indicate average EF value greater than 1.5 for all the elements (except Zn in middle estuary) suggesting significant anthropogenic enrichment in the estuary.

From Vashishti estuary mudflat and mangrove core collected from middle estuary were analyzed for sediment grain size, total organic carbon, total nitrogen, total phosphorous, pH and metals. Fine sediments i.e. silt and clay along with organic matter (total organic carbon, total nitrogen and total phosphorous) is relatively higher in mangrove while metals (except Ni, Cr and Pb) are higher in mudflats.

The different estuaries are compared for distribution of sediment components, TOC, TN, TP, C/N ratio, metals and diatoms at lower and middle estuary and discussed with respect to varying factor variables. A

summary of the thesis is presented which briefs the generalized observations and conclusions derived from the interpretations and discussions.

Chapter I

INTRODUCTION

1.1 Introduction

Tidal flats are an important part of coastal wetlands that are characterized by the accumulation of fine sediments and gentle bed slopes (Gao 2009a). Tidal flats are classified into three distinct zones viz. supratidal, intertidal and subtidal zone (Semeniuk 1981). The supratidal zone is above the mean high tidal level and has been mostly enclosed for cultivation or urban construction (Hu et al 2013). The subtidal zone, on the contrary, is permanently submerged by tides. The intertidal zone is between high water and low water during spring tide and is inundated periodically during spring-neap tidal cycle (Amos 1995). Mudflats and mangroves are adjacent sub-environments within intertidal zone in tropical and subtropical region (Harbison 1986; Wells and Coleman 1981).

Mudflats: Mudflats cover large “unvegetated” areas in intertidal zones that are exposed during low tide and submerged during high tide (Reineek 1972). They are often referred as “secret garden” of estuary because a diverse assemblage of cyanobacteria and eukaryotic algae thrive in such sediments (Sylvestre et al 2004; Miller et al 1996; MacIntyre et al 1996). Mudflats generally form in meso and macro tidal environment under large tidal range (Feng 1985, Cao et al 1989). Mudflats are characterized by extensive width and breadth and gentle-sloping surfaces. Mudflats can be divided into three sedimentological zones namely high, middle and low mudflats (Wang et al 1963). The high mudflats are less frequently inundated and predominantly composed of mud. The low mudflats, on the contrary, are submerged by tides in most cases. The middle mudflats are submerged during flood tides, but appear during ebb tides. The fine sediments across intertidal mudflats are delivered from rivers, erosion on the seabed and cliff recession, organisms living in coastal waters and mangroves produce shell debris and particulate organic matter (Gao 2009a). The sediment transport and deposition in intertidal mudflats is controlled by spring and neap tidal differences, waves, storms, flood-ebb tidal asymmetry and differences in water level. The development of intertidal mudflats takes as a response of intertidal profile to sediment supply, waves, tides and reclamation activities (Chen 1990, 1991). The intertidal mudflat profiles are mostly double "S" shaped consisting of an upper deposition zone, middle erosion zone and

lower deposition zone (Feng 1980). The variations in fine sediment supply and hydrodynamics determine whether the "S" shapes were upper concave or upper convex (Shi and Chen 1996). The estuarine mudflats are key habitats for a number of macrofaunal species and are consequently important areas for both avifaunal population (as roosting/feeding areas) and also act as important food sources or nursery grounds for fish communities (Boyes and Allen 2007). Both east and west coast of India are marked by extensive mudflats. Recent studies have highlighted the importance of these areas to study past changes in depositional environment (Singh and Nayak 2009; Fernandes and Nayak 2009, 2012a, b; Siraswar and Nayak 2011; Fernandes et al 2011; Pande and Nayak 2013a, b; Volvoikar and Nayak 2013a, b, c and Singh et al 2012, 2013).

Mangroves: Mangroves are salt tolerant shrubs and trees that act as buffer zone between land and sea (Ramanathan et al 1999). They harbour the most diverse and abundant fauna and flora of the tidal flats. The mangrove vegetation is associated with a unique horizontal root network that enhances the deposition of fine grained suspended sediments and prevents re-suspension and erosion of fine sediments (Soto-Jimenez and Paez-Osuna 2001; Kumaran et al 2004). Mangrove environments are highly productive and are sources of organic matter which may be transferred to adjacent coastal waters through the export of detritus and living organisms (Robertson and Duke 1990). The exchange of materials between mangroves and coastal waters is largely controlled by tides and river runoff (Wattayakorn et al 1990). Mangroves influence hydrodynamic activity by slowing down tidal currents and aiding in deposition of sediments and associated organic materials (Wolanski et al 1980). Recent geochemical studies indicate that the mangrove sediments are capable of trapping large quantities of pollutants, particularly trace metals, without significant effect on the vegetation (Delacerd 1983). Mangrove sediments are ideal for understanding hydrogeochemical processes (Ramanathan et al 1999). They may act as a sink or a source for trace metals in coastal environments because of their variable physical and chemical properties (Harbison 1986). Mangrove sediments have been extensively studied around the world viz. India,

Australia, Brazil, Malaysia, Arab, China, Thailand, etc. (Radojevic et al 2008). The Vashishti, Savitri, Kundalika, Amba, Dharamtar and Rajapuri are the major mangrove harbouring estuaries in Maharashtra along central west coast of India and harbours mangroves species like *Rhizophora mucronata*, *Avicennia officinalis*, *Sonneratia apetala*, *Kandelia candle*, *Acrostichum aureum* and *Acanthus ilicifolius* (Shindikar 2006).

Trace metals in the intertidal region may partially originate from the weathering of parent rocks (Wang and Zhu 2000), but mostly may stem from urban and industrial wastewater discharge (Zhang 1994; Birch and Taylor 1999; Ruiz 2001; Sakan et al 2009), or atmospheric deposition (Liu and Zhang 1996). In the water column, metals exist in different forms where they interact with suspended sediments, slowly settle down and finally get deposited in the sediment (Kennish 2002). Previous studies have shown that less than 1% of metals remain dissolved in the water column whereas over 99% are deposited and stored in the bottom sediments (Kalnejais et al 2010; Tankere et al 2007). However, several physical, chemical and biological processes which take place at sediment-water interface result in mobilization of metals. Intertidal sediments are therefore an important sink for a wide range of contaminants, trace metals in particular showing a high affinity for fine grained sediments (Cundy and Croudace 1995; Spencer et al 2003; Presley et al 1980; Jickells and Knap 1984; Williams et al 1994; Rae 1997; Liu et al 2000, 2003, 2006). With rapid industrialization and urbanization trace metal enrichment has increased over the years and must be bioaccumulating in the benthic organisms. Accumulated metals in the food chains cannot be eliminated chemically or biologically (Klavins et al 2000; Tam and Wong 2000). The accumulation of trace metals may have a toxic effect on intertidal ecosystems and also has potential to harm human health *via* the food chain. The study of spatial and temporal distribution of pollutants (e.g. trace metals) in the intertidal region can be used to forecast their accumulation at different sites. This would allow improved assessment of the environmental risks of trace metals thus finding better counter measures to protect the wetland ecosystem of the estuary (Hu et al 2013). Therefore, intertidal sediment pollution has received much attention as it is habitat for

variety of wildlife (Zhu 1991; Williams et al 1994; Jickells and Rae 1997; Jones and Turki 1997; Xu et al 1997; Zhang et al 2001, 2009; Wang et al 2002). Sediments within estuarine regions are composed of different sedimentological and geochemical phase that acts as binding sites for metals entering the estuarine environment. Organic matter also acts as a metal carrier and plays an important role in the metal distribution patterns (Lin and Chen 1998; Degroot et al 1982). Organic matter is generally preserved in fine-grained sediments (Salomons and Forstner 1984). After burial, early diagenetic processes such as post depositional migration and reprecipitation affects metal distribution. Under sub-oxic conditions, the degradation of organic matter involves the use of redox sensitive metals (e.g. Mn and Fe) as secondary oxidants and the reduction of Fe and Mn results in the mobilization and upward diffusion of these metals to oxic surface sediments where they are reprecipitated either as oxides, or occasionally as carbonates (Farmer and Lovell 1984). The adsorption of metals in Fe–Mn oxyhydroxides is a common phenomenon in estuarine sediments and their dissolution–reprecipitation reactions might lead to significant alteration in metal sediment profiles (Carman et al 2007). Under low oxygen concentrations Mn recycling is less important, allowing Fe oxide recycling to play an increasing role in other metals precipitation (Shaw et al 1993). Besides scavenging of metals by Fe–Mn oxide, variation in trace metal distribution is controlled by coatings on clays and other minerals, complexing by organic matter (Troup and Bricker 1975), the adsorption or precipitation of trace elements onto clay mineral surfaces, differences in hydrodynamics, churning, erosion, bioturbation, periodic dredging activities, sediment properties, coagulation due to mixing of salt and freshwater, agricultural, domestic and industrial runoffs, and from natural sources due to geological formation of the catchment area (Salomons et al 1988; Winkles et al 1993; Abu-Hilal and Badran 1990; Nohara and Yokoto 1978; El-Sayed 1982; Ridgway and Shimmiel 2002; Chatterjee et al 2007).

Clay minerals are a part of fine grained sediments (<2 μm) that are derived from parent-rocks through weathering processes (He and Liu 1997). They also form the major composition of suspended sediments in the estuary (You

and Tang 1992; Naidu et al 1995; Sionneau et al 2008). Clay minerals viz. smectite, illite, kaolinite and chlorite have been widely used in studies dealing with sedimentary provenance within estuarine environments (Allen 1991; Bukhari and Nayak 1996; Feuillet and Fleischer 1980; Gutierrez-Mas et al 1997; Li et al 1999; Rao and Rao 1995; Rao et al 2011; Kessarkar et al 2009, 2010, 2013). The clay mineral distribution can provide information on geology and topography of the continental source area (Chamley 1989). The compositions of clay mineral assemblages indicate the intensity of weathering and direction of the transport processes (Biscaye 1965; Griffin et al 1968; Petschick et al 1996; Chamley 1989; Chunyan et al 2010; Thamban and Rao 2002). The differential flocculation and size segregation of clay minerals is related to salinity change (Gibbs 1977). Amongst the clay minerals, kaolinite and illite usually are deposited in the upper estuary while smectite settle preferentially on distal areas of an estuary where the rate of flocculation increases due to higher salinity (Whitehouse et al 1960; Gibbs 1983; Chamley 1989).

Organic matter in estuaries can be derived from a range of sources which include autochthonous inputs of planktonic and benthic primary productivity, along with allochthonous inputs such as terrigenous, river run off and anthropogenic sources (Graham et al 2001). A significant portion of organic matter sinks through the water column and are ultimately preserved in sediments (Hu et al 2006) by the interaction of series of physical, chemical and biological processes (Liu et al 2006). The carbon/nitrogen ratio (C/N) in the sediments has been used to identify and characterize the source of organic matter (Wilson et al 2005; Ruiz-Fernández et al 2011). Marine algae typically have C/N ratio of 4-10, whereas terrestrial plants have C/N ratio of 20 or higher with characteristic ranges being 175–400 for wood, 20–50 for tree leaves, and 25–80 for grass and herbaceous plants (Hedges et al 1986; Prah et al 1980; Meyers 1994). Better understanding of sources of organic matter in estuarine sediments and the factors controlling their distribution is important to the understanding of global biogeochemical cycles (Hu et al 2006, Gireeshkumar et al 2013). Diagenetic processes may modify the C/N ratio in sediment columns after sedimentation (Pereira et al 1999). The impact of the diagenetic processes is related to the type of decomposing

material and the susceptibility to decomposition (Thornton and McManus 1994).

Diatoms are the major component of phytoplankton and are thought to be the dominant organisms in the estuarine and coastal environments due to their nutrient replete conditions (Schrader and Schuette 1981). Diatoms also form an important component of the microphytobenthos population (Mc Lusky 1989). These photosynthetic algae contribute more than 50% of primary production in estuarine and shallow coastal environments (Underwood and Kromkamp 1999). Diatoms are characterized by siliceous cell wall which gets preserved in sediments after their death (Round 1991). The diatom population is controlled by multiple factors which include sediment grain size, light, temperature, nutrients, pH, etc (Whitton and Rott 1996; Facca and Sfrico 2007; Pan and Stevenson 1996). Diatoms are ubiquitous organisms with high species diversity and short life cycle. Therefore, they react quickly to environmental conditions (Duong et al 2007). Diatoms are also good indicators of pollution levels (Duong et al 2007). Diatoms, single celled microscopic organisms belonging to class Bacillariophyceae, have been used as a proxy to reconstruct the depositional environment since these organisms are sensitive to changes in salinity, nutrient, pH, etc. Diatoms thrive in water of particular salinity and get preserved in sediments due to their siliceous cell wall. Diatom assemblages have been used to interpret changes in the degree of marine (Zong 1997) and fresh water influence (Almeida and Gil 2001). Diatoms have also been used as a biological indicator for erosion/accretion processes (Ribeiro et al 2010).

1.2 Literature review

Studies carried out in the recent years are listed in the table 1.1.

Table 1.1 Literature review of studies carried out in the recent years			
Authors	Objective	Parameters analyzed	Results
Pande	To understand	Grain size,	1) The distribution of metals is

and Nayak 2013a	sources and factors that control distribution of metals.	total organic carbon and metals (Fe, Mn, Al, Ni, Cr, Co, Zn and Pb)	largely controlled by Fe–Mn oxyhydroxides and organic carbon. 2) The middle flats of the lower estuary showed an anthropogenic source for Ni, Cr and Co while middle flats of the middle estuary showed a mainly lithogenic source.
Volvoikar and Nayak 2013a	To understand factors controlling metal distribution in sediments of creeks facing dissimilar anthropogenic pressures.	Grain size, total organic carbon and metals (Fe, Mn, Al, Cu, Zn, Co, Ni and Pb)	1) Most of the metals showed significant higher addition in Dudh creek (core DC) as compared to Khonda creek (core KC). However, Khonda creek sediments did show anthropogenic enrichment of Mn, Zn and Ni, while Dudh creek sediments showed anthropogenic enrichment of almost all the studied metals. 2) Large difference in metal concentration between the two creeks was attributed to their proximity to industries.
Singh et al 2013	To study the response of magnetic parameters in the environment to historical pollution, with changing sedimentation rates.	Grain size, total organic carbon, clay mineralogy, metals (Fe, Mn, Al, Ca, Mg, K, Zn, Cr, Co, Cu and Pb) and Pb ²¹⁰ dating	1) The sedimentation rate in the study area varied from 0.13 to 2 cm/yr. The rate was extremely low at the lower half of the cores (0.13–0.31 cm/yr, before ~1980) as compared to the near surface (1.21–2 cm/yr, after ~1980) with two clear phases of sedimentation rates. 2) The higher sedimentation rate in the upper portions of the cores was found to correspond to

			increased deposition of finer sediment components, metals and magnetic minerals which in turn were found to be mainly controlled by geology and/or human activities.
Rezaie-Boroon et al 2013	To assess the pollutant deposition processes in response to extensive human activities.	Metals (Ag, Al, As, Cd, Cr, Cu, Fe, Mn, Ni, Pb, Se, Sr, Ti, V and Zn)	<p>1) The Index of Geo-accumulation factor showed highest values for Pb, Mn, As, and Cu.</p> <p>2) Enrichment factors >1 for these elements, suggest anthropogenic inputs for most metals.</p> <p>3) The bioavailability of metals in lagoon sediments has the potential to be highly dynamic with local waste and natural H₂S discharge from existing fault line.</p>
Hamzeh et al 2013	To study the historical changes of some trace metals in core sediments collected in the docks basin of Rouen harbor. Also, the intensity of the sediment contamination using an EF and a geoaccumulation index (Igeo) by comparison with reference sediment quality guidelines.	Metals (Cd, Ni, Pb, Hg, Zn and Pb)	<p>1) The results of vertical distribution showed that the metal pollution in the past is much higher than in the surface sediment.</p> <p>2) Mercury was found to be the heaviest pollutant (with Igeo and EF exceeding 4 and 20, respectively), and Cd and Pb were the second most important pollutants. A slight contamination in Ni was observed with very low Igeo values.</p>

Hu et al 2013	To study the spatial and temporal variations in heavy metal contents in soils of the tidal flats in the Yangtze Estuary and to find the main factors controlling the contents of heavy metals in the tidal flats of the estuary.	Grain size, organic matter, pH, Fe, Mn, Cu, Zn, Pb, Cd, Cr, Ni and magnetic susceptibility	<p>1) The results showed that the heavy metal loads were commonly higher in the soils of nearshore high tidal flats and had a tendency of decreasing from land to sea at both of the study sites.</p> <p>2) The soils in the nearshore high tidal flats were finer and gradually got coarser seawards.</p> <p>3) The contents of heavy metals in the intertidal soils of both the sites EC and JS were significantly positively correlated with the clay (< 2 μm) and 2–20 μm fractions, but negatively with the sand (> 63 μm) and 20–63 μm fractions, which suggested that the heavy metals in the intertidal soils were primarily combined with the fine particulate fraction (< 20 μm), especially clay, and hence the spatial and seasonal variations in heavy metals were actually caused by the change of the grain-size characteristics of the intertidal soils due to the different sedimentary environments in the estuary.</p>
Fernandes and Nayak 2012b	1) To understand the dynamics of geochemical processes that govern the	Grain size, total organic carbon, total nitrogen, total	Ulhas Estuary with higher clay and organic matter contents, exhibited higher amounts of metals than Thane Creek.

	behaviour and fate of metals in estuarine subenvironments, and 2) identify the different factors responsible for the variability of metal concentrations in the sediments.	phosphorous, carbon/nitrogen ratio, pH and metals (Fe, Mn, Cu, Pb, Co, Ni, Zn, Cr, Al, Ca and V)	
Banerjee et al 2012	To examine the pattern and source of contaminant deposition along with the sediment accumulation rate in this ecologically sensitive area.	Trace metals (Fe, Zn, Co, Ni, Pb, Cu, Mn, Cr and Cd), organic carbon, Pb ²¹⁰ and Ra ²²⁶ dating.	<p>1) Both in mangroves and estuarine systems, Fe–Mn oxyhydroxides are observed to be a major controlling factor for trace metal accumulation when compared to organic carbon.</p> <p>2) Core collected from Hooghly estuary shows less contamination when compared to the mangrove region due to high energy and mostly coarse grained.</p> <p>3) The EFs are typically >1 for Cd, Pb, Co, and Cu indicating that these metals are highly enriched while other metals such as Zn, Ni, Cr, and Mn show no enrichment or depletion.</p> <p>4) This study suggests that the variation in trace metals content with depth or between mangrove and estuarine system results largely from metal input due to</p>

			anthropogenic activities rather than diagenetic processes.
Tue et al 2012	1) To understand the temporal variations of trace element concentrations. 2) To assess sediment quality of mangrove ecosystems from the Ba Lat Estuary (BLE).	Grain size, total organic carbon, porosity, trace metals (Pb, Zn, Cu, Cr, V, Mn, Cd, Co, Sb, Sn, Ag and Mo) and Pb ²¹⁰ dating.	1) Results from contamination factors, Pearson's correlation, and hierarchical cluster analysis suggest that the trace elements were likely attributed to discharge of untreated effluents from industry, domestic sewage, as well as non-point sources. 2) Geoaccumulation Index showed that mangrove sediments were moderately polluted by Pb and Ag, and from unpolluted to moderately polluted by Zn, Cu, and Sb.
Xia et al 2011	To reconstruct the pollution history of the metal inputs and to quantify the intensity of heavy metal pollution by using the metal enrichment factor and excess fluxes	Grain size, total organic carbon, total nitrogen, total phosphorous, C/N ratio and metals (Al, Fe, Hg, Cd, Cu, Cr, Pb, As and Zn)	When the erosion related to land-use modifications enhanced, it promoted higher accumulation rates of the sedimentary material. In the recent sediments they were found a moderate enrichment of Cd and Hg (maximum 3.5- and 2.8-fold corresponding to the local background levels, respectively) and a slight enrichment of Cr, Zn, As and Pb (maximum 1.3-, 1.3-, 1.3- and 1.2-fold, respectively). The excess metal fluxes also showed a consistently increasing trend since the early 1990s, which could be associated with the intensive use of phosphate

			fertilizers and the combustion of fossil fuels derived from human activities
Filho et al 2011	To estimate vertical distribution of trace metals in the sediment cores of Sundarban wetland in order to assess the degree of chemical enrichment contamination and the ecological quality of this region.	Grain size, organic carbon, pH and metals (Al, Fe, Mn, Zn, Cr, Cu, Ba, B, V, As and Hg).	1) The overall concentrations range is low to moderate, indicating the environmental conditions in the outfall zone (grain size, hydrodynamic regime, and confinement), which favors the in situ accumulation of pollutants. 2) The sediments are particularly enriched with Cr, Cu, B, V, and As. These enrichments seem to be due to the fine granulometry of the regions with Fe and Mn oxihydroxides being the main metal carriers.
Sundararajan and Natesan 2011	To identify the natural and anthropogenic imprints left by the accumulation of elements and to determine/identify the current level of enrichment of trace metals in the creek area.	Grain size, CaCO ₃ , organic carbon, major (Si, Al, Fe, Na, K, Ca, Mg and P) and trace (Mn, Cr, Cu, Ni, Co, Pb and Zn) metals.	1) Textural parameters, CaCO ₃ , OC and Al-normalized pattern of elements indicate depositional events in core samples that can be directly related to natural events during the last decade. 2) The calculated enrichment, anthropogenic factors and comparison of data indicate that the observed trace metals (especially Pb, Co) are enriched mainly due to the anthropogenic activities in the land as well as in the coastal zone (Palk Strait).
Thilagavathi et al	To determine the level of heavy	Soil texture, total	The minimum concentration was recorded in river mouth and the

2011	metals in Muthupettai lagoon mangroves in the southeast coast of India.	nitrogen, organic carbon, phosphorus and heavy metals (Fe, Mn, Cr, Cu, Ni, Pb, Zn and Cd).	maximum in lagoon.
Silva et al 2011	To determine concentration of metals.	pH, conductivity, salinity, DO, temperature, metals As, Br, Co, Cr, Cs, Fe, Rb, Sb, Ta, Th, U, Zn and rare earths (Sc, Ce, Eu, La, Lu, Nd, Sm, Tb and Yb)	The area is home to Brazil's most important and busiest port. It is concluded that As, La, Sm, Ne, Ce, Eu, Hf, Ta, Th, and U elements have a high background level in the region and that Fe and Zn were the main indicators of anthropogenic contribution in the sediments.
Rodríguez et al 2010	To evaluate the chronological evidence of human impacts and environmental degradation, which at the minimum can be used to advise the managers and	¹⁴ C dating, organic matter, metals (Zn, Cu, Cr and Pb) and diatoms.	A sediment core that spanned to 3000 yr BP was collected to reconstruct the Holocene natural changes in salinity and trophic state, and also the effect of human activities on the environmental quality of the system. Before the human impact, the system was controlled by a sea level decrease,

	government agencies about the consequences of bad environmental practices on coastal aquatic systems		during which an increase in trophic state was observed. After the human impact, an intensification of the eutrophication process was observed, mainly due to the industrial activities linked to lack of sanitation. In addition, sharp increase in heavy metal concentration were recorded after 1917, when the leather tanning activities together with the construction and operation of the oil refinery and the thermoelectric generation plant were first documented.
Ribeiro et al 2010	To infer the history of the paleoecological and paleohydrological changes during the last millennium.	Grain size, organic matter, diatoms, ¹⁴ C dating.	<p>1) The results revealed 58 diatoms species among benthic and planktonic life forms.</p> <p>2) Analysis applied to relative abundance of diatoms and associated sedimentary texture, OM contents and ¹⁴C dating, defined three ecozones.</p> <p>3) The lower sandy ecozone 1 dated at 930 ± 40 ¹⁴C yr BP (Beta 217590) was dominated by the benthic/epipsammic species <i>Staurosira obtusa</i>, <i>Staurosirella pinnata</i> and <i>Staurosirella crassa</i> (nov. comb.), that indicated more hydrodynamic energy than in present days, originating a shallow sedimentary environment, under</p>

			<p>erosive conditions, unfavorable to the colonization of vegetation. The intermediate grey clay ecozone 2 that was observed only in the IT1 core, dated at 520 ± 40 ^{14}C yr BP (Beta 217591) showed the prevalence of planktonic diatoms, providing evidence of a deeper and calmer environment, located in a probably protected area, with intense sedimentation of clay particles and with abundant plant remains, colonized by mangrove forest and alluvial palm forest. The upper organic-clay to organic-sand ecozone 3 much younger than 520 ± 40 ^{14}C yr BP, showed more agitated and erosive sedimentary conditions, however, with less energy than that in lower ecozones, indicated by higher abundance of <i>A. granulata</i>, strongly silicified.</p>
Zong et al 2010	To study relationship between diatom assemblages and environmental parameter (salinity, depth and sediment particle size)	Diatoms, salinity, water depth, sand content	<p>1) Marine diatoms were dominant in the high salinity environment and the outer part of the estuary.</p> <p>2) Brackish water diatoms were found in high abundance in the central part of the estuary. Both marine and brackish water diatoms were predominantly planktonic taxa.</p>

			<p>3) Freshwater diatoms dominated in low salinity environments, with planktonic taxa in the deep tidal channel and benthic species in the shallow deltaic distributaries.</p> <p>4) Statistical tests indicated that the modern diatom distribution is strongly correlated with salinity but is also influenced by several other environmental variables including sand content and water depth.</p>
Seshan et al 2010	<p>1) To evaluate the extent of heavy metal contamination from the surface to the bottom sediments.</p> <p>2) To determine relationship between metals and other sedimentological parameters such as grain size, pH, sediment composition, and organic matter.</p>	<p>Grain size, pH, organic matter, CaCO₃ and metals (Cd, Cr, Cu, Pb and Zn)</p>	<p>1) Grain size analysis and sediment composition shows sandy nature having a neutral pH.</p> <p>2) Cores collected within the canal showed a higher heavy metal concentration than the cores collected from Pulicat lagoon and 2 km into the Ennore Sea.</p> <p>3) The trace metal concentration for cadmium, lead and zinc in Ennore does not pose a threat to the sediment dwelling fauna whereas chromium and copper are likely to pose a threat.</p> <p>4) Quantitative indices place Ennore under moderately polluted. Ennore is likely to face a serious threat of metal pollution with the present deposition rates unless stringent pollution control norms</p>

			are adopted.
Sundararajan and Srinivasalu 2010	To study the origin and nature of the sediments and paleoenvironment	Sediment grain size, CaCO ₃ , organic matter, major (SiO ₂ , Al ₂ O ₃ , Na ₂ O, K ₂ O, CaO, MgO, Fe ₂ O ₃ , P ₂ O ₅) and trace (Mn, Cr, Cu, Ni, Co, Pb, Zn and Cd) elements.	<p>1) Textural studies indicate that the sediments have been poorly sorted and most of the sub samples are silty clay with few top samples sandy silty clay.</p> <p>2) The nature of organic matter also indicate high sedimentation rate.</p> <p>3) Based on the behaviors of CaCO₃, Organic matter (OM) and textural parameters the core was studied under the three units.</p> <p>4) The major oxide geochemistry shows higher concentration of detritus constituents.</p> <p>5) The trace element studies indicate ferruginous nature for all elements except Cu and Zn.</p>
Qi et al 2010	To study the geochemical sources in the estuarine sediments and to different depositional environments responded by vertical variation of indicative elements and enrichment and possible	Grain size, dating (Pb ²¹⁰ and Cs ¹³⁷), metals (Al, K, Mg, Ca, Fe, Mn, Co, Cr, Cu, Hg, Li, Ni, Pb, Zn), inorganic carbon, total carbon,	<p>1) The representative elements and related elemental ratio reflected different depositional environments in the four cores, which are controlled by the hydrodynamic conditions.</p> <p>2) Core IOW300 190 at the mid West Shoal maintained a constant sub-oxic environment with abundant fluvial deposits; core IOW300 480 at the mouth of the estuary formed an oxic environment influenced by the strong two-layer currents, while</p>

	contamination of heavy metals in the sediments using newly acquired geochemical natural background.	total sulphur and total nitrogen.	<p>two cores (IOW300 020 and IOW300 630) at the East Shoal experienced an evident change from marine anoxic condition to a weak anoxic or a sub-oxic condition caused by increasing riverine discharges.</p> <p>3) According to the enrichment factors (EFs) of heavy metals (Co, Cr, Cu, Hg, Ni, Pb and Zn), there was no significant metal enrichment and contamination in the core sediments in spite of that some metals increased and was partly enriched in the uppermost or surface sediments.</p> <p>4) Core IOW300 630, with a constant sedimentation rate of 0.45 cm/a by Cs137 and Pb210 dating, exhibits that heavy metals began to increase in the 1960s and increased progressively in the 1980s and 1990s, responding to the rapid economic development in the Pearl River delta region in the last three decades.</p>
Sundararajan and Natesan 2010	To identify the source and fate of metals and toxic elements in the study area, and its impact on the environment.	Grain size, CaCO ₃ , organic carbon, major (Si, Al, Na, K, Ca, Mg, Fe	The calculated enrichment factors and comparison indicate that the trace metals (especially Pb) are enriched mainly due to the external (anthropogenic) activities in the land as well as in the coastal zone (Palk Strait).

		and P) and trace (Mn, Cr, Cu, Ni, Co, Pb and Zn) elements.	
Jonathan et al 2010	<p>1) To identify the enrichment pattern of ALTMs (or labile metals) in the sediments to ascertain the Lability and</p> <p>2) mobility of these metals and their relationship with sediment quality parameters.</p>	<p>Grain size, pH, organic carbon, CaCO₃ and metals (Fe, Mn, Cr, Co, Ni, Pb, Cd, Mo, Ag, As and Ba)</p>	<p>1) Textural analysis reveals an overall predominance of mud.</p> <p>2) The results indicate that the change in pH values causes coagulation and precipitation of ALTMs.</p> <p>3) Fe and Mn have fairly close distribution patterns of enrichment in surface layers which might be ascribed to early diagenetic processes.</p> <p>4) The most prominent feature of ALTMs is the enrichment of Fe, Mn, Cr, Cu, Ni, Pb, and Ba in the surface–subsurface layers in the sediment cores, which is mainly attributed to the intense industrial and agricultural activities as well as drainage of untreated domestic sewage to this coastal region.</p> <p>5) The ALTMs also indicate their association with organic carbon and Fe–Mn oxyhydroxides. Anthropogenic Factor values indicated ALTMs enrichment for all trace metals due to intense anthropogenic activities.</p>

			6) Statistical analyses suggest that five ALTMs (Cu, Pb, As, Mo, Ba) are attached to the organic particles and the clustering of elements separately also indicates that they are from external source.
Alaoui et al 2010	To study (a) spatial and temporal differences, (b) the correlation among selected elements and major components of the samples, and (c) land use.	Clay, POC, Al, Fe, Pb, Zn, Cu, Cu, Mn, Ni, Cd, Hg and Cr.	<p>1) The results suggest that a major change in the sedimentary regime of the lagoon, associated with internal trapping and re-distribution of heavy metal, has been occurring in the past few decades. The cause would appear to be the construction of a Nador Canal at the lagoon.</p> <p>2) These comparisons suggest that sediment metal levels in the river are clearly high and probably pose an environmental risk at some stations. The levels of most of the metals were not greatly enriched, a consideration that is of the utmost importance when contamination issues are at stake.</p> <p>3) Metal concentrations found in Moulay Bouselham lagoon were comparable to aquatic systems classified as contaminated from other regions of the world.</p>
Katsuki et al 2009	To identify the influence of anthropogenic activity over the	Cs ¹³⁷ , Pb ²¹⁰ dating, diatoms, grain size	A distinct record of the succession of the dominant diatom taxa was preserved in core sediments. Low-oxygen water was prevalent in the

	past century.	and water content.	lake in 1929, before the first inlet excavation. Immediately after the first inlet excavation, the low-oxygen water in the western basin of the lake began to disappear, in a trend that became increasingly transparent, which has been attributed to an increasing rate of water exchange. The environmental change was reflected in a decrease of benthic diatom taxa and an increase of planktonic taxa, trends which have continued until today. Particularly, the numbers of diatom assemblage have been decreasing all over the lake during the last 10 years, which suggests that Lake Saroma's present-day deterioration and eutrophication will continue or become even worse.
Ruiz-Fernández et al 2009	To reconstruct the recent history of the metal enrichment (Cd, Cu, Hg, and Pb).	Grain size, organic carbon, CaCO ₃ , trace metals (Cd, Cu, Pb and Hg), Pb ²¹⁰ and Cs ¹³⁷ dating.	1) The metal fluxes ($\mu\text{g cm}^{-2} \text{y}^{-1}$) for the three lagoons fell within the ranges of 0.02–0.15 for Cd, 0.7–6.0 for Cu, 0.001–0.045 for Hg, and 0.7–20 for Pb. 2) The Hg pollution in Estero de Urías was attributed to the exhausts of the thermoelectric plant of Mazatlan and the metal enrichment in Chiricahueto and Ohuira was related to the

			agrochemical wastes from the crop lands surrounding these lagoons.
Badr et al 2009	To study the concentrations of nine metals Al, Fe, Mn, Cr, Cu, Zn, Cd, Ni and Pb in sediment cores and to investigate the processes that regulate them.	Grain size, CaCO ₃ , organic matter and metals (Al, Fe, Mn, Cd, Cr, Cu, Ni, Pb and Zn).	<p>1) Some metals like, Cr, Mn, Ni and Zn, were enriched in the upper 15 cm of core samples (recent deposition of sediments). Cd concentrations showed high fluctuations with depth and reverse pattern to that for Al, Fe and Mn which indicated land based source of these elements to the studied areas.</p> <p>2) Elevated concentrations of lead were recorded in the bottom layers of cores in Jeddah that indicated the most dramatic increase in usage of gasoline in early 1970s.</p> <p>3) The calculated contamination factors (CF's) were found in the following sequences: Cd > Pb > Ni > Cu > Zn > Cr > Mn for all studied areas.</p>
Chatterjee et al 2009	To evaluate the fluvio-marine and geochemical processes influencing the metal distribution.	Grain size, organic carbon, pH and metals (Al, As, Cd, Co, Cr, Cu, Fe, Mn, Ni, Pb and Zn)	1) The most interesting features are the downward increase of concentrations of majority of the elements reaching overall maximum values at a depth of 10–15 cm observed in station No.8 located along the main stream of the Ganges estuary as well as an overall elevated concentration of all the elements in the lower littoral zone.

			<p>2) The inter-elemental relationship revealed the identical behaviour of elements during its transport in the estuarine environment.</p> <p>3) The overall variation in concentration can be attributed to differential discharge of effluents originating from industrial and agricultural as well as from domestic sewage.</p>
Harikumar et al 2009	To determine distribution of trace elements along the core and to correlate the toxicity distribution with chemical concentration in sediment profiles.	Metals (Fe, Mn, Cu, Ni, Zn, Pb, Hg and Cd).	<p>1) Heavy metals such as Fe, Cu, Ni and Zn reported enrichment towards the surface of the core sediment sample collected from the centre of the lake. Pb, Cd and Hg showed uniform distribution throughout the core.</p> <p>2) Results of the analysis showed that Vembanad lake is facing serious metal pollution with increased rate of deposition.</p>
Hwang et al 2009	To reconstruct historical changes in terms of trace metal pollution in the tidal flat of outer Stege Marsh.	Metals (Ag, Al, As, Cd, Co, Cr, Cu, Fe, Li, Mg, Mn, Ni, Pb, Se, V and Zn).	<p>1) Aluminum-normalized enrichment factors indicate that inputs from anthropogenic sources were predominant over natural input for Ag, Cu, Pb, and Zn. Among these, lead was the most anthropogenically impacted metal with enrichment factors ranging from 32 to 108.</p> <p>2) Depth profiles and coefficients of variation show that As, Cd, and Se were also influenced by</p>

			<p>anthropogenic input.</p> <p>3) The levels of these anthropogenically impacted metals decline gradually towards the surface due to regulation of the use of leaded gasoline, municipal and industrial wastewater discharge control, and closure of point sources on the upland of Stege Marsh.</p>
Zourarah et al 2009	To evaluate the contamination sources, the historical evolution of contamination and the fluxes of heavy metals to the sediments.	Grain size, organic carbon, metals (Cd, Hg, Cr, Cu, Fe, Mn, Ni, Pb and Zn), Pb ²¹⁰ and Cs ¹³⁷ dating.	<p>1) These data indicate that the mean sedimentation rates are 0.38–0.68 cm per year. The analytical results and the radiometric dating of sediment cores show extremely high concentrations of Zn, Pb and Cu in the sediments that can be ascribed mostly to the discharge of the liquid effluent from the sewage since the late 1960s, which shows decreasing trend towards the present day.</p> <p>2) The pollution intensity of the estuary is determined by the enrichment factor, which shows that the Oum Er Bia estuary is moderately polluted.</p>
Wang et al 2008	1) To determine the total concentration and spatial distribution of trace elements in the	Grain size, total organic carbon and metals (Co, Cu, Ni, Cr,	1) The results demonstrated that terrigenous sediment received by the rivers are main sources of the trace metal elements and TOM, and the lithology of parent material

	<p>surficial sediments in the west-four Pearl river estuary region; 2) to evaluate the sedimentological and geochemical factors that control the distribution pattern and the source of trace elements;</p> <p>3) to explore the natural and anthropogenic input of heavy metals and to assess the pollution status on the area</p>	<p>Pb, Zn, Sr, Zr and Ba)</p>	<p>is a dominating factor controlling the trace metal composition in the surficial sediment. In addition, the hydrodynamic condition and landform are the dominating factors controlling the large-scale distribution, while the anthropogenic input in the coastal area alters the regional distribution of heavy metals Co, Cu, Ni, Pb, Cr and Zn.</p> <p>2) The results indicate prevalent enrichment of Co, Cu, Ni, Pb and Cr, and the contamination of Pb is most obvious, further more the peculiar high EF value sites of Zn and Pb probably suggest point source input.</p>
Liu et al 2008	<p>Diatoms from a sediment core were analyzed in order to date the historical changes in phytoplankton assemblages, and to relate these changes to anthropogenic and natural changes that have occurred during the last century.</p>	<p>Diatoms, nutrients (phosphate, silicate, nitrate and ammonium), Pb^{210} and Cs^{137} dating.</p>	<p>1) The flora was mainly composed of centric diatoms (59–96%).</p> <p>2) The concentration of diatoms declined sharply above 30 cm (after ~1981 A.D.), while the dominant species changed from <i>Thalassiosira anguste-lineatus</i>, <i>Thalassiosira eccentrica</i>, <i>Coscinodiscus excentricus</i>, <i>Coscinodiscus concinnus</i> and <i>Diploneis gorjanovici</i> to <i>Cyclotella stylorum</i> and <i>Paralia sulcata</i>.</p> <p>3) Species richness decreased slightly, and the cell abundance of</p>

			<p>warm-water species increased. They argued that these floral changes were probably caused by climate change in combination with eutrophication resulting from aquaculture and sewage discharge.</p>
Tang et al 2008	To assess the spatial and temporal changes of metal contaminants.	Metals (Cu, Ni, Pb, Zn, Al, Fe, Mn, Co and Ca) and Pb^{210} dating.	<p>1) The spatial distribution of trace metals can probably be attributed to the proximity of major urban and industrial discharge points, and to the effect of tidal flushing in the harbour.</p> <p>2) In the sediment cores, the highest concentrations of trace metals were observed to have accumulated during the 1950s–1980s, corresponding with the period of rapid urban and industrial development in Hong Kong. From the late 1980s, there has been a major decline in the concentrations of trace metals, due to a reduction in industrial activities and to the enactment of wastewater pollution controls in the territory.</p> <p>3) The $^{206}Pb/^{207}Pb$ ratios varied from 1.154 to 1.190, which were</p>

			lower than those of background geological materials in Hong Kong (206Pb/207Pb: 1.201–1.279).
Dai et al 2007	To assess how the sediment records reflect the environmental changes of Jiaozhou Bay, a semi-enclosed bay adjacent to Qingdao, China.	Grain size, pH, Eh, Metals (Cr, Cu, Zn, Pb, Co, Ni, Cd, Li), organic carbon, total nitrogen, total phosphorous, biogenic silica, organic phosphorous, C/N, OC/OP, Si/N and Pb ²¹⁰ dating.	Based on the research, the development of Jiaozhou Bay environment in the past hundred years can be divided into three stages: (1) before the 1980s characterized by relatively low sedimentation rate, weak heavy metal pollution and scarce eutrophication; (2) from the 1980s to 2000, accelerating in the 1990s, during which high sedimentation rates, polluted by heavy metals and the frequent occurrence of red tide; (3) after 2000, the period of the improvement of environment, the whole system has been meliorated including the heavy metal pollution and hypernutrification.
Carman et al 2007	1) To examine trace metal concentrations in the sediments in the Pearl river estuary (PRE) and its surrounding SCS area, 2) to investigate the relationship of trace	Grain size, metals (Co, Cr, Cu, Ni, Pb, Zn, Al, Ca, Fe, Mg and Mn), speciation and Pb ²¹⁰ dating.	1) The distribution of Cu, Cr, Pb, and Zn demonstrated a typical diffusion pattern from the land to the direction of the sea. Two hotspots of trace metal contamination were located at the mixed zone between freshwater and marine waters. 2) The enrichment of metals in the sediments could be attributed to

	<p>metal contamination between the PRE and its surrounding coastal area, 3) to evaluate the geochemical cycling process of trace metals in sediments between the PRE and its surrounding coastal area (e.g. physical and chemical transportation processes of trace metals in estuarine and coastal areas).</p>		<p>the deposition of the dissolved and particulate trace metals in the water column at the estuarine area.</p>
<p>Conrad et al 2007</p>	<p>To examine the historical record of trace metal contamination in the highly industrialized Elizabeth River subestuary, Virginia.</p>	<p>Specific surface area, organic carbon, major (Fe, Mn and Al), trace (Ni, Cr, Co, Zn and Pb) elements, Cs¹³⁷ and Pb²¹⁰ dating.</p>	<p>The concentrations in the surface sediments of many trace metals were elevated to levels 2–5 times higher than the levels at the bottom of the cores in both the Southern and Western Branches of the river.</p>

Lorenzo et al 2007	1) To evaluate the historical levels and sources of Pb, Cd, Cu, Cr, Co and Zn pollution in the estuaries of north Galicia, 2) to determine the background values of pollutants and the identification of non-polluted samples using PCA.	Grain size, total organic carbon, C/N and metals (Pb, Cu, Co, Cr, Cd and Zn).	1) The pollution levels obtained bear a strong resemblance to those documented for a moderately industrialised area. 2) PCA identifies factors that reflect mainly temporal associations with metals. 3) Sedimentation rates between 0.9 and 1.1 cm/year were determined. 4) In Viveiro core levels of Cr pollution are associated with tanneries. In Ortigueira, high core levels of Cu and Co are linked to mining, and Cr levels to adjacent ultramafic rocks. Erosion of Holocene sediment causes high values of Co and Cr in the Barqueiro core. Cu increase in the three estuaries is related to fungicide use since 1910.
Vaalgamaa and Korhola 2007	To compare sediment profiles in a lake and an estuary from both sedimentological and paleoenvironmental points of view in a situation where catchment-driven differences were minimized.	Grain size, total carbon, total nitrogen, total phosphorous, organic carbon, biogenic silica, C/N ratio, metals	1) Differences between the sediment cores were studied by using linear regression analysis and principal components analysis (PCA). 2) Despite similarities in catchment land-use and history, the sediment geochemical profiles of the sites varied significantly. 3) Some of the differences could be related to differences in chemical sedimentation

		<p>(Al, K, Mg, Ca, Na, Fe, Mn, Cu and Zn), Pb^{210}, Ra^{226} and Cs^{137} dating.</p>	<p>environment (lacustrine versus estuarine).</p> <p>4) TP concentration was found to be positively correlated with sediment iron content in estuarine sediment but negatively correlated with Fe in lake sediment.</p> <p>5) In the estuarine core sedimentary iron was not correlated to lithogenic potassium and aluminum but in the lake core the iron seemed to be lithogenic in origin, as suggested by the strong positive correlations ($r^2 = 0.95-0.96$) between these three variables.</p> <p>6) Most similarities among the cores were found in Al concentrations. Estuarine nutrient profiles appeared relatively monotonous compared to the lake core. This is probably due to more vigorous mixing of the sediments that may ensure more rapid and complete consumption of the organic matter deposited on the bottom of the estuary. Therefore the lake sediment appeared to preserve the historical record of eutrophication better. Biologically less active and more particle-bound materials like the trace metals Cu and Zn seemed to</p>
--	--	---	---

			retain good records of anthropogenic impact also in the estuarine core.
Church et al 2006	To investigate historical records of urban and industrial activities.	Pb210, Cs137, organic carbon, total nitrogen, phosphorus, C/N, Isotopes (C and N) and metals (As, Ag, Cd, Co, Cr, Cu, Ni, Mn, Pb, Sn, U, V and Zn)	Recorded dramatic increase in total phosphorus (TP) starting in 1950–1960 in the freshwater marsh sediment upstream in the Delaware River water, tracks the introduction of P detergent use. Although this might include increased use of P fertilizers, there is a substantial decrease after removal of the P detergent source in the mid-1970s. Carbon stable isotopes (d13C) track P changes after 1955. The heavier carbon isotope (13C) corresponds to higher levels of P in the sediments (and water), while the lighter carbon (12C) isotope in recent times corresponds to decreased discharge of P. In more recent times since the 1970s, there is a significant relationship (p < 0.05) between d13C and sediment P, while before 1965 there is a significant but different relationship. As such, the lower d13C of the sediment organic matter may record decreased growth/eutrophication when P loadings and concentrations are reduced. The N stable isotope

			<p>record shows a marked increase in $\delta^{15}\text{N}$ (ca. 3.5x to 7.5x) starting in the early 1960s. This corresponds to a substantial increase in the concentration of dissolved nitrogen (mainly as nitrate) from population growth, fertilizer applications, or changes in the processing of wastewater leading to reduction in chemical oxygen demand.</p>
<p>Karbassi and Shankar 2005</p>	<p>To understand the geological history of the area, the geochemical nature of sediments deposited at different times and association of base metals with the various constituent phases of sediments.</p>	<p>Cu, Pb, Zn, Ni, Co, Mn, Al, Ca, magnetic susceptibility and loss on ignition.</p>	<p>The sediments have high Al and organic matter contents due to the high sedimentation rate and their proximity to river mouths.</p> <p>Down-core variations of elements indicate a decrease of lithogenous component during probably the past few centuries. While abundance of calcareous shells in some zones has lead to the dilution of most of the metals, it appears that Pb and Mn are associated with this phase. Copper, Zn and Fe are associated with organic matter and detrital particles, whereas Ni and Co are predominantly associated with the insoluble fraction.</p> <p>Oxides/hydroxides of Fe and Mn are absent because of the reducing conditions and the high terrigenous influx. Geochemically, Mn and Fe are present in different</p>

			phases of sediments (in the insoluble fraction and organic matter respectively). The Fe content of one of the cores is positively correlated with magnetic susceptibility.
Yang et al 2004	To determine historical variations in heavy metals and possible anthropogenic impacts on the southern Yangtze Estuary tidal flats using a long sediment core and ^{210}Pb dating	Grain size, total organic carbon, bulk density, metals (Al, Fe, Mg, Cu, Pb, Cr, Zn, Ni and As), Pb^{210} dating.	1) Over the last 100 years, human impact was minimal. However, over the last few decades, vertical metal concentrations have been affected by human activities such as local industrialization, urbanization and construction of major sewage outlets. 2) Copper, lead and arsenic were identified as contaminants in the Yangtze Estuary on the basis of national pollution standards and a comparison of metals in the upper core with those in the lower core.

1.3 Objectives

The objectives of the thesis are-

- 1) To study the distribution and abundance of sediment components, organic carbon, clay minerals and selected elements in sediments with space and time, along the coast between Mumbai and Ratnagiri.
- 2) To understand the depositional environment and post depositional processes.
- 3) To investigate the past climate from the study of fossil diatoms.

1.4 Study area

1.4.1 Background of the study area

The coastal Maharashtra, popularly known as Konkan region, comprises of six districts namely Thane, Greater Mumbai, Mumbai, Raigad, Ratnagiri and Sindhudurg. The coastline of Maharashtra stretches 720 km in length covering 240 km of Raigad district. The coastline is indented by the openings of numerous river mouths, creeks, beaches, bays, cliffs, etc. The rivers and creeks of west coast in general form drainage in east-west direction. The region is surrounded by Western Ghats (Sahyadris) to the east and Arabian Sea to the west. The area experiences tropical warm, moist and humid climate throughout the year. The temperature range varies between 25 and 35 °C. The south-west monsoon period is from June to September. The normal average annual rainfall is 3028.9 mm of which nearly 95 percent occurs during the monsoon period. The rainfall pattern is not uniform and increases rapidly from the coast towards the Sahyadri. The tides are semidiurnal and currents within estuaries are entirely governed by tides during non-monsoon period. Geologically, the collision of Indian and Eurasian plate during early Tertiary period initiated the tectonic upliftment and resulted in the evolution of Western Ghats. The basalt lava flows are predominant rock type commonly known as Deccan trap which appear as table top hills. The entire catchment area consists of dark colored volcanic lava of Mesozoic period and laterites. The different types of soils are forest soil, varkas soil, rice soil, khar soil, alluvial soil, lateritic soil and residual soil. The residual soil occurs on the slopes, alluvial soil on the river valleys and the lateritic soil on hilly upland where the rainfall is more than 2000 mm. The color of soil may vary from bright red to brownish red owing to the preponderance of hydrated iron oxide.

The study area (Figure 1.1) is bounded between 15° 36' N to 19° 80' N latitude and 72° 51' to 74° 36' E longitude along central west coast of India. The Amba, Kundalika, Rajapuri and Savitri are the major rivers of Raigad while Vashishti is one of the main rivers of Ratnagiri district form the study area. The industrial development in the region started in 1970 after industries

were banned in Mumbai Metropolitan. The industrial policy of Maharashtra state encourages industries to be set up in the developing and under-developed areas in order to disperse them from heavily congested areas of Mumbai, Thane and Pune city. The Raigad district is situated very close to these cities. Due to its location, Maharashtra industrial development corporation (MIDC) has set up several industrial estates in Raigad district like petrochemical industry at Nagothane near Roha, fertilizer industry at Thal-Vayshet near Alibag, Hindustan Oil Corporation (HOC) and Reliance Chemical Industries at Rasayani and Patalganga, Natural Gas (ONGC), Bharat Petro Chemicals Ltd (BPCL) and Nhava-Sheva (JNPT) at Uran, etc.

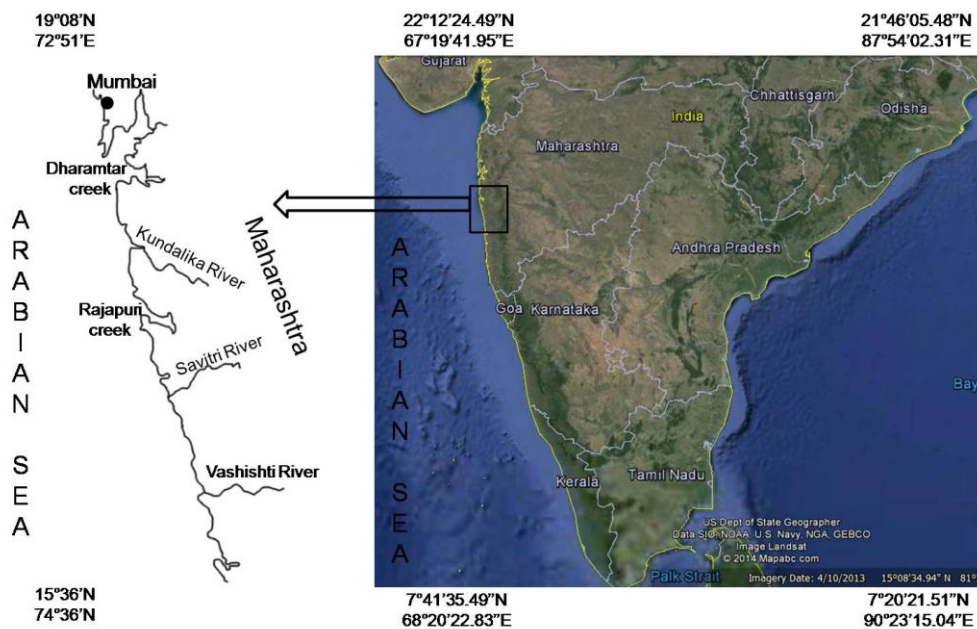


Figure 1.1 Study area map

1.4.2 Dharamtar creek

Dharamtar creek is the confluence of Amba River, Patalganga River and Karanza creek, opening in the southern part of Mumbai harbor. The Dharamtar creek is 9-10 m deep, 1 km wide near its mouth and accessible by small boats during high tide (Kulkarni et al 2011). The creek is substantially crisscrossed with many sub-creeks and channels.

The Amba River forms a major estuarine system of Dharamtar creek. The river originates from the mountain range of Sahyadri, follows a narrow and meandering course of over 140 km before opening finally into Dharamtar

creek (Tiwari and Nair 2002). The basin perimeter of Amba River is 164.96 km and basin area is 570.58 km² (Shindikar 2006). The catchment area of river is 740 km² and average annual rainfall is 3050 mm. The estuary is shallow with average depth of 3 m during an average tide and 2.6 km wide near its mouth during spring tide (Kumar and Sarma 1991; Paulinose et al 2004). The lower estuary is characterized by high and variable suspended load due to dispersion of bed sediment in the water column as a result of strong tidal current. The estuarine limits of Amba vary considerably with the flood and ebb tides. A bund in the river at Bandhara gate controls the flow of freshwater into the tidal waters during the monsoon period (Paulinose et al 2004). The high river discharge during the monsoons completely flushes out even the traces of sea water in the inner estuary. Mangroves mainly *Avicenia marina*, *A. alba* and *Sonneratia* species occur in fringes as well as in large patches surrounding the mudflats (Kulkarni et al 2011). The estuary receives substantial amount of waste water from a petrochemical complex and other industries that opens into Dharamtar creek (Ram et al 2009). The river is not only the main source of water supply for industries located on its bank but also used for drinking purpose to nearby cities and villages. The physicochemical properties in the water column of Amba estuary ranges from 24-33.6°C temperature, 7.5-8.3 pH, 0.1-38 salinity, 3-5.3 ml⁻¹ dissolved oxygen and 0.2-5.3 ml⁻¹ biological oxygen demand (Tiwari and Nair 2002; Kulkarni et al 2011). The Amba estuary opens into Dharamtar creek and latter joins the Thane creek-Mumbai harbour complex. The rate of sedimentation of Thane creek-Mumbai harbour complex varies from 0.73 to 1.94 cm/year (Sharma et al 1994) which is comparable with 0.24 to 2.72 cm/year of thane creek (Fernandes 2011).

1.4.3 Kundalika estuary

Kundalika is one of the major rivers along the central west coast of India that originates in the Sahyadris at an altitude of 820 m near Hirdewadi and meets the Arabian Sea near Revdanda in Raigad district of Maharashtra. Towards its north Amba River catchment and in its south Savitri River basin is situated. The important towns located on the banks of Kundalika are Kolad, Roha and Salav. The river is fed by the excess water released from Tata

Power's Mulshi Dam and other dams, including Ravalje, Bhira and Dholvan. The total length of the river is 67.9 km. The basin perimeter of Kundalika River is approximately 166.96 km and basin area is 489.44 km² (Shindikar 2006). The catchment area of river is 825 km² and average annual rainfall is 3143 mm. The width of the channel increases considerably from upper to lower reaches where it meets the Arabian Sea. The soil is of an alluvial type rich in phosphorous, manganese and copper (Shindikar 2006). Kundalika is a tide-dominated estuary. The spring tidal range decreases considerably from lower to middle estuary (Dineshkumar et al 2001). The highest tide near Revdanda is 4.12 m (Chauhan et al 2004). However, neap tides show only a small decrease. The limit of tidal flooding is 30 km approximately. The physicochemical properties in the water column of Kundalika estuary ranges from 7.1-7.9 pH, 20.1-32.8 salinity, 4.9-7.3 ml⁻¹ dissolved oxygen and 1.5-12.4 ml⁻¹ biological oxygen demand (Inamdar 2010). The middle region of Kundalika Estuary is an ideal sink for suspended sediment matter. Mangrove species from genera like *Acanthus*, *Avicennia* and *Rhizophora* form the dominant vegetation in upper tidal flats of Kundalika River. Maharashtra industrial development corporation (MIDC) has set up several chemical industries at Dhatav- Roha located in the middle region of Kundalika Estuary. These industries discharge their effluents directly into the river without any treatment (Maharashtra Pollution Control Board 2004–2005). Large quantity of river water is consumed by industries, including RCF's THAL Project and many MIDC situated all along the river.

1.4.4 Rajapuri creek

Rajapuri creek lies along the west coast of India in Raigad district of Maharashtra. The creek is fed by Mandad River which originates in Western Ghats follows a meandering course and opens in Rajapuri creek. The total length of the river is 24.99 km. The basin perimeter of Mandad River is 92.69 km and basin area is 166.92 km² (Shindikar 2006). The river length from Mandad to Rajapuri is 14 km. The catchment area of Rajapuri creek is covered by forest land and agricultural area. Mandad River receives effluents from domestic, urban and other diffuse sources as the river passes through the cities. Several industries located in the coastal areas of Arabian Sea are

discharging untreated or semi-treated effluents into the creek (Maharashtra Pollution Control Board 2004-2005). The physicochemical properties in the water column of Rajapuri creek ranges from 25.2-30.2°C temperature, 7.6-8.3 pH, 35.1-36.8 salinity, 17-193 ml^{-1} suspended solid, 3.5-4.6 ml^{-1} dissolved oxygen and 0.5-3.0 ml^{-1} biological oxygen demand (Gajbhiye et al 1995). The biological characteristics of Rajapuri creek ranges from 0.5-13.4 mgm^{-3} chlorophyll a, 0.1-8.1 mgm^{-3} phaeophytin, 0.5-120.3 $\text{mg}(100\text{m}^3)^{-1}$ zooplankton biomass, 1.6-150.7 zooplankton population (no. $\cdot 10^3 \cdot 100 \text{m}^3)^{-1}$, 9-20 zooplankton total groups (no.), 0.5-52.9 macrobenthos biomass (gm^{-2} wet wt.), 713-6076 population (no. m^{-2}) and 2-9 total group (no.) (Gajbhiye et al 1995).

1.4.5 Savitri estuary

Savitri River originates in Mahabaleshwar and flows through Raigad district and eventually meets Arabian Sea at Harehareshwar. It passes through Poladpur, Mahad, Mangaon and Shrivardhan taluks. The total length of river is 97.47 km. The basin perimeter of Savitri River is 267.44 km and basin area is 1445.91 km^2 (Shindikar 2006). The catchment area of river is 2889 km^2 and average annual rainfall is 3493 mm. The major tributaries of Savitri River are Gandari River, Ghod nala, Kal nadi, Negeshri nadi. There are three major industrial estates developed by Maharashtra industrial development corporation (MIDC), of which one is the MIDC Mahad, located in the catchment area of the Savitri River basin. Mainly chemical industries like pharmaceutical, pesticide, dye and dye intermediate are located in Mahad industrial area that discharges large quantities of waste water in to the river (Lokhande et al 2009). Sewage of Mahad city is also discharged into the river. The water from this river is used by the industries and people from nearby villages for their daily needs. pH in the water column of Savitri estuary ranges from 7.42 to 7.65 (Yardi et al 2012).

1.4.6 Vashishti estuary

The river originates in the Western Ghats and drains to the Arabian Sea. The riverine flow is regulated by water released from the hydal power station at Popheli and varies between 32 and 108 m^3s^{-1} with an average of 80 m^3s^{-1} (Zingde et al 1995). The Jog River is the main tributary of the Vashishti.

Kolkiwadi Dam, near Alore has a vast reservoir which feeds the tributary of the river. The town of Chiplun lies on the banks of Vashishti. The total length of river is 87.41 km. The basin perimeter of Vashishti River is 254.94 km and basin area is 1393.62 km² (Shindikar 2006). The catchment area of river is 2238 km² and average annual rainfall is 3391 mm. The tidal range is between 2 to 3.3 m for spring tide and 0.7 to 0.9 m for neap tide (Zingde et al 1995). The estuarine mouth is shallow due to sand bar. The freshwater influx during monsoons results in excellent flushing of the estuarine system (Nair et al 1998). pH in the water column of Vashishti estuary ranges from 7 to 7.7 (Zingde et al 1995). The biological characteristics of Vashishti estuary ranges from 1.4-4.8 mgm⁻³ chlorophyll a, 52.8-129.7 mgCm⁻³h⁻¹ primary productivity, 0.2-28.4 ml/100m³ zooplankton biomass, 821-89481 zooplankton population (no./100 m³), 3-12 zooplankton groups (no.), 0.3-17.5 macrobenthos biomass (g/m²wet wt.) and 3-7 macrobenthic group (no.) (Nair et al 1998). MIDC has set up chemical industries at Lote Parshuram about 12 km from Chiplun.

Chapter II

METHODOLOGY

2.1 Introduction

To achieve the objectives of the study detailed in chapter 1, carefully chosen sampling and analytical techniques were implemented to eliminate sampling errors and biases. The methodology comprises of a systematic set of procedures including field survey, sediment core collection, laboratory analysis and data computations. The details of the methodological approach are described below in figure 2.1.

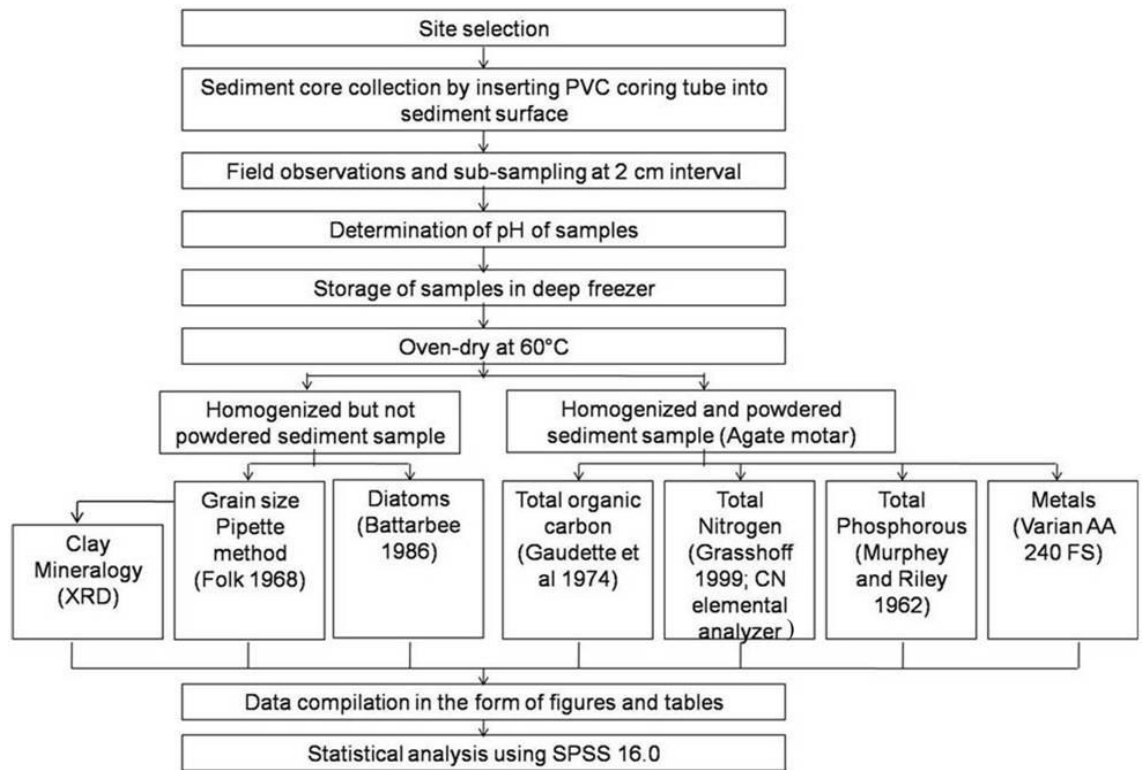


Figure 2.1 Sampling and sample processing techniques

2.2 Field studies and sampling

The sampling was carried out in the month of December (2008) and January (2010) along the major rivers of Raigad district and in one of the main rivers of Ratnagiri district in Maharashtra. During the first phase of sampling total of 17 cores from Vasishti, Savitri, Rajapuri and Kundalika Rivers were collected while the second phase comprise of total 3 cores from Amba River and Dharamtar creek. The sampling positions were located by hand held global positioning system (GPS).

2.2.1 Location of sampling area

The location of sampling area is shown in figure 2.2. The sampling sites were located mainly in lower and middle estuarine regions. These sites differ from each other with respect to tidal settings and distance from the mouth of estuary.

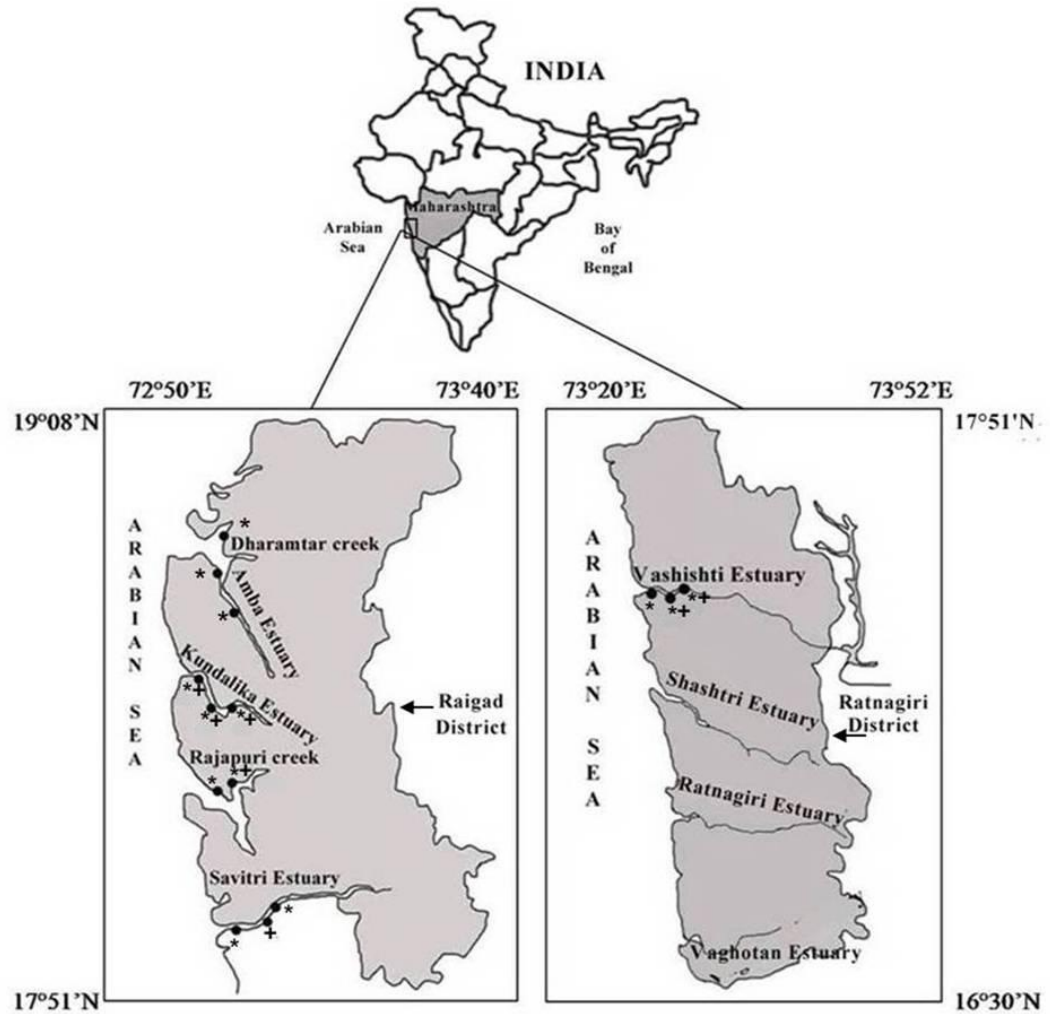


Figure 2.2 Study area map with sampling locations (filled circles) .

* Mudflat core + Mangrove core

2.2.2 Collection of sediment cores

Total of 20 cores were collected using pre-cleaned acid washed PVC coring tube of 2 m length and 63 mm diameter. The hand driven coring tube was inserted gently into the exposed sediment surface during low tide then pushed to ensure that it reached the maximum depth and slowly retrieved back. The length and colour was noted immediately after core collection. Cores were sub-sampled at an interval of 2 cm with a plastic knife. The samples were placed in clean labeled plastic bags, stored in ice-box and transported to the laboratory. Care was taken to avoid any contamination of samples. The core length varied from 46 to 108 cm due to nature of substratum. The details of sampling and field observations are shown in table 2.1.

S.No	River	Sampling Location	Station code	Latitude	Longitude	Sub-environment	Core length (cm)	No. of sub-samples	Color	
									Length	Color
1	Amba	Dharamtar Bridge	S-2	18°41'47.6"N	73°01'45.6"E	Mudflats	82	41	0-25 cm 25-80 cm	Light Grey Dark Grey
			2	Dharamtar creek	Revas	S-3	18°48'13.5"N	72°56'47.2"E	Mudflats	46
		Karanza			S-1	18°52'27.4"N	72°59'55.9"E	Mudflats	60	30
		3	Kundalika Estuary	Salav	S-62	18°32'20.76"N	73°56'11.41"E	Mudflats	66	33
Salav	S-47			18°32'18.26"N	72°56'12.30"E	Mangroves	82	41	0-82 cm	Uniform Brown
Kopri	S-63			18°27'41.56"N	73°00'19.86"E	Mudflats	66	33	0-9 cm 10-6 cm	Brown Mixed Black Brown
Kopri	S-42			18°27'41.61"N	73°00'18.71"E	Mangroves	84	42	0-84 cm	Uniform Brown
Gophan	S-45			18°28'29.14"N	73°01'48.01"E	Mudflats	66	33	0-66 cm	Uniform Grey
Gophan	S-40			18°28'26.86"N	73°01'48.22"E	Mangroves	80	40	0-80 cm	Uniform Grey
4	Rajapuri creek	Chinchghar	S-60	18°16'55.39"N	73°00'30.59"E	Mudflats	98	49	0-39 cm 39-98cm	Light Grey Dark Grey
		Khajni	S-61	18°18'5.47"N	73° 2'31.47"E	Mudflats	74	37	0-30 cm 30-74 cm	Light Grey Dark Grey
		Khajni	S-65	18°18'7.09"N	73° 2'25.56"E	Mangroves	80	40	0-12cm 12-80 cm	Brown Dark Grey
5	Savitri Estuary	Vesvi	S-18	17°59'4.54"N	73° 3'53.18"E	Mudflats	100	50	0-100 cm	Uniform Brown
		Veral	S-21	17°58'54.85"N	73° 3'51.79"E	Mangroves	90	45	0-25 cm 25-78 cm	Brown Grey Black
		Panderi	S-41	18° 1'58.10"N	73° 9'15.97"E	Mudflats	78	39	0-14 cm 14-78 cm	Brown Grey
6	Vashishti Estuary	Dhopave	S-7	17°34'59.8"N	73°11'36.3"E	Mudflats	102	51	0-102 cm	Uniform Grey
		Telewadi	S-10	17°35'13.13"N	73°12'41.05"E	Mudflats	108	52	0-108 cm	Uniform Brown
		Telewadi	S-20	17°35'6.84"N	73°12'40.73"E	Mangroves	78	39	0-78 cm	Uniform Brown
		Sakhari Bandar	S-16	17°34'56.86"N	73°13'22.26"E	Mudflats	82	41	0-82 cm	Uniform Brown
		Sakhari Bandar	S-15	17°34'54.33"N	73°13'20.34"E	Mangroves	80	40	0-5 cm 5-80 cm	Brown Mixed Black Brown
Total 20 cores			Mudflat core = 13 Mangrove core = 7				Number of sub-samples = 799			

Some of the photographs taken during the field work are shown below in figure 2.3a-d.



Figure 2.3a-d Photographs depicting field work and sampling

2.3 Laboratory procedures and analysis

pH was measured soon after the samples reached the laboratory. Then the samples were stored in deep freezer until further analysis.

The sediment samples were dried in oven at 60°C for 48 hours. Part of the dried sediments were homogenized and ground to fine powder using agate mortar and pestle kept in pre-cleaned vials for the analysis of total organic carbon (TOC), total nitrogen (TN), total phosphorous (TP) and selected metals (Fe, Mn, Al, Ni, Cr, Co, Zn and Pb), while the other un-powdered part of sediment was used for the analysis of sediment components (sand, silt and clay), clay minerals and fossil diatoms. All the reagents used were of analytical grade. Instruments were calibrated prior to analysis. The glasswares and teflon beakers were thoroughly washed with chromic acid, rinsed in double distilled deionized water (milli Q) and completely dried in oven at 60°C. Double distilled deionized water (milli Q) was used throughout the experiments.

2.3.1 pH

The pH was analyzed using pH meter (Thermo Orion 420 A+ model). To check its accuracy, pH meter was calibrated with standard buffers of pH 4.0, 7.0 and 9.2 with regular interval.

2.3.2 Sediment components

The analysis of sediment components i.e sand, silt and clay was carried out by using Pipette method detailed by Folk (1968). Accordingly, around 10 grams of homogenized, not powdered sediment was taken in 1000 ml beaker with milli Q water. After 24 hours when sediment was settled, the water was decanted by using decanting pipe up to approximately 300 ml of water remaining in the beaker. The solution was made up to 1000 ml with milli Q water. The process of decantation was repeated 5 to 6 times to remove salinity. After decanting, the sample was treated with 10 ml of 10% sodium hexametaphosphate to dissociate the clay particles and after 24 hours, 5 ml of 30% of hydrogen per oxide (H_2O_2) was added to oxidize the organic matter. Next day, the solution was passed through a 63 micron sieve attached through funnel to 1000 ml cylinder. The sieve was washed with milli Q water till a 1000 ml mark was reached. The contents of sieve (>63 micron) representing sand fraction was transferred to a pre-weighed 100 ml beaker

and kept in oven for drying. The solution in the 1000 ml cylinder was stirred homogenously for about 2 minutes by using a stirrer and the stirring time was noted. The solution was allowed to settle at room temperature. At specified time calculated by referring table 2.2, 25 ml of the solution was pipetted out at 8 Ø by inserting pipette up to 10 cm in the cylinder. The solution representing clay fraction (<2 micron) was transferred to pre-weighed 100 ml beaker and kept in oven for drying. After drying, the weight of beakers with sand and clay fraction was noted.

Calculation: The sand, silt and clay percentages were calculated by applying the following formula

Sand:

Weight of sand = (Weight of sand + beaker) – (Weight of empty beaker)

Sand % = (Weight of sand / Total amount of sediment taken in 1000 ml beaker) * 100

Clay:

Weight of clay = [(Weight of clay + beaker) – (Weight of empty beaker) * 1000/25] -1

Clay % = (Weight of clay / Total amount of sediment taken in 1000 ml beaker) * 100

Silt:

Silt (%) = 100 - (sand % + clay %)

Table 2.2 Time schedule used for pipette analysis

Size Ø	Depth to which pipette was inserted (cm)	Time after which water was pipetted out				
		Hours: Minutes: Seconds				
		28°C	29°C	30°C	31°C	32°C
4	20	0:00:48	0:00:46	0:00:46	0:00:44	0:00:44
5	10	0:01:36	0:01:34	0:01:32	0:01:29	0:01:28
6	10	0:06:25	0:06:15	0:06:06	0:06:57	0:05:52
7	10	0:25:40	0:25:02	0:24:25	0:24:49	0:23:27
8	10	1:42:45	1:40:13	0:37:42	1:37:15	0:33:51
9	10	6:30:00	6:40:40	6:32:50	6:32:10	6:11:30
10	10	27:06:00	26:30:00	-	-	-

2.3.3 Clay mineralogy

The mineralogical composition was determined on the clay fraction (<2 micron) obtained by wet sieving Pipette method. After stirring the solution homogenously, the solution was allowed to settle. At specified time calculated by referring table 2.2 for 9 Ø, the solution was pipetted out up to 10 cm in a 500 ml beaker. 5 ml of acetic acid and 10 ml of hydrogen peroxide (H₂O₂) was added to remove carbonates and organic matter respectively. After treating the sample, solution was allowed to settle. The water was decanted 6 – 8 times at an interval of 24 hours to ensure that clay was free from excess of reagents that were added earlier. Slides for clay minerals were prepared by pipetting 1 ml of the clay and spreading uniformly over pre-labeled slide. The slides were allowed to dry at room temperature. The air dried slides were exposed to ethylene glycol for 1 hour at 100°C. The slides were scanned from 3° to 30° at 2/3° 2 theta on a Philips X-ray diffractometer (PW 1840 model) using Nickel filtered Cu-K, radiation equipped with an automatic divergent slit. The minerals were identified using procedures outlined by Brindley and Brown (1980). Following the semi-quantitative method (Biscaye 1965), the weighted peak area percentages of the major clay minerals were calculated from the X-ray diffractograms of the glycolated samples (Rao and Rao 1995).

2.3.4 Total organic carbon (TOC)

Total organic carbon was estimated following the method given by Gaudette et al (1974) which involves exothermic heating and oxidation with K₂Cr₂O₇ and concentrated H₂SO₄ followed by titration of excess dichromate with 0.5 N Fe(NH₄)₂(SO₄)₂·6H₂O. The procedure involves, 0.5 g of finely ground sediment sample was treated with 10 ml of standard K₂Cr₂O₇ and 20 ml of concentrated H₂SO₄ with silver sulphate (Ag₂SO₄) in 500 ml conical flask. Silver sulfate was used to prevent the oxidation of chloride ions. The conical flask was gently rotated for about 1 minute so that the solution was well mixed. The solution was allowed to stand for 30 minutes. After 30 minutes, 200 ml of milli Q, 10 ml of 85% phosphoric acid and 0.2 g of sodium fluoride was added. The solution was then titrated with standard ferrous ammonium sulphate using diphenylamine as an indicator to a one drop end point of

brilliant green. For standard, a blank without sediment was followed with procedure mentioned above. Dextrose was taken as a reference standard for the determination of organic carbon.

Calculation

$$\text{Organic carbon (\%)} = 10 (1-T/S) * F$$

where,

S = Standardization blank titration, ml of ferrous solution

T = Sample titration, ml of ferrous solution

F = Factor which is derived as follows:

$$F = (1.0 \text{ N}) * 12/4000 * 100/\text{Sample weight}$$

= 0.6 when sample weight is exactly 0.5 g

where,

$$12/4000 = \text{m. eq. wt. carbon}$$

2.3.5 Total nitrogen (TN)

Total nitrogen was determined by two methods namely one detailed by Grasshoff (1999) and other using nitrogen carbon soil elemental analyzer. In the first method, 1 g of finely ground sediment sample was autoclaved in an oxidation flask with a mixture of potassium persulfate and boric acid in sodium hydroxide solution for 30 minutes. The solution was allowed to cool. 1 ml of this solution was made up to 50 ml by adding milli Q water. This was then passed through a cadmium reductor column and analyzed for total nitrogen as diazo dye measured at 543 nm with spectrophotometer. The standard was prepared with reagents potassium nitrate, sulphanyl amide and alpha naphthyl amine hydrochloride following the procedure mentioned above. In the second method, 12-14 mg of finely ground sediment sample packed in tin capsule was used to determine total nitrogen in an elemental analyzer (FLASH 2000 Organic Elemental analyzer). Recalibration check was performed at regular intervals. Together with the samples, natural sediment certified standards were run to test the analytical and instrument accuracy of the method. The precision of this method based on replicate measurements of a reference standard was 0.005% for nitrogen.

2.3.6 Total phosphorous (TP)

The analysis of total phosphorous was done by following the standard procedure given by Murphy and Riley (1962). This procedure is based on the reaction of orthophosphate ions with an acidified molybdate reagent to form a phosphomolybdenum complex which is reduced with ascorbic acid to form molybdenum blue in the presence of potassium antimony tartarate. The total phosphorous was determined on the digested samples obtained by procedure followed for total nitrogen. 5 ml of digested mixture was made up to 50 ml by adding milli Q water with 1 ml of mixed reagent (ammonium molybdate solution + H₂SO₄ + potassium antimony tartarate) and 1 ml of ascorbic acid was added to the solution. The solution was thoroughly mixed. The absorbance was measured at 880 nm against a blank using spectrophotometer. The standard reagent was prepared with potassium dihydrogen orthophosphate following the procedure mentioned above.

2.3.7 Digestion of sediments

0.2 g of finely ground powdered sediment was transferred in a Teflon beaker and treated with 10 ml of HF, HNO₃ and HClO₄ (ratio 7:3:1) on the hot plate at 150°C. After drying, 5 ml of the same above mixture was added, then after 1 hour, 2 ml of concentrated HCl was added and allowed to dry completely. The dried mixture was treated with 10 ml of 1:1 HNO₃. After the clear solution was obtained the solution was transferred to polypropylene volumetric flasks and the solution was made up to 50 ml with milli Q water (Jarvis and Jarvis 1985). Together with sediment samples, certified sediment (BCSS-1) was digested using the same procedure to test and maintain the accuracy of dataset.

2.3.8 Metal analysis

The digested sediment samples were analyzed for elemental concentration by using Varian AA 240 FS flame Atomic Absorption Spectrometry (AAS) with an air/acetylene flame for all the elements (Fe, Mn, Ni, Cr, Co, Zn and Pb) except for Al for which nitrous oxide/acetylene flame was employed at specific wavelength. The accuracy was checked at regular intervals. The recoveries were between 86-91% for Fe, Ni and Al; 87-92% for Mn and Co; 80-85% for Pb and Zn; 90-95% for Cr, with a precision of ±6% standard deviation. Precision was calculated by analyzing certified reference standard

from the Canadian National Bureau of Standards (BCSS-1) together with the some selected samples in triplicates.

2.3.9 Diatoms

The homogenized and not powdered sediment samples were used for diatom isolation using the method described by Battarbee (1986), in which ~0.5–1.0 gram of the sediment was heated with 30% H₂O₂ and 10% HCl to remove organic matter and carbonates, respectively. After treating sediment with acids, samples were washed by using Milli Q water and 6-8 decantations were applied. Clay was removed in the final wash by adding few drops of 1% weak ammonia solution. A small quantity of the sample (0.2 ml) was poured over a cover slip and left to evaporate. These cover slips were subsequently mounted onto the glass slide using Canada balsam as a mounting medium. Diatoms were identified and counted by using an Olympus light microscope Normanski optics, under 1000x magnification in oil immersion lens. A minimum of 200-300 complete diatom valves were counted for each sample. The identification of diatoms was done using the identification keys (Desikachary 1986-1989; Gonzalves and Gandhi 1952-1954; Mishra 1956). A flowchart representing the procedure followed for diatoms is shown in figure 2.4.

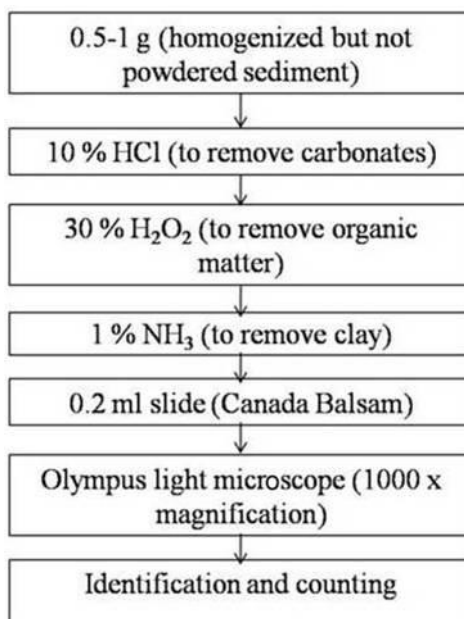


Figure 2.4 Procedure followed for diatom analysis after Battarbee (1986)

2.4 Data processing

The software Excel and C2 were used for computations and plotting graphs of different parameters. Different statistical analysis namely Pearson correlation coefficient, Varimax R-mode factor analysis and ANOVA t-test were performed on SPSS for analyzing large dataset. Only significant values ($p < 0.01$ and $p < 0.05$) are reported in the thesis.

To distinguish between anthropogenic and natural input of trace metals, enrichment factor (EF) was used as an index, which is obtained from metal to aluminum ratio in the sample divided by the background metal/aluminum ratio (Seshan et al 2012; Xia et al 2012). It is expressed mathematically as

$$EF = [(M/Al)_{\text{sediment}} / (Me/Al)_{\text{shale}}]$$

where $(M/Al)_{\text{sediment}}$ is the metal to Al ratio in the samples of interest and $(Me/Al)_{\text{shale}}$ is the metal to Al ratio in average shale (Turekian and Wedepohl 1961). If EF value is between 0.5 and 1.5, it suggests natural input and if EF value is greater than 1.5, it suggest anthropogenic input of metals (Sarkar et al 2011; Zhang and Liu 2002). Further, to evaluate the level of pollution in sediments, the index of geo-accumulation using the formula of Muller (1979) was used and is given below

$$I_{geo} = \log_2 C_n / 1.5 * B_n$$

Where, I_{geo} is Index of geo-accumulation, C_n is measured concentration of an element “ n ” and B_n is element content in “average shale” (Turekian and Wedepohl 1961) and the factor 1.5 is used because of possible variation of the background data due to lithogenic effects. Muller (1979) classified the level of pollution into seven classes based upon Index of geo-accumulation (I_{geo}) values viz “very strongly polluted” - I_{geo} class 6 ($I_{geo} > 5$); “Strong to very strong” - I_{geo} class 5 (I_{geo} 4-5); “Strongly polluted” - I_{geo} class 4 (I_{geo} 3-4); “Moderately to strongly polluted” - I_{geo} class 3 (I_{geo} 2-3); “Moderately polluted” - I_{geo} class 2 (I_{geo} 1-2); “Unpolluted to moderately polluted” - I_{geo} class 1 (I_{geo} 0-1) and “Unpolluted” - I_{geo} class 0 ($I_{geo} < 0$).

Chapter III

RESULT AND DISCUSSION

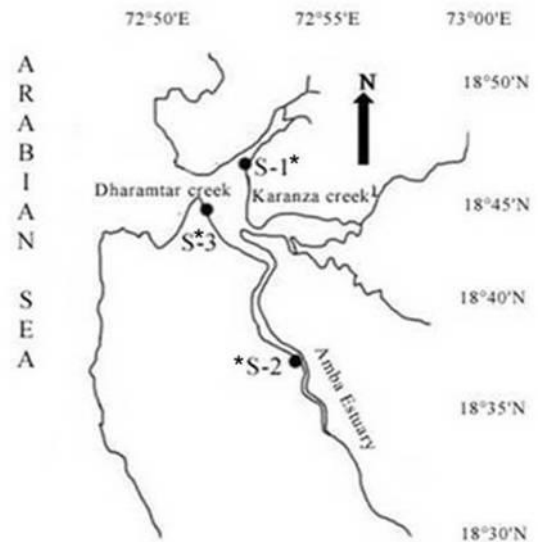


Figure 3.1 Study area map with core location. *Mudflat core

3.1 Dharamtar creek

3.1.1 Collection of sediment core

Total three sediment cores (S-1, S-2 and S-3) were collected from intertidal mudflats of Dharamtar creek (Figure 3.1). The core S-1 and S-3 were located near the mouth of Karanza and Dharamtar creek respectively while core S-2 was located from the middle estuarine region of Amba estuary (Figure 3.1). The core length varied from 46 to 82 cm. S-1, S-2 and S-3 were analyzed for sediment grain size, total organic carbon (TOC) and pH; S-2 and S-3 were further analyzed for total nitrogen (TN), total phosphorous (TP) and metals while selected samples of core S-2 were studied for fossil diatoms.

3.1.2 Colour

The colour variations between light grey and dark grey to black were seen visually. The sediment was light grey from 0 to 25 cm in core S-2, 0 to 46 cm in core S-3 and 0 to 30 cm in core S-1. The remaining part of core S-1 and S-2 was dark grey to black.

3.1.3 Sediment grain size

The data showed a range of 1.54 to 23.66% with a mean of 7.87% sand, 26.8 to 55.34% with a mean of 34.09% silt, 40.64 to 67.64% with a mean of 58.04% clay for core S-2; 0.42 to 2.76% with a mean of 1.08% sand, 41.57 to 65.15% with a mean of 52.39% silt and 33.96 to 57.76% with a mean of

46.53% clay for core S-3 and 0.09 to 21.9% with a mean of 3.3% sand, 13.4 to 50.92% with a mean of 34.17% silt and 43.24 to 79.96% with a mean of 62.52% clay for core S-1. Each core has been divided into three zones depending upon the distribution pattern of sediment components namely zone 1, 2 and 3 wherein zone 3 represents recent sediments. The mean and standard deviation of sediment grain size in each zone for cores S-2, S-3 and S-1 are given in table 3.1.

Table 3.1 Mean and standard deviation (values in parenthesis) of different parameters in each zone for core S-2, S-3 and S-1. The p-value denotes results of one-way ANOVA statistically significant at p<0.05. n=number of samples.

Core S-2				
	Zone 1 (82-60 cm) n=12	Zone 2 (60-42 cm) n=10	Zone 3 (42-0 cm) n=21	p value (*statistical significant at p<0.05)
	Mean (Standard deviation)	Mean (Standard deviation)	Mean (Standard deviation)	
Sand (%)	14.50 (±5.35)	8.55 (±7.13)	4.25 (±4.22)	0.00*
Silt (%)	31.20 (±3.49)	33.77 (±3.4)	36.01 (±5.84)	0.03*
Clay (%)	54.30 (±7.92)	57.68 (7.73)	59.74 (±5.15)	0.09
TOC (%)	1.29 (±0.36)	1.52 (0.23)	1.71 (±0.21)	0.00*
TN (%)	0.08 (±0.03)	0.11 (±0.03)	0.13 (±0.03)	0.00*
TP (%)	0.02 (±0.01)	0.03 (±0.01)	0.03 (±0.00)	0.00*
C/N	18.37 (±11.12)	15.05 (±5.89)	14.08 (±4.69)	0.27
pH	7.69 (±0.10)	7.76 (±0.20)	7.74 (±0.24)	0.66
Fe (%)	7.66 (±0.48)	7.56 (±0.27)	7.57 (±0.26)	0.75
Mn (ppm)	834.50 (±58.53)	814.10 (±55.49)	766.44 (±36.92)	0.00*
Al (%)	7.89 (±0.42)	8.44 (±0.31)	8.32 (±0.20)	0.00*
Ni (ppm)	94.14 (±7.80)	91.93 (±9.8)	97.60 (±6.98)	0.16
Cr (ppm)	265.97 (±29.55)	240.30 (±11.90)	233.76 (±29.69)	0.00*
Co (ppm)	71.03 (±3.27)	71.33 (±3.90)	69.97 (±3.42)	0.53
Zn (ppm)	118.03 (±5.30)	118.43 (±6.91)	151.65 (±25.21)	0.00*
Pb (ppm)	63.75 (±12.76)	85.40 (±16.10)	102.22 (±17.25)	0.00*
Core S-3				
	Zone 1(46-28 cm) n=10	Zone 2 (28-6 cm) n=12	Zone 3 (6-0 cm) n=3	p value (*statistical significant at p<0.05)
	Mean (Standard deviation)	Mean (Standard deviation)	Mean (Standard deviation)	
Sand (%)	1.26 (±0.66)	0.79 (±0.19)	1.43 (±0.66)	0.04*
Silt (%)	52.87 (±4.26)	50.66 (±6.34)	52.51 (±10.11)	0.68
Clay (%)	45.86 (±4.79)	48.55 (±6.44)	46.07 (±10.75)	0.59
TOC (%)	1.87 (±0.13)	1.59 (±0.16)	1.00 (±0.34)	0.00*
TN (%)	0.06 (±0.02)	0.03 (±0.02)	0.03 (±0.01)	0.01*
TP (%)	0.04 (±0.01)	0.04 (±0.00)	0.03 (±0.01)	0.08
C/N	35.40 (±10.76)	58.70 (±22.5)	38.20 (±26.60)	0.03*
pH	7.97 (±0.09)	7.87 (±0.09)	7.36 (±0.41)	0.00*
Fe (%)	8.49 (±0.49)	8.36 (±0.46)	8.90 (±0.35)	0.21
Mn (ppm)	769.67 (±44.19)	680.22 (±34.33)	775.11 (±8.86)	0.00*
Al (%)	9.36 (±0.33)	9.59 (±0.26)	9.13 (±1.15)	0.24
Ni (ppm)	98.97 (±7.35)	102.39 (±8.34)	119.67 (±8.08)	0.00*
Cr (ppm)	241.30 (±5.72)	232.83 (±9.42)	261.78 (±11.34)	0.00*
Co (ppm)	58.17 (±2.66)	52.81 (±2.64)	50.11 (±3.29)	0.00*
Zn (ppm)	135.53 (±4.46)	131.53 (±4.79)	133.89 (±1.95)	0.13
Pb (ppm)	53.97 (±27.09)	74.50 (±16.82)	95.89 (±21.47)	0.02*
Core S-1				
	Zone 1 (60-32 cm) n=15	Zone 2 (32-12 cm) n=11	Zone 3 (12-0 cm) n=6	
	Mean (Standard deviation)	Mean (Standard deviation)	Mean (Standard deviation)	
Sand (%)	1.0527 (±1.35)	7.27 (±5.82)	0.75 (±0.74)	
Silt (%)	38.6327 (±8.15)	29.89 (±7.65)	29.028 (±7.44)	
Clay (%)	60.3147 (±8.86)	62.83 (±6.33)	70.22 (±8.01)	
TOC (%)	1.6757 (±0.26)	1.63 (±0.14)	1.90 (±0.11)	
pH	7.3707 (±0.27)	7.16 (±0.35)	6.83 (±0.21)	

In the core S-2 collected from the middle estuarine region of Amba estuary, in zone 1, sand showed relatively higher values with gradual decrease from 82 to 74 cm and gradual increase from 74 to 60 cm (Figure 3.1.1). Clay displayed greater fluctuations and compensated both silt and sand distribution. In zone 2, silt varies around its average line while clay and sand

compensated each other. This indicates deposition of sediments in phases and fluctuating supply of fine and coarse sediments into the tidal flats (Figure 3.1.1). The strong tidal currents in the study area are responsible for re-suspension and transportation of fine sediments, thus leaving coarser sediment as bed load deposits (Nair and Ramchandran 2002). Alternatively, Amba estuary receives an average of 2100 mm rainfall of which 95% occurs during monsoon period (Paulinose et al 2004). Both varying rainfall and runoff must be responsible for the formation of sediment beds with coarser sediments between finer sediments. In zone 3, sand showed relatively low values except a major peak at 20 cm depth. The distribution of silt and clay largely compensated each other. The major positive peak of silt at 30 cm depth is compensated by major negative peak of clay (Figure 3.1.1).

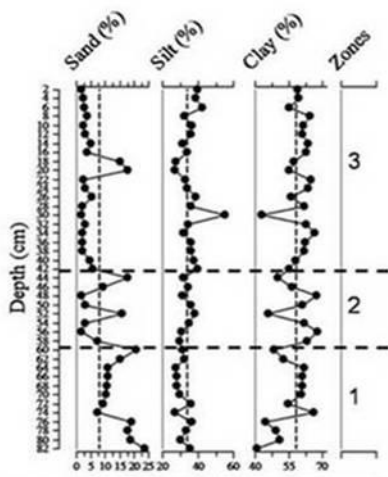


Figure 3.1.1 Down-core variation of sediment grain size in different zones with zone 1 representing bottom while zone 3 represents the top for core S-2. The vertical line represents average value

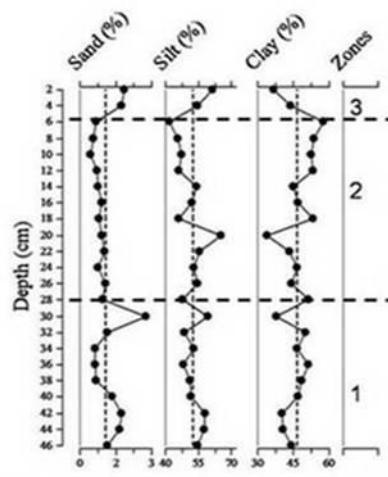


Figure 3.1.2 Down-core variation of sediment grain size in different zones with zone 1 representing bottom while zone 3 represents the top for core S-3. The vertical line represents average value

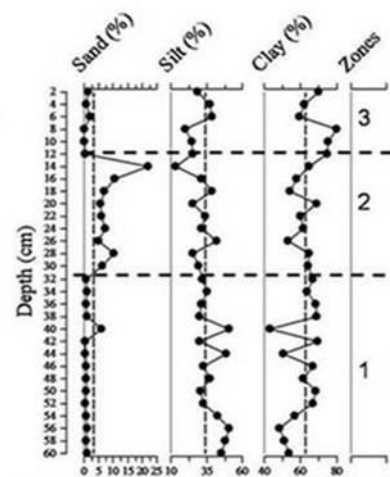


Figure 3.1.3 Down-core variation of sediment grain size in different zones with zone 1 representing bottom while zone 3 represents the top for core S-1. The vertical line represents average value

In the core S-3 collected near the mouth of Dharamtar creek, in zone 1, sand and silt showed nearly similar distribution pattern (Figure 3.1.2). Clay compensated the distribution of both silt and sand. At 30 cm depth, sand and silt showed a major positive peak which is compensated by negative peak of clay. In zone 2, sand and silt showed a gradual decrease with silt displaying larger fluctuations. The decreasing trend of silt is compensated by increasing trend of clay (Figure 3.1.2). In zone 3, sand and silt showed an increasing trend while clay showed a decreasing trend (Figure 3.1.2). The relatively

higher percentage of fine sediments in the lower estuarine region can be attributed to two main reasons, first construction of jetty near Revas Bandar which reduced the tidal flow and second dredging of main channel of the harbor and the dumping of these finer sediments in the adjoining area (Swamy et al 1980).

In zone 1 and 3 of core S-1 collected near the mouth of Karanza creek, sand is nearly constant, silt and clay compensate each other (Figure 3.1.3). In zone 2, sand and clay showed a gradual increase while silt showed a gradual decrease. In zone 3 sand maintains lower than average value.

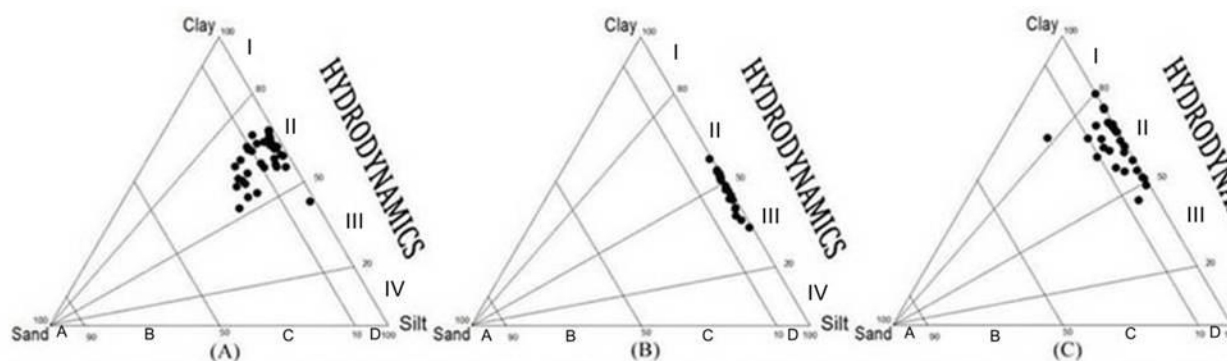


Figure 3.1.4 Ternary diagram for the classification of hydrodynamic conditions after Pejrup (1988) for core S-2 (A), S-3 (B) and S-1 (C)

Further, an attempt has been made to understand the hydrodynamic conditions of depositional environment using ternary diagram proposed by Pejrup (1988). The plot reveals that the core S-1 and S-2 collected from lower and middle estuarine regions respectively falls within section 2, indicating that sediments must have deposited under less violent conditions (Figure 3.1.4). Core S-3 collected from lower estuarine region falls within sections II and III, indicating relatively violent to less violent hydrodynamic condition (Figure 3.1.4). Both S-1 and S-3 collected from the lower estuarine region fall within “D type” indicating presence of poor sand and high concentration of silt and clay components while some samples of core S-2 that fall within “C type” indicating the presence of slightly sand-dominated sediment (Figure 3.1.4).

3.1.4 Nutrients (TOC, TN and TP)

The data showed a range of 0.55 to 2.13% with a mean of 1.56% TOC, 0.02 to 0.18% with a mean of 0.11% TN and 0.013 to 0.04 with a mean of 0.03% TP for core S-2; 0.68 to 2.10% with a mean of 1.63% TOC, 0.01 to 0.1 with a mean of 0.04% TN and 0.02 to 0.04% with a mean of 0.037% TP for core S-3 and 0.91 to 2.02% with a mean of 1.71% TOC for core S-1. The mean and standard deviation of TN, TP and TOC in each zone are given in table 3.1.

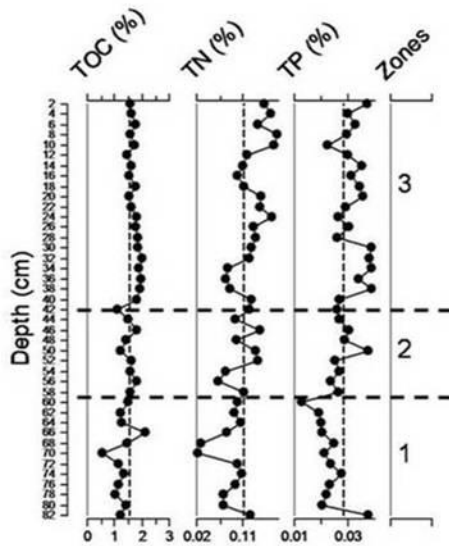


Figure 3.1.5 Down-core variation of total organic carbon (TOC), total nitrogen (TN) and total phosphorous (TP) in different zones with zone 1 representing bottom while zone 3 represents the top for core S-2. The vertical line represents average value

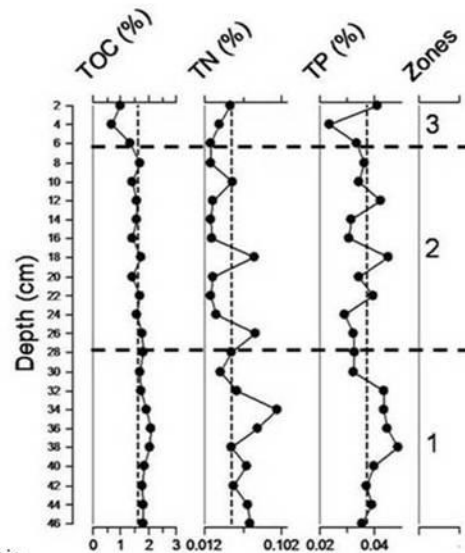


Figure 3.1.6 Down-core variation of total organic carbon (TOC), total nitrogen (TN) and total phosphorous (TP) in different zones with zone 1 representing bottom while zone 3 represents the top for core S-3. The vertical line represents average value

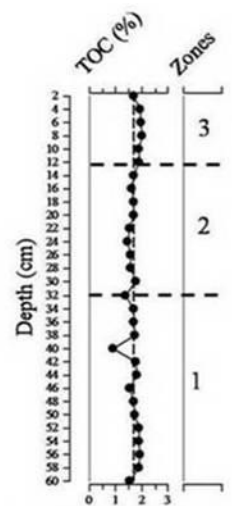


Figure 3.1.7 Down-core variation of total organic carbon (TOC) in different zones with zone 1 representing bottom while zone 3 represents the top for core S-1. The vertical line represents average value

In core S-2 collected from middle estuarine region of Amba estuary TOC, TN and TP showed a gradual increase from zone 1 to zone 3 (Figure 3.1.5). In zone 1 TOC, TN and TP showed relatively low values which may be attributed to poor absorbability of nutrients on negatively charged quartz grains, which predominate in this zone (Sarkar et al 2004) (Figure 3.1.5). In zone 2 TOC, TN and TP fluctuate near their respective average lines, peak value agree with that of clay distribution (Figure 3.1.1, Figure 3.1.5). In zone 3 TOC, TN and TP showed relatively higher values which may be attributed to additional supply of terrestrial organic matter in the recent years (Wahyudi and Minagawa 1997).

In core S-3 collected near the mouth of Dharamtar creek TOC, TN and TP showed a gradual decrease from zone 1 to zone 3 (Figure 3.1.6). The relatively higher values of TOC, TN and TP noted in zone 1 where fine

sediments showed higher corresponding values may therefore be attributed to association with higher surface area of finer particles (Meyers, 1994). In zone 2 and 3 the relatively low TOC, TN and TP may be due to constant flushing activity by tides and waves which mobilizes litter and leaches out organic matter near the mouth (Meyers 1997).

In core S-1 collected near the mouth of Karanza creek, relatively higher TOC coincides with relatively higher silt and clay percentage in zone 1 and 3 respectively (Figure 3.1.7).

3.1.5 C/N ratio

C/N ratio in the present study ranged between 9-49 in core S-2 and 20-97 in core S-3 (Figure 3.1.8). The mean and standard deviation of C/N ratio in each zone for cores S-2 and S-3 are given in table 3.1.

The higher range of C/N ratio noted in core S-3 may be due to deposition of mangrove derived detritus as the site location of core S-3 was surrounded by large extensions of mangroves like *Avicenia marina*, *Avicenia alba* and *Sonneratia apetala* (Kulkarni et al 2011). Earlier studies have reported higher C/N ratio ranging between 24-78 (Rao et al 1994) and 31-66 (Alongi and Christoffersen 1992) for mangrove detritus. Additionally, enhanced decomposition rates of N may also account for higher C/N ratio.

The large variations in C/N ratio noted in core S-3 probably reflects the degree of organic matter preservation (Muller 1977; Waples and Sloan 1980) as core S-3 is located in lower estuarine region which is characterized by dynamic interaction of waves and river water currents (Figure 3.1.8). On the other hand, the lack of such variability in core S-2 may suggest changes in rate of input. For example, higher C/N ratio noted at 72-64 cm in zone 1 where sand showed higher corresponding values suggest deposition of terrestrially derived organic matter (Figure 3.1.8). Similarly, in zone 3, a slight increase in C/N ratio from 42-36 cm followed by slight decrease from 36-0 cm reflects changing source of organic matter where an increase in the C/N ratio may represent greater input of terrestrial organic matter while a

decrease may indicate increasing contribution of marine derived organic matter (Cupery 2011).

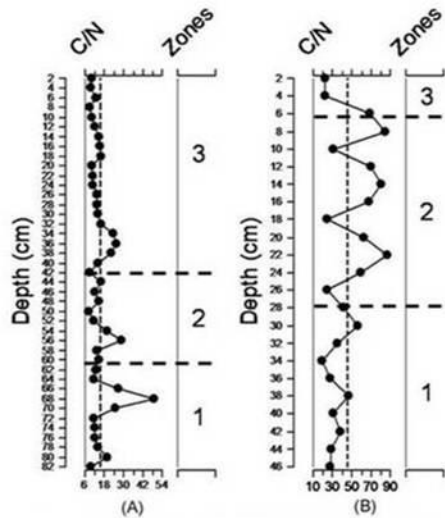


Figure 3.1.8 Down-core variation of C/N ratio in different zones with zone 1 representing bottom while zone 3 represents the top for core S-2 (A) and S-3 (B). The vertical line represents average value

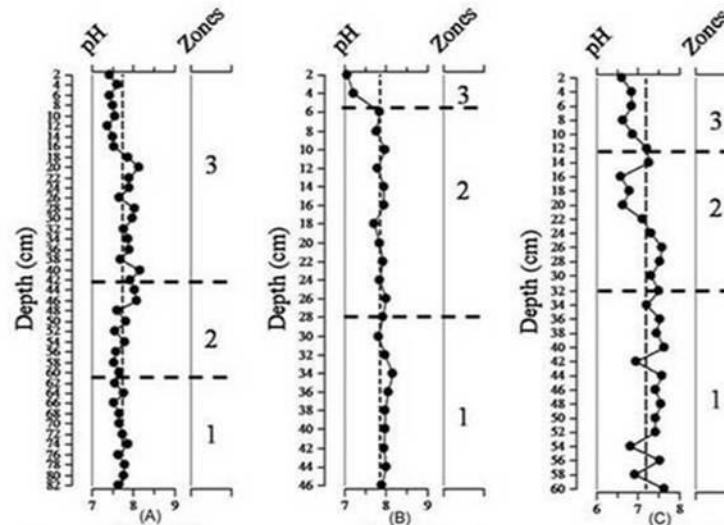


Figure 3.1.9 Down-core variation of pH in different zones with zone 1 representing bottom while zone 3 represents the top for core S-2 (A) S-3 (B) and S-1 (C). The vertical line represents average value.

3.1.6 pH

pH showed a range of 7.38 to 8.17 with a mean of 7.73 for core S-2; 7.05 to 8.15 with a mean of 7.85 for core S-3 and 6.57 to 7.63 with a mean of 7.19 for core S-1. The mean and standard deviation of pH in each zone for cores S-2, S-3 and S-1 are given in table 3.1. pH decreases from zone 1 to zone 3 in all the three cores (S-2, S-3 and S-1) (Figure 3.1.9).

3.1.7 Major elements (Fe, Mn and Al)

The data showed a range of 7.00 to 8.63% with a mean of 7.6% Fe, 693.67 to 923 ppm with a mean of 794 ppm Mn and 6.71 to 8.93% with a mean of 8.23% Al for core S-2 and 7.83 to 9.32% with a mean of 8.44% Fe, 645.67 to 828.33 ppm with a mean of 726 ppm Mn and 7.85 to 10.06% with a mean of 9.43% Al for core S-3. The mean and standard deviation of Fe, Mn and Al in each zone are given in table 3.1.

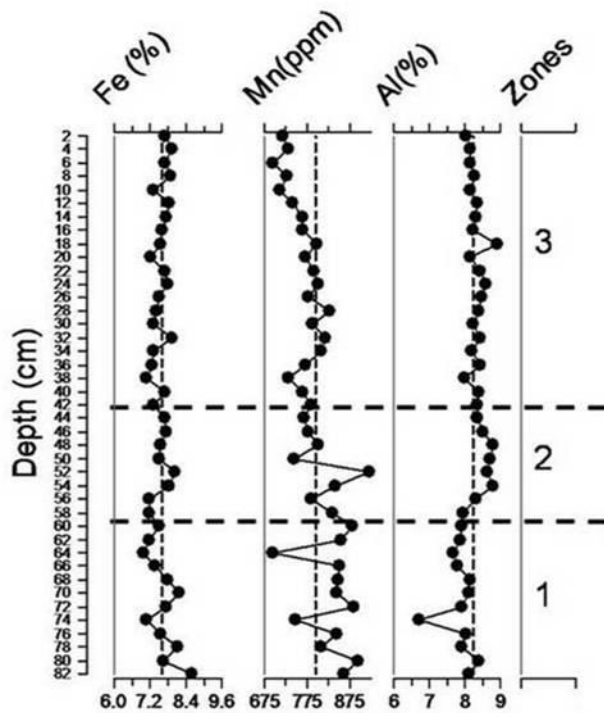


Figure 3.1.10 Down-core variation of major metals (Fe, Mn and Al) in different zones with zone 1 representing bottom while zone 3 represents the top for core S-2. The vertical line represents average value

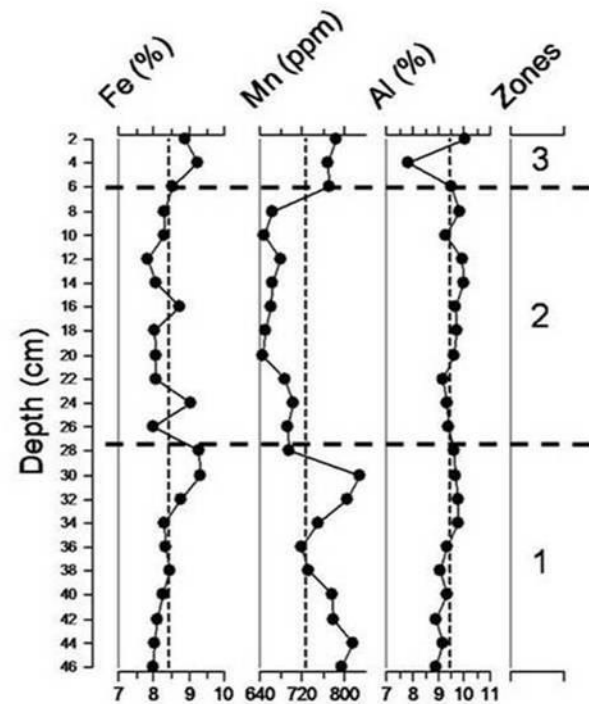


Figure 3.1.11 Down-core variation of major elements (Fe, Mn and Al) in different zones with zone 1 representing bottom while zone 3 represents the top for core S-3. The vertical line represents average value.

In core S-2 collected from middle estuarine region of Amba estuary, the relatively low Al concentration in zone 1 is attributed to higher sand percentage as Al is mostly associated with fine fraction (Windom et al 1989; Loring 1991; Din 1992) (Figure 3.1.10). The relatively higher Fe concentration from 82 to 68 cm agrees with sand distribution (Figure 3.1.10, Figure 3.1.1). The distribution pattern of Mn is similar to that of Fe in zone 1 and zone 2 which may reflect similar source and/or post-depositional behaviors (Figure 3.1.10). Peak value of Fe and Mn at 52 cm depth coincides with peak value of sand. In zone 2, Al showed a gradual increase from 60 to 54 cm and a gradual decrease from 54 to 42 cm (Figure 3.1.10). In zone 3, the distribution of Al largely agrees with that of clay. Mn showed gradual decrease near surface (18-0 cm) which may be attributed to removal of Mn from sediment to water for biotic uptake, since Mn sulfides are less stable (Santschi et al 1990) in the top layers of sediments. Fe values fluctuate around average line in this portion of the core.

In core S-3 collected near the mouth of Dharamtar creek, in zone 1, Al and Fe concentration increases. Mn showed gradual decrease at 46-38 cm and gradual increase at 38-28 cm (Figure 3.1.11). Fe, Mn, sand and silt displayed a peak value at 30 cm depth. In zone 2, Al showed relatively higher concentration while Fe and Mn showed relatively low concentrations. In zone 3, Fe, Mn, sand and silt showed fairly similar distribution patterns of enrichment near surface which might be due to the early diagenetic processes (Figure 3.1.11). Klinkhammer et al (1982) and Santschi et al (1990) stated that Fe^{+2} and Mn^{+2} species get precipitated in the top layers in the sediments as these elements diffuse upward from subsurface. This must have resulted in lower values of Fe and Mn in zone 2 of the core (Figure 3.1.11).

3.1.8 Trace elements (Ni, Cr, Co, Zn and Pb)

The data showed a range of 80.67 to 113 ppm with a mean of 95.72 ppm Ni, 117.3 to 321.67 ppm with a mean of 244 ppm Cr, 59 to 81 ppm with a mean of 70.55 ppm Co, 112.33 to 218.33 ppm with a mean of 135 ppm Zn and 44 to 132.67 ppm with a mean of 87.32 ppm Pb for core S-2 and 88.33 to 127 with a mean of 103 ppm Ni, 217.33 to 273.33 ppm with a mean of 239 ppm Cr, 46.33 to 62.67 ppm with a mean of 54.62 ppm Co, 124 to 144 ppm with a mean of 133 ppm Zn and 6.67 to 120.67 ppm with a mean of 69.57 ppm Pb for core S-3. The mean and standard deviation of Ni, Cr, Co, Zn and Pb in each zone are given in table 3.1.

In core S-2, average values of trace metal concentration displayed the following order, $Cr > Zn > Ni > Pb > Co$. The metal concentrations of Ni, Co and Cr did not show much fluctuation with depth (Figure 3.1.12). The Pb profile showed gradual increase in zone 1, 2 and higher values in zone 3 (Figure 3.1.12). Zn showed almost constant trend in zone 1, 2 and in lower part of zone 3. Zn in the upper part of zone 3 i.e. from 20 cm to surface showed increasing trend (Figure 3.1.12). The peak values obtained at 52 cm and 24 cm depth for Ni, Co and Cr coincides with that of Fe and Mn which suggests post-depositional changes namely coprecipitation of trace metals (Sawlan and Murray 1983; Millward and Moore 1982). Higher concentration of Ni, Co and Cr in zone 1 also agreed largely with that of Fe and Mn

distribution (Figure 3.1.12, Figure 3.1.10). The relatively low TOC in zone 1 causes redox cycling of the metals to occur at relatively deeper depth in the core sediments (Nath et al 1989) (Figure 3.1.5). The increased and high value of Pb and Zn in the upper portion of zone 3 is attributed to enhanced anthropogenic input in recent years (Figure 3.1.10). These elements must have preserved as adsorbed metals on the finer fraction of sediments and not due to precipitation on Fe and Mn oxy-hydroxides or complexation with organic matter as distribution trend of Fe, Mn and TOC decreases towards surface in the upper portion (Wang and Cappellen 1996).

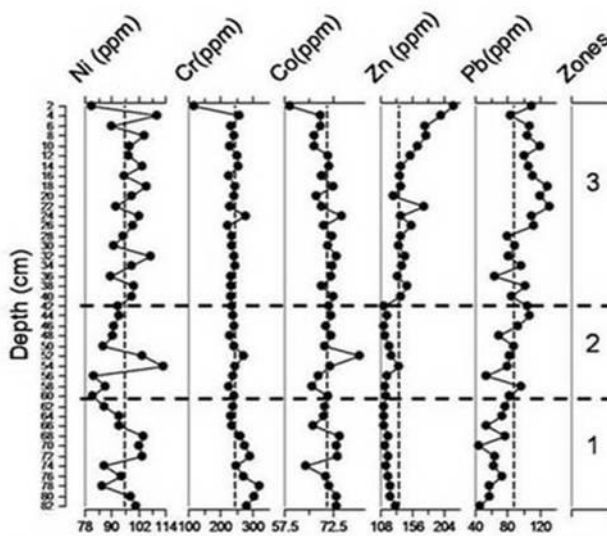


Figure 3.1.12 Down-core variation of trace elements (Ni, Cr, Co, Zn and Pb) in different zones with zone 1 representing bottom while zone 3 represents the top for core S-2. The vertical line represents average value

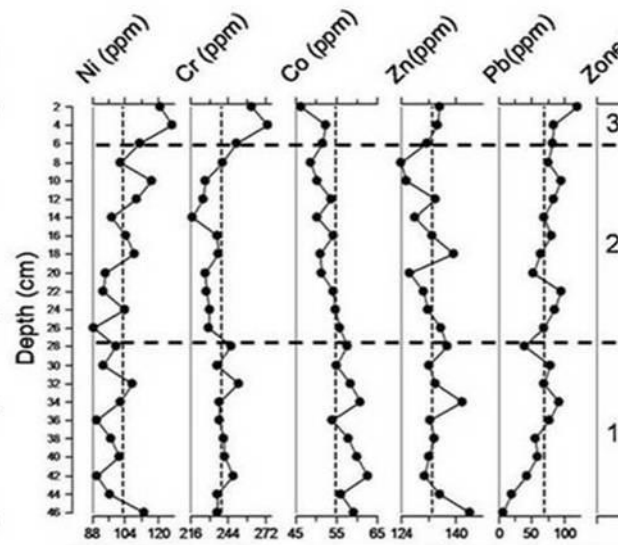


Figure 3.1.13 Down-core variation of trace elements (Ni, Cr, Co, Zn and Pb) in different zones with zone 1 representing bottom while zone 3 represents the top for core S-3. The vertical line represents average value

In core S-3, average values of trace metal concentration displayed the following order, Cr > Zn > Ni > Pb > Co. In zone 1, Pb displayed an overall increasing trend while Co showed decreasing trend (Figure 3.1.13). Other elements maintained almost constant values (Figure 3.1.13). In zone 2, Ni and Pb and to some extent Cr showed gradual increasing trend whereas Co and Zn showed decreasing trend (Figure 3.1.13). In zone 3, most elements except Co showed higher values (Figure 3.1.13). Higher values of most of the elements in zone 3 indicate diagenetic redistribution by Fe and Mn

oxyhydroxides and trapping of these elements in aerobic conditions (Lacerda 1998).

3.1.9 Diatoms

A total of 23 genera of diatoms were recorded in core S-2. Diatoms were represented by *Cyclotella*, *Nitzschia*, *Thalassiosira*, *Surirella*, *Raphoneis*, *Diploneis*, *Pinnularia*, *Grammatophora*, *Gyrosigma*, *Skeletonema*, *Hyalodiscus*, *Amphora*, *Navicula*, *Coscinodiscus*, *Biddulphia*, *Campylodiscus*, *Cerataulina*, *Hemidiscus*, *Triceratium*, *Cymbella*, *Eucampia*, *Stauroneis* and *Eunotia*. Out of 23 genera recorded, a few diatom genera like *Cyclotella*, *Nitzschia*, *Triceratium*, *Thalassiosira*, *Surirella*, *Raphoneis* and *Diploneis* were present throughout the core and were used for interpretation.

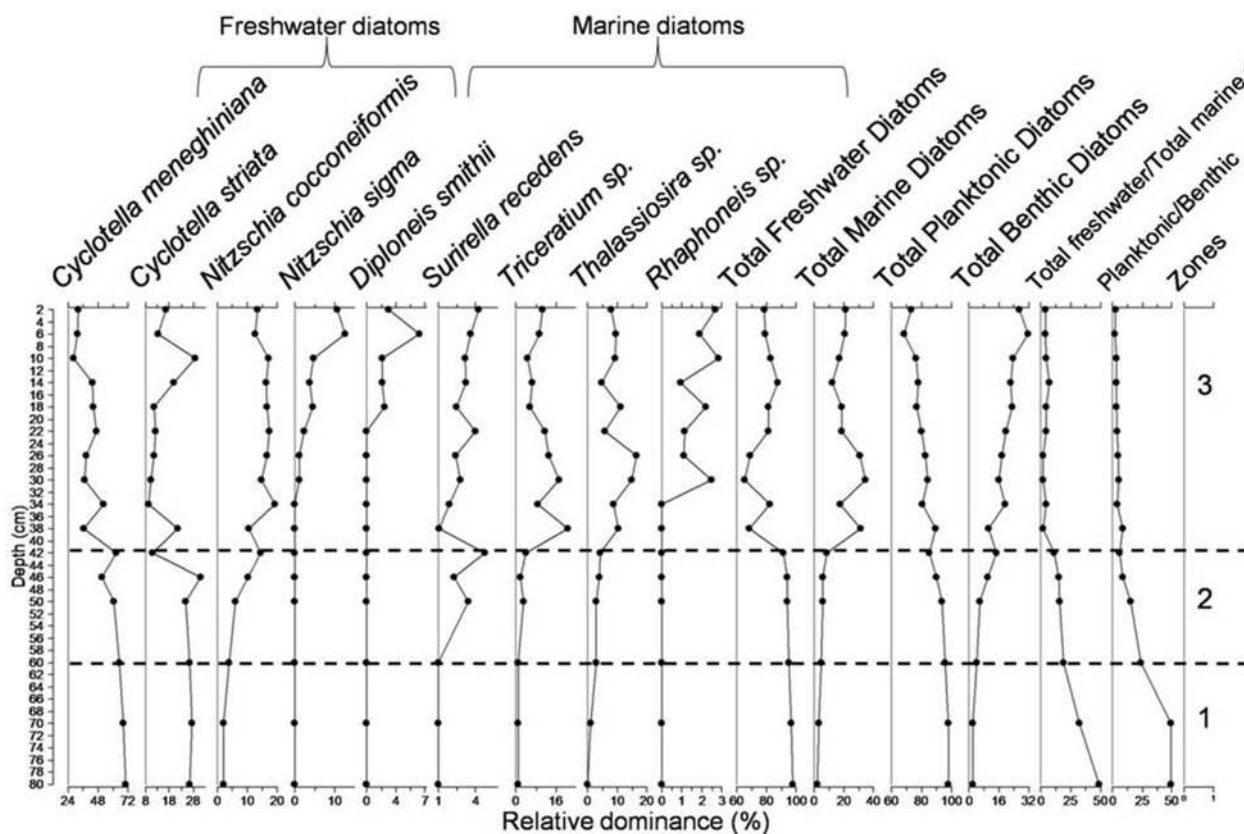


Figure 3.1.14 Down-core variation of diatoms for core S-2. Individual species >1% of relative abundance were retained for the profile

The down-core records of diatoms showed a mixed assemblage of marine and freshwater diatoms (Figure 3.1.14). The fresh water diatoms, however, dominated over the marine diatoms. The freshwater diatoms were

represented by two genera viz. *Cyclotella* and *Nitzschia* whereas marine diatoms were represented by *Surirella*, *Triceratium*, *Thalassiosira*, *Rhaphoneis* and *Diploneis*. Genus *Cyclotella* was dominant among the diatoms throughout the core (Figure 3.1.14) and represented by two species viz. *Cyclotella meneghiniana* and *Cyclotella striata*.

The relative dominance of freshwater and marine diatoms is shown in the figure 3.1.14. The freshwater diatoms are relatively higher between 82-42 cm and 22-10 cm whereas marine diatoms show higher values between 42-22 cm and 10-0 cm. The occurrence of freshwater diatoms in the estuarine environment could be due to the extensive freshwater runoff from the Amba River. *Cyclotella meneghiniana*, a cosmopolitan planktonic diatom species (Finlay et al 2002) is the dominant freshwater diatom (Figure 3.1.14). The increased freshwater runoff which ultimately led to the dominance of *Cyclotella meneghiniana* is further supported by the investigations of Tuchman et al (1984) who documented that the advantageous nature of this species is to survive under different salinity range. Further, Roubex and Lancelot (2008) have demonstrated that *Cyclotella meneghiniana* can survive under wide range of salinity ranging from 5–35 psu, however, its growth generally increases with a salinity optimum of 18 psu which provides the compelling evidence for freshwater runoff. The abundances of marine diatom genera *Thalassiosira* and *Triceratium* showed their peak abundance from 42 to 22 cm and increasing trend from 10 to 0 cm where *Thalassiosira* increased from 1 to 16% between 82 and 22 cm. Similarly, *Triceratium* increased from 1 to 21% between 82 and 22 cm. The overall increase in marine diatoms from 42 to 22 cm and from 10 to 0 cm suggests increased marine influence through the tidal effect at this depth interval.

3.1.10 Paired t-test analysis

Statistical paired t-test analysis ($p < 0.05$) indicated significant differences in the distribution of sediment grain size, TN, TP, C/N ratio and metals (except Cr) (Table 3.1.1).

Table 3.1.1 Summary of paired samples t-test comparing core S-2 and S-3 ($p < 0.05$)

Variables	Difference of means	t	df	Sig. (2-tailed)
Sand S2 – Sand S3	3.98649	3.8	22	0.001
Silt S2 – Silt S3	-16.6344	-10.358	22	0
Clay S2 – Clay S3	12.6479	10.054	22	0
TOC S2 – TOC S3	0.0731	1.119	22	0.275
TN S2 – TN S3	0.86657	8.909	22	0
TP S2 – TP S3	-0.05399	-4.184	22	0
C/N S2 – C/N S3	-32.0945	-6.467	22	0
pH S2 – pH S3	-0.07522	-1.294	22	0.209
Fe S2 – Fe S3	-0.84953	-7.914	22	0
Mn S2 – Mn S3	40.087	2.817	22	0.01
Al S2 – Al S3	-1.09802	-10.578	22	0
Ni S2 – Ni S3	-5.81159	-2.416	22	0.024
Cr S2 – Cr S3	-4.57971	-0.631	22	0.534
Co S2 – Co S3	15.4493	22.552	22	0
Zn S2 – Zn S3	15.2029	2.638	22	0.015
Pb S2 – Pb S3	32.4638	5.624	22	0

3.1.11 Correlation

In core S-2 (Table 3.1.2), sand showed significant positive correlation with Mn ($r=0.544$) and Cr ($r=0.476$); silt showed significant positive correlation with Zn ($r=0.381$) while TOC, TN and TP showed significant positive correlation with Zn ($r=0.319$, $r=0.564$, $r=0.418$) and Pb ($r=0.349$, $r=0.591$, $r=0.37$) thus indicating the role of sediment grain size and organic elements as carriers of trace metals (Harbison 1986; Bernardello et al 2006). The significant positive correlation of most of the trace metals (except Zn and Pb) with Fe and Mn indicates that they are associated with Fe-Mn oxyhydroxides (Chatterjee et al 2007; Jonathan et al 2010). Inter-relationships among trace metals indicate a common source or a similar enrichment mechanism (Table 3.1.2).

The data computed showed average EF value greater than 1.5 for all elements except Mn, Ni and Zn suggesting anthropogenic enrichment of these metals in both S-2 and S-3. However, EF value for Zn in upper section of zone 3 in cores S-2 is more than 1.5 suggesting increase in Zn contamination in recent years (Figure 3.1.15, Figure 3.1.16). Among the metals, EF values of Pb and Co are very high. Increasing trend for Pb is noted.

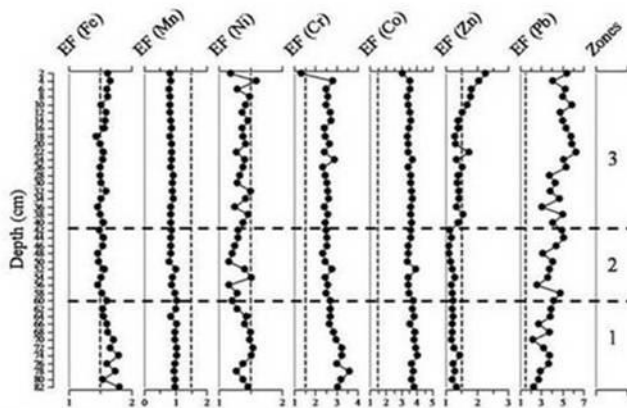


Figure 3.1.15 Down-core variation of Enrichment factor (EF) in different zones with zone 1 representing bottom while zone 3 represents the top for core S-2. The vertical line represents EF value of 1.5

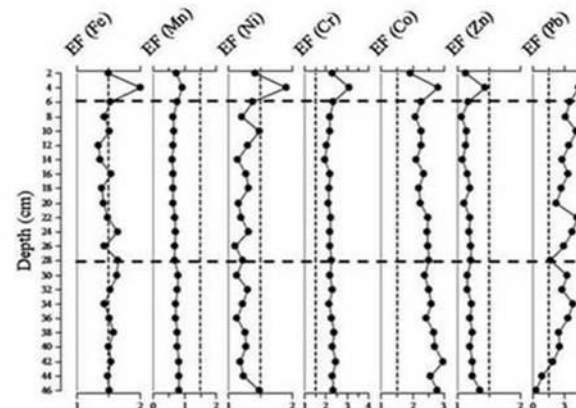


Figure 3.1.16 Down-core variation of Enrichment factor (EF) in different zones with zone 1 representing bottom while zone 3 represents the top for core S-3. The vertical line represents EF value of 1.5

The average Igeo values for Mn and Fe fall in class 0 and class 1 respectively in both cores S-2 and S-3 indicating that sediments are close to background values with respect to Mn and unpolluted to moderately polluted with respect to Fe (Figure 3.1.17; Figure 3.1.18). In core S-2, average Igeo value for Co and Pb falls in class 2 suggesting that sediments are moderately polluted (Figure 3.1.17).

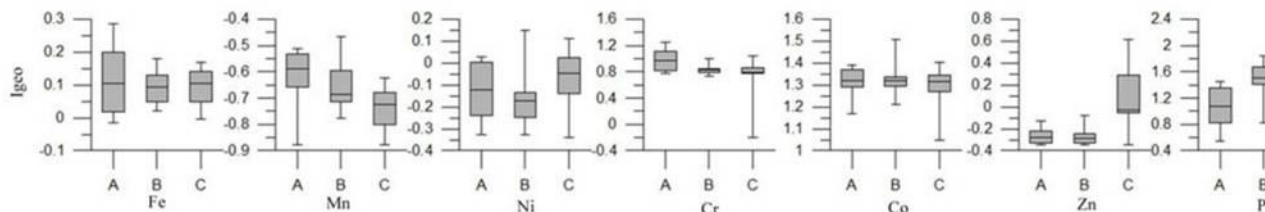


Figure 3.1.17 Box and Whisker plot of Index of geo-accumulation (Igeo) in zone 1 (A), zone 2 (B) and zone 3 (C) for core S-2

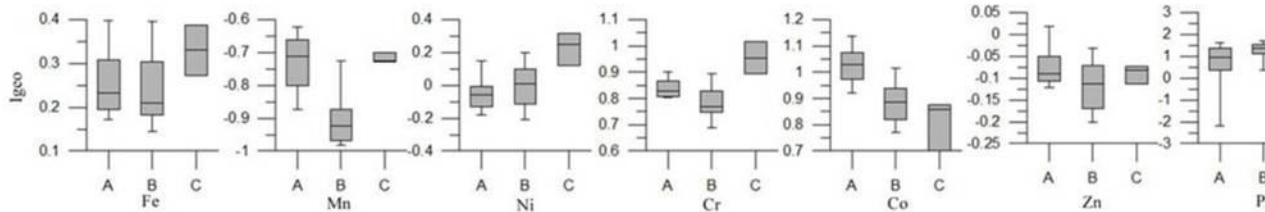


Figure 3.1.18 Box and Whisker plot of Index of geo-accumulation (Igeo) in zone 1 (A), zone 2 (B) and zone 3 (C) for core S-3

In core S-3, Igeo value for Pb in zone 1, 2 and 3 and Co in zone 1 falls in class 2. Co in zone 2 and 3 falls in class 1 reflecting decrease in Co contamination over the years (Figure 3.1.18).

Igeo value for Cr falls in class 1 in core S-3 (zone 1 and 2) and S-2 (zone 2 and 3) indicating that sediments are unpolluted to moderately polluted with respect to Cr. However, Cr in zone 3 of core S-3 and zone 1 of core S-2 falls in Igeo class 2 reflecting that surface and bottom sediments of core S-3 and S-2 respectively are moderately contaminated. Igeo value for Zn falls in class 0 in core S-3 (zone 1, 2 and 3) and S-2 (zone 1 and 2) indicating that sediments are unpolluted with Zn. Igeo value for Ni falls in class 0 in core S-3 (zone 1 and 2) and S-2 (zone 1, 2 and 3). The average Igeo value of Ni in zone 3 of core S-3 falls in Igeo class 1 reflecting an increase in Ni contamination over the recent years.

3.1.13 Factor analysis

In core S-2 and S-3, the five factors (F1, F2, F3, F4, F4 and F5) correspond to 75.56% and 84.02% respectively. F1, F2, F3, F4 and F5 account for 19.09, 18.32, 17.12, 11.05 and 10.00% respectively in core S-2 and 21.93, 17.82, 17.09, 15.71 and 11.47% respectively in core S-3 (Table 3.1.4, Table 3.1.5).

Factor	F1	F2	F3	F4	F5
Variance (%)	19.09	18.12	17.12	11.05	10.00
Sand	-.172	-.898	.039	-.160	.131
Silt	.167	.089	.022	.930	-.045
Clay	.042	.803	-.054	-.543	-.093
TOC	.263	.576	.041	.205	.313
pH	.041	-.038	.081	.016	.845
TN	.831	-.003	.020	.236	.022
TP	.387	.431	.173	.387	.046
Fe	.008	-.344	.671	.194	-.450
Mn	-.593	-.426	.344	.029	.132
Al	.147	.246	.665	.244	.236
Ni	.124	.078	.831	-.159	-.087
Cr	-.422	-.474	.508	-.159	.073
Co	-.401	-.211	.748	.124	.297
Zn	.677	.305	.055	.245	-.490
Pb	.841	.204	.059	-.040	.199
Number of samples = 42 Positive loadings highlighted in Bold are >0.6 significant at p<0.05					

Factor	F1	F2	F3	F4	F5
Variance (%)	21.93	17.82	17.09	15.71	11.47
Sand	-.065	-.680	.019	.626	-.081
Silt	-.012	-.978	-.036	.000	-.061
Clay	.017	.984	.032	-.057	.065
TOC	.847	.180	.419	-.136	.047
pH	.869	.251	.123	-.266	-.101
TN	.280	-.012	.848	-.058	-.024
TP	.228	.145	.702	-.132	.412
Fe	-.204	.031	-.302	.815	.048
Mn	.028	-.292	.397	.722	-.208
Al	.180	.058	.085	-.195	.829
Ni	-.881	.250	.060	.144	-.107
Cr	-.519	.043	.156	.700	-.204
Co	.610	-.011	.426	.264	-.474
Zn	-.106	.000	.793	.177	-.278
Pb	-.421	.123	-.251	.120	.660
Number of samples = 23 Positive loadings highlighted in Bold are >0.6 significant at p<0.05					

In core S-2 (Table 3.1.4), F1 showed significant loadings on TN (0.831), Pb (0.841) and Zn (0.677). F2 showed significant positive loadings on clay (0.803) and good positive loadings on TOC (0.576). F3 showed significant positive loadings on Fe (0.671), Al (0.665), Ni (0.831), Co (0.748) and good positive loadings on Cr (0.508). F4 showed significant positive loadings on silt (0.93) while F5 showed significant positive loadings on pH (0.845).

In core S-3 (Table 3.1.5), F1 showed significant loadings on TOC (0.847), pH (0.869) and Co (0.61). F2 showed significant positive loadings on clay (0.984). F3 showed significant positive loadings on TN (0.848), TP (0.702) and Zn (0.793). F4 showed significant positive loadings on sand (0.626), Fe (0.815), Mn (0.722) and Cr (0.70) while F5 showed significant positive loadings on Al (0.829) and Pb (0.66).

F1 in core S-2 and F1, F3 in core S-3 can be associated as nutrient controlled factor as the distribution of Pb and Zn in core S-2 and Co and Zn in core S-3 is controlled either by TOC, TN or TP. F3 in core S-2 can be

associated as Fe-Al controlled factor while F4 and F5 in core S-3 can be associated as Fe-Mn-Al controlled factor.

3.1.14 Isocon

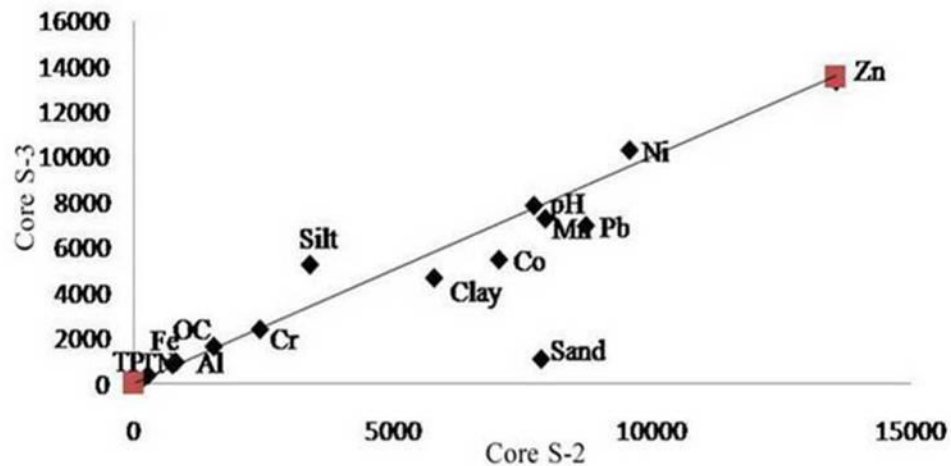


Figure 3.1.19 Isocon diagram. Individual point represents average value

When two locations (core S-2 and core S-3) are compared relatively higher sand, clay, Pb, Mn and Co are deposited at the middle estuarine region of Amba estuary while silt and Ni are found to be relatively higher near the mouth of Dharamtar creek (Figure 3.1.19). The higher values of Fe at surface/subsurface layers (10-0 cm) in core S-2 and S-3 could be also attributed to industrial plants and port around Dharamtar. The barges around industries can be sources for particulate Fe which settle down and mix with the bottom sediments in these regions. The precipitated Fe in the form of oxyhydroxides has the affinity to scavenge other metals such as Ni, Pb, Cr etc., as they pass through the water en route to the sediment (Davis and Leckie 1978).

3.1.15 Conclusion

The distribution of metals is largely controlled by sediment grain size, TOC, TN and TP both near the mouth and in the middle portion of the creek. When the average values are considered, Mn and Co showed higher concentration in middle portion whereas, Fe and Al are higher near the mouth. Geo-accumulation index computed for the metals indicated that Dharamtar creek is moderately polluted with Pb and Co, unpolluted to moderately polluted

with Ni, Cr and Fe and practically unpolluted with Zn and Mn, source being both natural and anthropogenic as indicated by factor analysis. Enrichment factor indicated increase in the level of pollution near mouth over the recent years. Diatoms showed mixed assemblages of fresh and marine diatoms with predominance of freshwater planktonic diatom *Cyclotella meneghiniana* throughout the core and is attributed to monsoon regulated high river runoff.

3.2 Kundalika estuary

Total six cores, three from mudflats (S-62, S-63 and S-45) and remaining three from mangroves (S-47, S-42 and S-40), were collected along Kundalika estuary (Figure 3.2).

3.2 A Mudflats

3.2A.1 Collection of sediment cores

Amongst the three cores collected from mudflats, one represented lower estuary (S-62) while the other two cores (S-63 and S-45) were representing lower middle (S-63) and upper middle (S-45) estuarine regions (Figure 3.2). Each core was 66 cm in length. All the three cores viz. S-62, S-63 and S-45 were analyzed for sediment grain size and TOC; S-62 and S-45 were also analyzed for metals; S-62 was further analyzed for TN while S-45 for TP.

3.2A.2 Colour

Sediment colour was brown from 0 to 10 cm in S-62 and 0 to 9 cm in S-63. The remaining part of S-62 and S-63 was mixed black to grey colour. The core S-45 was uniform grey colour from 0 to 66 cm.

3.2A.3 Sediment grain size

The data showed a range of 1.21 to 19.97% with a mean of 11.52% sand, 35.38 to 76.21% with a mean of 49.58% silt, 6.48 to 59.12% with a mean of 38.90% clay for core S-62; 0.15 to 9.1% with a mean of 3.46% sand, 19.93 to 75.85% with a mean of 46.57% silt and 23.12 to 79.8% with a mean of 49.97% clay for core S-63 and 0.06 to 4.91% with a mean of 0.76% sand, 13.47 to 45.58% with a mean of 24.62% silt and 54.16 to 86.4% with a mean of 74.62% clay for core S-45. Each core has been divided into three zones depending upon the distribution pattern of sediment components namely zone 1, 2 and 3 wherein zone 3 represents recent sediments. The mean and

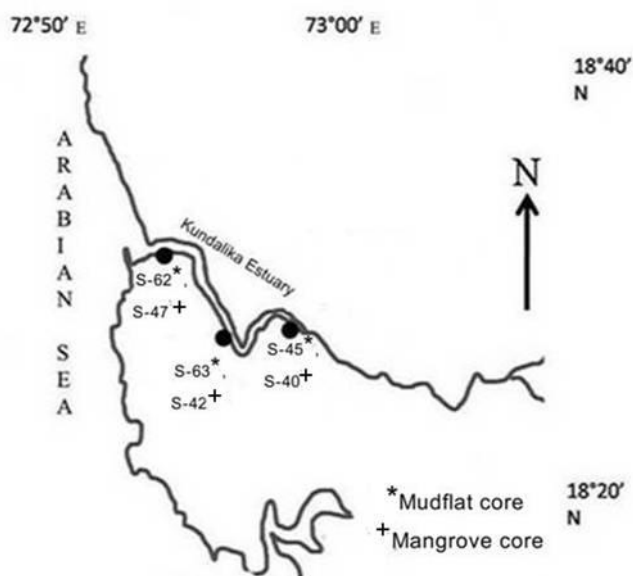


Figure 3.2 Location of core collection from Kundalika estuary

standard deviation of sediment grain size in each zone for cores S-62, S-63 and S-45 are given in table 3.2a.

Table 3.2a Mean and standard deviation (values in parenthesis) of different parameters in each zone for core S-62, S-45 and S-63. The p value denotes results of one-way ANOVA statistically significant at $p < 0.05$. n = number of samples.

Core S-62				
	Zone 1 (66-50 cm) n = 9	Zone 2 (50-28 cm) n = 12	Zone 3 (28-0 cm) n = 14	p value (*statistically significant at $p < 0.05$)
	Mean (Standard deviation)	Mean (Standard deviation)	Mean (Standard deviation)	
Sand (%)	6.71 (± 5.17)	15.55 (± 3.12)	10.92 (± 2.73)	*0.00
Silt (%)	49.90 (± 12.12)	45.21 (± 9.23)	54.19 (± 10.74)	0.12
Clay (%)	43.39 (± 14.67)	39.09 (± 8.30)	34.89 (± 12.19)	0.25
TOC (%)	1.24 (± 0.24)	0.76 (± 0.26)	1.24 (± 0.31)	*0.00
TN (%)	0.14 (± 0.03)	0.16 (± 0.03)	0.14 (± 0.05)	0.47
C/N	9.44 (± 3.19)	4.75 (± 1.41)	9.37 (± 3.42)	*0.00
Fe (%)	11.40 (± 0.75)	11.70 (± 0.66)	11.60 (± 0.68)	0.61
Mn (ppm)	889.85 (± 94.58)	936.28 (± 81.18)	883.64 (± 53.09)	0.19
Al (%)	6.96 (± 0.27)	7.07 (± 0.31)	6.81 (± 0.30)	0.09
Ni (ppm)	119.37 (± 9.42)	116.14 (± 6.23)	105.38 (± 9.00)	*0.00
Cr (ppm)	328.07 (± 51.52)	356.25 (± 42.06)	233.83 (± 73.67)	*0.00
Co (ppm)	91.26 (± 4.64)	90.78 (± 4.88)	82.55 (± 7.80)	*0.00
Zn (ppm)	235.59 (± 64.06)	167.89 (± 32.06)	196.33 (± 60.95)	*0.03
Pb (ppm)	81.19 (± 8.43)	97.72 (± 11.17)	134.64 (± 25.22)	*0.00
Core S-45				
	Zone 1 (66-50 cm) n = 9	Zone 2 (50-28 cm) n = 12	Zone 3 (28-0 cm) n = 14	p value (*statistically significant at $p < 0.05$)
	Mean (Standard deviation)	Mean (Standard deviation)	Mean (Standard deviation)	
Sand (%)	0.27 (± 0.21)	0.40 (± 0.20)	1.34 (± 1.31)	*0.00
Silt (%)	27.81 (± 13.21)	25.37 (± 11.09)	22.70 (± 3.44)	0.46
Clay (%)	71.91 (± 13.26)	74.23 (± 11.16)	75.95 (± 3.94)	0.62
TOC (%)	1.00 (± 0.09)	1.15 (± 0.08)	1.70 (± 0.33)	*0.00
TP (%)	0.03 (± 0.00)	0.03 (± 0.01)	0.03 (± 0.01)	0.07
Fe (%)	8.30 (± 0.30)	8.81 (± 0.44)	8.73 (± 0.92)	0.19
Mn (ppm)	877.96 (± 101.57)	967.39 (± 87.63)	1006.60 (± 70.45)	*0.01
Al (%)	8.04 (± 0.07)	8.25 (± 0.32)	8.02 (± 0.87)	0.57
Ni (ppm)	88.30 (± 5.14)	91.33 (± 6.77)	101.29 (± 13.96)	*0.01
Cr (ppm)	337.89 (± 14.04)	316.58 (± 20.50)	358.60 (± 47.56)	*0.01
Co (ppm)	69.93 (± 1.48)	69.53 (± 4.02)	73.00 (± 10.75)	0.43
Zn (ppm)	141.59 (± 2.26)	140.92 (± 6.87)	139.31 (± 14.95)	0.86
Pb (ppm)	92.30 (± 8.01)	101.67 (± 11.21)	146.29 (± 26.88)	*0.00
Core S-63				
	Zone 1 (66-50 cm) n = 9	Zone 2 (50-28 cm) n = 12	Zone 3 (28-0 cm) n = 14	
	Mean (Standard deviation)	Mean (Standard deviation)	Mean (Standard deviation)	
Sand (%)	2.03 (± 2.47)	4.62 (± 2.4)	3.35 (± 1.77)	
Silt (%)	33.79 (± 13.56)	53.47 (± 15.57)	50.41 (± 15.66)	
Clay (%)	64.17 (± 14.37)	41.91 (± 13.85)	46.25 (± 14.59)	
TOC (%)	1.49 (± 0.40)	1.69 (± 0.13)	1.74 (± 0.39)	

In the core S-62, collected from lower estuary, in zone 1, sand percentage increases, silt and clay show fluctuating trends (Figure 3.2a.1). In zone 2, sand is relatively higher, clay percentage increases and silt percentage

decreases with some variations. In zone 3, sand is nearly constant; silt percentage increases while clay percentage decreases (Figure 3.2a.1). In zone 1 of core S-63 (Figure 3.2a.2), sand and silt percentage increases while clay percentage decreases. In zone 2, sand, silt and clay showed fluctuating trends. In zone 3, sand percentage decreases while silt and clay showed fluctuating trends. In zone 1 and 2 of core S-45 (Figure 3.2a.3), sand remain constant while silt and clay showed large fluctuations compensating each other. In zone 3, sand and silt percentage increases while clay decreases.

Further, to understand the hydrodynamic conditions of depositional environment, ternary diagram proposed by Pejrup (1988) is plotted. Plots (Figure 3.2a.4) reveal that core collected from lower estuary (S-62) falls largely within section III and II indicating that sediment deposition took place under relatively violent to less violent conditions. Core S-63 collected from lower middle estuary falls largely within sections III and II (Figure 3.2a.4) while core S-45 collected from upper middle estuary falls largely within sections II and I indicating that sediment deposition took place under less violent to calm conditions. Further, the sediments from middle estuary (S-63 and S-45) fall within D type while in core from lower estuary (S-62) majority of the points of sediments fall within C type indicating presence of sand dominated sediments.

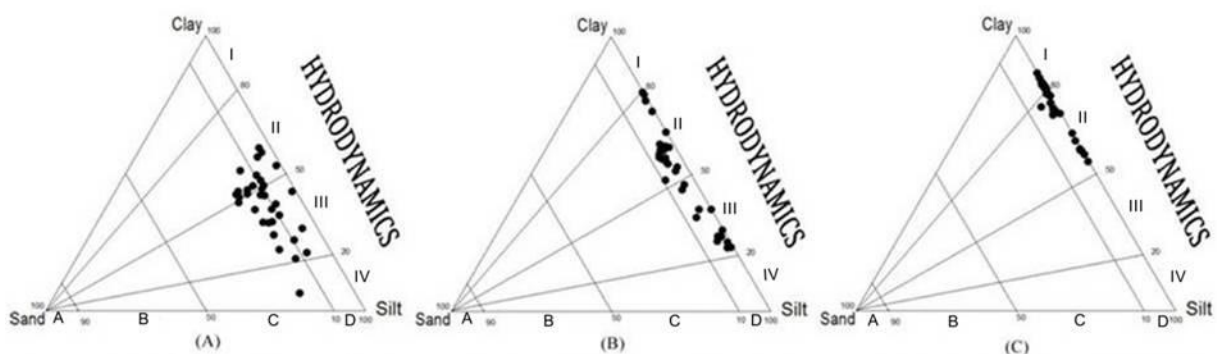


Figure 3.2a.4 Ternary diagram for the classification of hydrodynamic conditions after Pejrup (1988) for core S-62 (A), S-63 (B) and S-45 (C)

When the distribution of sediment grain size along the estuary (S-62, S-63, S-45) is compared, it is observed that sand showed a “band-type” distribution. The sand content increases from the minimum at upper region of middle estuary (S-45) to the maximum at lower estuary (S-62). This indicates

increasing energy conditions from middle to lower estuary (Lorenzo et al 2007). The average sand is less than 1% in upper region of middle estuary (S-45) while more than 11% in lower estuary (S-62). The relatively higher tidal energy in lower estuary results in higher hydro dynamics near the mouth which facilitates the deposition of coarser sediments. The finer sediments are more mobile and are carried to the middle estuary where tidal currents are relatively weaker resulting in the deposition of mud (Manning et al 2010). Thus, variations in average sand percentage were due to differences in tidal range at different places (Feng 1985; Cao et al 1989). The high range (13.7–20 %) and average (~17 %) sand percentage observed in zone 2 of lower estuary (S-62) (Table 3.2a) is attributed to factors such as high river discharge (Walsh and Nittrouer 2004) or during extreme events such as storm surges (Gao 2009b), agricultural practices/anthropogenic activities, including sand mining (Dandekar 2010). On the other hand, the upper middle estuary (S-45) consist primarily of clay component with an average of 75%, deposited possibly from turbidity maxima (Dyer 1986) developed within this part of estuary.

3.2A.4 Nutrients (TOC, TN and TP)

The data showed a range of 0.3 to 1.71% with a mean of 1.10% TOC and 0.07 to 0.31% with a mean of 0.15% TN for core S-62; 1.01 to 2.6% with a mean of 1.66% TOC for core S-63 and 0.87 to 2.37% with a mean of 1.35% TOC and 0.02 to 0.06% with a mean of 0.03% TP for core S-45. The mean and standard deviation of TN, TP and TOC in each zone are given in table 3.2a.

In core S-62, collected from lower estuary, zone 1 and 3 are characterized by relatively higher TOC concentration while in zone 2 TN is relatively high (Figure 3.2a.5). In middle estuary (S-63), in zone 1 TOC is relatively low, in zone 2 TOC is nearly constant whereas in zone 3 from 28-10 cm TOC is relatively high and from 10-0 cm TOC is relatively low (Figure 3.2a.7). In core S-45 relatively low TOC and TP are noted in zone 1 and 2 respectively while in zone 3 they show relatively higher concentration (Figure 3.2a.6).

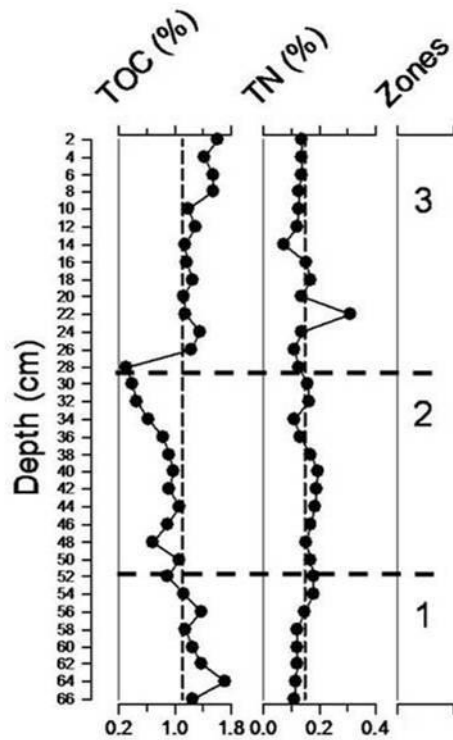


Figure 3.2a.5 Down-core variation of TOC and TN in different zones with zone 1 representing bottom while zone 3 represents the top for core S-62. The vertical line represents average value.

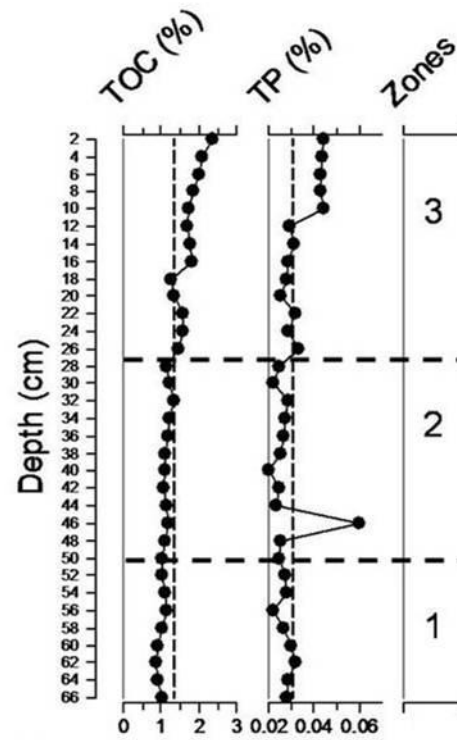


Figure 3.2a.6 Down-core variation of TOC and TP in different zones with zone 1 representing bottom while zone 3 represents the top for core S-45. The vertical line represents average value.

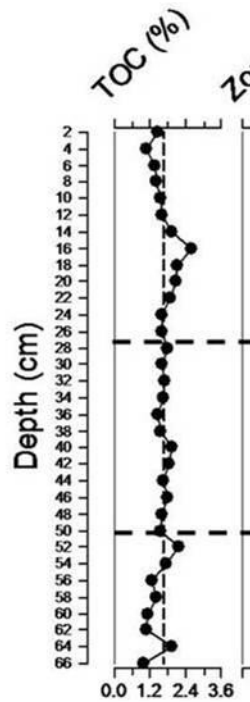


Figure 3.2a.7 Down-core variation of TOC in different zones with zone 1 representing bottom while zone 3 represents the top for core S-63. The vertical line represents average value.

When the distribution of TOC along the estuary (S-62, S-63 and S-45) is compared, it is observed that TOC also showed a “band-type” distribution which decreases with increasing coarser fraction from maximum in middle to minimum in lower estuary. The relatively higher TOC concentration is noted in the middle estuary (S-63 average 1.65 %; S-45 average 1.35 %) where sediments are muddy (average 95 % mud). On the other hand, relatively low TOC (S-62 average 1.1 %) is noted near the mouth where sediments are slightly sandy mud (75–95 % mud) (Flemming 2000). According to Muzuka and Shaghude (2000), muddier sites contain higher content of TOC relative to sandier sites which is mainly attributed by them to factors such as surface area/volume ratio of sediment grain. However, in addition, the terrestrial input from the adjacent land masses (Jonathan et al 2004) must be responsible for higher TOC concentration in the middle estuary. Further, relatively higher TOC along with higher percentage of finer fraction (95 %) in the middle estuary suggests calm environment of deposition (Kumar and Edward 2009).

The depth-wise distribution of TOC showed high and increased percentage (S-62 and S-45) in zone 3 and relatively low percentage (S-63; S-45) in zone 1 indicating degradation of organic material with depth (Figure 3.2a.5; Figure 3.2a.6; Figure 3.2a.7). The high and increased TOC (S-45 1.2–2.4 %; S-63 1.07–2.6 %; S-62 0.3–1.6 %), TN (S-62 0.07–0.31 mg/g) and TP (S-45 0.2–0.6 mg/g) in zone 3 is mainly attributed to extensive use of fertilizers, population growth and increased inputs of particulate sedimentary matter and urban waste (Ruiz-Fernández et al 2003; Zourarah et al 2009). However, in lower estuary (S-62), relatively low TOC concentration (0.4–1.1 %) in zone 2 reflects their dilution by addition of coarse grained (>63 μm , 14–20 %) sediments (Pichaimani et al 2008) because of poor absorbability of organics on negatively charged quartz (Chatterjee et al 2007). In core S-62, the relatively higher TOC from 66 to 54 cm (1.12–1.71%) and TN concentration from 56 to 50 cm (0.07–0.31%) may be attributed to relatively higher percentage of finer sediments at corresponding depth intervals. When the two cores (S-63 and S-45), one from lower region (S-63) and other from upper region (S-45) of middle estuary are compared relatively higher average TOC concentration is found in lower region of middle estuary (S-63). Although TOC generally depends upon the grain size and is enriched in fine grained sediments (Falco et al 2004), factors such as balance between accumulation and degradation rate of organic matter and the source and type of organic material are keys which control the concentration of organic carbon in sediments (Schorer 1997).

3.2A.5 C/N ratio

In core S-62, C/N ratio is relatively low in zone 2 where sand had shown relatively higher values reflecting increase in marine processes and input (Figure 3.2a.8).

3.2A.6 Major elements (Fe, Mn and Al)

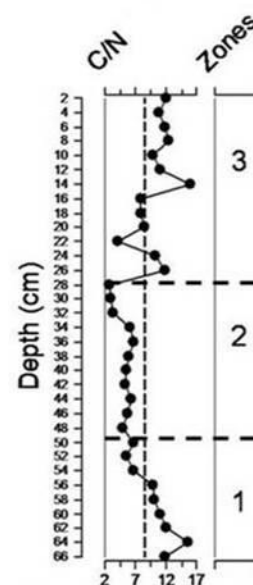


Figure 3.2a.8 Down-core variation of C/N ratio in different zones with zone 1 representing bottom while zone 3 represents the top for core S-62. The vertical line represents average value.

The data showed a range of 10.02 to 12.84% with a mean of 11.61% Fe, 789.67 to 1083 ppm with a mean of 899.14 ppm Mn and 6.36 to 7.53% with a mean of 6.95% Al for core S-62 and 5.83 to 9.57% with a mean of 8.61% Fe, 741.67 to 1134.33 ppm with a mean of 954.05 ppm Mn and 5.31 to 8.97% with a mean of 8.10% Al for core S-45. The mean and standard deviation of Fe, Mn and Al in each zone are given in table 3.2a.

In core S-62 collected from lower estuary, in zone 1, Fe and Mn fluctuate with an overall increasing trend while Al concentration increases up to 56 cm (Figure 3.2a.9). Negative peak of Fe at 54 cm depth coincides with that of Al indicating their common terrigenous source. In zone 2, Al showed an increasing trend while Fe and Mn showed a decreasing trend. In zone 3 Fe, Mn and Al showed large variations with values falling around their respective average line. The reduced Fe and Mn concentration at surface (8-0 cm) may indicate that Fe and Mn ions with greater mobility are removed from surface sediments to the water column through active diffusion and advective processes (Janaki-Ramann et al 2007; Badr et al 2009).

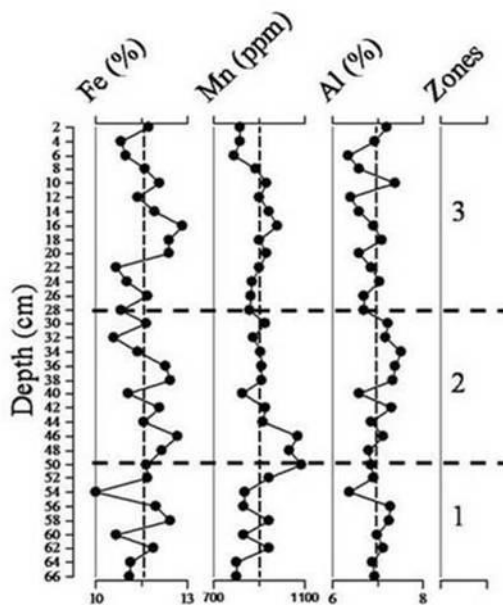


Figure 3.2a.9 Down-core variation of major elements (Fe, Mn and Al) in different zones with zone 1 representing bottom while zone 3 represents the top for core S-62. The vertical line represents average value.

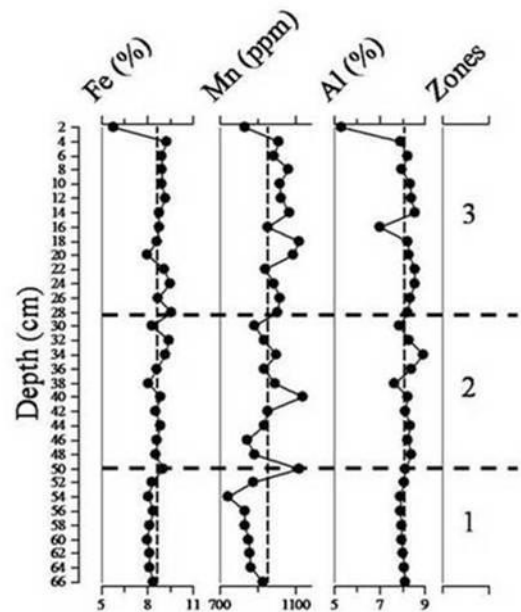


Figure 3.2a.10 Down-core variation of major elements (Fe, Mn and Al) in different zones with zone 1 representing bottom while zone 3 represents the top for core S-45. The vertical line represents average value.

In core S-45 collected from middle estuary, in zone 1, Al is nearly constant with values falling on the average line, Fe and Mn values are less than their

respective averages (Fig. 3.2a.10). In zone 2 Fe, Mn and Al values fluctuate around the average line. In zone 3 concentrations of Fe, Mn and Al is more than their respective averages.

When the distribution of major elements (Fe, Mn and Al) along the estuary (S-62 and S-45) is compared, it is observed that average Al and Mn content is greater in the middle estuary (S-45), while average Fe content is more in lower estuary (S-62). The Al content is considered as a good indicator of the amount of finer clay material (Ram et al 2003) of terrestrial origin. The result of sediment grain size analysis clearly indicated twofold increase in clay content in middle estuary (S-45) when compared to lower estuary (S-62). Therefore, the observed higher concentration of Al is attributed to high clay content in middle estuary (S-45). The relatively higher Al and Mn content in middle estuary (S-45) also reflect greater input by mechanical and chemical weathering of rocks (Decarlo and Anthony 2002). On the other hand, elevated Fe content in lower estuary (S-62) could be attributed to terrigenous supply of ferromagnesian minerals, industrial and municipal discharges (Sagheer 2004; Bhagure and Mirgane 2011) and greater recycling of Fe by resuspension of bottom sediments due to tidal mixing in lower estuarine region (Kumar and Edward 2009). The depth-wise distribution of Fe and Mn in middle estuary (S-45) indicated enrichment in zone 3 due to the precipitation of these redox sensitive elements as hydroxides and oxides, whereas the low Fe and Mn concentrations in zone 1 reflect their dissolution.

3.2A.7 Trace elements (Ni, Cr, Co, Zn and Pb)

The data showed a range of 93.00 to 138.67 ppm with a mean of 112.54 ppm Ni, 159.67 to 457 ppm with a mean of 298.44 ppm Cr, 69 to 93 ppm with a mean of 87.60 ppm Co, 134 to 368.33 ppm with a mean of 199 ppm Zn and 69.67 to 177.67 ppm with a mean of 109.66 ppm Pb for core S-62 and 72.67 to 132.67 with a mean of 94.64 ppm Ni, 226.67 to 408 ppm with a mean of 340.81 ppm Cr, 44 to 83.67 ppm with a mean of 71.19 ppm Co, 96.33 to 156.67 ppm with a mean of 140.67 ppm Zn and 80.33 to 176.67 ppm with a mean of 118.64 ppm Pb for core S-3. The mean and standard deviation of Ni, Cr, Co, Zn and Pb in each zone are given in table 3.2a.

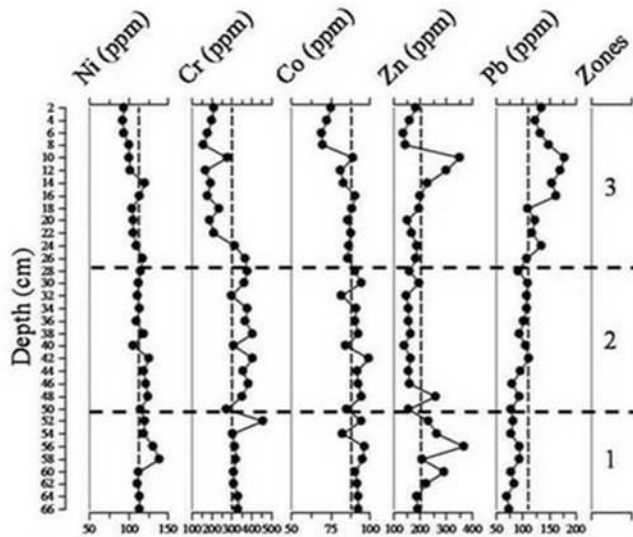


Figure 3.2a.11 Down-core variation of trace elements (Ni, Cr, Co, Zn and Pb) in different zones with zone 1 representing bottom while zone 3 represents top for core S-62. The vertical line represents average value.

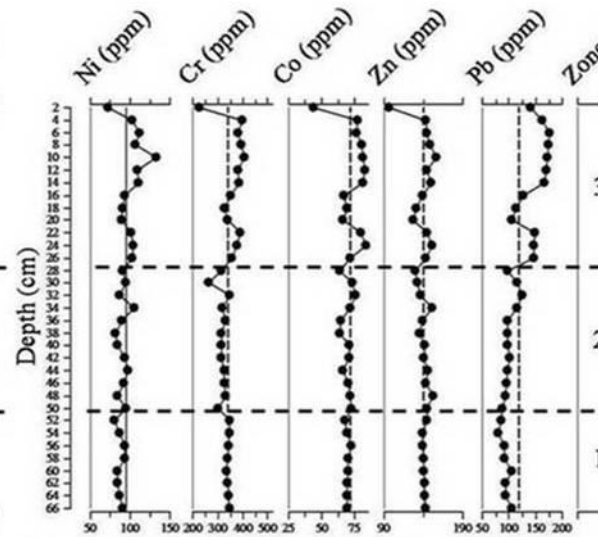


Figure 3.2a.12 Down-core variation of trace elements (Ni, Cr, Co, Zn and Pb) in different zones with zone 1 representing bottom while zone 3 represents top for core S-45. The vertical line represents average value.

In core S-62, the average values of trace metal concentrations displayed the following order, $Cr > Zn > Ni > Pb > Co$. In zone 1, concentrations of Ni, Cr and Co decreases while Pb increases with some variations (Fig. 3.2a.11). Zn showed an overall increase till 56 cm then showed a gradual decrease. In zone 2, concentrations of Ni, Cr and Co were higher while Zn and Pb were lower than their respective average. Ni, Cr, Co showed decreasing trend, Zn remain constant and Pb showed an increasing trend (Figure 3.2a.11). In zone 3, Ni, Co and Cr showed a decreasing trend from 28 to 6 cm whereas Zn and Pb displayed an increase in concentration reaching the highest value at 10 cm (Figure 3.2a.11). All the metals showed increase in concentration at surface (0–6 cm) (Figure 3.2a.11). The vertical profile of trace elements indicated a decreasing trend in lower estuary (S-62) with almost all metals exceeding their average values in zone 1 and 2. Sand and TOC also exceeded their average value in zone 2 and 1, respectively (Figure 3.2a.1; Figure 3.2a.5). The elevated metal concentration may therefore be due to their association with detrital sand (i.e. mining and smelt products) particles and organic matter in zone 2 and 1, respectively. Similar enrichment of trace metals in coarse particles has been reported in estuaries subjected to mining (Cundy et al 2003). The reduced concentration of trace elements in surface

sediments (0–12 cm) is similar to that of Fe–Mn and is attributed to diagenetic removal or diffusion process (Fig. 3.2a.9).

In core S-45, the average values of trace metal concentrations displayed the following order, Cr > Zn > Pb > Ni > Co. In zone 1 and 2, almost all the metals except Pb displayed constant trend with values below or around the average line while in zone 3, between 28 and 4 cm all the metals showed values above the average line followed by drastic decrease at surface (Figure 3.2a.12). Pb values, however, were much less than average in zone 1 and 2 and showed an overall increasing trend in zone 2 and zone 3 (Figure 3.2a.12).

When the distribution of trace elements (Ni, Cr, Co, Zn and Pb) along the estuary (S-62 and S-45) is compared, it is observed that average content of Ni, Co and Zn is more in the lower estuary (S-62) whereas average Cr and Pb content is more in middle estuary (S-45). The distribution of metals depends upon factors such as the distance of element sources to estuary, hydrodynamics, the chemical characteristics (e.g. sorption-adsorption capacity of trace metals, flocculation, etc.), and the chemical and biochemical condition of sedimentary environment (Williams et al 1994). The depth-wise distribution showed different trends in metal profiles in lower (S-62) and middle (S-45) estuary (Figure 3.2a.11; Figure 3.2a.12). In middle estuary (S-45) the metals analyzed are enriched in the zone 3 (28–4 cm) with a constant trend in zone 1 and 2 (Fig. 3.2a.12). Clay, TOC and major elements (Al, Fe and Mn) also showed enrichment in zone 3 similar to trace elements thus indicating a common source (Fig.3.2a.3 Figure 3.2a.6; Figure 3.2a.10; Figure 3.2a.12). However, at surface all the metals including Fe, Mn and Al showed drastic decrease which may be due to diffusion of elements or disturbance due to dredging activities.

3.2A.8 Paired t-test analysis

Paired t-test analysis ($p < 0.05$) indicated significant differences in the distribution of

Variables	Paired Differences	t	df	Sig. (2-tailed)
SandS62 - SandS45	10.7554	11.845	32	0
SiltS62 - SiltS45	24.967	10.837	32	0
ClayS62 - ClayS45	-35.7224	-15.314	32	0
TOCS62 - TOCS45	-0.24583	-3.531	32	0.001
FeS62 - FeS45	2.99845	16.214	32	0
MnS62 - MnS45	-54.9091	-2.75	32	0.01
AlS62 - AlS45	-1.15073	-9.337	32	0
NiS62 - NiS45	17.899	5.856	32	0
CrS62 - CrS45	-42.3636	-2.39	32	0.023
CoS62 - CoS45	16.404	8.326	32	0
ZnS62 - ZnS45	58.3333	5.756	32	0
PbS62 - PbS45	-8.9798	-3.031	32	0.005

sediment grain size, TOC and metals (Table 3.2a.1) between the two locations.

3.2A.9 Correlation

The significant positive association of clay with Cr ($r=0.383$) and Co ($r=0.495$) in lower estuary (S-62) (Table 3.2a.2) and of TOC with Ni ($r=0.442$) and Pb ($r=0.856$) in middle estuary (S-45) (Table 3.2a.3) indicated interaction of trace metals with clay particles and organic matter in the process of removal and fixation of Cr and Co in lower estuary (S-62) and Ni and Pb in middle estuary (S-45), respectively. Other elements do not show significant positive association with clay and TOC as the interaction among metals, clay and TOC depends upon many factors including charge on metal ions (Bartoli et al 2012).

Table 3.2a.2 Pearson correlation coefficient for core S-62

	Sand	Silt	Clay	TOC	pH	TN	Fe	Mn	Al	Ni	Cr	Co	Zn	Pb
Sand	1													
Silt	-0.061	1												
Clay	-380*	-900**	1											
TOC	-.535**	0.323	-0.066	1										
pH	0.042	.408*	-.397*	.387*	1									
TN	0.297	-0.184	0.041	-0.176	-0.108	1								
Fe	0.284	0.012	-0.135	-0.027	-0.012	-0.135	1							
Mn	.445**	0.012	-0.205	-.386*	-0.243	0.161	.606**	1						
Al	0.107	-.508**	.424*	-0.253	-0.246	0.005	.383*	0.176	1					
Ni	-0.047	-0.299	0.298	-.348*	-.772**	-0.007	0.307	.395*	0.251	1				
Cr	0.216	-.514**	.383*	-.543**	-.752**	0.057	0.072	0.162	.469**	.619**	1			
Co	-0.002	-.534**	.495**	-.426*	-.777**	0.126	.383*	.368*	.523**	.759**	.723**	1		
Zn	-.344*	-0.13	0.271	0.181	-0.155	-0.195	0.048	-0.006	0.074	0.232	-0.014	0.28	1	
Pb	0.128	0.34	-.372*	0.223	.779**	-0.141	0.178	-0.02	-0.151	-.493**	-.659**	-.468**	0.142	1

*. Correlation is significant at the 0.05 level (2-tailed). ** Correlation is significant at the 0.01 level (2-tailed).
number of samples = 33

Table 3.2a.3 Pearson correlation coefficient for core S-45

	Sand	Silt	Clay	TOC	pH	TP	Fe	Mn	Al	Ni	Cr	Co	Zn	Pb
Sand	1													
Silt	-0.034	1												
Clay	-0.072	-.994**	1											
TOC	.687**	-0.124	0.051	1										
pH	-0.198	0.174	-0.152	-.561**	1									
TP	.363*	0.158	-0.197	.552**	-.372*	1								
Fe	-0.039	-0.094	0.098	-0.041	0.027	-0.097	1							
Mn	0.318	0.105	-0.138	0.25	-0.144	-0.088	.480**	1						
Al	-0.165	-0.114	0.132	-.388*	0.26	-0.209	.777**	0.326	1					
Ni	.372*	-0.18	0.141	.442**	-.345*	0.32	.562**	.411*	.465**	1				
Cr	0.29	-0.068	0.037	0.275	-0.164	0.263	.586**	0.23	.534**	.679**	1			
Co	0.184	-0.043	0.023	0.103	-0.074	0.07	.748**	0.324	.708**	.732**	.785**	1		
Zn	-0.006	0.047	-0.046	-0.202	0.19	-0.009	.703**	0.183	.787**	.601**	.709**	.807**	1	
Pb	.617**	-0.123	0.057	.856**	-.608**	.494**	0.257	.400*	0.013	.724**	.566**	.506**	0.174	1

** Correlation is significant at the 0.01 level (2-tailed). * Correlation is significant at the 0.05 level (2-tailed).
number of samples = 33

Further, TOC and clay content alone cannot be a decisive factor in the mechanism of metal accumulation in sediments. TP showed significant positive correlation with sand ($r = 0.36$), TOC ($r = 0.55$) and Pb ($r = 0.49$) in middle estuary (S-45). The significant positive association between sand and Mn ($r=0.45$) in lower estuary (S-62) is attributed to Mn oxide coatings on the sand grains (Badr et al 2009). The mudflat sediments are dominated by finer components which consist of larger surface-active fractions and Fe–Mn oxide coating. The Fe–Mn oxides provide metal adsorbing sites and are known to co-precipitate trace elements (Carman et al 2007). Strong relationship of trace metals with Fe–Mn therefore indicates that they are associated with Fe–Mn oxyhydroxides (Chatterjee et al 2007; Jonathan et al 2010) (Table 3.2a.2; Table 3.2a.3). Inter-relationships among metals in lower

and middle estuary indicated a common source or a similar enrichment mechanism at their respective places. Further, good association of metals with Al indicates that these metals have terrigenous origin. Thus, in addition to Fe–Mn oxyhydroxides and aluminosilicates, nature as well as texture of the sediments, i.e. clay, silt or sand, organic carbon is important factors controlling the distribution and fate of metals along lower and middle estuary.

3.2A.10 Enrichment factor (EF) and geoaccumulation index (I_{geo})

Figure 3.2a.13 and Figure 3.2a.14 shows EF plots of metals. In the present study, EF value of nearly all elements (except Mn in core S-62 and S-45 and Ni in zone 1 and 2 of core S-45) is greater than 1.5 suggesting anthropogenic input. Cr, Co and Pb show high EF values in both the cores.

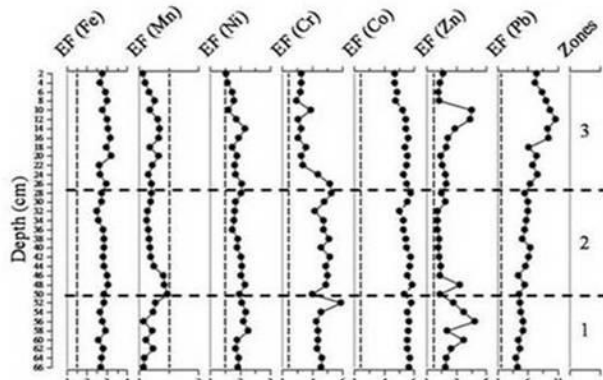


Figure 3.2a.13 Downcore variation of enrichment factor for core S-62

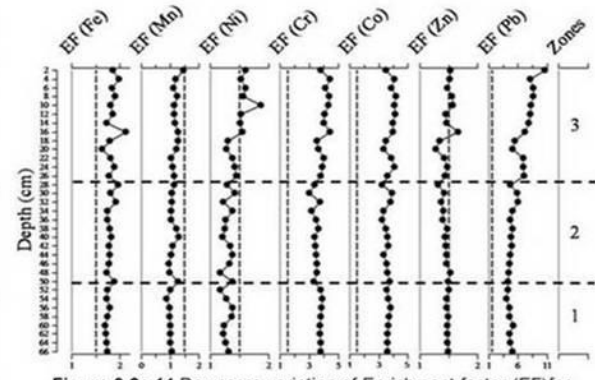


Figure 3.2a.14 Downcore variation of Enrichment factor (EF) for core S-45

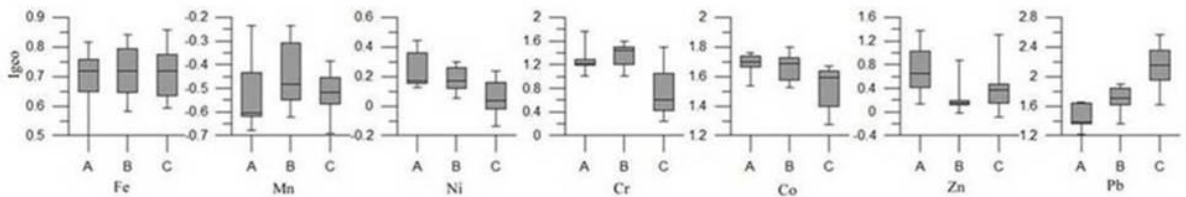


Figure 3.2a.15 Box and Whisker plot of Index of geo-accumulation (I_{geo}) in zone 1 (A), zone 2 (B) and zone 3 (C) for core S-62

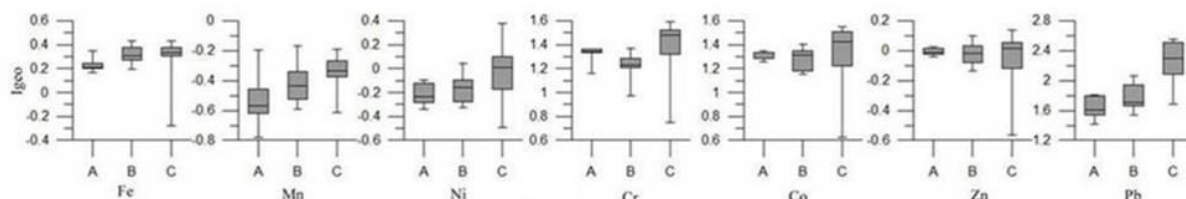


Figure 3.2a.16 Box and Whisker plot of Index of geo-accumulation (I_{geo}) in zone 1 (A), zone 2 (B) and zone 3 (C) for core S-45

The average geo-accumulation index (I_{geo}) computed for the metals studied along Kundalika estuary is presented in Figure (Figure 3.2a.15; Figure

3.2a.16). The average Igeo for Ni and Zn falls in class 0 and class 1 in core S-45 and S-62 respectively, suggesting that sediments are within background with respect to Ni and Zn in middle estuary (S-45) and unpolluted to moderately polluted in lower estuary (S-62). In core S-45 and S-62 (Figure 3.2a.15; Figure 3.2a.16), the average Igeo for Fe falls in class 1 in zone 1, 2 and 3 while Pb falls in class 2 in zone 1 and 2 and in class 3 in zone 3 reflecting that estuary is unpolluted to moderately polluted with Fe and moderately to strongly polluted with Pb. The average Igeo for Cr in zone 1, 2 and 3 of core S-45 and zone 1, 2 of core S-62 falls in class 2 indicating that sediments are moderately polluted, average Igeo for Cr in zone 3 of core S-62 falls in class 1 reflecting decrease in Cr contamination over the years. In core S-45, average Igeo for Mn falls in class 0 in zone 1 and 3, class 1 in zone 2 while in core S-62 in class 0 in zone 1 and 3 and class 1 in zone 2. The possible sources of anthropogenic input of metals into the river are (1) domestic waste directly discharged into the river without any treatment (2) accidental discharges of effluents directly or indirectly into the river through nallas, from industrial areas (3) unauthorized disposal of hazardous waste and (4) washing of chemical tankers in the river (Maharashtra Pollution Control Board 2004–2005; Maharashtra Pollution Control Board 2002–2003; Dandekar 2010).

3.2A.11 Factor analysis

In the lower estuary (S-62), the four factors (F1, F2, F3 and F4) correspond to 76.11%. F1, F2, F3, F4 account for 26.91%, 18.29%, 16.64% and 14.28% respectively (Table 3.2a.4). In middle estuary (S-45), the four factors correspond 83.38% with F1, F2, F3 and F4 explaining 32.19%, 27.08%, 15.26% and 8.85% respectively (Table 3.2a.5). In lower estuary (S-62) F1 showed significant loadings on Ni (0.82), Cr (0.77) and Co (0.72) and in F2 clay (0.85) and Al (0.72) showed significant loadings. Fe (0.89) and Mn (0.79) showed significant loadings in F3 and, in F4 TOC (0.61) and Zn (0.69) showed significant loadings (Table 3.2a.4; Table 3.2a.5).

Table 3.2a.4 R-mode factor analysis for core S-62

Factor	F1	F2	F3	F4
Variance (%)	26.905	18.289	16.639	14.279
Sand	-0.089	-0.039	0.472	-0.766
Silt	-0.269	-0.898	0.085	0.14
Clay	0.288	0.849	-0.285	0.205
TOC	-0.4	-0.182	-0.271	0.606
pH	-0.946	-0.168	-0.034	0.001
TN	0.064	0.122	-0.099	-0.583
Fe	-0.022	0.085	0.888	0.134
Mn	0.238	-0.108	0.794	-0.208
Al	0.114	0.72	0.375	-0.039
Ni	0.82	0.114	0.342	0.169
Cr	0.766	0.363	0.106	-0.242
Co	0.719	0.464	0.378	0.08
Zn	0.085	0.225	0.133	0.686
Pb	-0.832	-0.088	0.29	0.133
Loadings highlighted in bold are >0.6 significant at p<0.05				

Table 3.2a.5 R-mode factor analysis for core S-45

Factor	F1	F2	F3	F4
Variance (%)	32.19	27.08	15.26	8.85
Sand	0.026	0.724	0.097	0.212
Silt	-0.043	-0.085	0.984	0.017
Clay	0.04	0.008	-0.992	-0.039
TOC	-0.078	0.948	-0.046	0.059
pH	0.067	-0.69	0.203	0.04
TP	0.067	0.659	0.264	-0.499
Fe	0.824	-0.045	-0.084	0.338
Mn	0.269	0.273	0.136	0.862
Al	0.855	-0.327	-0.103	0.204
Ni	0.716	0.536	-0.119	0.097
Cr	0.82	0.349	0.003	-0.104
Co	0.916	0.181	0.001	0.081
Zn	0.934	-0.128	0.09	-0.048
Pb	0.33	0.898	-0.052	0.11
Loadings highlighted in bold are >0.6 significant at p<0.05				

In the middle estuary (S-45) (Table 3.2a.5) F1 showed significant loadings on Fe (0.82), Al (0.86), Ni (0.72), Cr (0.82), Co (0.92) and Zn (0.93); F2 showed significant loadings on sand (0.72), TOC (0.95), TP (0.66) and Pb (0.90); F3 showed significant loadings on silt (0.98) and F4 showed significant loadings on Mn (0.86).

F3 in lower estuary (S-62) can be called Fe-Mn controlled factors. In middle estuary (S-45), Al and Fe played major role in trace metal distribution (Ni, Cr, Co and Zn). Factor 1 in middle estuary can be called Fe-Al controlled factor. In lower estuary (S-62) Al showed significant loadings with clay. Fe and Al are the major component of silica minerals that are the products of rock and soil weathering on land (Zhou et al. 2004). This group can be called as a lithogenic group, as the variability of these elements appears to be controlled by terrestrial and natural sources. However, in the lower estuary (S-62) Ni, Cr and Co are grouped together in Factor 1 and showed no significant association with Fe, Mn or Al. The weak correlations of these trace metals with Fe, Mn and Al suggest different source. The significant association of these metals among each other suggest common source possibly anthropogenic such as industrial and agricultural activities. In the lower estuary (S-62) and middle estuary (S-45) organic matter (total organic carbon, total nitrogen and total phosphorous) seems to play minor role in distribution of metals except for Zn and Pb in lower (S-62) and middle (S-45) estuary respectively where they show good association.

3.2B Mangroves

3.2B.1 Collection of sediment cores

Amongst three cores, S-47 was collected from lower estuary while S-42 and S-40 were collected representing lower middle and upper middle estuarine regions respectively (Figure 3.2). The core length varied between 82 cm in S-47, 84 cm in S-42 and 80 cm in S-40. The cores S-47, S-42 and S-40 were analyzed for sediment grain size and TOC; S-42 and S-40 were also analyzed for pH; S-47 and S-40 were analyzed for metals while S-47 was analyzed for TN.

3.2B.2 Colour

The colour was uniform brown in S-47 and S-42 and uniform grey in S-40.

3.2B.3 Sediment grain size

The data showed a range of 0.3 to 8.13% with a mean of 3.29% sand, 20.62 to 86.7% with a mean of 53.83% silt, 9.2 to 72.4% with a mean of 42.88% clay for core S-47; 0.06 to 2.82% with a mean of 0.68% sand, 6.4 to 69.53% with a mean of 35.12% silt and 30.24 to 92.64% with a mean of 64.2% clay for core S-42 and 0.13 to 18.47% with a mean of 2.30% sand, 5.01 to 50.06% with a mean of 30.49% silt and 49.16 to 91.72% with a mean of 67.21% clay for core S-40. Each core has been divided into three zones depending upon the distribution pattern of sediment components namely zone 1, 2 and 3 wherein zone 3 represents recent sediments. The mean and standard deviation of sediment grain size in each zone for cores S-47, S-42 and S-40 are given in table 3.2b.

Table 3.2b Mean and standard deviation (values in parenthesis) of different parameters in each zone for core S-47, S-40 and S-42. The p-value denotes results of one-way ANOVA statistically significant at $p < 0.05$. n = number of samples.

Core S-47				
	Zone 1 (82-50 cm) n=17	Zone 2 (50-28 cm) n=12	Zone 3 (28-0 cm) n=14	p value (*statistically significant at $p < 0.05$)
	Mean (Standard deviation)	Mean (Standard deviation)	Mean (Standard deviation)	
Sand (%)	3.94±1.8	2.06±2.11	3.61±2.59	0.07
Silt (%)	57.76±19.85	48.27±15.14	52.23±11.04	0.29
Clay (%)	38.31±18.84	49.66±13.65	44.16±10.32	0.15
TOC (%)	0.92±0.19	1.03±0.15	1.24±0.20	*0.00
TN (%)	0.27±0.10	0.21±0.03	0.19±0.02	*0.00
C/N	3.65±1.25	5.08±0.94	6.57±1.43	*0.00
pH	7.37±0.04	7.82±0.27	7.93±0.10	*0.00
Fe (%)	8.21±0.38	7.93±0.35	8.48±0.53	*0.01
Mn (ppm)	760.00±50.07	722.83±58.60	773.57±61.03	0.07
Al (%)	7.04±0.25	7.53±0.29	7.53±0.34	*0.00
Ni (ppm)	104.12±9.56	97.08±11.50	96.29±6.61	*0.047
Cr (ppm)	238.37±15.19	224.36±9.70	220.74±25.92	*0.03
Co (ppm)	62.16±2.40	58.67±2.98	60.55±3.39	*0.01
Zn (ppm)	130.69±4.70	130.97±4.43	130.71±4.10	0.98
Pb (ppm)	105.61±7.98	119.86±11.49	120.24±19.24	*0.01
Core S-40				
	Zone 1 (80-40 cm) n= 21	Zone 2 (40-22 cm) n = 10	Zone 3 (22-0 cm) n= 11	p value (*statistically significant at $p < 0.05$)
	Mean (Standard deviation)	Mean (Standard deviation)	Mean (Standard deviation)	
Sand (%)	0.60±0.41	2.44±2.95	5.19±6.63	*0.01
Silt (%)	31.84±13.37	29.46±6.02	29.83±13.11	0.84
Clay (%)	67.56±13.22	68.10±7.47	64.99±10.55	0.79
TOC (%)	1.33±0.29	1.91±0.37	1.94±0.21	*0.00
pH	7.04±0.45	6.42±0.12	6.63±0.11	*0.00
Fe (%)	8.83±0.45	9.34±0.45	9.37±0.53	*0.00
Mn (ppm)	954.67±108.63	1002.50±37.11	1171.80±100.18	*0.00
Al (%)	9.01±0.59	9.15±0.50	9.26±0.32	*0.40
Ni (ppm)	99.62±13.19	109.93±8.65	97.91±10.06	*0.04
Cr (ppm)	212.63±19.34	282.80±7.56	290.97±6.42	*0.00
Co (ppm)	108.11±4.40	95.17±7.29	82.97±4.17	*0.00
Zn (ppm)	156.51±18.84	162.00±8.89	156.88±9.29	0.61
Pb (ppm)	84.73±35.13	104.00±19.60	106.12±16.99	0.08
Core S-42				
	Zone 1 (84-34 cm) n=26	Zone 2 (34-10 cm) n=13	Zone 3 (10-0 cm) n=5	
	Mean (Standard deviation)	Mean (Standard deviation)	Mean (Standard deviation)	
Sand (%)	0.43±0.26	0.75±0.15	1.80±0.68	
Silt (%)	37.02±17.13	29.43±3.79	36.56±6.82	
Clay (%)	62.55±17.10	69.82±3.85	61.64±6.88	
TOC (%)	1.46±0.27	1.41±0.11	1.75±0.23	
pH	7.54±0.38	7.56±0.41	7.49±0.19	

In zone 1 of core S-47 (Figure 3.2b.1) between 74 and 54 cm, sand decreases, silt is relatively higher while clay percentage is relatively low compensating each other (Figure 3.2b.1). In zone 2, sand is low while silt and clay fluctuates around average line. In zone 3, silt percentage increases while clay percentage decreases. Sand percentage increases between 28 and 18 cm and then decreases further up to 6 cm before showing increasing trend towards surface. When the average values of the different components are compared with the distribution profiles of respective sections, they also support the division into three zones described above.

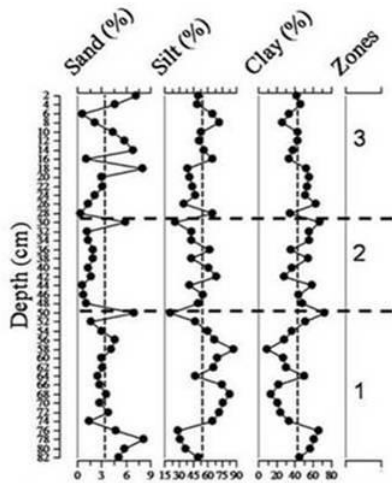


Figure 3.2b.1 Down-core variation of sediment grain size in different zones with zone 1 representing bottom while zone 3 represents the top for core S-47. The vertical line represents average value.

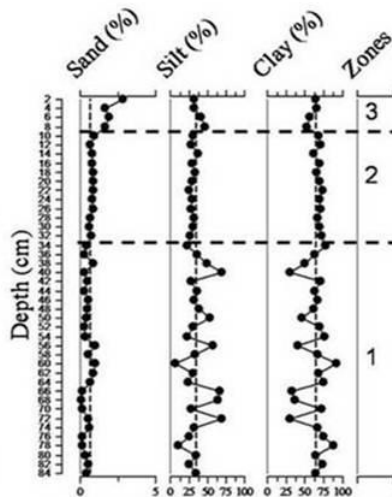


Figure 3.2b.2 Down-core variation of sediment grain size in different zones with zone 1 representing bottom while zone 3 represents the top for core S-42. The vertical line represents average value.

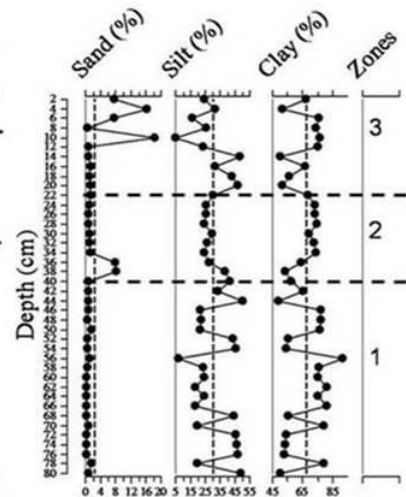


Figure 3.2b.3 Down-core variation of sediment grain size in different zones with zone 1 representing bottom while zone 3 represents the top for core S-40. The vertical line represents average value.

In the core S-42 collected from lower region of middle estuary, in zone 1, silt and clay fluctuate compensating each other while in zone 2 and 3 they showed uniform distribution (Figure 3.2b.2). Sand maintains constant trend in zone 1 and 2 with values below average line in zone 1 and values on average line in zone 2. However, in zone 3 (10 to 0 cm), sand shows increasing trend with values falling above average line.

In zone 1 of core S-40 from 80 to 54 cm silt decreases while clay increase. In zone 2 silt and clay showed uniform distribution with values falling near the average line. In zone 3, silt and clay fluctuate near the average line. Sand showed a constant trend in zone 1 and 2. In zone 3 i.e. from 12 cm up to surface sand fluctuates with values above the average line (Fig 3.2b.3).

The major difference amongst the three cores is that core collected from lower estuary is dominated by silt component whereas cores collected from middle estuary are dominated by clay component. The fine sediment namely silt and clay constitutes more than 95% in all the three cores. This is attributed to the mangrove vegetation which is associated with a unique horizontal root network (Kumaran et al 2004) that enhances the deposition of fine grained suspended sediments and prevents re-suspension and erosion of fine sediments (Soto-Jimenez and Paez-Osuna 2001).

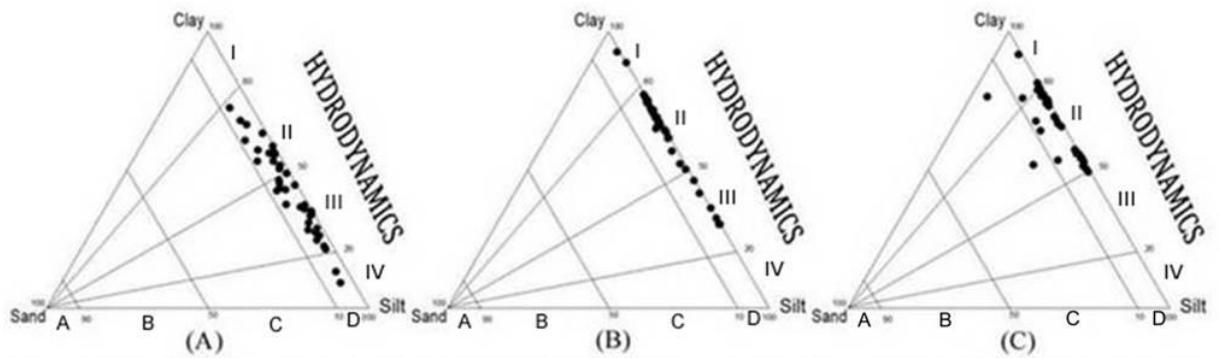


Figure 3.2b.4 Ternary diagram for the classification of hydrodynamic condition after Pejrup (1988) for core S-47 (A), S-42 (B) and S-40 (C)

The hydrodynamic plots (Pejrup 1988) reveals that the cores collected from lower estuary (S-47) and lower region of middle estuary (S-42) falls largely within III and II sections indicating that sediment deposition took place under relatively violent to less violent conditions (Figure 3.2b.4). However, the sediments in the upper middle estuary (S-40) falls largely within sections II indicating that sediment deposition took place under less violent conditions. The cores (S-47, S-42 and S-40) fall within D type, suggesting presence of poor sand and high concentration of silt and clay components, in lower and middle estuary.

3.2B.4 Nutrients (TOC and TN)

The data showed a range of 0.47 to 1.71% with a mean of 1.05% TOC and 0.15 to 0.56% with a mean of 0.23% TN for core S-47; 1.21 to 2.67% with a mean of 1.48% TOC for core S-42 and 0.95 to 2.46% with a mean of 1.63% TOC for core S-40. The mean and standard deviation of TN, TP and TOC in each zone are given in table 3.2b.

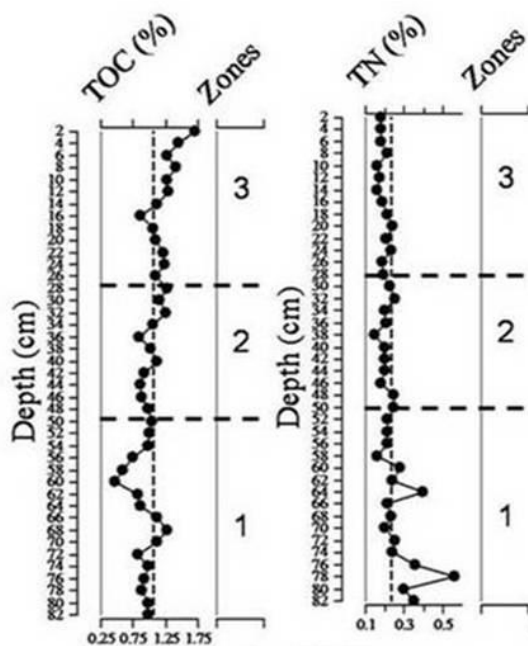


Figure 3.2b.5 Down-core variation of TOC and TN in different zones with zone 1 representing bottom while zone 3 represents the top for core S-47. The vertical line represents average value.

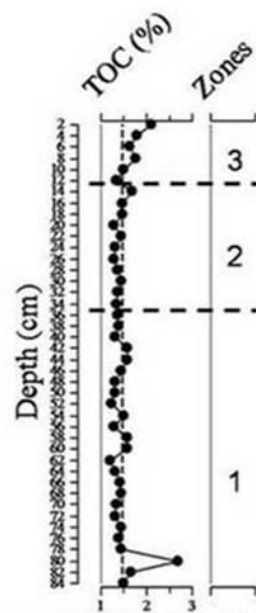


Figure 3.2b.6 Down-core variation of TOC in different zones with zone 1 representing bottom while zone 3 represents the top for core S-42. The vertical line represents average value.

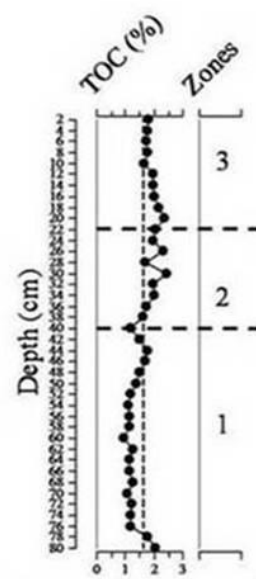


Figure 3.2b.7 Down-core variation of TOC in different zones with zone 1 representing bottom while zone 3 represents the top for core S-40. The vertical line represents average value.

TOC showed similar trend in all the three cores (S-47, S-42 and S-40) i.e. increases from zone 1 to zone 3. (Figure 3.2b.5; Figure 3.2b.6; Figure 3.2b.7). In the core S-47, collected from lower estuary, TOC is nearly constant with values falling near the average line except between 64–56 cm and 16–0 cm where TOC falls below and above the average line, respectively (Figure 3.2b.5). TN shows decreasing trend with values falling above average line in zone 1 and below average line in zone 2 and 3 (Figure 3.2b.5).

In core S-42 collected from lower region of middle estuary, TOC is constant with values falling near average line except from 10 to 0 cm where gradual increase is observed (Figure 3.2b.6). In core S-40 collected from upper middle estuary, in zone 1 TOC is constant with values below average line (Figure 3.2b.7). In zone 2, TOC increases and in zone 3 TOC decreases but values fall above the average line (Figure 3.2b.7).

3.2B.5 C/N ratio

C/N ratio in core S-47 ranged from 1.58 to 9.45 with a mean of 4.98 suggests greater marine influence. The C/N ratio in zone 1 falls below the average line, in zone 2 and 3 from 50 to 16 cm values are constant falling on the average line and from 16 to 0 cm C/N ratio increases with values above the average line (Figure 3.2b.8).

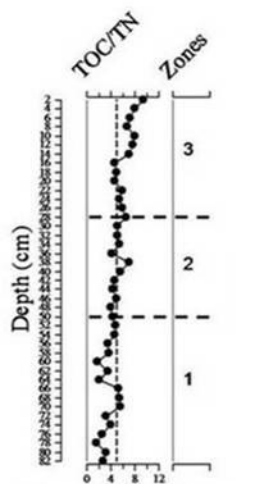


Figure 3.2b.8 Down-core variation of C/N ratio in different zones with zone 1 representing bottom while zone 3 represents the top for core S-47

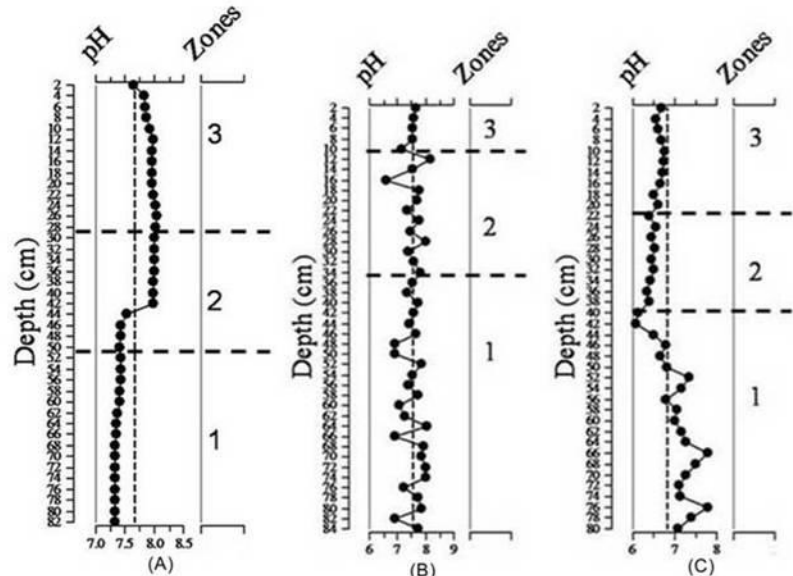


Figure 3.2b.9 Down-core variation of pH in different zones with zone 1 representing bottom while zone 3 represents top for core S-47 (A), S-42 (B) and S-40 (C). The vertical line represents average value.

3.2B.6 pH

pH showed a range of 7.33 to 8.04 with a mean of 7.68 for core S-47; 6.58 to 8.19 with a mean of 7.55 for core S-42 and 6.09 to 7.8 with a mean of 6.81 for core S-40. The mean and standard deviation of pH in each zone for cores S-47, S-42 and S-40 are given in table 3.2b.

In core S-42 pH varies around the average line in zone 1 and 2 and is relatively constant in zone 3. In core S-40 pH is mainly basic in zone 1 while slightly acidic in zone 2 and 3 (Figure 3.2b.9). In core S-47 pH is constant except for sudden increase at 44 cm depth.

3.2B.7 Major elements (Fe, Mn and Al)

The data showed a range of 7.39 to 9.59% with a mean of 8.23% Fe, 641.67 to 878 ppm with a mean of 756.7 ppm Mn and 6.66 to 8.21% with a mean of 7.33% Al for core S-47 and 8.01 to 10.46% with a mean of 9.08% Fe, 839 to 1302.67 ppm with a mean of 1025 ppm Mn and 7.64 to 9.87% with a mean of 9.08% Al for core S-40. The mean and standard deviation of Fe, Mn and Al in each zone are given in table 3.2b.

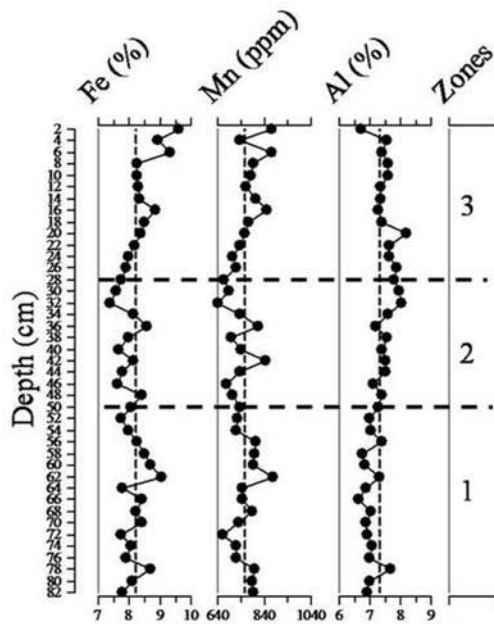


Figure 3.2b.10 Downcore variation of major elements (Fe, Mn and Al) in different zones with zone 1 representing bottom while zone 3 represents the top for core S-47. The vertical line represents average value.

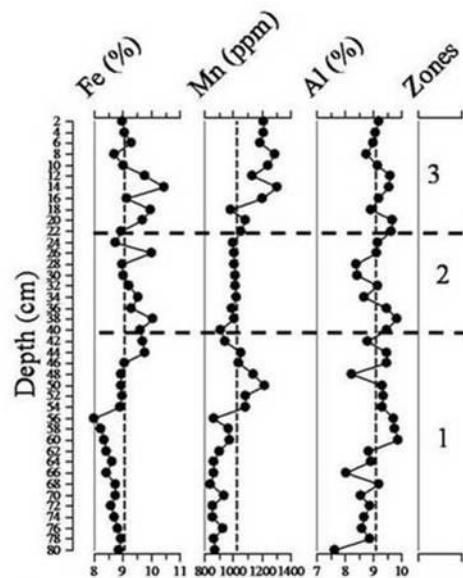


Figure 3.2b.11 Downcore variation of major elements (Fe, Mn and Al) in different zones with zone 1 representing bottom while zone 3 represents the top for core S-40. The vertical line represents average value.

In the core S-47 collected from lower estuary, in zone 1, Fe and Mn generally fluctuate around average line while Al is lower than their average values (Figure 3.2b.10). In zone 2, Al increases with values more than average while Fe and Mn concentration decreases with values less than their respective averages. In zone 3, Al content decreases while Fe and Mn concentration increase with values mostly more than their respective averages. The vertical profiles of Fe and Mn show enrichment in the top section of zone 3 (20–0 cm) (Figure 3.2b.10) due to early diagenetic process. Klinkhammer et al (1982) stated that Fe^{+2} and Mn^{+2} species get precipitated in the top layers in mangrove sediments as these elements diffuse upwards. The synchronous decrease of Fe and Mn profile between 32 and 20 cm (Figure 3.2b.10), suggests oxic/sub-oxic interface (Santschi et al 1990).

The core S-40 collected from middle estuary, in zone 1, Fe and Mn is less than their respective average up to 56 cm (Figure 3.2b.11). In zone 2 and 3, Fe decreases with values above average line. Mn concentration decreases from 50 to 40 cm, remains constant from 40 to 16 cm and increases from 16 to 0 cm. Al fluctuates around average line in zone 1, 2 and 3 with an overall increasing trend (Figure 3.2b.11). The variability in Al profile probably reflect influence of terrigenous and authogenic material supply (Badr et al 2009).

3.2B.8 Trace elements (Ni, Cr, Co, Zn and Pb)

In core S-47 (Figure 3.2b.12), Ni ranges from 86 to 128 ppm with a mean value of 99 ppm; Cr ranges from 170 to 279 ppm with a mean value of 229 ppm; Co ranges from 54 to 66 ppm with a mean value of 61 ppm; Zn concentration ranges from 124 to 140 ppm with a mean value of 131 ppm and Pb ranges from 95 to 182 ppm with a mean value of 114 ppm. The average values of trace metal concentrations displayed the following order, Cr > Zn > Pb > Ni > Co. In zone 1, Ni, Cr, Co and Zn to some extent is higher while Pb shows lower than their respective averages. Ni and Cr show decreasing trend while Pb increases, Co and Zn show large fluctuations with overall decreasing trend (Figure 3.2b.12). In zone 2, Ni, Co and Zn display an overall decreasing pattern while Cr and Pb show constant trend. In zone 3, Ni, Co, Zn and to some extent Pb show an increasing trend while Cr decreases with large variations. A fluctuating trend with metal enrichment in the top section (0–28 cm) is observed in this core. Zorana et al (2009) stated that metal enrichment in the upper layer is not necessarily due to anthropogenic input only. This enrichment also may be explained by the redox sensitive elements (Fe and Mn) which show similar increase toward the surface (20–0 cm). The fluctuating metal profile may be attributed to varying hydrodynamic energy conditions prevailing in upper flats as mentioned earlier as well as bioturbation by organisms associated with mangroves (Clark et al 1998; Gao 2009a).

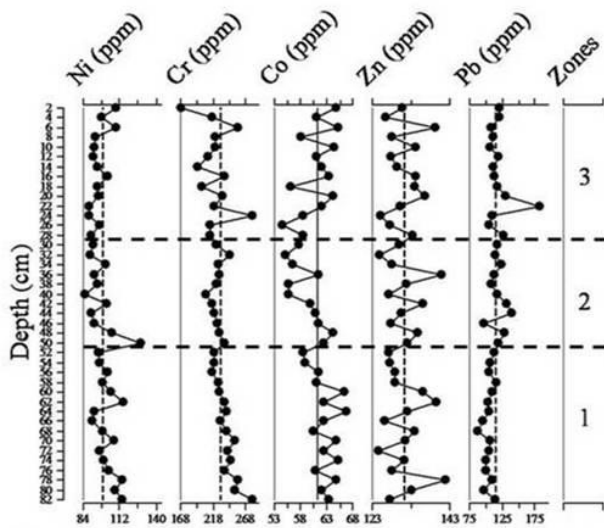


Figure 3.2b.12 Down-core variation of trace elements (Ni, Cr, Co, Zn and Pb) in different zones with zone 1 representing bottom while zone 3 represents the top for core S-47. The vertical line represents average value.

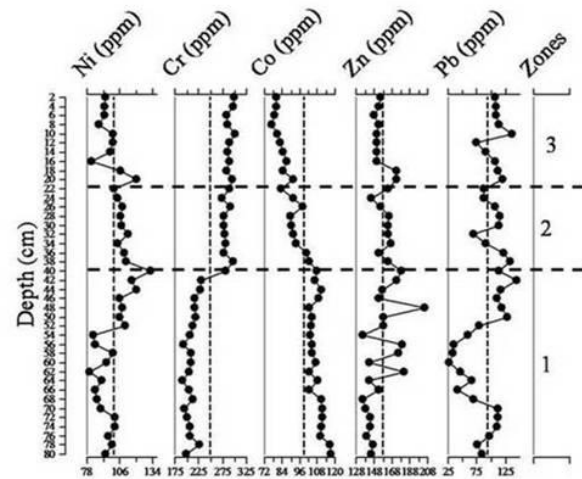


Figure 3.2b.13 Downcore variation of trace elements (Ni, Cr, Co, Zn and Pb) in different zones with zone 1 representing bottom while zone 3 represents the top for core S-40. The vertical line represents average value.

In core S-40 (Figure 3.2b.13), Ni ranges from 81 to 132 ppm with a mean value of 101 ppm; Cr ranges from 191 to 302 ppm with a mean value of 248 ppm; Co ranges from 77 to 117 ppm with a mean value of 99 ppm; Zn concentration ranges from 135 to 205 ppm with a mean value of 157 ppm and Pb ranges from 26 to 145 ppm with a mean value of 95 ppm. The average values of trace metal concentrations displayed the following order, Cr > Zn > Ni > Co > Pb. In zone 1, values of Ni, Zn and Pb vary around average line with fluctuations; Cr shows values less than average and Co values fall above average line. Except for Co which shows decreasing trend, other metals studied show increasing trend. In zone 2, metals except Cr show decreasing trend. In zone 3, metals except Zn and Cr show decreasing trend. Zn and Cr remain constant.

3.2B.9 Paired t-test analysis

Paired t-test analysis ($p < 0.05$) indicated significant differences in the distribution of silt, clay, TOC, Fe, Mn, Al, Cr, Co, Zn and Pb (Table 3.2b.1).

Table 3.2b.1 Summary of Paired sample t-test comparing core S-47 and S-40

Variables	Paired Differences	t	df	Sig. (2-tailed)
sandS47 - sandS40	0.94151	1.334	39	0.19
SiltS47 - siltS40	23.452	6.986	39	0
ClayS47 - clayS40	-24.3935	-7.472	39	0
TOCS47 - TOCS40	-0.57387	-9.588	39	0
FeS47 - FeS40	-0.84091	-7.058	39	0
MnS47 - MnS40	-269.167	-12.64	39	0
AlS47 - AlS40	-1.74481	-18.176	39	0
NiS47 - NiS40	-2.1	-0.799	39	0.429
CrS47 - CrS40	-20.3917	-2.557	39	0.015
CoS47 - CoS40	-37.95	-20.332	39	0
ZnS47 - ZnS40	-26.4583	-11.265	39	0
PbS47 - PbS40	19.2333	4.04	39	0

3.2B.10 Correlation

Concentrations and vertical distributions of trace metals in sediment may be controlled by numerous factors such as particle size (granulometric composition), mineral composition of sediments, carrier substances (e.g. hydroxides, carbonates, sulfides), sediment surface area, organic matter content, individual and combined effects of Eh and pH, etc. (Förstner and Wittmann 1979; Zorana et al 2009). In core S-47 and S-40, most of the trace metals show good correlation with Fe and Mn (Table 3.2b.2; Table 3.2b.3). This suggests the possible role of Fe and Mn as carrier of trace metals. Fe-Mn oxyhydroxides are known to scavenge trace metals from solution, before or during the diagenesis (Chester and Hughes 1967; Salomons and Förstner 1984). In core S-40, Ni exhibited different level of significance of correlation with Fe and Mn. For instance, Ni showed good correlation with Fe ($r=0.56$) and weak correlation with Mn ($r=-0.01$). This may be strongly influenced by redox conditions (Zwolsman et al 1996). Similar weak correlation of Ni with Mn and good correlation with Fe in sediments was also observed by Magesh et al (2011) from Tamiraparani estuary, southeast coast of India. Zn showed weak correlation with both Fe ($r=0.13$) and Mn ($r=0.06$).

Table 3.2b.2 Pearson correlation coefficient for core S-47

	Sand	Silt	Clay	TOC	pH	TN	Fe	Mn	Al	Ni	Cr	Co	Zn	Pb
Sand	1													
Silt	-.341*	1												
Clay	0.21	-.991**	1											
TOC	0.119	-0.152	0.141	1										
pH	-0.176	-0.19	0.223	.441**	1									
TN	.329*	-.329*	0.294	-0.288	-.484**	1								
Fe	0.266	0.251	-0.299	0.165	-0.012	-0.09	1							
Mn	0.26	0.299	-.349*	-0.032	-0.025	0	.768**	1						
Al	-0.139	-.445**	.484**	0.294	.709**	-0.093	-0.2	-0.238	1					
Ni	.388*	-0.12	0.068	-0.192	-.502**	.364*	.440**	.440**	-0.284	1				
Cr	-0.161	-0.005	0.029	-0.262	-.336*	.496**	-0.182	-0.11	-0.047	0.28	1			
Co	0.188	0.212	-0.248	-0.2	-.523**	.336*	.479**	.408**	-.450**	.455**	0.242	1		
Zn	0.071	0.038	-0.05	-0.222	-0.012	0.266	.526**	.570**	0.096	.411**	0.084	.442**	1	
Pb	-0.075	-0.248	0.269	0.146	.422**	-0.16	-0.001	-0.048	.413**	-0.169	-0.259	-0.059	0.04	1

*. Correlation is significant at the 0.05 level (2-tailed). ** . Correlation is significant at the 0.01 level (2-tailed).

Table 3.2b.3 Pearson correlation coefficient for core S-40

	Sand	Silt	Clay	TOC	pH	Fe	Mn	Al	Ni	Cr	Co	Zn	Pb
Sand	1												
Silt	-0.296	1											
Clay	-0.054	-.938**	1										
TOC	0.134	0.078	-0.13	1									
pH	-0.246	0.047	0.04	-.574**	1								
Fe	0.125	.382*	-.445**	.592**	-.573**	1							
Mn	.431**	-0.119	-0.032	.387*	-.381*	.368*	1						
Al	0.141	0.004	-0.055	-0.037	-0.294	0.218	0.247	1					
Ni	-0.019	0.3	-0.307	0.291	-.580**	.559**	-0.007	0.218	1				
Cr	.483**	-0.047	-0.127	.736**	-.701**	.630**	.601**	0.253	.322*	1			
Co	-.456**	0.253	-0.099	-.557**	.477**	-0.304	-.746**	-0.159	0.081	-.814**	1		
Zn	-0.07	-0.198	0.232	0.146	-.475**	0.134	0.056	0.038	.405**	0.154	-0.129	1	
Pb	.359*	0.183	-.322*	.397*	-.532**	.550**	.374*	-0.121	.517**	.471**	-0.22	0.096	1

** . Correlation is significant at the 0.01 level (2-tailed). * . Correlation is significant at the 0.05 level (2-tailed).

In addition, most trace metals showed weak correlation with Al in both cores (S-47 and S-40), except for Pb in S-47 (Table 3.2b.2; Table 3.2b.3). The Al content is considered as a good indicator of the amount of fine material (Windom et al 1989; Loring 1991; Din 1992) and is primary source of aluminosilicate minerals. The weak correlation with majority of trace elements probably suggests that metals are not bound to aluminosilicates.

Most of the metals show good positive relationship with organic carbon in core S-40 (Table 3.2b.3). Organic matter is an important controlling factor in the abundance of trace metals (Rubio et al 2000). Salomans and Foerstner (1984) suggested that during initial deposition, trace metals may become associated with organic particulate matter. The strong positive correlation of organic carbon with Cr (r=0.74), Fe (r=0.59), Pb (r=0.40) and Mn (0.39)

suggest adsorption and complexation of metals in the form of organometallic complexation in sediments (Marchand et al 2006; Samuel and Phillips 1988).

The positive correlation of Mn ($r=0.43$), Cr ($r=0.48$) and Pb ($r=0.36$) with sand and Fe ($r=0.38$) with silt in core S-40 (Table 3.2b.3) suggest that granulometric composition also control concentrations of metals in sediment (Foerstner and Wittmann 1979).

3.2B.11 Factor analysis

The four factors (F1, F2, F3 and F4) explained 74.02% and 77.73% of the total variance in lower (S-47) and middle (S-40) estuary respectively (Table 3.2b.4). F1, F2, F3 and F4 account for 22.59%, 18.36%, 17.90% and 15.17% respectively in core S-47 and 27.93%, 21.52%, 19.41% and 8.87% respectively in core S-40 (Table 3.2b.5).

In lower estuary (S-47), F1 showed significant positive loadings on Fe (0.87), Mn (0.87), Ni (0.61), Co (0.63) and Zn (0.79); F2 on pH (0.80), Al (0.86) and Pb (0.63); F3 on clay (0.85) and sand (0.65) while F4 showed significant positive loadings on TN (0.61) and Cr (0.78) (Table 3.2b.4). In middle estuary (S-40) F1 showed significant positive loadings on sand (0.69), Mn (0.82) and Cr (0.84); F2 on Ni (0.83) and Zn (0.74), F3 on silt (0.93) while F4 showed significant loadings on Al (0.95) (Table 3.2b.5). The significant association of sand with metals may be attributed to the formation of oxide coating on the sand grain (Badr et al 2009).

Table 3.2b.4 R-mode factor analysis for core S-47

Factor	F1	F2	F3	F4
Variance (%)	22.591	18.362	17.902	15.169
Sand	0.328	-0.373	0.647	-0.325
Silt	0.176	-0.309	-0.903	-0.014
Clay	-0.231	0.375	0.846	0.062
TOC	-0.042	0.201	0.158	-0.662
pH	-0.111	0.804	-0.071	-0.442
TN	0.146	-0.229	0.537	0.613
Fe	0.873	-0.055	-0.106	-0.277
Mn	0.868	-0.063	-0.156	-0.142
Al	-0.166	0.855	0.233	-0.038
Ni	0.61	-0.338	0.365	0.256
Cr	-0.043	-0.106	0.06	0.78
Co	0.633	-0.344	-0.018	0.317
Zn	0.785	0.286	0	0.335
Pb	0.061	0.626	0.104	-0.146
Loadings highlighted in bold are >0.6 significant at p<0.05				

Table 3.2b.5 R-mode factor analysis for core S-40

Factor	F1	F2	F3	F4
Variance (%)	27.93	21.521	19.413	8.87
Sand	0.685	-0.107	-0.052	0.057
Silt	-0.213	0.05	0.933	0.002
Clay	-0.026	-0.013	-0.956	-0.023
TOC	0.584	0.454	0.16	-0.286
pH	-0.461	-0.781	-0.004	-0.108
Fe	0.41	0.558	0.525	0.036
Mn	0.821	0.047	0.009	0.126
Al	0.181	0.143	0.062	0.947
Ni	-0.07	0.829	0.334	0.105
Cr	0.838	0.411	0.107	0.043
Co	-0.893	-0.096	0.168	-0.027
Zn	-0.095	0.744	-0.384	0.028
Pb	0.414	0.465	0.365	-0.357
Loadings highlighted in bold are >0.6 significant at p<0.05				

3.2B.12 Isocon

When the distribution of metals is compared between the lower and middle estuary almost all the metals (except Pb) showed higher concentration in the middle estuary (S-40) along with TOC and clay. Sand and silt showed higher concentration in the lower estuary (S-47) (Figure 3.2b.14).

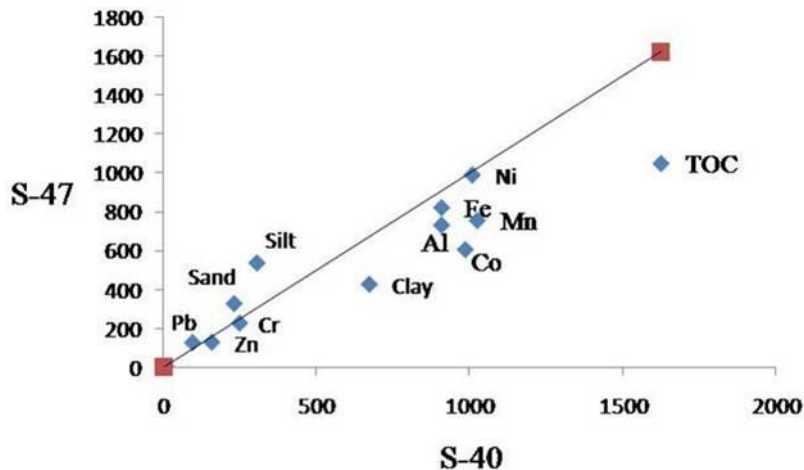


Figure 3.2b.14 Isocon diagram. Individual point represents average value.

When the distribution of metals along mudflats (S-62 and S-45) and mangroves (S-47 and S-40) is compared (Figure 3.2b.15, 3.2b.16), it is observed in the lower estuary average Mn, Cr, Zn, Ni, Co content is greater in the mudflat (S-62). On the other hand, in the middle estuary average Mn, Zn, Ni and Co content is greater in mangrove (S-40) in comparison to

mudflat sediments (S-45). The intertidal sediment is redistributed by tidal waters which carry suspended sediment from sub tidal to intertidal areas. Semeniuk (1981) stated that the mudflats are inundated by flowing tidal waters for 80 % of their time and for about 50% of the time in mangroves. Wave attenuation along with frequency of tidal inundation rate must be responsible for landward decrease in trace metals content.

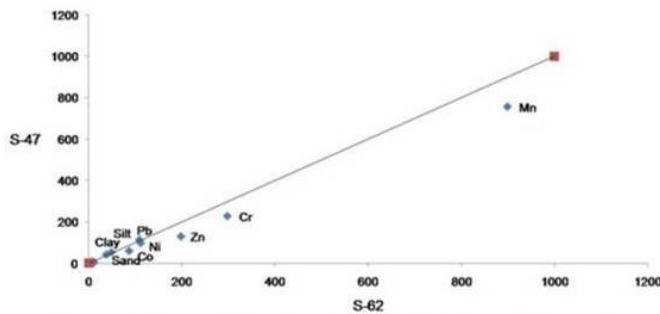


Figure 3.2b.15 Isocon diagram comparing mudflat (S-62) and mangrove (S-47) of lower estuary

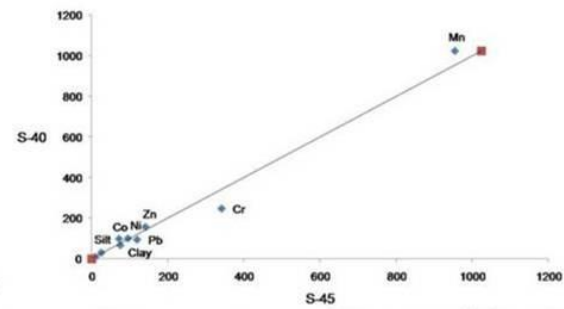


Figure 3.2b.16 Isocon diagram comparing mudflat (S-45) and mangrove (S-40) of middle estuary

3.2B.13 Conclusion

The grain size distribution across the lower and middle estuary is controlled by factors such as wave and tide-controlled hydrodynamics and anthropogenic activities including sand mining. Depth-wise distribution of organic carbon indicated enrichment in zone 3 (0–28 cm) at all the locations studied, possibly due to extensive use of fertilizers, population growth and urban waste. When the EF values are considered, nearly all elements (except Mn) show anthropogenic enrichment in Kundalika Estuary. In mudflats of middle estuary, organic carbon played a major role in the distribution of trace metals.

3.3 Rajapuri creek

Total three cores, two from mudflats (S-60 and S-61) and one from mangroves (S-65), were collected along Rajapuri creek (Figure 3.3).

3.3A Mudflats

3.3A.1 Collection of sediment cores

Amongst two mudflat cores, one represented lower channel of Mandad River (S-61) and other the main channel of Rajapuri creek (S-60). The core length varied from 74 cm in core S-61 to 98 cm in core S-60. The cores (S-60 and S-61) were analyzed for sediment grain size, TOC, TN, pH, metals and diatoms (Figure 3.3).

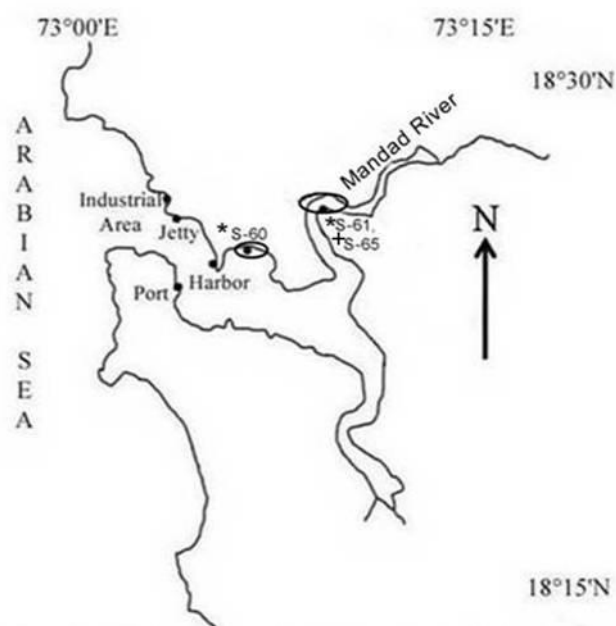


Figure 3.3 Study area with core location for Rajapuri creek
* Mudflat core + Mangrove core

3.3A.2 Colour

Colour variations from brown to light grey and dark grey to black were seen visually in both the cores from surface to bottom. Sediment colour was brown to light grey from 0 to 30 cm in core S-61 and from 0 to 39 cm in core S-60. The remaining part of the core (S-61 and S-60) was dark grey to black.

3.3A.3 Sediment grain size

The data showed a range of 1.67 to 18.42% with a mean of 7.73% sand, 23.47 to 58.27% with a mean of 34.53% silt, 37.44 to 72.4% with a mean of 57.74% clay for core S-61 and 0.1 to 36% with a mean of 4.96% sand, 19.62 to 93.52% with a mean of 43.60% silt and 6.12 to 77.92% with a mean of 51.41% clay for core S-60. Each core has been divided into two zones depending upon the distribution pattern of sediment components namely zone 1 and 2 wherein zone 2 represents recent sediments. The mean and standard deviation of sediment grain size in each zone for cores S-61 and S-60 are given in table 3.3.

Table 3.3 Mean and standard deviation (values in parenthesis) of different parameters in each zone for core S-61 and S-60. The p-value denotes results of one-way ANOVA statistically significant at $p < 0.05$.
N=number of samples.

Core S-61					
	Zone 1 (74-28 cm)		Zone 2 (28-0 cm)		p value (*statistically significant at $p < 0.05$)
	N	Mean(Standard deviation)	N	Mean (Standard deviation)	
Sand (%)	24	8.44 (± 4.80)	14	6.58 (± 0.97)	0.16
Silt (%)	24	36.13 (± 7.34)	14	31.69 (± 1.50)	*0.03
Clay (%)	24	55.43 (± 8.01)	14	61.73 (± 2.00)	*0.01
TOC (%)	24	3.33 (± 0.75)	14	1.97 (± 0.33)	*0.00
TN (%)	11	0.20 (± 0.06)	7	0.20 (± 0.07)	0.99
C/N	11	21.18 (± 4.68)	7	12.88 (± 4.10)	0.00
pH	24	7.48 (± 0.15)	14	7.41 (± 0.21)	0.23
Fe (%)	24	7.69 (± 1.13)	14	8.37 (± 0.72)	0.05
Mn (ppm)	24	505.9 (± 101.13)	14	645.62 (± 39.42)	*0.00
Al (%)	24	7.09 (± 0.69)	14	8.03 (± 0.36)	*0.00
Ni (ppm)	24	100.57 (± 11.06)	14	109.81 (± 10.30)	*0.02
Cr (ppm)	24	337.82 (± 59.89)	14	389.21 (± 74.93)	*0.03
Co (ppm)	24	61.82 (± 8.55)	14	70.07 (± 3.95)	*0.00
Zn (ppm)	24	72.47 (± 13.09)	14	82.45 (± 6.83)	*0.01
Pb (ppm)	24	72.47 (11.20)	14	76.02 (± 11.05)	0.35
S-60					
	Zone 1 (98-40 cm)		zone 2 (40-0 cm)		p value (*statistically significant at $p < 0.05$)
	N	Mean (Standard deviation)	N	Mean Standard deviation)	
Sand (%)	30	0.80 (± 0.78)	20	11.00 (± 9.46)	*0.00
Silt (%)	30	49.73 (± 26.18)	20	34.22 (± 5.89)	*0.01
Clay (%)	30	49.46 (± 25.93)	20	54.70 (± 6.51)	0.38
TOC (%)	30	3.23 (± 0.52)	20	2.60 (± 0.40)	*0.00
TN (%)	12	0.06 (± 0.02)	10	0.11 (± 0.02)	*0.00
C/N	12	84.86 (± 28.89)	10	32.72 (± 12.55)	*0.00
pH	30	7.27 (± 0.19)	20	7.03 (± 0.27)	*0.00
Fe (%)	30	5.13 (± 0.46)	20	7.98 (± 0.89)	*0.00
Mn (ppm)	30	663.77 (± 49.24)	20	700.12 (± 38.45)	*0.01
Al (%)	30	5.66 (± 0.42)	20	7.03 (± 0.83)	*0.00
Ni (ppm)	30	88.30 (± 11.08)	20	97.95 (± 10.38)	*0.00
Cr (ppm)	30	169.07 (± 14.43)	20	297.85 (± 44.99)	*0.00
Co (ppm)	30	42.89 (± 7.49)	20	65.92 (± 6.87)	*0.00
Zn (ppm)	30	76.19 (± 4.97)	20	101.08 (± 10.51)	*0.00
Pb (ppm)	30	68.34 (± 27.00)	20	53.98 (± 14.52)	*0.04

In core S-61 (Figure 3.3a.1), zone 1 is characterized by large variations in sand, silt and clay percentages. Sand percentage is relatively higher in this zone (average ~8%). In zone 2, from 28 to 10 cm, clay shows an overall increasing trend while silt and sand show an overall decreasing trend. From 10 cm to surface, clay shows an overall decreasing trend while sand and silt show an overall increasing trend. In core S-60 (Figure 3.3a.1), zone 1 is

characterized by the dominance of mud (silt+clay), sand percentage being very low (average <1%). Silt and clay show large variations in this zone. In zone 2, sand shows a rapid increase from 38 to 24 cm, with highest positive peak at 32 cm (average ~20%). Silt and clay values are less than their respective average value up to 16 cm. From 16 cm to surface, sand, silt and clay show almost uniform profiles.

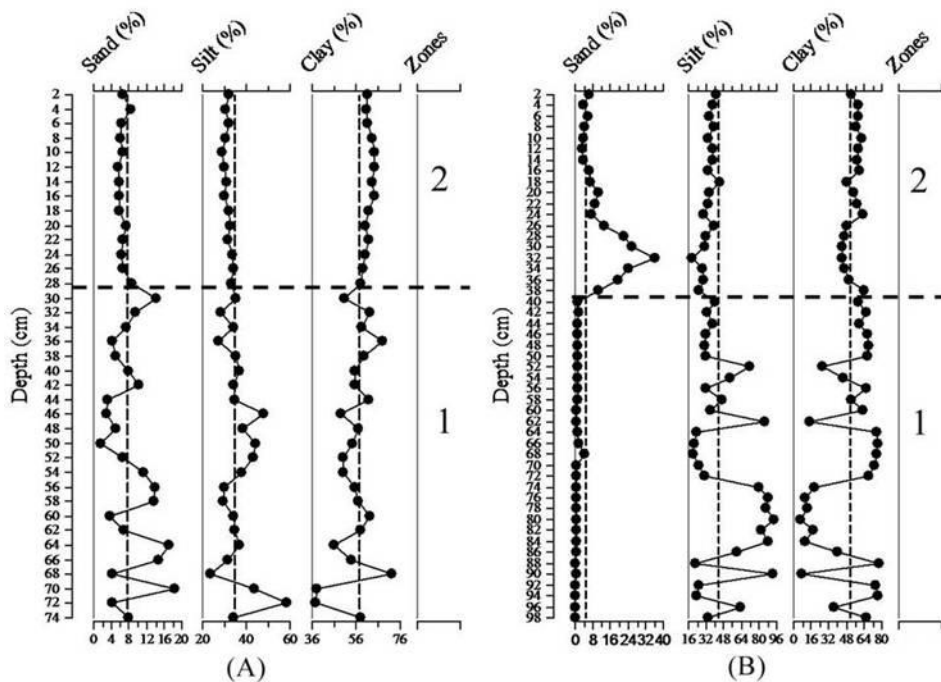


Figure 3.3a.1 Down-core variation of sediment grain size in different zones with zone 1 representing bottom while zone 2 represents the top for core (A) S-61 and (B) S-60. The vertical line represents average value.

To understand the hydrodynamic conditions of depositional environment ternary diagram proposed by Pejrup (1988) was plotted. Plot (Figure 3.3a.2) reveals that the core collected from the sub-channel (S-61) falls largely within section II indicating that sediment deposition took place under less violent condition while the core S-60 which was collected from main channel falls largely within sections IV, III and II indicating violent to less violent hydrodynamic conditions (Figure 3.3a.2).

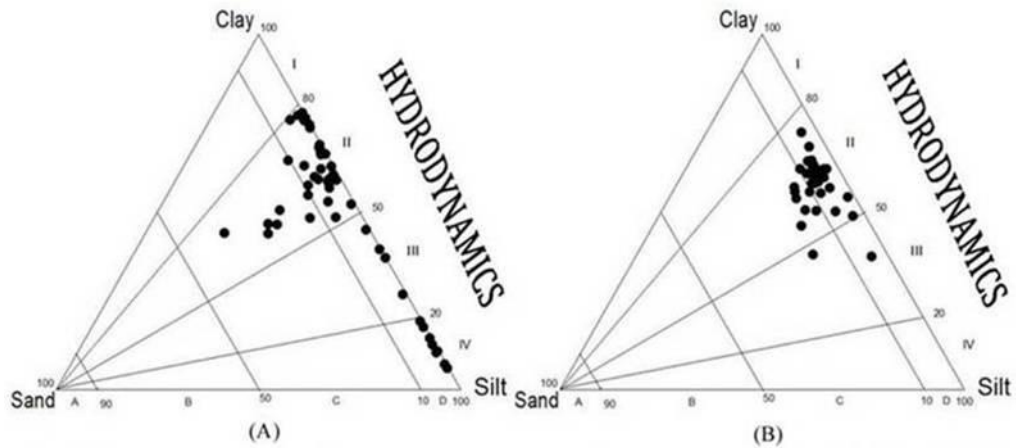


Figure 3.3a.2 Ternary diagram for the classification of hydrodynamic conditions after Pejrup (1988) for core S-60 (A) and S-61 (B)

3.3A.4 Nutrients (TOC and TN)

The data showed a range of 1.53 to 4.82% with a mean of 2.84% TOC and 0.14 to 0.32% with a mean of 0.20% TN for core S-61 and 1.64 to 4.59% with a mean of 2.97% TOC and 0.03 to 0.16% with a mean of 0.08% TN for core S-60. The mean and standard deviation of TOC and TN in each zone for cores S-61 and S-60 are given in table 3.3.

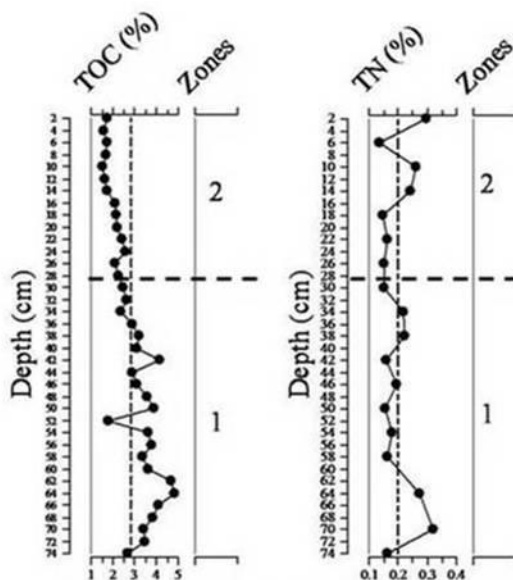


Figure 3.3a.3 Down-core variation of TOC and TN in different zones with zone 1 representing bottom while zone 2 represents the top for core S-61. The vertical line represents average value.

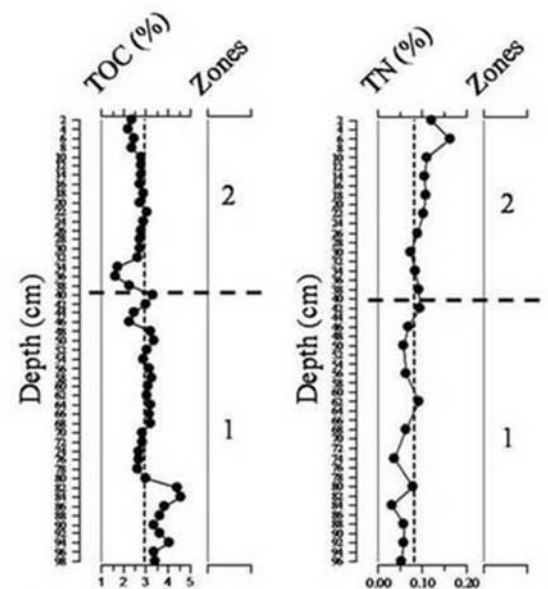


Figure 3.3a.4 Down-core variation of TOC and TN in different zones with zone 1 representing bottom while zone 2 represents the top for core S-60. The vertical line represents average value.

In zone 1 of core S-61 (Figure 3.3a.3) major portion of TOC fall above average line while in zone 2 TOC falls below average line. TN concentration is relatively higher in zone 1 (range 0.15-0.32%) (Figure 3.3a.3). In core S-60

(Figure 3.3a.4), zone 1 and 2, show a nearly constant trend for TOC except from 98 to 82 cm, where values fall above the average lines and from 46 to 32 cm and 10 cm to surface, where the values fall below the average lines. In zone 1, TN values fall below average line. In zone 2, TN concentration increases towards surface.

3.3A.5 C/N ratio

C/N ratio ranged from 7.44 to 29.61 with a mean of 17.95 for core S-61 and 16.49 to 147.91 with a mean of 61.16 for core S-60. The mean and standard deviation of C/N ratio in each zone are given in table 3.3. In core S-60 and S-61, in zone 1 (Figure 3.3a.5) major portion of C/N ratio falls above average line while in zone 2 C/N ratio fall below average line. The enhanced C/N ratio in all the samples in core S-60 (Figure 3.3a.5) may be due to deposition of terrestrially transported organic matter which contains vascular plant debris with lower nitrogen content since the site location of core S-60 is surrounded by reserved forest area. Hay et al (2009) and Meyers (1997) also made a similar observation.

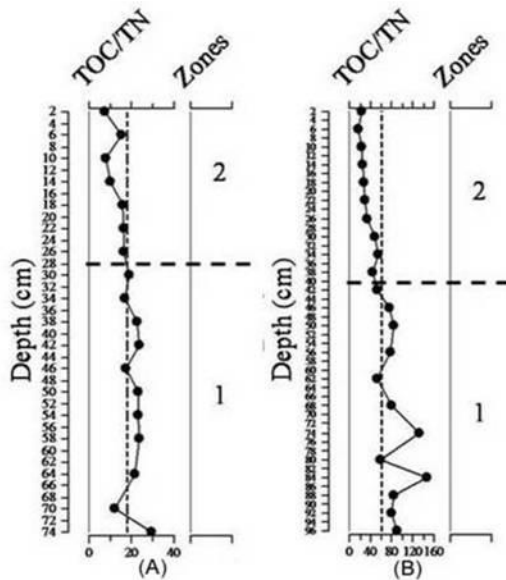


Figure 3.3a.5 Down-core variation of C/N ratio in different zones with zone 1 representing bottom while zone 2 represents the top for core S-61 (A) and S-60 (B). The vertical line represents average value.

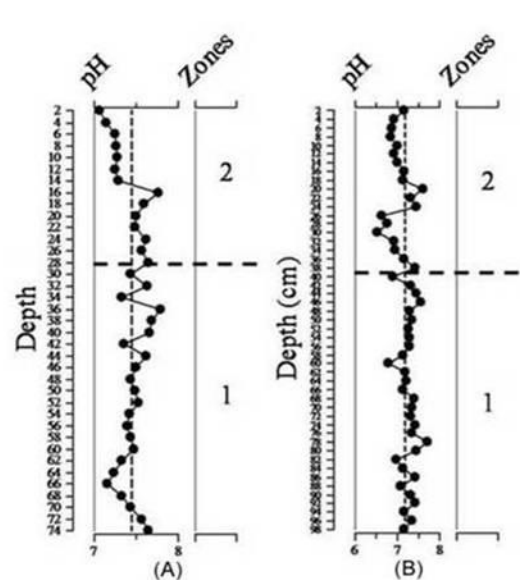


Figure 3.3a.6 Down-core variation of pH in different zones with zone 1 representing bottom while zone 2 represents the top for core S-61 (A) and S-60 (B). The vertical line represents average value.

3.3A.6 pH

pH showed a range of 7.07 to 7.79 with a mean of 7.45 for core S-61 and 6.53 to 7.70 with a mean of 7.18 for core S-60. The mean and standard deviation of pH in each zone for cores S-61 and S-60 are given in table 3.3.

In core S-61, pH is basic in zone 1 and zone 2. pH in core S-60 is basic in zone 1 and acidic in zone 2 (Figure 3.3a.6).

3.3A.7 Major elements (Fe, Mn and Al)

The data showed a range of 3.97 to 9.66% with a mean of 7.89% Fe, 373.33 to 711.33 ppm with a mean of 553.23 ppm Mn and 5.26 to 8.47% with a mean of 7.41% Al for core S-61 and 3.37 to 9.33% with a mean of 6.28% Fe, 460.67 to 792 ppm with a mean of 677.93 ppm Mn and 4.28 to 8.52% with a mean of 6.22% Al for core S-60. The mean and standard deviation of Fe, Mn and Al in each zone are given in table 3.3.

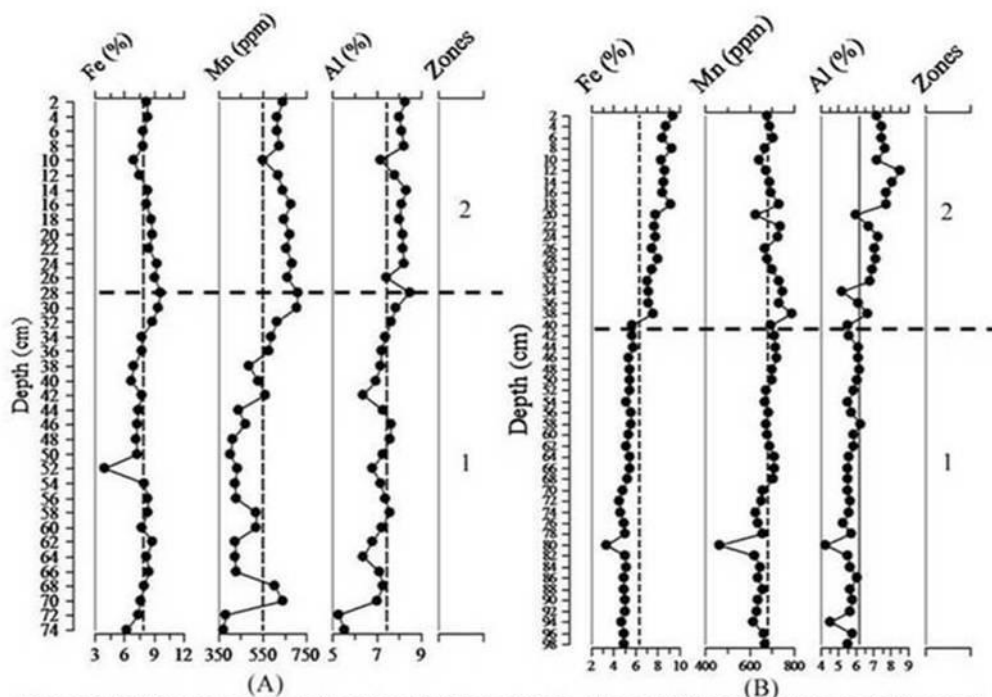


Figure 3.3a.7 Down-core variation of major elements (Fe, Mn and Al) in different zones with zone 1 representing bottom while zone 2 represents the top for core S-61 (A) and S-60 (B). The vertical line represents average value.

In zone 1 of core S-61 (Figure 3.3a.7), significant variations in Mn and Al profiles are noted. They show overall increasing trend. Fe fluctuates around its average line. In zone 2, from 28 to 10 cm, Fe, Mn and Al show an overall decreasing trend while from 10 cm to surface they show an overall

increasing trend. In zone 1 of core S-60 (Figure 3.3a.7), Fe, Mn and Al are nearly constant with values falling below their respective average lines. In zone 2, Fe and Al show an increasing trend while Mn shows a decreasing trend with values falling above their respective average lines. The diagenetic enhancement in Fe and Mn concentration in zone 2 in both the cores (S-61 and S-60) (Figure 3.3a.7) is also confirmed by variation in sediment colour with brown to light grey in zone 2 which indicated more oxic environment and dark grey to black sediments in zone 1 which indicated reducing environment (Spencer 2002).

3.3A.8 Trace elements (Ni, Cr, Co, Zn and Pb)

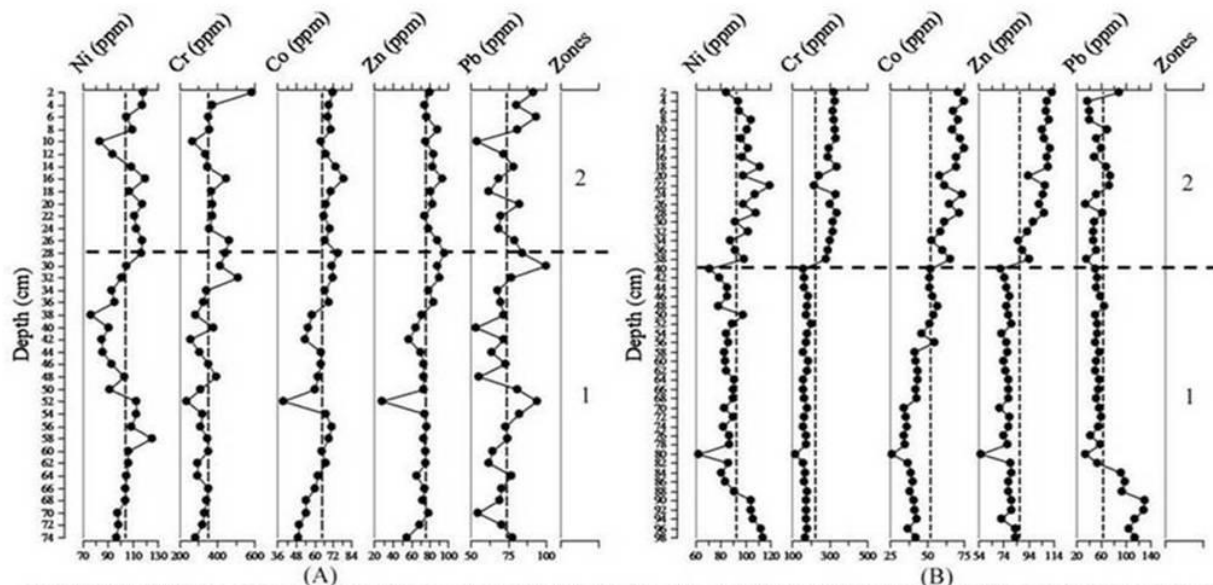


Figure 3.3a.8 Down-core variation of trace elements (Ni, Cr, Co, Zn and Pb) in different zones with zone 1 representing bottom while zone 2 represents the top for core S-61 (A) and S-60 (B). The vertical line represents average value.

The data showed a range of 76 to 125.33 ppm with a mean of 103.63 ppm Ni, 238 to 584.33 ppm with a mean of 354.41 ppm Cr, 34.67 to 79 ppm with a mean of 64.58 ppm Co, 28.67 to 95.67 ppm with a mean of 75.62 ppm Zn and 53.33 to 100 ppm with a mean of 73.50 ppm Pb for core S-61 and 62.33 to 119.33 with a mean of 92.60 ppm Ni, 114.33 to 337.33 ppm with a mean of 221.89 ppm Cr, 26 to 75 ppm with a mean of 52.10 ppm Co, 55.67 to 112.67 ppm with a mean of 86.46 ppm Zn and 34 to 130.33 ppm with a mean of 62.86 ppm Pb for core S-60. The mean and standard deviation of Ni, Cr, Co, Zn and Pb in each zone are given in table 3.3.

In zone 1 of core S-61 (Figure 3.3a.8), trace metal profiles show wide variability with an overall increasing trend except Ni which seems to follow the trend of Fe. In zone 2, from 28 to 10 cm, trace metals show an overall decreasing trend while from 10 cm to surface they show an overall increasing trend. In core S-60 (Figure 3.3a.8), zone 1 shows nearly constant profiles of trace metals with values below their respective average lines while in zone 2, trace metals (except Pb) show an overall increasing trend with values above their respective average lines. The higher value of Pb from 98 to 84 cm and Ni from 98 to 90 cm roughly coincides with intervals of high total organic carbon content (Figure 3.3a.8). The trace metal profiles indicate that their distribution is regulated by Fe and Mn oxyhydroxides.

3.3A.9 Diatoms

A total 18 diatom genera were identified. Diatoms were mainly represented by genera *Cyclotella*, *Nitzschia*, *Pleurosigma*, *Coscinodiscus*, *Chaetoceros*, *Thalassionema*, *Surirella*, *Navicula*, *Diploneis*, *Grammatophora*, *Hyalodiscus*, *Campylodiscus*, *Triceratium*, *Pinnularia*, *Biddulphia*, *Cerataulina*, *Thalassiosira* and *Syndra*. Most genera identified in the present study have also been recorded in the water column of Rajapuri creek (Gajbhiye et al 1995) and other estuaries along west coast of India (D'Costa and Anil 2010; Patil and Anil 2008; Garg and Bhaskar 2000). Diatoms genera with <1% representation were not used for interpretation.

In core S-61 (Figure 3.3a.9), *Cyclotella meneghiniana* and *Nitzschia cocconeiformis* are the dominant diatoms present in every sediment sample. Other diatoms with representation up to 10% included *Hyalodiscus subtilis*, *Chaetoceros* sp., *Nitzschia sigma*, *Coscinodiscus* sp., *Grammatophora oceanica*, *Thalassiosira* sp., *Diploneis* sp., *Campylodiscus* sp. and *Pinnularia* sp. Less common diatoms with 1% relative abundance included *Biddulphia reticulate*, *Triceratium* sp., *Cerataulina bicornis* and *Surirella recedens*. Freshwater diatoms ranged from 56 to 94% while marine diatoms ranged from 6 to 44%. Zone 1, is characterized by predominance of freshwater forms like *Cyclotella meneghiniana* (range 33-67%) and *Nitzschia cocconeiformis* (range 12-30%) while in zone 2 marine forms like

Chaetoceros sp., *Hyalodiscus subtilis*, *Grammatophora oceanica* and *Diploneis* sp. show relatively high abundance. *Nitzschia sigma* was mainly present in the surface layers (18 cm to surface).

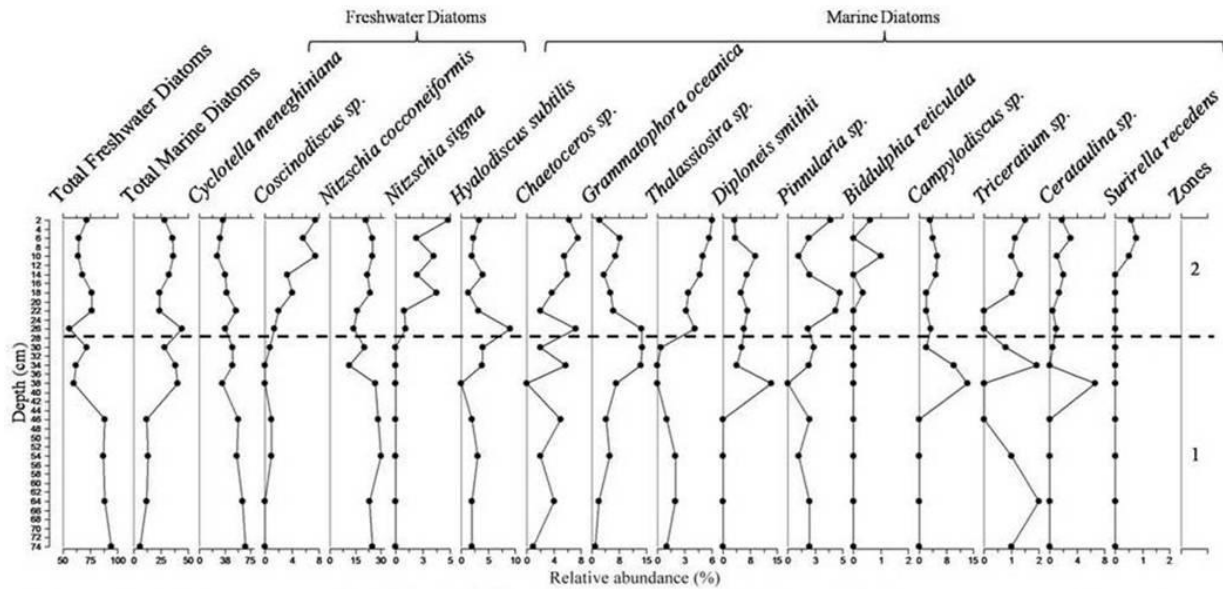


Figure 3.3a.9 Down-core distribution of diatoms in different zones with zone 1 representing bottom while zone 2 represents the top for core S-61. Individual species >1% of relative abundance were retained for the profile.

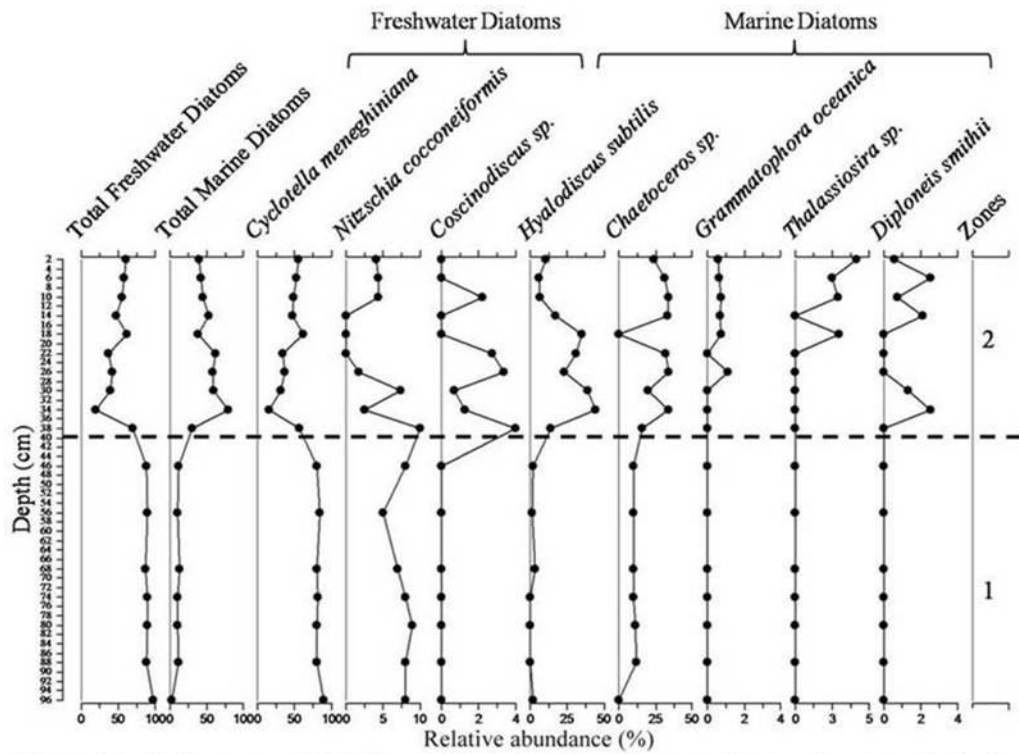


Figure 3.3a.10 Down-core distribution of diatoms in different zones with zone 1 representing bottom while zone 2 represents the top for core S-60. Individual species >1% of relative abundance were retained for the profile.

In core S-60 (Figure 3.3a.10), *Cyclotella meneghiniana* is most common diatom occurring in every sample, in some cases with relative abundance >50%. Other diatoms with maximum relative abundance >30% in some samples included *Chaetoceros sp.* and *Hyalodiscus subtilis*. The freshwater diatoms ranged from 20 to 77% while marine diatoms ranged from 23 to 80%. *Cyclotella meneghiniana* was most dominant throughout in zone 1 (range 80-90%) and in zone 2, *Hyalodiscus subtilis* and *Chaetoceros sp.* were predominant.

3.3A.10 Correlation

Fe, Mn and Al correlates well with trace metals (except Pb) (Table 3.3a.1; Table 3.3a.2). Pb does not show any significant correlation with Fe, Mn and Al suggesting that it is from different source (Table 3.3a.1; Table 3.3a.2). In core S-60, significant positive correlation between Pb and TOC ($r=+0.53$) may indicate that Pb is trapped by organic matter. In core S-60 (Table 3.3a.1), significant positive correlation of sand and TN with Fe ($r=+0.48$; $r=+0.75$), Al ($r=+0.31$; $r=+0.64$), Cr ($r=+0.64$; $r=+0.69$), Co ($r=+0.45$; $r=+0.72$) and Zn ($r=0.44$; $r=+0.68$) suggest that these metals might have a similar source in the sediment and/or they have undergone similar post depositional processes. While in core S-61 (Table 3.3a.2), metals show poor or weak correlation with sand and TN. Inter-relationship among the elements indicated a common source or involved in similar enrichment mechanism (Table 3.3a.1; Table 3.3a.2).

Table 3.3a.1 Pearson correlation coefficient for core S-61

	Sand	Silt	Clay	TOC	pH	Fe	Mn	Al	Ni	Cr	Co	Zn	Pb	TN
Sand	1													
Silt	-0.073	1												
Clay	-0.488**	-0.835**	1											
TOC	0.308	0.253	-0.391*	1										
pH	-0.276	0.163	0.009	0.022	1									
Fe	0.247	-0.371*	0.189	0.029	-0.108	1								
Mn	0.013	-0.471**	0.405*	-0.612**	0.006	0.561**	1							
Al	-0.144	-0.489**	0.508**	-0.561**	-0.131	0.499**	0.730**	1						
Ni	0.221	-0.213	0.064	-0.224	-0.148	0.425**	0.350*	0.449**	1					
Cr	-0.025	-0.225	0.211	-0.355*	-0.015	0.537**	0.563**	0.552**	0.473**	1				
Co	0.002	-0.505**	0.441**	-0.319	-0.074	0.755**	0.560**	0.751**	0.415*	0.569**	1			
Zn	-0.008	-0.361*	0.32	-0.248	0.034	0.795**	0.622**	0.613**	0.255	0.627**	0.849**	1		
Pb	0.085	0.001	-0.048	-0.321	-0.204	0.091	0.182	0.24	0.407*	0.241	0.115	-0.009	1	
TN	0.327	0.113	-0.305	0.021	-0.473*	-0.211	0.051	-0.046	-0.131	0.103	-0.066	0.042	-0.349	1

** . Correlation is significant at the 0.01 level (2-tailed).

* . Correlation is significant at the 0.05 level (2-tailed).

Table 3.3a.2 Pearson correlation coefficient for core S-60

	Sand	Silt	Clay	TOC	pH	Fe	Mn	Al	Ni	Cr	Co	Zn	Pb	TN
Sand	1													
Silt	-0.347*	1												
Clay	-0.011	-0.934**	1											
TOC	-0.473**	0.267	-0.104	1										
pH	-0.455**	0.239	-0.084	0.064	1									
Fe	.483**	-0.375**	0.216	-0.522**	-0.457**	1								
Mn	.385**	-0.544**	.432**	-0.412**	-0.147	.452**	1							
Al	.310*	-0.278	0.179	-0.383**	-0.422**	.883**	.417**	1						
Ni	0.266	-0.316*	0.235	-0.034	-0.135	.463**	.301*	.454**	1					
Cr	.636**	-0.348*	0.128	-0.559**	-0.527**	.934**	.402**	.832**	.481**	1				
Co	.450**	-0.456**	.314*	-0.497**	-0.417**	.935**	.523**	.872**	.436**	.883**	1			
Zn	.436**	-0.312*	0.167	-0.405**	-0.435**	.950**	.394**	.907**	.613**	.908**	.885**	1		
Pb	-0.266	0.072	0.025	.531**	0.235	-0.262	-0.253	-0.238	.368**	-0.26	-0.291*	-0.121	1	
TN	0.24	-0.262	0.197	-0.538**	-0.359	.751**	0.26	.640**	0.217	.689**	.715**	.675**	-0.306	1

*. Correlation is significant at the 0.05 level (2-tailed). **. Correlation is significant at the 0.01 level (2-tailed).

3.3A.11 Principal component analysis (PCA)

A PCA allows an easy visualization of the relationships existing amongst the variables in large data sets (Reid and Spencer 2009; Passos et al 2010). It represents correlation between the variables, directions and intensities of the variation (arrow length) (Virkanen 1998). The first two components in a PCA biplot represent relationship between diatoms and environmental variables and accounted for 55.7% of the total variance (Figure 3.3a.11). In core S-60, sand and marine diatom *Hyalodiscus subtilis* are closely associated in group 1 and *Cyclotella meneghiniana*, silt and TOC are closely associated in group 2 while in core S-61 TN, *Grammatophora oceanica*, *Nitzschia cocconeiformis*, *Diploneis* sp., *Thalassiosira* sp. and *Triceratium* sp. are closely associated in group 3 (Figure 3.3a.11).

3.3A.12 Factor analysis

Factor analysis was employed to identify the important variables that control trace metal distribution (Selvaraj et al 2004). In core S-61 (Table 3.3a.3), the five factors (F1, F2, F3, F4 and F5) correspond to 87.50% of the total variance. F1, F2, F3, F4 and F5 accounted for 30.69%, 19.79%, 13.71%, 12.83% and 10.47% respectively. In core S-60 (Table 3.3a.4), four factors (F1, F2, F3 and F4) correspond to 86.55% of the total variance. F1, F2, F3 and F4 accounted for 35.29%, 19.46%, 18.88% and 12.93% respectively.

Table 3.3a.3 R-mode factor analysis

Factor	F1	F2	F3
Variance (%)	30.694	19.792	13.707
sand	-0.04	0.978	0.051
silt	-0.136	-0.062	0.977
clay	0.129	-0.613	-0.765
Mud	0.04	-0.978	-0.051
pH	-0.156	-0.114	0.211
Fe	0.756	0.379	-0.122
Mn	0.853	0.115	-0.269
Al	0.84	-0.316	-0.084
Ni	0.492	0.332	-0.205
Cr	0.685	-0.102	0.007
Co	0.767	-0.126	-0.246
Zn	0.941	-0.051	0.085
Pb	0.121	-0.08	0.042
TOC	-0.578	0.469	0.48
TN	0.038	0.204	0.177

Positive loadings highlighted in **bold** at $p < 0.05$

Sub channel (core S-61)

Sediment sources

Sub channel largely consists of river brought terrigenous supply of sediments. The transportation and deposition of sediment is controlled by processes such as river runoff, tides and waves. At the time of high river runoff, sediments are

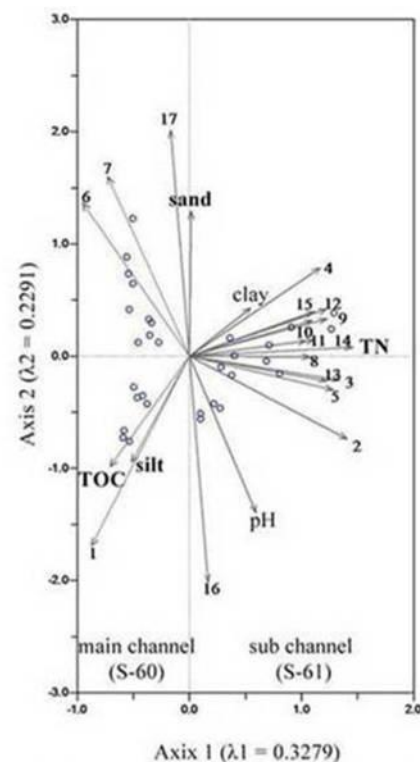


Figure 3.3a.11 Statistical relationship between diatoms and environmental variables by using multivariate Principal component analysis (PCA)
 Note: 1-Cyclotella meneghiniana, 2-Nitzschia cocconeiformis, 3-Nitzschia sigma, 4-Coscinodiscus sp., 5-Pinnularia sp., 6-Chaetoceros sp., 7-Hyalodiscus sp., 8-Grammatophora sp., 9-Thalassiosira sp., 10-Biddulphia sp., 11-Campylodiscus sp., 12-Diploneis sp., 13-Triceratium sp., 14-Cerataulina sp., 15-Surirella sp., 16-Total Freshwater diatoms, 17-Total marine diatoms, TN Total nitrogen, TOC-Total organic carbon, ○ samples.

transported downstream near the channel outlet whereby coarse grained sediments selectively settle down as the flow velocity declines while the fine sediments move to a greater distance. The dominance of sand (range 4-18%) noted between 74 and 52 cm probably reflects high river runoff conditions (Figure 3.3a.1). The alternating high proportion of sand (74-52 cm), silt (52-40 cm) and clay (40-32 cm) may reflect tide and wave induced variations in flow strength (Dalrymple and Choi 2007) (Figure 3.3a.1). The large variations in Mn (range 373-711 ppm) and Al (range 5.3-8.5%) profiles in zone 1 (Figure 3.3a.7) strongly support the changes in flow conditions (Zwolsman et al 1993). The organic matter input into the river channel also increases during the periods of high river discharge (Simenstad 1983). Peak TOC (range 1.8-4.8%), TN (range 0.15-3.2%), elevated C/N ratio (range 12-30) and predominance of freshwater forms (range 60-94%) throughout in zone 1 (Figure 3.3a.3; Figure 3.3a.5) strongly suggest large contribution from fluvial land derived terrestrial organic matter and small input from marine sources (Meyers and Ishiwatari 1993).

Zone 2 (Figure 3.3a.1) has almost homogenous grain size distribution suggesting uniform sediment transport and depositional processes. This is attributed to conditions when the river runoff is less and there is regular resuspension, transport and deposition in response to tidal inflow and waves. The decreasing trend of C/N ratio from 26 cm to surface (range 17-7) in zone 2 provides evidence of greater marine input (Figure 3.3a.5). This coincides with relatively high proportion of total marine diatoms (range 44-23%) (Figure 3.3a.9). Here, marine genera *Grammatophora oceanica*, *Chaetoceros sp.*, *Hyalodiscus subtilis*, *Diploneis sp.* and *Campylodiscus sp.* showed their peak abundance (Figure 3.3a.9). The increase in

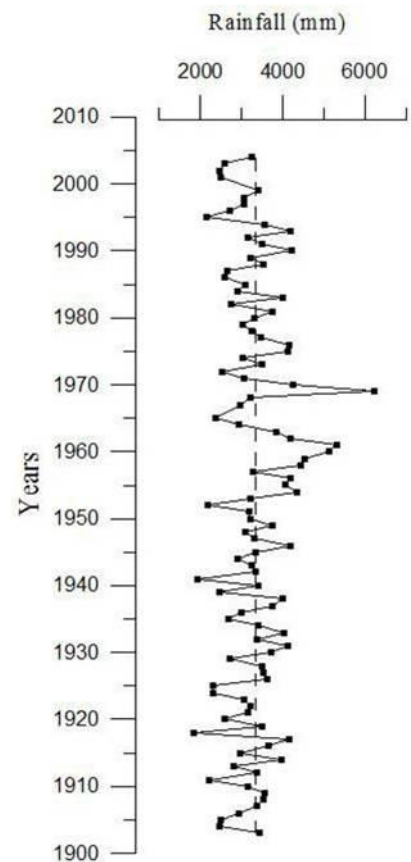


Figure 3.3a.12 Rainfall data of last 100 years for station Mahad in Raigad district of Maharashtra.

Nitzschia sigma (range 1-5%) from 26 cm to surface possibly indicates some degree of water column disturbance, probably due to tidal action (Figure 3.3a.9) (Wachnicka et al 2011). The higher proportion of finer sediments (range 58-65%) noted from 28 cm to surface in zone 2 is attributed to decrease in rainfall in recent years thus favouring the deposition of finer particles (Volvoikar and Nayak 2013a; Selvaraj et al 2003). The sedimentation rates (^{210}Pb dating) reported from mudflats located close to the study area are 2.72 cm/year (Fernandes 2011) and 1.21 cm/year in lower estuary (Singh et al 2013) and 1.46 cm/year in middle estuary (Fernandes 2011). The sedimentation rate reported from near shore and estuarine areas are 1.94 cm/year (Sharma et al 1994) and 0.62 cm/year (Borole 1988). The sedimentation rate in intertidal region is mainly controlled by tidal inundation, wind-wave activities, sediment grain size, organic carbon and vegetation cover (Temmerman et al 2003). Taking the average sedimentation rate of lower estuary and near shore and estuarine areas as 1.28 cm/year and 1.97 cm/year respectively, it can be said that the sediment cores of the present study may represent not more than 100 years. The rainfall data of last 100 years for Raigad district shows intervals of higher rainfall than average in past (1950-1970) and intervals of lower rainfall than average in the recent years (1995-2005) (Figure 3.3a.12).

Sediment geochemistry

The increasing distribution pattern of trace metals in zone 1 (Figure 3.3a.8) may be due to non-uniform grain size responsible for sorption and also varying amount of anthropogenic contribution (Vaithiyanathan et al 1993). It is important to mention here that the rock type in the catchment area is mainly basalts. Higher Fe concentration (range 6.24-8.76%) compared to lower Al concentration (range 5.25-7.56%) in zone 1 is attributed to high coarser size fraction (Achyuthan et al 2002). In zone 2, the enrichment of Fe (range 7.9-8.3%) and Mn (range 615-643 ppm) from 8 cm to surface reflects early diagenetic process. A sharp decrease in Fe (8.3-6.9%) and Mn (644-552 ppm) at 14-10 cm is the suggestive of oxic/sub-oxic interface (Santschi et al 1990; Ayyamperumal et al 2006). This probably explains the dissolution of Fe and Mn in partly reduced sediment layers producing Fe^{+2} and Mn^{+2}

species, which migrate upward in the sediment column and get precipitated near the oxic-suboxic interface (Santschi et al 1990; Shaw et al 1990). The similar distribution of trace metals with Fe and Mn at 14-0 cm may indicate readsorption by Fe and Mn oxyhydroxides (Zwolsman et al 1993). Fe and Al are major constituents of clay mineral, feldspars and amorphous aluminosilicate gels (Bortleson and Lee 1972). The significant positive correlation between Fe and Al ($r=+0.88$) and similar distribution profiles at 40-28 cm and 14-0 cm may indicate that Fe is mainly associated with the clay mineral fraction and that the sediments come from the same detrital source (Ruiz-Fernández et al 2011) (Table 3.3a.1). Factor 1 (Table 3.3a.3) showed significant positive loadings on Fe (0.76), Mn (0.85), Al (0.84), Cr (0.69), Co (0.77) and Zn (0.94) and is associated as natural factor, since the variability of these elements is controlled by natural or terrestrial sources (Fe, Mn and Al) (Zhou et al 2004). Factor 2 and factor 3 showed significant positive loadings on sand (0.98) and silt (0.98) respectively and are associated as grain size controlled factor. Factor 4 showed significant positive loadings on Pb (0.89) and good positive loadings on Ni (0.58). Factor 4 is associated as anthropogenic factor since the variability of Pb and to some extent Ni is not controlled Fe, Mn or Al. Factor 5 showed significant positive loadings on TN (0.84) and is associated as organic matter controlled factor. The average Igeo value for Mn and Zn falls in class 0 which suggests background value for these elements. The Igeo value for Fe falls in class 1 which indicates that sediments are unpolluted to moderately polluted. The Igeo value for Cr, Co and Pb falls in class 2 indicating that the channel is moderately polluted with respect to these metals (Table 3.3a.5). Ni falls in class 0 in zone 1 and class 1 in zone 2 reflecting an increase in contamination over the recent years.

Table 3.3a.5 Range and average of Index of geo-accumulation index in zone 1 and zone 2 for core (A) S-61 and (B) S-60

(A) Sub channel (S-61)					(B) Main channel (S-60)				
Metals	Range	Average	Igeo class	Pollution Intensity	Metals	Range	Average	Igeo class	Pollution Intensity
Zone 1 (74-28 cm)					Zone 1 (98-40 cm)				
Fe	-0.83 to 0.45	0.10	1	UP to MP	Fe	-1.07 to -0.30	-0.47	0	UP
Mn	-1.77 to -0.84	-1.36	0	UP	Mn	-1.47 to -0.82	-0.95	0	UP
Ni	-0.42 to 0.30	-0.03	0	UP	Ni	-0.71 to 0.15	-0.22	0	UP
Cr	0.04 to 1.93	1.27	2	MP	Cr	-0.24 to 0.57	0.32	1	UP to MP
Co	0.48 to 1.40	1.10	2	MP	Co	-0.13 to 1.00	0.57	1	UP to MP
Zn	-2.31 to -0.57	-1.01	0	UP	Zn	-1.36 to -0.78	-0.91	0	UP
Pb	0.83 to 1.74	1.26	2	MP	Pb	0.19 to 2.12	1.10	2	MP
Zone 2 (28-0 cm)					Zone 2 (40-0 cm)				
Fe	-0.05 to 0.45	0.24	1	UP to MP	Fe	-0.31 to 0.40	0.16	1	UP to MP
Mn	-1.21 to -0.84	-0.98	0	UP	Mn	-1.03 to -0.69	-0.87	0	UP
Ni	-0.29 to 0.23	0.10	1	UP to MP	Ni	-0.53 to 0.23	-0.07	0	UP
Cr	0.99 to 2.11	1.50	2	MP	Cr	0.21 to 1.32	1.12	2	MP
Co	1.17 to 1.47	1.30	2	MP	Co	0.88 to 1.40	1.20	2	MP
Zn	-0.93 to -0.57	-0.79	0	UP	Zn	-1.01 to -0.34	-0.50	0	UP
Pb	0.84 to 1.64	1.33	2	MP	Pb	0.18 to 1.55	0.80	1	UP to MP

Note : UP = Unpolluted, MP=Moderately polluted

Main channel (core S-60)

Sediment sources

The possible sediment source for the main channel comes from the adjacent watersheds and their drainage systems, the sea and the sub channels. The enhanced deposition of mud (silt+clay) and paucity of sand noted in zone 1 (Figure 3.3a.1) probably reflects high river runoff when river carry a large amount of suspended sediments and continuous winnowing transports fine sediments near sheltered areas (Semeniuk 1981). The variations in fine grained sediments (Figure 3.3a.1) may be due to regular resuspension by changing fresh water interaction with tidal currents which are more likely to affect fine (<63µm) rather than coarse grained particles (>63µm) in a protected sheltered environment (Zhang et al 1988; Stephens et al 1992). The similar distribution of major (Fe, Mn and Al) and trace metal (Ni, Cr, Co, Zn and Pb) (Figure 3.3a.7; Figure 3.3a.8) indicates that sediments are derived from same source or have undergone similar post-depositional processes. TOC shows significant positive correlation with mud ($r=+0.48$) (Table 3.3a.2). This is because the ratio of TOC to surface area is higher for finer particles than for coarser sand particles (Meyers, 1994). The predominance of silt between 98 and 74 cm roughly coincides with intervals of high TOC content (Figure 3.3a.4). This may be due to adsorption effects (Guerzoni et al 1984; Faganeli et al 1991; Soto and Martinez 2012). The

decline in TOC from 46 to 42 cm coincides with decrease in pH (Figure 3.3a.4; Figure 3.3a.6). The organic matter content depends on both the retention capacity of the sediment and the rate of microbial degradation (Clarke and Wharton 2001). The organic matter in zone 1 is enriched in TOC (range 2.25-4.59%) but depleted in TN (range 0.03-0.09%) (Figure 3.3a.4). The microbial decomposition of organic matter would result in more loss of nitrogen as nitrogen is more easily degraded than carbon (Rice and Tenore 1981; Zhou et al 2007; Soto and Martinez 2012). The large changes in C/N ratio (range 52-148) can occur during decomposition of organic matter (Figure 3.3a.5) (Yu et al 2010). The elevated C/N ratio suggests that the decomposed organic matter has lost more nitrogen in comparison to carbon and/or changes in land and marine derived organic matter content.

Sand is transported as bedload from the seaward direction when strong tidal currents capable of transporting the coarse particles and deposit them as the tidal currents velocity weakens. The high percentage of sand (range 7-36%) noted from 38 to 22 cm must have been transported from the seaward direction (Figure 3.3a.1). This is supported by significant decrease in C/N ratio (range 54-22) from 38 to 22 cm which indicated increase in marine influence (Figure 3.3a.5). Also, the relative abundance of marine diatom assemblages from 38 to 22 cm vary between 30 and 80%, with a large number of samples representing >50%, indicating a constant marine supply to the main channel (Figure 3.3a.10). *Hyalodiscus subtilis* a marine benthic species (Federico and Marcela 2009) show its peak abundance (range 44%-39%) from 34 to 30 cm (Figure 3.3a.10). The significant positive correlation of marine diatom *Hyalodiscus subtilis* with sand further supports a strong marine influx from seaward direction (Figure 3.3a.10). *Chaetoceros sp.* another marine planktonic diatom (Suto 2006) appeared more frequently (range 34-20%) from 34 to 22 cm (Figure 3.3a.10). Diatom genera *Thalassiosira*, *Grammatophora*, *Diploneis*, *Coscinodiscus* and *Nitzschia cocconiformis* were either totally absent or less frequent at this depth interval (Figure 3.3a.10). This may be attributed to substrate disturbance by sudden change in depositional conditions (Ribeiro et al 2010; Garcia 1996). The low TOC (range 3.33%-1.64%) and TN concentration (range 0.09-0.07%) from

40 to 30 cm is because of dilution by large supply of coarser sediments and oxidation of organic matter due to constant decrease in pH (range 7.43-6.53) (Figure 3.3a.4; Figure 3.3a.6) (Zourarah et al 2009; Ramaswamy et al 2008).

The C/N ratio is fairly constant between 18 and 0 cm (range 23-28) except at a depth of 6 cm (Figure 3.3a.5). The significant increase in TN concentration from 18 cm to surface also coincides with increase in fine sediments probably due to better preservation of nitrogen by adsorption onto fine grained sediment (Figure 3.3a.4; Figure 3.3a.1) (Stevenson and Chen 1972; Muller 1977; Maeda et al 2002). The low TOC value at surface (8 cm to surface) probably reflects mixing processes and decomposition of organic matter under oxic conditions (Canuel and Martens 1993). The decrease in pH from 8 cm to surface (Fig. 6b) might be due to higher decomposition leading to accumulation of organic acids (Dean 1999).

Sediment geochemistry

The similarity in Fe and Mn profiles particularly in zone 1 (Figure 3.3a.7) indicates strong association of geochemical matrix between the two elements (Chatterjee et al 2007). The uniform distribution profiles of trace metals, major elements together with sand and TOC in zone 1 are likely to reflect the background concentration (Figure 3.3a.1; Figure 3.3a.4). In zone 2, the peak of Ni, Cr, Co and Zn at 38 cm coincide with Fe-Mn peak (Figure 3.3a.8). This probably reflects reprecipitation of trace metal on Fe-Mn oxide and hydroxides coatings (Millward and Moore 1982). The decrease in Mn concentration in zone 2 (Figure 3.3a.7) is attributed to preferential reduction of Mn (Wu et al 2001) or its diffusion to water column. Factor 1 (Table 3.3a.4) showed significant positive loadings on Fe (0.90), Al (0.94), Cr (0.82), Co (0.85), Zn (0.92) and TN (0.79) and good positive loading on Ni (0.50). Factor 1 is associated as natural and/or organic matter controlled factor. Factor 2 showed significant positive loadings on sand (0.93). Factor 3 showed significant positive loadings on clay (0.93) and Mn (0.69). Factor 2 and factor 3 are associated as grain size controlled factor. Factor 4 showed significant positive loadings on TOC (0.76), Pb (0.85) and good positive loadings on Ni (0.51). Factor 4 is associated as organic matter controlled

factor. The average Igeo values (Table 3.3a.5) of Mn, Ni and Zn falls in class 0 suggesting that sediments are in background with respect to these metals. The Igeo value of Fe falls in class 0 in zone 1 and class 1 in zone 2. Cr and Co falls in class 1 in zone 1 and class 2 in zone 2 reflecting increase in contamination over the recent years. While Pb on the other hand, falls in class 2 in zone 1 and class 1 in zone 2 indicating decrease in Pb contamination over the years.

Sub channel (S-61) Vs main channel (S-60)

The two channels differ from each other with respect to catchment area, hydrodynamics and industrial activities. Statistical paired t-test analysis ($p < 0.05$) indicate significant difference in the distribution of metals (Table 3.3a.6).

Table 3.3a.6 Paired t-test analysis comparing core S-61 and S-60

	Variables	Mean	t	df	Sig. (2-tailed)	Significant difference at $p < 0.05$
Pair1	sand(S-61)-sand(S-60)	1.23716	0.807	36	0.425	No
Pair2	silt(S-61)-silt(S-60)	-2.70384	-1.071	36	0.292	No
Pair3	clay(S-61)-clay(S-60)	1.46668	0.534	36	0.596	No
Pair4	pH(S-61)-pH(S-60)	0.30541	6.516	36	0.000	Yes
Pair5	Fe(S-61)-Fe(S-60)	1.14311	4.669	36	0.000	Yes
Pair6	Mn(S-61)-Mn(S-60)	-140.973	-7.868	36	0.000	Yes
Pair7	Al(S-61)-Al(S-60)	0.93725	8.576	36	0.000	Yes
Pair8	Ni(S-61)-Ni(S-60)	11.1892	4.996	36	0.000	Yes
Pair9	Cr(S-61)-Cr(S-60)	114.766	9.587	36	0.000	Yes
Pair10	Co(S-61)-Co(S-60)	7.84685	4.977	36	0.000	Yes
Pair11	Zn(S-61)-Zn(S-60)	-14.045	-6.401	36	0.000	Yes
Pair12	Pb(S-61)-Pb(S-60)	19.0991	7.166	36	0.000	Yes
Pair13	TN(S-61)-TN(S-60)	0.09653	6.642	13	0.000	Yes
Pair14	TOC(S-61)-TOC(S-60)	0.06597	0.495	36	0.623	No

The observed major differences between the two channels are, First, in the sub channel (S-61), metals are associated with Fe and Mn while in the main channel (S-60) metals show significant association with Fe only (Table 3.3a.1; Table 3.3a.2). The association of metals with Fe and/or Mn depends upon the metals and the nature of its source, ability of environment to buffer or disperse input of metals through tidal energy (Turner 2000). The significant association of metals with Fe and no significant correlation with Mn could indicate faster co-precipitation in a protected sheltered environment of relatively low tidal energy. The precipitated Fe in the form of

oxyhydroxide has the affinity to scavenge other metals such as Cr, Co and Zn as they pass through the water (Chatterjee et al 2007).

Second, in the main channel (S-60), the distribution of metals is regulated by organic matter (TN and TOC) (Table 3.3a.2). This indicates that organic matter is the main geochemical carrier of metals in the main channel. While in sub channel (S-61) lack of association of metals with organic matter suggest different depositional processes (Figure 3.3a.2). Third, sand showed significant positive correlation with metals and marine diatoms in the main channel (S-60) while in the sub channel (S-61) sand does not control their distribution (Table 3.3a.1; Table 3.3a.2; Figure 3.3a.11). This can be explained by considering marine influx from the seaward side which carry some metals along with sand as sand shows significant positive association with metals and marine diatoms. Further, this may cause remobilization of particle-bound trace metals and would gradually increase the trace metal concentration. Aloupi and Angelidis (2002) found significant correlation of metals with sand fraction in areas affected by pollution from harbour and industries located in coastal areas. Main channel is surrounded by old, rusty and stranded barges around Agardanda harbour, Dighi Port and Rajapuri jetty (Figure 3.3a). Fourth, highest numbers of diatoms were recorded in the sub channel (S-61). Average TN concentration is more than double in sub channel (S-61) when compared to the main channel (S-60) (S-61 average TN 0.2%; S-60 average TN 0.08%). TN and diatoms are closely situated in group 3 in the river channel (S-61) (Figure 3.3a.11). Therefore high diatom abundance in the river channel (S-61) is attributed to higher nitrogen content, resulting in increase in primary productivity and phytoplankton abundances (Weikert 1987).

3.3B Mangroves

The core S-65 collected from lower channel of Mandad River was analyzed for sediment grain size, TOC and pH. The core is divided into two zones depending upon the distribution pattern of sediment grain size namely, zone 1 and zone 2 wherein zone 2 represents recent sediments (Figure 3.3b.1). Zone 1 is characterized by large variations in sand, silt and clay

percentages. In zone 2 sand, silt and clay show almost uniform profiles. TOC and pH is relatively higher in zone 1 in comparison to zone 2. The sediment component plotted on ternary diagram indicated that sediment deposition took place under less violent conditions (Figure 3.3b.2).

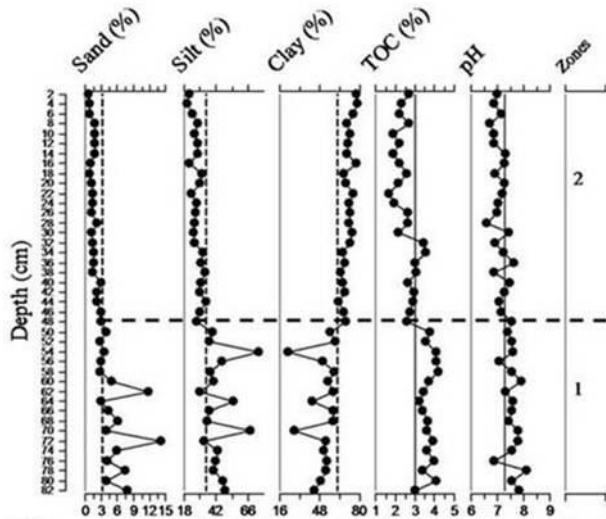


Figure 3.3b.1 Down-core variation of sediment grain size, TOC and pH in different zones with zone 1 representing bottom while zone 2 represents the top for core S-65. The vertical line represents average value.

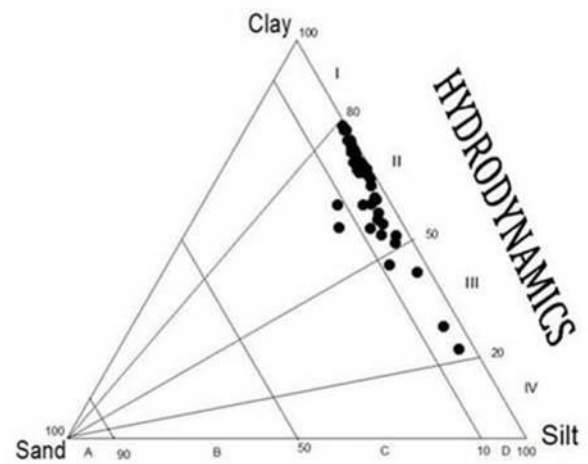


Figure 3.3b.2 Ternary diagram for the classification of hydrodynamic conditions after Pejrup (1988) for core S-65

Conclusion

The distribution of sediments in an estuarine channel is controlled mainly by river runoff, tides and waves. During the periods of higher rainfall, mix coarse and fine sediments are deposited in the sub channel (S-61) while in the main channel (S-60) fine sediments are deposited. In the sub channel (S-61), in zone 1, organic matter showed enrichment in total organic carbon and total nitrogen concentration. The major and trace metal profiles showed variations in distribution. On the other hand, in the main channel (S-60), in zone 1, organic matter is depleted in total nitrogen concentration. The major and trace metal showed nearly constant profiles. During the periods of lower rainfall, tidal influence provides quiet depositional site in the sub channel (S-61) while in the main channel (S-60) tide dominated coarser sediments are deposited. The increasing proportion of marine diatoms and decreasing trend of carbon/nitrogen ratio in zone 2 suggests stronger tidal influence in the main channel (S-60) as compared to the sub channel (S-61). The rainfall

data also indicated a higher rainfall in the past and a decreased rainfall pattern over the recent years. The Igeo value of Pb, Cr and Co suggest that sub channel is moderately polluted while main channel is unpolluted to moderately polluted with respect to these trace metals.

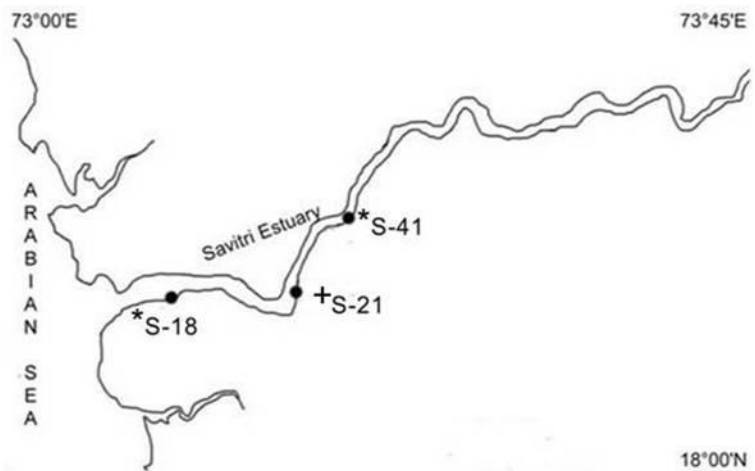


Figure 3.4 Study area map with core location for Savitri Estuary
* Mudflat core + Mangrove core

3.4 Savitri estuary

Total three cores, two from mudflats (S-18 and S-41) and one from mangroves (S-21) were collected along Savitri estuary (Figure 3.4).

3.4 A Mudflats

3.4A.1 Collection of sediment core

Amongst the two cores collected from mudflats, one represented lower estuary (S-18) while other represented middle estuary (S-41). The core length ranged from 78 cm for core S-41 to 100 cm for core S-18. The two cores (S-18 and S-41) were analyzed for sediment grain size, TOC, TN, TP, pH, metals, clay minerals and diatoms.

3.4A.2 Colour

The sediment colour varied from brown to grey for core S-41 and a uniform brown colour was noted for core S-18.

3.4A.3 Sediment grain size

The data showed a range of 29.8 to 52.1% with a mean of 29.8% sand, 28.14 to 55.9% with a mean of 40.3% silt and 16.2 to 48.9% with a mean of

29.9% clay for core S-18 and 1.1 to 19.9% with a mean of 5.1% sand, 4.4 to 58.8% with a mean of 42.2% silt and 35.8 to 92.6% with a mean of 52.8% clay for core S-41. Depending upon the distribution pattern of sediment component core S-18 can be divided into three zones namely zone 1, 2 and 3 while core S-41 can be divided into two zones namely zone 1 and 2. The mean and standard deviation of sediment grain size in each zone for cores S-18 and S-41 are given in table 3.4.

Table 3.4 Mean and standard deviation of different parameters in each zone for core S-18 and S-41. The p-value represent result of one way ANOVA significant at $p < 0.05$

Core S-18							
	Zone 1 (100-78 cm)		Zone 2 (78-14 cm)		Zone 3 (14-0 cm)		p value
	N	Mean	N	Mean	N	Mean	
Sand (%)	12	19.97±6.72	33	35.89±7.96	7	18.67±7.55	0.00
Silt (%)	12	44.79±4.64	33	37.83±5.33	7	44.30±3.68	0.00
Clay (%)	12	35.23±6.50	33	26.27±4.36	7	37.02±7.73	0.00
pH	12	7.57±0.11	33	7.38±0.14	7	6.88±0.04	0.00
Fe (%)	12	11.92±1.33	33	14.22±5.29	7	16.43±1.49	0.09
Mn (ppm)	12	2082.40±682.97	33	1857.20±399.15	7	2191.90±135.13	0.13
Al (%)	12	8.77±0.95	33	9.18±1.44	7	9.18±0.66	0.62
Ni (ppm)	12	148.89±9.16	33	152.90±17.91	7	139.90±6.40	0.13
Cr (ppm)	12	262.53±21.62	33	241.29±42.77	7	194.43±22.90	0.00
Co (ppm)	12	103.06±7.43	33	94.07±11.57	7	74.95±6.61	0.00
Zn (ppm)	12	158.59±11.34	33	175.31±23.87	7	157.54±8.34	0.02
Pb (ppm)	12	53.19±7.21	33	49.80±16.38	7	71.62±18.20	0.00
TOC (%)	12	1.30±0.16	33	1.04±0.19	7	2.10±0.48	0.00
TN (%)	6	0.11±0.03	17	0.07±0.01	4	0.14±0.04	0.00
TP (%)	6	0.05±0.01	17	0.04±0.01	4	0.05±0.01	0.02
C/N ratio	6	16.77±1.89	17	18.36±1.66	4	17.53±0.9	0.17
Smectite (%)	3	51.70±3.94	8	50.38±9.42	2	57.93±5.20	0.53
Illite (%)	3	19.69±0.21	8	19.40±7.09	2	15.89±5.05	0.75
Kaolinite (%)	3	13.97±1.54	8	15.26±2.53	2	16.55±0.83	0.47
Chlorite (%)	3	14.64±4.27	8	14.96±3.30	2	9.62±0.98	0.18
Core S-41							
	Zone 1 (78-18 cm)		Zone 2 (18-0 cm)				p value
	N	Mean	N	Mean			
Sand (%)	31	5.75±3.53	9	2.68±1.50			0.02
Silt (%)	31	42.08±13.68	9	43.90±11.53			0.72
Clay (%)	31	52.17±13.25	9	53.42±11.41			0.8
pH	31	6.65±0.46	9	5.73±0.22			0
Fe (%)	31	11.22±2.20	9	10.10±0.92			0.15
Mn (ppm)	31	1987.90±268.78	9	2018.70±353.49			0.78
Al (%)	31	9.26±1.61	9	10.49±1.19			0.04
Ni (ppm)	31	138.99±23.20	9	130.41±12.57			0.3
Cr (ppm)	31	261.83±60.43	9	195.44±16.25			0
Co (ppm)	31	105.76±12.35	9	100.00±8.38			0.2
Zn (ppm)	31	156.30±21.29	9	143.30±11.04			0.09
Pb (ppm)	31	47.06±9.25	9	57.19±4.75			0
TOC (%)	31	1.85±0.36	9	2.20±0.16			0
TN (%)	14	0.15±0.03	5	0.18±0.03			0.03
TP (%)	14	0.04±0.01	5	0.05±0.02			0.35
C/N ratio	14	14.06±1.44	5	13.86±1.60			0.79
Smectite (%)	4	56.11±7.22	2	55.35±4.46			0.9
Illite (%)	4	16.14±5.80	2	12.94±4.78			0.54
Kaolinite (%)	4	12.75±3.29	2	12.81±6.14			0.99
Chlorite (%)	4	14.99±3.39	2	18.89±3.11			0.25

In core S-18, in zone 1 and 3, major portion of silt and clay falls above average line while sand falls below average line. However, in zone 2, major portion of sand falls above average line while silt and clay falls below average line. The higher and variable sand percentage in zone 2 reflects conditions of high river discharge where coarse grained sediments are

transported and deposited in lower estuary (Walsh and Nittrouer 2004). In zone 1 of core S-41, silt and clay show large fluctuations. Sand percentage increases reaching highest at 26 cm. In zone 2, sand and silt percentage decreases while clay increases (Figure 3.4a.1). Silt and clay compensates each other throughout in zone 1 and zone 2. The higher sand percentage in zone 1 probably reflects high river runoff conditions. The variations in fine grained sediments may reflect regular resuspension by changing freshwater interaction with tidal current (Zhang et al 1988). The higher proportion of fine sediments in zone 3 of core S-18 and zone 2 of core S-41 is attributed to decrease in rainfall favoring the deposition of finer particles (Selvaraj et al 2003).

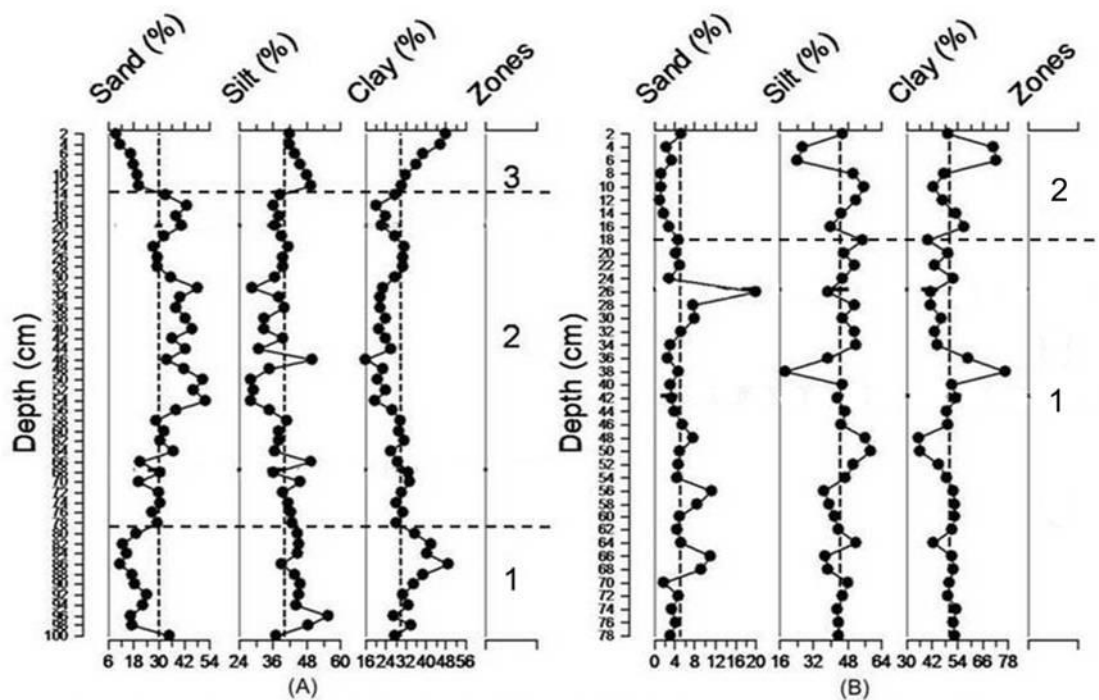


Figure 3.4a.1 Down-core variation of sediment grain size in different zones with zone 1 representing bottom while zone 3 in core S-18 (A) and zone 2 in core S-41 (B) represents the top. The vertical line represents average value.

The hydrodynamic plots (Pejrur 1988) reveal that the core collected from lower estuary (S-18) falls largely within section III (Figure 3.4a.2) indicating that sediment deposition took place under relatively violent conditions while the core S-41 which was collected from middle estuary falls largely within sections III and II indicating relatively violent to less violent hydrodynamic conditions (Figure 3.4a.2). Further, the sediments from middle estuary (S-41) fall within D type while in the core from lower estuary (S-18) sediments fall

within C type indicating presence of sand dominated sediments, in the lower estuary.

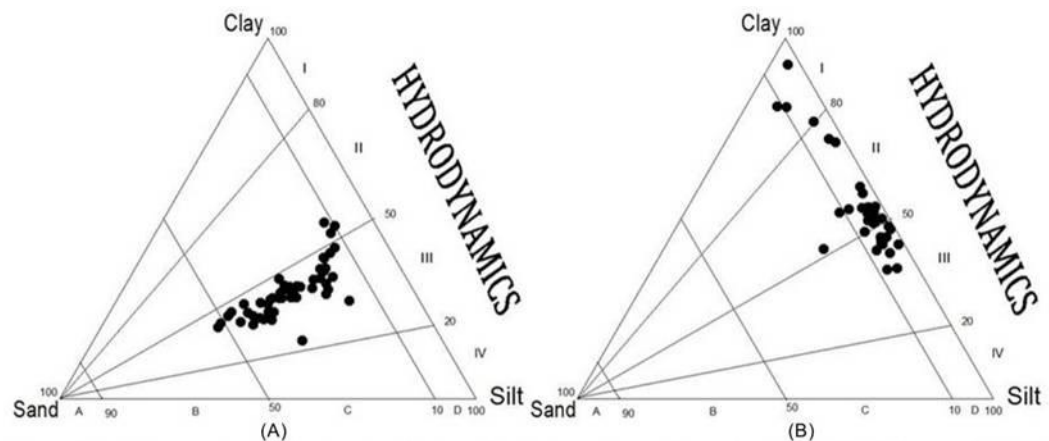


Figure 3.4a.2 Ternary diagram for the classification of hydrodynamic conditions after Pejrup (1988) for core S-18 (A) and S-41 (B)

3.4A.4 Nutrients (TOC, TN and TP)

The data showed a range of 0.69 to 2.96% with a mean value of 1.28% TOC, 0.04 to 0.17% with a mean of 0.09% TN and 0.03 to 0.06% with a mean of 0.05% TP for core S-18 and 0.87 to 2.67% with a mean value of 1.92% TOC, 0.08 to 0.21% with a mean of 0.16% TN, 0.02 to 0.08% with a mean of 0.04% TP for core S-41. The mean and standard deviation of TN, TP and TOC in each zone for cores S-18 and S-41 are given in table 3.4.

In core S-18 TOC, TN and TP concentrations are more than average in zone 1 and 3 while in zone 2 their concentrations are less than average (Figure 3.4a.3). The relatively higher values of TOC, TN and TP noted in zone 1 and 3 where fine sediments showed higher corresponding values may therefore be attributed to association with higher surface area of finer particles (Meyers 1994) while TOC, TN and TP showed relatively low values in zone 2 which may be attributed to poor absorbability of nutrients on negatively charged quartz grains which predominate in this zone (Sarkar et al 2004).

In zone 1 of core S-41, TOC is nearly constant with major points falling near average line except the decreasing trend between 56-46 cm and 32-26 cm which coincide with decreasing trend of clay and increasing trend on sand respectively. TN shows less variation in comparison to TP around average line. In zone 2 TOC, TN and TP increases (Figure 3.4a.3). The high and

increased TOC, TN and TP in zone 2 is mainly attributed to extensive use of fertilizers, population growth, increased inputs of terrestrial sedimentary matter associated with urban waste (Ruiz-Fernández et al 2003; Jonathan et al 2004; Zourarah et al 2009).

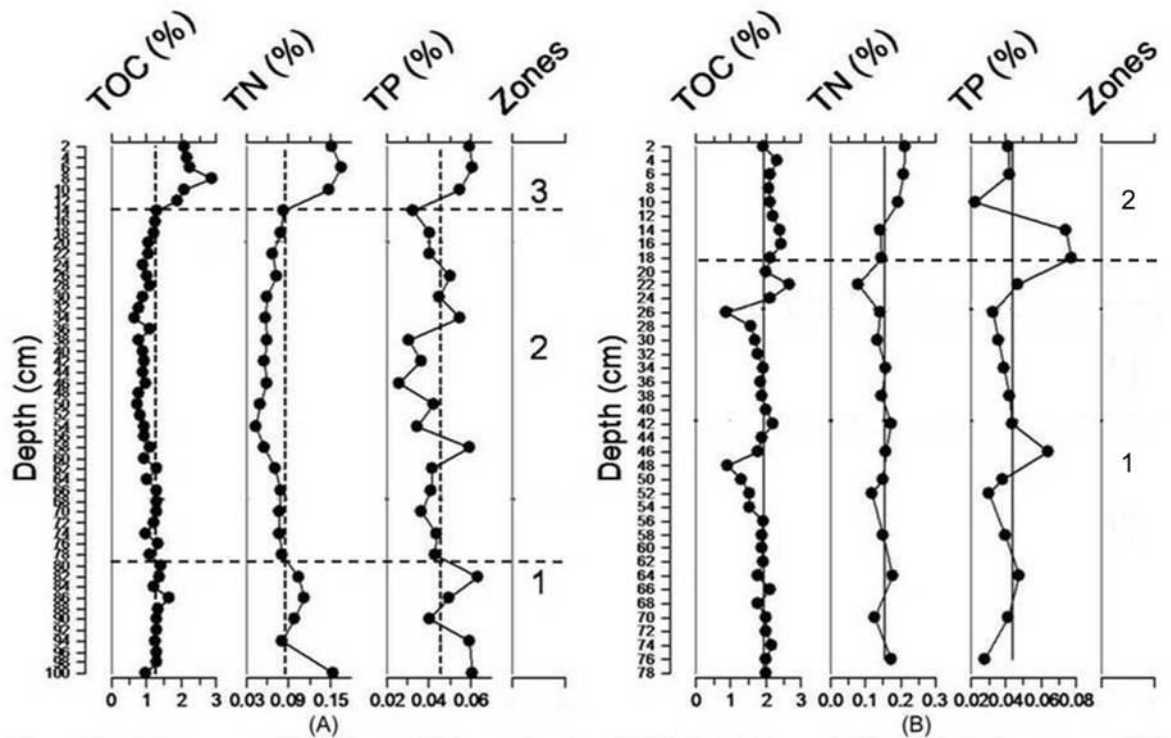


Figure 3.4a.3 Down-core distribution of total organic carbon (TOC), total nitrogen (TN) and total phosphorous (TP) in different zones with zone 1 representing bottom while zone 3 in core S-18 (A) and zone 2 in core S-41 (B) represents the top. The vertical line represents average value.

3.4A.5 C/N ratio

C/N ratio in the present study ranges from 14 to 22 with a mean of 18 for core S-18 and 12 to 17 with a mean of 14 for core S-41.

In core S-18 C/N values in zone 1 (6-18) indicated both marine and terrestrially derived organic matter. In zone 2 C/N values (12-22) indicated mainly terrestrially derived organic matter while in zone 3 the decreasing trend of C/N ratio suggest increasing contribution from marine derived organic matter (Cupery 2011) (Figure 3.4a.4).

In core S-41, the large variations in C/N values in zone 1 is attributed to dynamic interaction of wave and river (Muller 1977) while in zone 2 C/N

values shows overall decreasing trend which suggest increasing contribution of marine derived organic matter (Figure 3.4a.4).

3.4A.6 pH

In core S-18 ranges from 6.84 to 7.69 with a mean of 7.37 for core S-18 and 5.42 to 7.23 with a mean of 6.46 for core S-41.

In core S-18, pH showed slightly basic conditions in zone 1 and 2 while slightly acidic conditions in zone 3 (Figure 3.4a.5). In core S-41, pH conditions varied from slightly basic in zone 1 to acidic in zone 3 (Figure 3.4a.5).

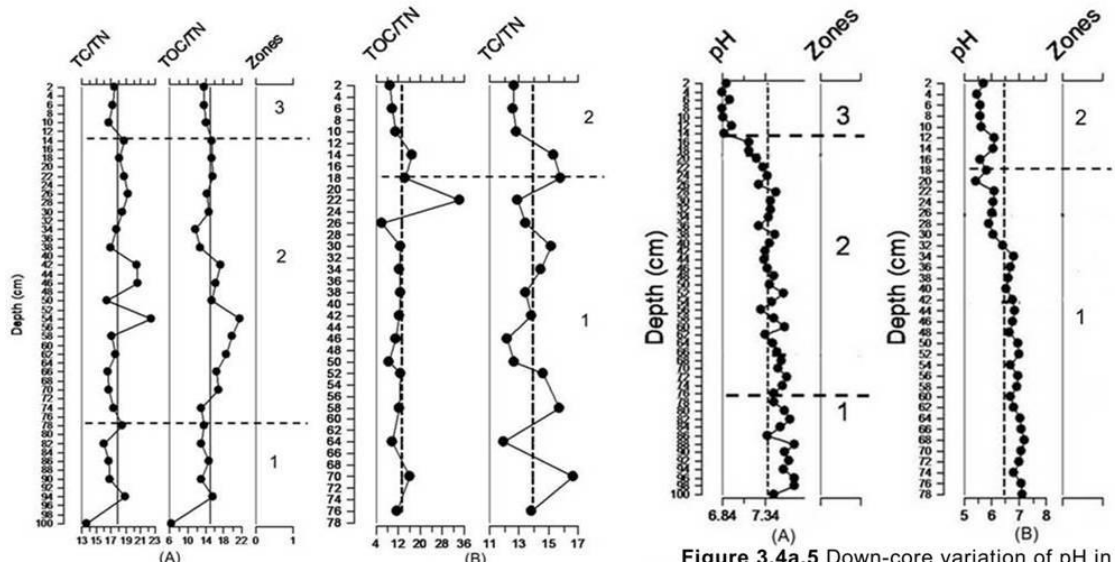


Figure 3.4a.4 Down-core variation of C/N ratio in different zones with zone 1 representing bottom while zone 3 in core S-18 (A) and zone 2 in core S-41 (B) represents the top. The vertical line represents average value.

Figure 3.4a.5 Down-core variation of pH in different zones with zone 1 representing bottom while zone 3 in core S-18 (A) and zone 2 in core S-41 (B) represents the top. The vertical line represents average value.

3.4A.7 Major elements (Fe, Mn and Al)

The data showed a range of 8.52 to 26.89% with a mean of 13.97% Fe, 1174 to 3184 ppm with a mean of 1969.58 ppm Mn and 6.55 to 13.51% with a mean of 9.08% Al for core S-18 and 8.17 to 17.91% with a mean of 11.01% Fe, 1412.67 to 2620.33 ppm with a mean of 1990.26 ppm Mn and 6.7 to 12.87% with a mean of 9.55% Al for core S-41. The mean and standard deviation of Fe, Mn and Al in each zone are given in table 3.4.

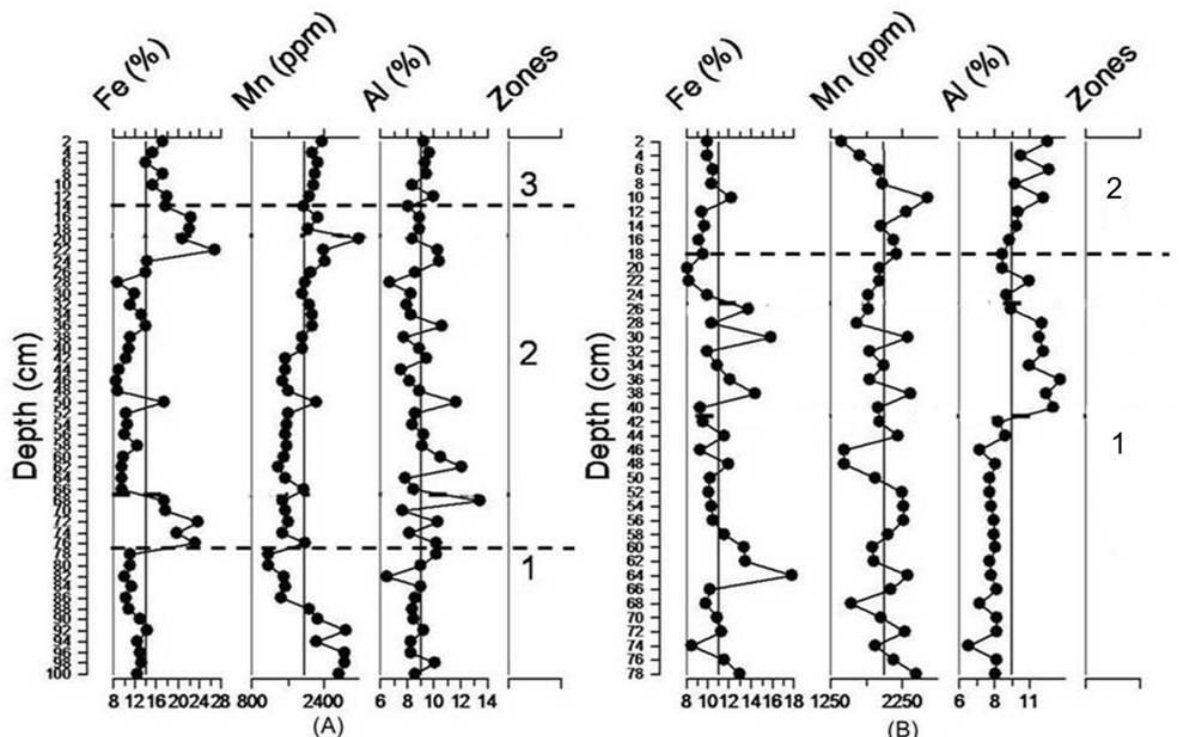


Figure 3.4a.6 Down-core variation of major elements (Fe, Mn and Al) in different zones with zone 1 representing bottom while zone 3 in core S-18 (A) and zone 2 in core S-41 (B) represents the top. The vertical line represents average value.

In zone 1 of core S-18 Fe and Mn show an overall decrease. In zone 2, Fe and Mn show an overall increase with Fe displaying greater variations (Figure 3.4a.6). In zone 3, Mn increases and Fe decreases. However, in surface layers (6-0 cm) Fe concentration increases. Al is nearly constant in zone 1 and 3 but shows greater variations in zone 2. In zone 1 of core S-41 Fe and Mn vary around average line. Al concentration remains constant below the average line (Figure 3.4a.6). In zone 2 Fe and Al showed relatively higher concentration. In zone 3 between 26 cm and 10 cm Fe, Mn and Al increased gradually and from 10 cm to surface Fe and Mn decreased gradually while Al showed fluctuations (Figure 3.4a.6).

3.4A.8 Trace elements (Ni, Cr, Co, Zn and Pb)

The data showed a range of 130 to 219 with a mean of 150.53 ppm Ni, 152 to 343.67 with a mean of 239.86 ppm Cr, 66 to 120.67 ppm with a mean of 93.49 ppm Co, 140.67 to 261 ppm with a mean of 169.40 Zn and 24.33 to 98 ppm with a mean of 53.67 ppm Pb for core S-18 and 109 to 226.33 with a mean of 137.65 ppm Ni, 177.67 to 422 with a mean of 248.67 ppm Cr, 87.67 to 147 ppm with a mean of 104.82 ppm Co, 124.7 to 215.1 ppm with a mean

of 153.92 Zn and 15.67 to 65.67 ppm with a mean of 49.3 ppm Pb for core S-41. The mean and standard deviation of Ni, Cr, Co, Zn and Pb in each zone are given in table 3.4.

In zone 1 of core S-18, trace metals show higher concentration which roughly coincides with intervals of higher silt, clay, TOC, TN and TP concentration (Figure 3.4a.7). In zone 2 trace metals show different trends with Ni, Zn and Pb displaying an overall increase while Cr and Co displaying an overall decrease. The peak values of trace metals (Ni, Co, Zn and Pb) at 20 cm depth agrees with Mn peak probably indicates precipitation of Mn-oxides in the oxic sediments (Caetano et al 2009) while the peak of Al and Cr at 68 cm indicates their common terrigenous source. In zone 3, trace metals (except Pb) show overall decrease. In core S-41 trace metals show greater variations in zone 1 (Figure 3.4a.7). The peak value of trace metals at 64 cm agrees with Fe and Mn peak indicate readsorption by Fe and Mn oxyhydroxides (Zwolsman et al 1993). In zone 2, trace metals concentration is almost uniform. Pb concentration increases towards surface (Figure 3.4a.7). The peak value of trace metals (except Pb) at 10 cm agrees with Fe, Mn, Al peak probably suggest their natural or terrestrial sources (Zhou et al 2004).

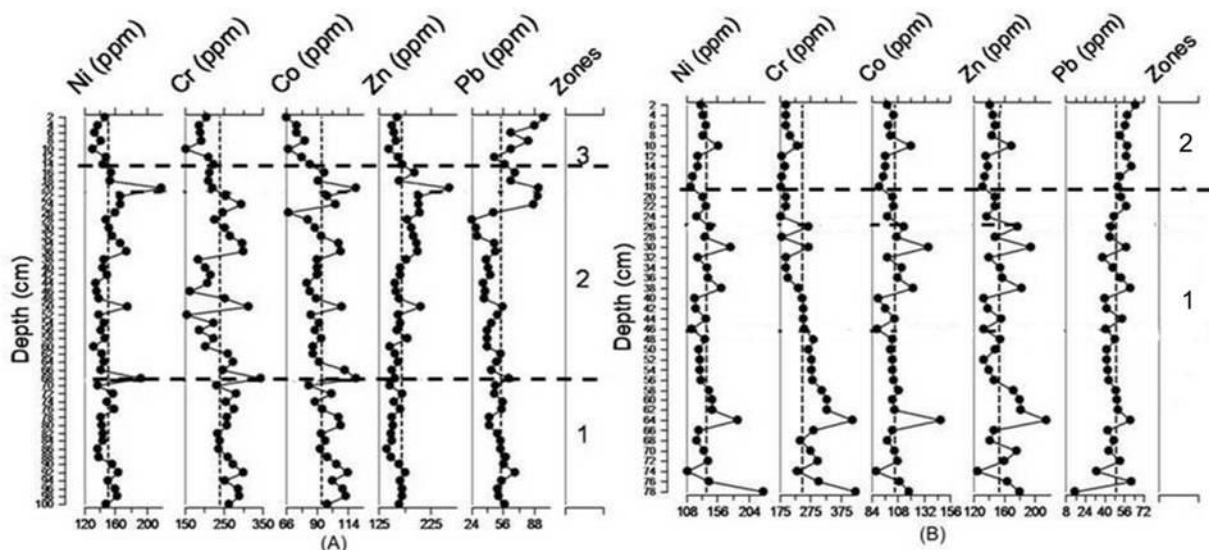


Figure 3.4a.7 Down-core variation of trace elements (Ni, Cr, Co, Zn and Pb) in different zones with zone 1 representing bottom while zone 3 in core S-18 (A) and zone 2 in core S-41 (B) represents the top. The vertical line represents average value.

3.4A.9 Clay minerals

The data showed a range of 37.9-63.6% with a mean of 51.8% smectite, 10.6-29.8% with a mean of 18.9% illite, 12.2-19.1% with a mean of 15.2% kaolinite and 8.9-19.9% with a mean of 14.1% chlorite for core S-18 and 47.4-65% with a mean of 55.9% smectite, 8.3-22.3% with a mean of 15% illite, 8.5-17.2% with a mean of 13% kaolinite and 10.4-21.1% with a mean of 16% chlorite for core S-41.

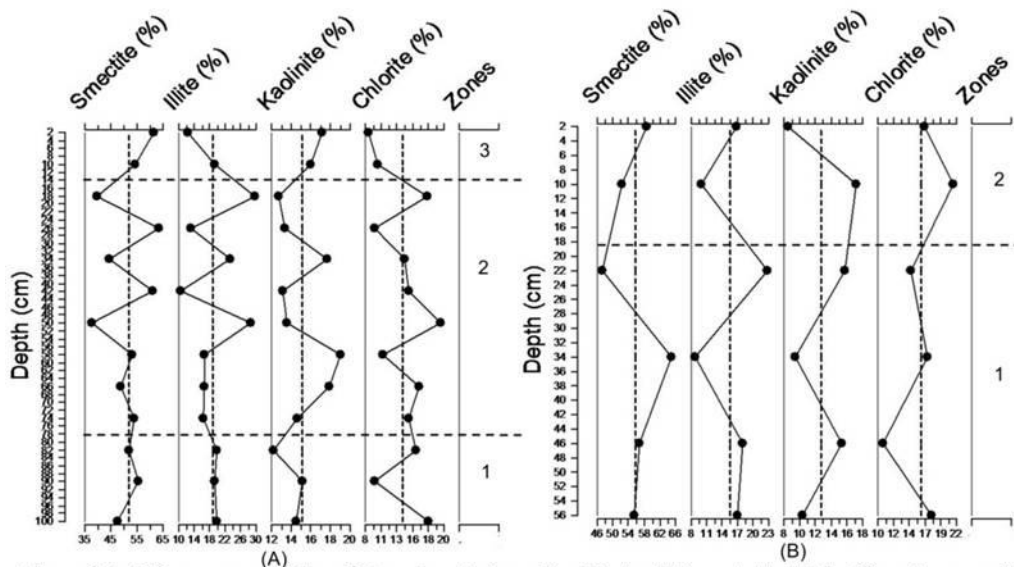


Figure 3.4a.8 Down-core variation of clay minerals (smectite, illite, kaolinite and chlorite) in different zones with zone 1 representing bottom while zone 3 in core S-18 (A) and zone 2 in core S-41 (B) represents the top. The vertical line represents average value.

Amongst the clay minerals, smectite was the dominant mineral and relatively higher in the middle estuary (S-41) (Figure 3.4a.8). The smectite is mainly derived from weathering of Deccan trap basalt. Alternatively, smectite may be transported by adjacent rivers discharging the smectite into the Arabian sea which in turn enters into the estuary during high tide. Rao and Rao (1995) reported that smectite is abundant in the inner shelf sediments. Since, the grain size of smectite is much smaller than that of kaolinite and illite, smectite tends to remain in suspension longer time and selectively winnows farther from its source. On the other hand, kaolinite is coarser than other clay minerals so it settles quickly in lower estuary. Smectite also chemically alters to illite and chlorite. Chlorite survives under low weathering while illite is transformed to kaolinite with enhanced weathering. The marginally higher proportion of smectite observed in zone 3 (14-0 cm) of lower estuary (S-18) may be attributed to higher proportion of fine sediments and bonding with organic elements. The relatively higher illite and kaolinite concentration is

observed in lower estuary (S-18) which may indicate strong hydrolytic conditions (Chamley 1989). The rivers along central west coast of India originates from mountain ranges of Sahayadris and receives average annual rainfall of 3750 mm of which 95% occurs during the monsoon period (June-September). The heavy rainfall during monsoons causes vigorous drainage leading to strong hydrolytic processes on parent rocks. As a result intense leaching takes place in the parent rocks. Further, illite and kaolinite are predominantly present as suspension load in the estuary and continental shelf region of the Arabian sea. Therefore it can be inferred that these clay minerals might be contributed by the sea. The distribution of clay minerals is therefore closely associated with factors including river runoff, tidal currents, wave energy, differential flucculations, size segregation, physical sorting, resuspension of bottom sediments and chemical alteration.

3.4A.10 Diatoms

A total of 32 diatom genera were identified. Diatoms were mainly represented by genera *Diploneis*, *Cyclotella*, *Hydrosera*, *Cymatotheca*, *Nitzschia*, *Aulacosira*, *Tryblioptychus*, *Navicula*, *Epithemia*, *Achnanthes*, *Triceratium*, *Pinnularia*, *Biddulphia*, *Schuattia*, *Amphora*, *Thalassiosira*, *Rhaphoneis*, *Surirella*, *Gomphonema*, *Hyalodiscus*, *Rhopalodia*, *Grammatophora*, *Stauroneis*, *Cymbella*, *Synedra*, *Pleurosigma*, *Coscinodiscus*, *Distephanus*, *Thalassionema*, *Eunortia*, *Cerataulina* and *Achnanthes*. Diatoms genera with <1% representation were not used for interpretation.

In core S-18 (Figure 3.4a.9), *Cyclotella*, *Nitzschia*, *Cymatotheca*, *Coscinodiscus*, *Thalassiosira*, *Rhaphoneis* and *Diploneis* were the dominant diatom genera. Freshwater diatoms ranged from 32 to 84% while marine diatoms ranged from 18 to 69%. Zone 1, is characterized by predominance of freshwater forms like *Cyclotella meneghiniana* (range 40-45%), *Cymatotheca weissflogii* (range 7-8%), *Nitzschia cocconeiformis* (range 10-12%) and *Coscinodiscus halose* (range 8-10%). In zone 2, between 80 and 38 cm, diatom genera were either totally absent or less frequent. This may be attributed to higher sand content and low nutrient concentration noted at

this depth. Zone 3 shows higher relative dominance of marine diatoms. In core S-41, freshwater diatoms ranged from 50 to 78% while marine diatoms ranged from 22 to 50% (Figure 3.4a.10). In zone 1 freshwater namely *Cyclotella*, *Nitzschia*, *Coscinodiscus* and marine diatom genera namely *Rhaphoneis*, *Thalassiosira*, *Hyalodiscus*, *Thalassionema* and *Triceratium* showed their peak dominance. In zone 2, relative dominance of freshwater diatoms decreased and marine diatoms increased.

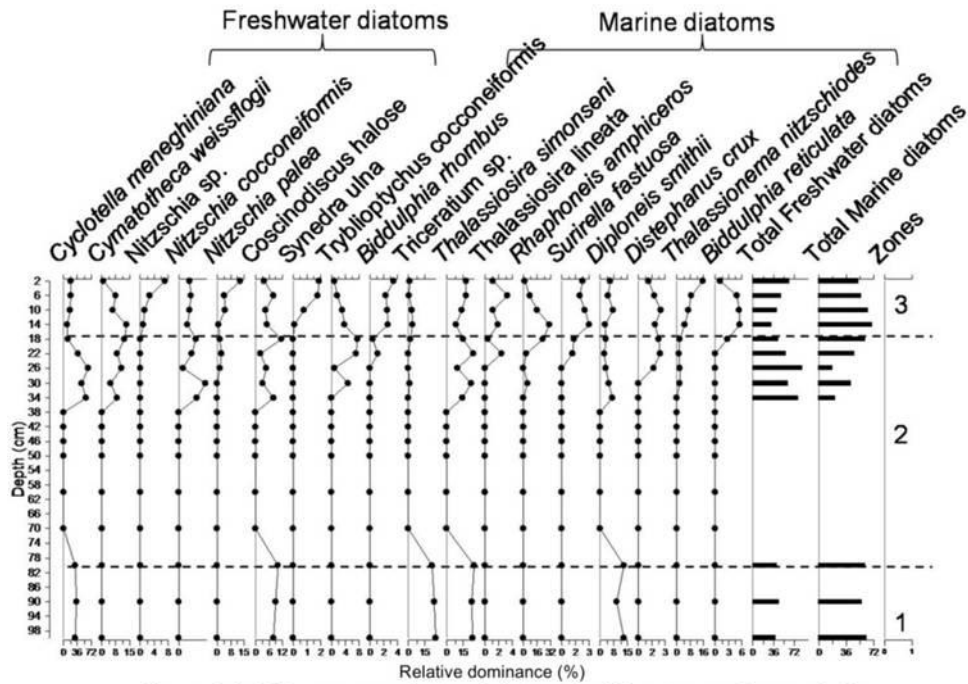


Figure 3.4a.9 Down-core variation of diatoms in different zones for core S-18

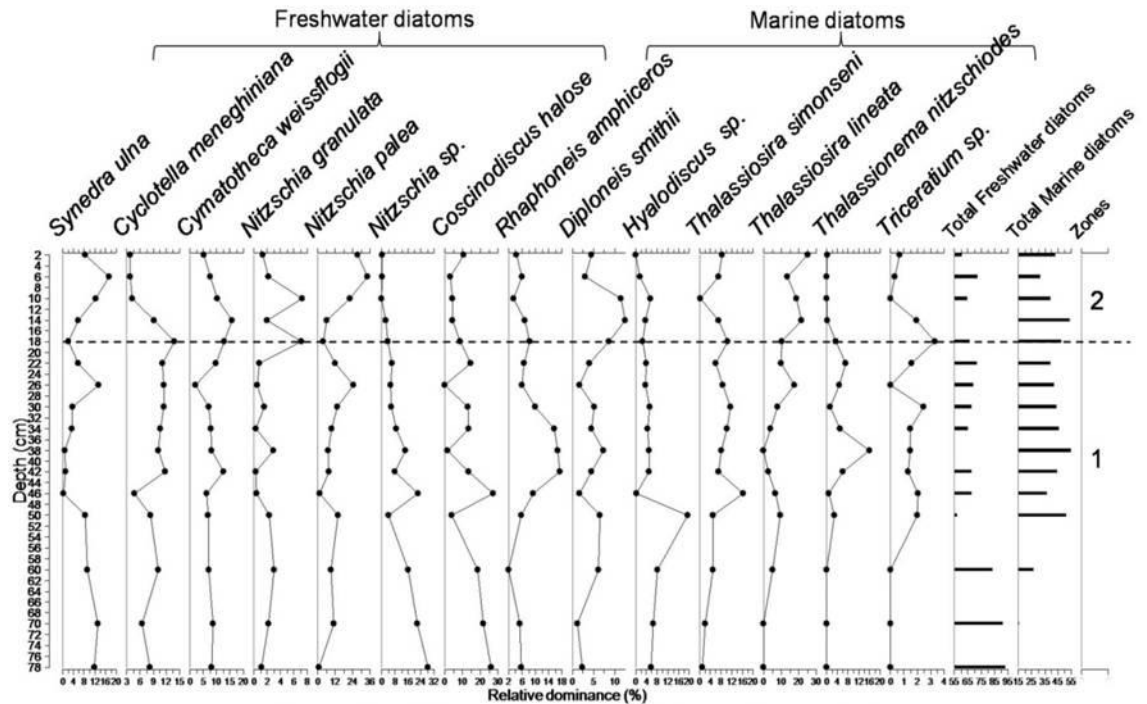


Figure 3.4a.10 Down-core variation of diatoms for core S-41

4A.11 Paired t-test analysis

Statistical t-test analysis ($p < 0.05$) indicated significant differences in the distribution of

Variables	Difference of means	t	df	Sig. (2-tailed)
S18sand - S41sand	27.80	16.25	38	0.00
S18silt - S41silt	-3.20	-1.37	38	0.18
S18clay - S41clay	-24.60	-11.90	38	0.00
S18pH - S41pH	0.85	12.62	38	0.00
S18Fe - S41Fe	3.52	3.61	38	0.00
S18Mn - S41Mn	-75.79	-0.92	38	0.37
S18Al - S41Al	-0.35	-0.94	38	0.36
S18Ni - S41Ni	13.15	2.80	38	0.01
S18Cr - S41Cr	-15.35	-1.39	38	0.17
S18Co - S41Co	-13.93	-4.92	38	0.00
S18Zn - S41Zn	18.30	3.63	38	0.00
S18Pb - S41Pb	4.21	1.52	38	0.14
S18TOC - S41TOC	-0.65	-7.20	38	0.00
S18TN - S41TN	-0.07	-9.67	14	0.00
S18TP - S41TP	0.00	-0.14	14	0.89

sand, clay, pH, Fe, Ni, Co, Zn, TOC, TN between the two cores (Table 3.4a.1).

3.4A.12 Correlation

In core S-18, the significant positive correlation of Ni and Pb with Fe-Mn indicates their association with Fe-Mn oxyhydroxides (Chatterjee et al 2007). Al did not show significant correlation with trace metals (except Cr). Al, Fe and Mn did not show any significant correlation with each other (Table 3.4a.2). Further, no significant association of trace metals (except Zn) with sand, silt, clay or TOC indicates that they are derived from different sources.

The significant positive correlation between nutrients (TN and TP) and clay is attributed to higher surface area for fine particles (Meyers 1994). The significant correlation of Cr and Co with pH suggests that their distribution is controlled by pH. Cr also showed significant positive association with Al. In core S-41, trace metals (except Pb) are positively correlated with Fe and/or Mn (Table 3.4a.3). Al did not show any significant positive correlation with trace elements (except Pb). Trace metals show no significant positive association with sand, silt, clay, TOC or Al. Cr is positively correlated with pH (Table 3.4a.3).

Table 3.4a.2 Pearson correlation coefficient for core S-18

	Sand	Silt	Clay	TOC	pH	Fe	Mn	Al	Ni	Cr	Co	Zn	Pb	TN	TP
Sand	1														
Silt	-0.809**	1													
Clay	-0.872**	0.417**	1												
TOC	0.386**	0.224	-0.784**	1											
pH	0.086	0	-0.133	0.099	1										
Fe	-0.031	0.057	0.001	0.044	-0.310*	1									
Mn	-0.108	0.218	-0.014	0.157	-0.166	0.355*	1								
Al	0.023	-0.075	0.027	-0.093	-0.064	0.304*	-0.027	1							
Ni	0.234	-0.136	-0.249	0.177	0.132	0.450**	0.499**	0.350*	1						
Cr	-0.006	0.026	-0.013	0	0.502**	0.149	0.176	0.408**	0.566**	1					
Co	0.122	0.041	-0.222	0.248	0.597**	0.077	0.227	0.295*	0.651**	0.712**	1				
Zn	0.473**	-0.316*	-0.467**	0.300*	-0.049	0.356*	0.550**	0.042	0.786**	0.26	0.340*	1			
Pb	-0.338*	0.176	0.376**	-0.249	-0.454**	0.597**	0.521**	0.287*	0.344*	0	0.022	0.222	1		
TN	-0.665**	0.375	0.666**	-0.479*	-0.494*	0.059	0.449*	-0.123	-0.452*	-0.314	-0.428*	-0.479*	0.534**	1	
TP	-0.505**	0.17	0.587**	-0.526**	-0.092	-0.035	0.376	-0.088	-0.003	0.124	-0.125	-0.048	0.285	0.611**	1

** Correlation is significant at the 0.01 level (2-tailed). * Correlation is significant at the 0.05 level (2-tailed).

Table 3.4a.3 Pearson correlation coefficient for core S-41

	Sand	Silt	Clay	TOC	pH	Fe	Mn	Al	Ni	Cr	Co	Zn	Pb	TN	TP
Sand	1														
Silt	-0.24	1													
Clay	-0.025	-0.965**	1												
TOC	-0.589**	-0.125	0.289	1											
pH	0.181	-0.198	0.155	-0.267	1										
Fe	0.249	-0.099	0.034	-0.387*	0.248	1									
Mn	-0.181	-0.08	0.132	0.241	0.124	0.338*	1								
Al	-0.172	0.069	-0.024	0.145	-0.528**	0.059	0	1							
Ni	0.03	-0.309	0.31	-0.122	0.174	0.762**	0.460**	0.094	1						
Cr	0.235	-0.234	0.177	-0.313	0.671**	0.639**	0.318*	-0.498**	0.660**	1					
Co	0.176	-0.075	0.029	-0.234	0.136	0.871**	0.487**	0.149	0.819**	0.522**	1				
Zn	0.204	-0.11	0.058	-0.244	0.238	0.919**	0.343*	0.026	0.810**	0.662**	0.879**	1			
Pb	-0.148	0.231	-0.198	0.232	-0.434**	0.179	0.021	0.373*	-0.08	-0.330*	0.246	0.189	1		
TN	-0.155	-0.221	0.282	-0.047	-0.262	0.137	-0.106	0.264	0.07	0.017	0.01	0.006	0.29	1	
TP	-0.189	0.058	0.017	0.364	-0.166	-0.311	-0.297	-0.209	-0.43	-0.334	-0.425	-0.38	0.023	-0.167	1

** Correlation is significant at the 0.01 level (2-tailed). * Correlation is significant at the 0.05 level (2-tailed).

3.4A.13 Factor analysis

Table 3.4a.4 Varimax R-mode factor analysis for core S-18 (A) and S-41 (B)

	(A)			(B)			
Variance (%)	30.58	22.49	20.19	Variance (%)	30.88	20.72	18.70
Sand (%)	-0.98	-0.03	0.02	Sand (%)	0.07	-0.85	0.15
Silt (%)	0.79	0.05	0.11	Silt (%)	-0.16	-0.14	-0.78
Clay (%)	0.86	0.01	-0.11	Clay (%)	0.14	0.37	0.76
Mud (%)	0.99	0.03	-0.02	Mud (%)	-0.07	0.85	-0.15
TOC (%)	0.67	0.15	-0.47	TOC (%)	-0.16	0.83	0.06
pH	-0.06	-0.40	0.81	pH	0.20	-0.33	0.60
Fe (%)	0.02	0.77	-0.09	Fe (%)	0.92	-0.26	-0.05
Mn (ppm)	0.06	0.72	0.08	Mn (ppm)	0.56	0.35	0.11
Al (%)	0.06	0.39	0.23	Al (%)	0.12	0.34	-0.53
Ni (ppm)	-0.28	0.73	0.53	Ni (ppm)	0.90	0.07	0.21
Cr (ppm)	0.03	0.24	0.85	Cr (ppm)	0.65	-0.32	0.50
Co (ppm)	-0.10	0.24	0.88	Co (ppm)	0.95	-0.10	-0.12
Zn (ppm)	-0.56	0.65	0.21	Zn (ppm)	0.94	-0.18	-0.02
Pb (ppm)	0.33	0.80	-0.21	Pb (ppm)	0.20	0.24	-0.65

Positive loadings highlighted in bold are > 0.5 significant at $p < 0.05$

In core S-18, the three factors (F1, F2 and F3) correspond to 73.25% of the total variance. F1, F2 and F3 accounted for 30.58%, 22.49% and 20.19% respectively (Table 3.4a.4). F1 showed positive loadings on silt (0.79), clay (0.86), mud (0.99) and TOC (0.67). F2 showed significant positive loadings on Fe (0.77), Mn (0.72), Ni (0.73), Zn (0.65) and Pb (0.80) (Table 3.4a.4). F3 showed significant loadings on pH (0.81), Cr (0.86), Co (0.88) and Ni (0.53). In core S-41, three factors correspond to 70.3% of the total variance. F1 showed positive loadings on Fe (0.92), Mn (0.56), Ni (0.9), Cr (0.65), Co (0.95) and Zn (0.94). F2 showed significant loadings on mud (0.85) and TOC (0.83). F3 showed significant loadings on clay (0.76), pH (0.60) and Cr (0.50).

3.4A.14 Enrichment factor (EF) and index of geoaccumulation (Igeo)

In the present study (Table 3.4a.5), EF value showed a range of 1.33 to 4.41 with a mean of 2.62 Fe, 1.04 to 3.60 with a mean of 2.08 Mn, 1.38 to 3.06 with a mean of 1.98 Ni, 1.60 to 3.18 with a mean of 2.37 Cr, 3.01 to 6.00 with a mean of 4.39 Co, 0.97 to 2.60 with a mean of 1.60 Zn and 1.35 to 4.38 with a mean of 2.37 Pb for core S-18 and 1.27 to 3.27 with a mean of 2.00 Fe, 1.11 to 2.73 with a mean of 2.01 Mn, 1.13 to 3.15 with a mean of 1.74 Ni,

1.38 to 4.49 with a mean of 2.42 Cr, 3.04 to 7.57 with a mean of 4.73 Co, 0.9 to 2.20 with a mean of 1.39 Zn and 0.74 to 3.01 with a mean of 2.09 Pb for core S-41 (Table 3.4a.5). Igeo value showed a range of 0.27 to 1.93 with a mean of 0.91 Fe, -0.12 to 1.32 with a mean of 0.59 Mn, 0.35 to 1.1 with a mean of 0.55 Ni, 0.17 to 1.35 with a mean of 0.81 Cr, 1.21 to 2.08 with a mean of 1.70 Co, -0.02 to 0.87 with a mean of 0.24 Zn and -0.3 to 1.71 with a mean of 0.77 Pb for core S-18 and 0.21 to 1.34 with a mean of 0.61 Fe, 0.15 to 1.04 with a mean of 0.63 Mn, 0.1 to 1.15 with a mean of 0.42 Ni, 0.4 to 1.64 with a mean of 0.84 Cr, 1.62 to 2.37 with a mean of 1.87 Co, -0.19 to 0.59 with a mean of 0.1 Zn and -0.94 to 1.13 with a mean of 0.68 Pb for core S-41.

Table 3.4a.5 Mean and standard deviation of enrichment factor (EF) and index of geoaccumulation (Igeo) for core S-18 and S-41					
S-18			S-41		
	Zone 1 (100-78) N=12	Zone 2 (78-14 cm) N=33	Zone 3 (14-0 cm) N=7	Zone 1 (78-18 cm) N=31	Zone 2 (18-0 cm) N=9
Enrichment Factor (EF)					
Fe	2.33±0.29	2.64±0.94	3.06±0.38	2.10±0.49	1.64±0.14
Mn	2.25±0.72	1.95±0.51	2.26±0.17	2.07±0.41	1.84±0.39
Ni	2.03±0.26	2.00±0.31	1.81±0.15	1.81±0.39	1.47±0.11
Cr	2.68±0.31	2.36±0.40	1.89±0.26	2.62±0.83	1.67±0.15
Co	5.00±0.47	4.38±0.61	3.46±0.45	4.91±0.84	4.04±0.36
Zn	1.53±0.19	1.64±0.32	1.47±0.16	1.45±0.28	1.16±0.09
Pb	2.46±0.44	2.18±0.68	3.10±0.75	2.07±0.46	2.19±0.19
Index of geoaccumulation (Igeo)					
Fe	0.74±0.16	0.92±0.50	1.21±0.13	0.64±0.26	0.51±0.12
Mn	0.63±0.50	0.51±0.29	0.78±0.09	0.63±0.20	0.64±0.26
Ni	0.54±0.09	0.58±0.16	0.45±0.07	0.43±0.21	0.35±0.14
Cr	0.96±0.12	0.82±0.26	0.52±0.18	0.92±0.32	0.53±0.12
Co	1.85±0.10	1.71±0.17	1.39±0.13	1.88±0.6	1.81±0.11
Zn	0.15±0.10	0.29±0.18	0.14±0.08	0.12±0.19	0.00±0.11
Pb	0.81±0.20	0.66±0.44	1.21±0.37	0.61±0.36	0.93±0.12

In zone 1, 2 and 3 of core S-18, the average EF value for Mn, Ni, Cr and Zn falls between 1 and 3 indicating minor enrichment; the average EF value for Co falls between 3 and 5 indicating moderate enrichment (Table 3.4a.5). The average EF value for Fe and Pb falls between 3 and 5 in zone 3 reflecting an increase in Fe and Pb contamination in the recent years. In zone 1 and 2 of core S-41, the average EF value for Fe, Mn, Ni, Zn and Pb falls between 1 and 3 indicating minor enrichment. In zone 2, average EF value for Cr falls between 1 and 3 and Co falls between 5 and 10 indicating minor and moderate enrichment of Cr and Co respectively. Zhang and Liu (2002) recommended using EF=1.5 as an assessment criterion, i.e. if EF value between 0.5 and 1.5 (i.e. $0.5 \leq EF \leq 1.5$) suggest that the trace element may be

entirely from crustal materials or natural weathering process while EF values greater than 1.5 (i.e. $EF \geq 1.5$) suggests that the significant portion of the trace metal is derived from non crustal material. In the present study, average values for all the elements is more than 1.5 in both the cores (S-18 and S-41) suggesting significant anthropogenic impact on metal levels in the estuary.

In zone 1, 2 and 3 of core S-18, the average Igeo value for Mn, Ni, Cr and Zn falls in class 1 which indicates that sediments are unpolluted to moderately polluted; Pb and Zn falls in class 1 in zone 1 and 2 and in class 3 in zone 3 reflecting an increase in Fe and Pb contamination in the recent years (Table 3.4a.5). Co falls in class 2 in zone 1, 2 and 3. In zone 1 and 2 of core S-41, the average Igeo value for Fe, Mn, Ni, Zn and Pb falls in class 1; Co falls in class 2 in zone 1 and 3 indicating that sediments are moderately polluted, Cr falls in class 2 in zone 1 and in class 1 in zone 2.

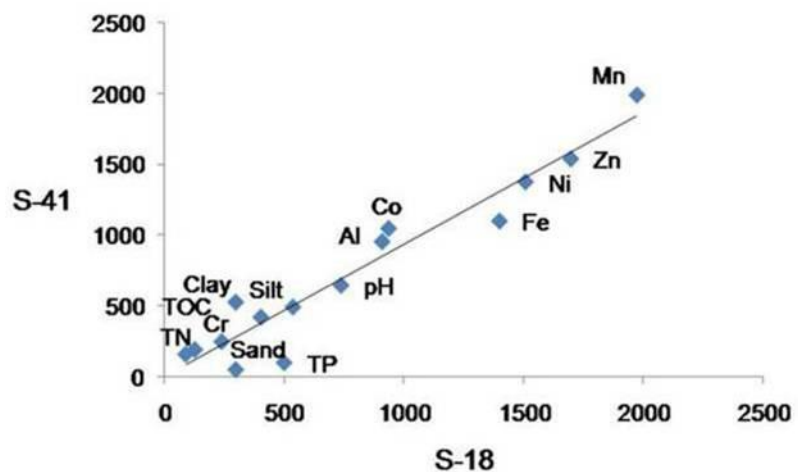


Figure 3.4a.11 Isocon diagram. Individual point represents average value.

3.4A.15 Isocon

When two locations are compared relatively higher Zn, Ni, Fe, sand, TP and pH are deposited at lower estuary while TOC, TN, clay, silt, Al, Co and Mn are found to be higher in the lower estuary (Figure 3.4a.11).

3.4 B Mangroves

Core S-21 was collected from lower middle estuarine region. The sediment colour was brown from 0 to 25 cm. The remaining part of the core was dark grey to black.

The data showed a range of 0.79 to 10.89% with a mean of 3.45% sand, 32.84 to 77.27% with a mean of 44.60% silt and 19.80 to 65.36% with a mean of 51.95% clay. The core is dominated by clay component and the fine sediment constitutes more than 95% (Figure 3.4b.1). The hydrodynamic plots (Pejrur 1988) reveal that the sediment deposition took place under relatively violent to less violent conditions (Figure 3.4b.2).

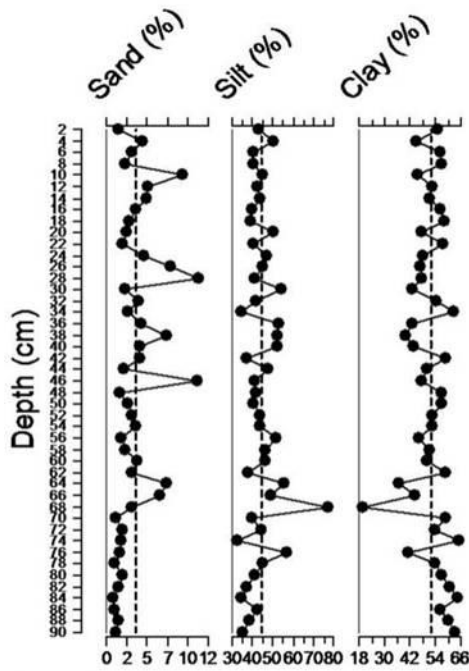


Figure 3.4b.1 Down-core variation of sediment grain size for core S-21

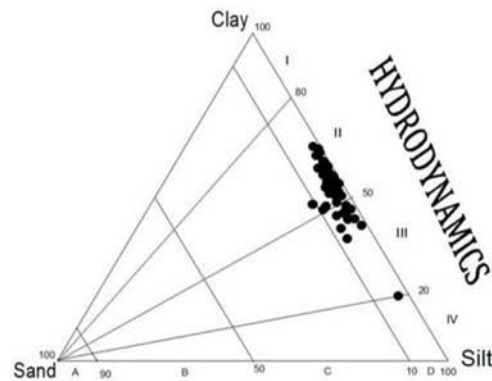


Figure 3.4b.2 Ternary diagram for the classification of hydrodynamic condition after Pejrup (1988)

Conclusion

The distribution of sediment grain size indicated silt and clay as the major sediment components in lower (S-18) and middle (S-41) estuary respectively. Smectite was the major clay mineral and is relatively higher in the middle estuary (S-41). Marine diatoms showed higher relative dominance in lower estuary (S-18) while in the middle estuary (S-41) freshwater diatoms were predominant. The trace metal distribution is mainly controlled by Fe-Mn oxyhydroxides. However, in the lower estuary (S-18) pH also regulated trace metals (Ni, Cr and Co) distribution. Index of geo-accumulation (I_{geo}) computed indicated that Savitri estuary is unpolluted to moderately polluted with respect to Fe, Mn, Ni, Cr, Zn and Pb and moderately polluted with respect to Co. Enrichment factor (EF) calculated indicate average EF value

greater than 1.5 for all the elements (except Zn in middle estuary) suggesting significant anthropogenic enrichment in the estuary.

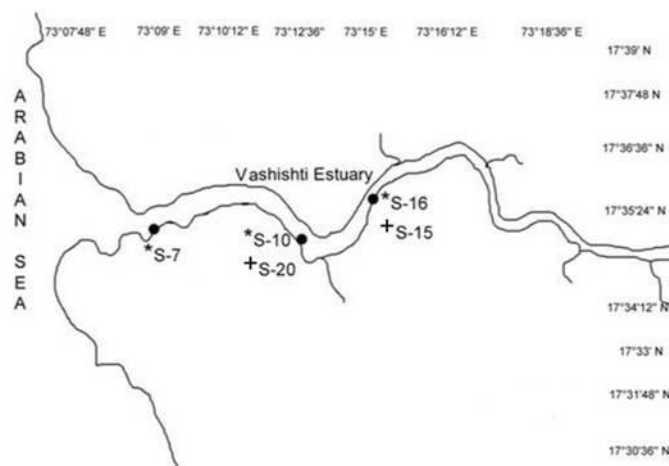


Figure 3.5 Location of core collection from Vashishti Estuary
*Mudflat core +Mangrove core

3.5 Vashishti estuary

Total five cores, three from mudflats (S-7, S-10 and S-16) and remaining two from mangroves (S-20 and S-15) were collected along Vashishti estuary (Figure 3.5).

3.5A Mudflats

3.5A.1 Collection of sediment cores

Amongst the three cores collected from mudflats one represented lower estuary (S-7) while the other two cores (S-10 and S-16) represented lower middle (S-10) and upper middle (S-16) estuarine regions (Figure 3.5). The core length varied from 82 cm to 108 cm. All the three cores (S-7, S-10 and S-16) were analyzed for sediment grain size, TOC and pH; S-10 was further analyzed for TN, TP and metals.

3.5A.2 Colour

Sediment colour was uniform grey in core S-7 and uniform brown in core S-10 and S-16.

3.5A.3 Sediment grain size

The data showed a range of 6.77 to 25.19% with a mean of 13.66% sand, 39.1 to 54.29% with a mean of 47.73% silt and 30.16 to 46.08% with a mean of 38.61% clay for core S-7; 0.71 to 12.65% with a mean of 4.82% sand, 39.22 to 61.85% with a mean of 49.99% silt and 37.16 to 59.52% with a mean of 45.19% clay for core S-10 and 0.77 to 15.65% with a mean of

4.51% sand, 28.5 to 79.63% with a mean of 55.73% silt and 18.36 to 61.76% clay with a mean of 39.75% clay for core S-16. The core has been divided into different zones depending upon the distribution pattern of sediment components. The mean and standard deviation of sediment grain size in each zone is given are table 3.5a.

Table 3.5a Mean and standard deviation (values in parenthesis) of different parameters in each zone from core S-7, S-10 and S-16. The p-value denotes results of one way ANOVA statistically significant at $p < 0.05$. N=number of samples.

S-7				
	Zone 1 (102-58 cm) N=23	Zone 2 (58-26 cm) N=17	Zone 3 (26-0 cm) N=13	
	Mean (Standard deviation)	Mean (Standard deviation)	Mean (Standard deviation)	
Sand (%)	11.02 (± 2.34)	16.76 (± 4.19)	13.97 (± 2.25)	
Silt (%)	48.29 (± 2.93)	45.89 (± 3.76)	49.36 (± 2.35)	
Clay (%)	40.68 (± 3.04)	37.34 (± 3.44)	36.66 (± 2.93)	
TOC (%)	3.03 (± 0.54)	3.21 (± 0.32)	2.97 (± 0.50)	
pH	7.28 (± 0.15)	7.27 (± 0.11)	6.99 (± 0.13)	
S-10				
	Zone 1 (108-62 cm) N=24	Zone 2 (62-26 cm) N=19	Zone 3 (26-0 cm) N=13	p value (*statistically significant at $p < 0.05$)
	Mean (standard deviation)	Mean (standard deviation)	Mean (standard deviation)	
Sand (%)	6.28 (± 3.36)	4.98 (± 2.64)	2.37 (± 1.00)	*0.00
Silt (%)	48.23 (± 3.23)	50.53 (± 3.05)	52.87 (± 4.20)	*0.00
Clay (%)	45.49 (± 4.66)	44.49 (± 3.76)	44.75 (± 4.42)	0.74
TOC (%)	2.24 (± 0.45)	2.55 (± 0.58)	2.80 (± 0.26)	*0.00
TN (%)	0.13 (± 0.08)	0.14 (± 0.08)	0.13 (± 0.06)	0.83
TP (%)	0.02 (± 0.01)	0.03 (± 0.01)	0.03 (± 0.01)	*0.00
C/N	22.57 (± 13.52)	22.64 (± 10.94)	26.52 (± 11.70)	0.60
pH	7.20 (± 0.18)	7.19 (± 0.17)	6.94 (± 0.11)	*0.00
Fe (%)	9.66 (± 0.97)	9.24 (± 0.94)	10.10 (± 1.50)	0.10
Mn (ppm)	1489.60 (± 185.35)	1361.50 (± 137.84)	1357.20 (± 159.69)	*0.02
Al (%)	9.80 (± 1.61)	11.30 (± 1.83)	10.35 (± 1.99)	*0.03
Ni (ppm)	119.64 (± 9.36)	122.70 (± 8.94)	120.28 (± 11.95)	0.59
Cr (ppm)	179.18 (± 16.77)	181.23 (± 15.51)	220.44 (± 24.52)	*0.00
Co (ppm)	84.00 (± 7.18)	78.98 (± 5.94)	75.00 (± 6.61)	*0.00
Zn (ppm)	140.88 (± 13.85)	145.81 (± 12.28)	154.86 (± 16.42)	*0.02
Pb (ppm)	47.19 (± 6.10)	38.81 (± 4.06)	58.03 (± 9.43)	*0.00
S-16				
	Zone 1 (84-34 cm) N=25	Zone 2 (34-0 cm) N=17		
	Mean (Standard deviation)	Mean (Standard deviation)		
Sand (%)	6.45 (± 3.54)	1.60 (± 0.72)		
Silt (%)	54.14 (± 15.67)	58.01 (± 10.20)		
Clay (%)	39.40 (± 14.11)	40.38 (± 10.11)		
TOC (%)	2.57 (± 0.38)	2.40 (± 0.22)		
pH	7.21 (± 0.14)	6.93 (± 0.09)		

In core S-7 silt and clay showed values higher than average in zone 1 while in zone 2 they are less than average (Figure 3.5a.1). Sand is higher than average in zone 2. In zone 3 sand varies around average line, silt is generally higher while clay is lower than their respective averages. Sand showed opposite trend to that of finer sediments in zone 1 and 2. In zone 3 it

fluctuated around average line. In zone 1 of core S-10 sand and silt showed an overall increasing trend while clay showed an overall decreasing trend (Figure 3.5a.1). In zone 2 clay increases, silt varies around average line. In zone 3 from 26 to 14 cm silt decreases, clay increases and from 14 to 0 cm silt increases and clay decreases. Sand showed over decreasing trend in zone 2 and 3. In zone 1 of core S-16 sand is higher than average while in zone 2 sand is uniform. Silt and clay fluctuate around average line in zone 1 and 2 (Figure 3.5a.1).

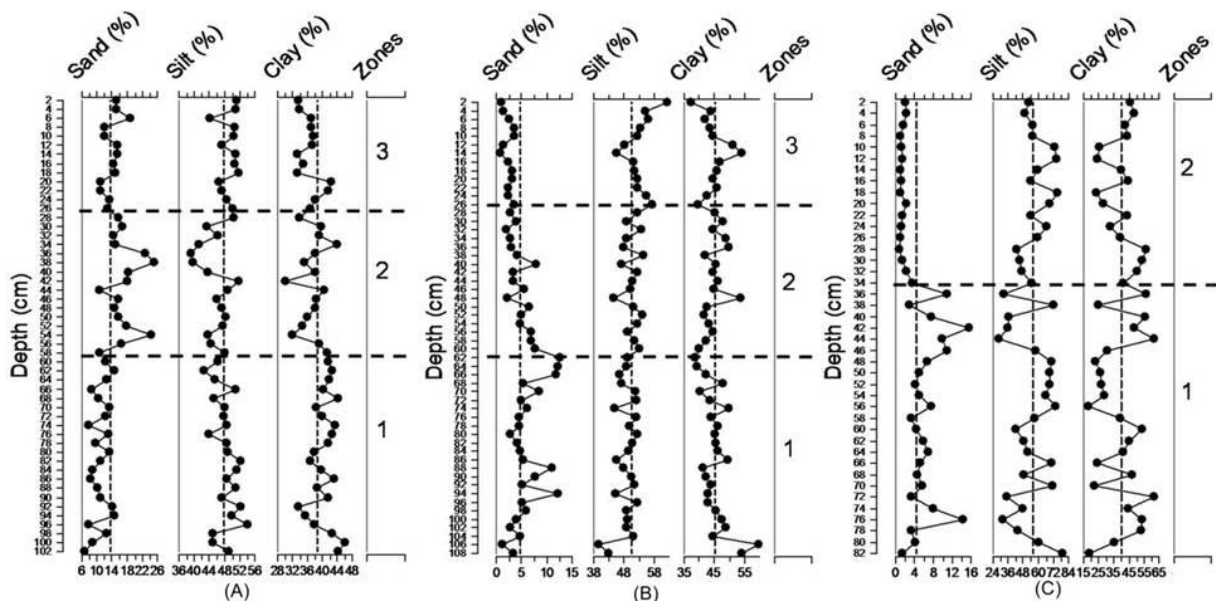


Figure 3.5A.1 Down-core variation of sediment grain size in different zones with zone 1 representing bottom while zone 3 represents the top for core S-7 (A), S-10 (B) and S-16 (C). The vertical line represents the average value

The hydrodynamic conditions of depositional environment revealed that the core S-7 collected from lower estuary fall within section III indicating that sediments must have deposited under relatively violent conditions (Figure 3.5a.2). Core S-10 and S-16 collected from lower middle and upper middle regions fall within section II and III indicating varying hydrodynamic conditions. Both S-10 and S-16 collected from middle estuarine region fall within “D type” indicating presence of poor sand and high concentration of silt and clay components while core S-7 fall within “C type” indicating the presence of slightly sand-dominated sediment, in the lower estuary.

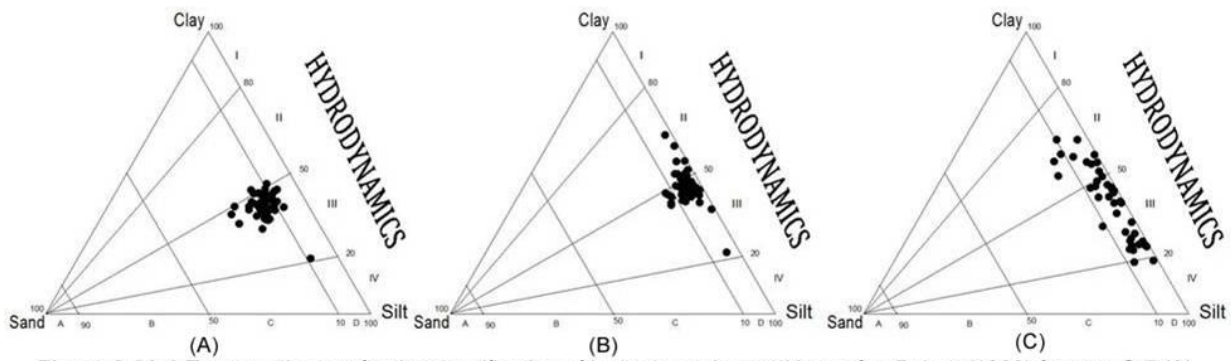


Figure 3.5A.2 Ternary diagram for the classification of hydrodynamic conditions after Pejrup (1988) for core S-7 (A), S-10 (B) and S-16 (C)

3.5A.4 Nutrients (TOC, TN and TP)

The data showed a range of 2.07 to 4.23% with a mean of 3.09% TOC for core S-7; 1.61 to 3.72% with a mean value of 2.48% TOC, 0.01 to 0.36% with a mean of 0.14% TN and 0.01 to 0.05% with a mean of 0.03% TP for core S-10 and 1.92 to 3.12% with a mean value of 2.52% TOC for core S-16. The mean and standard deviation of TN, TP and TOC in each zone is given in table 3.5a.

In core S-7, TOC fluctuates around average line in zone 1 (Figure 3.5a.3). Major portion of TOC falls above average line in zone 2 and below average line in zone 3. In zone 1 of core S-10, major portion of TOC and TP fall below their respective average line while TN fluctuates around average line (Figure 3.5a.3). TOC, TN and TP show an overall increasing trend in zone 2 and an overall decreasing trend in zone 3. TOC is relatively uniform except between 32 and 48 cm which coincide with intervals of high sand content in core S-16 (Figure 3.5a.3).

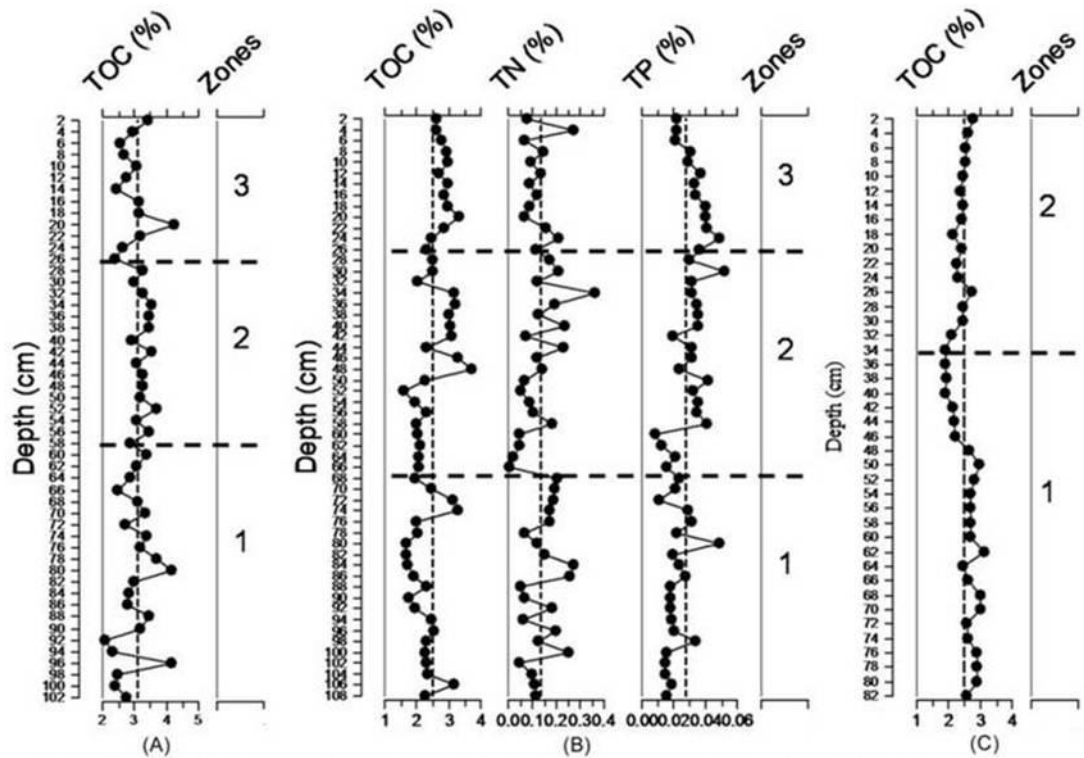


Figure 3.5A.3 Down-core variation of nutrients (TOC, TN and TP) for core S-7 (A), S-10 (B) and S-16 (C) in different zones with zone 1 representing bottom and zone 3 represents the top. The vertical line represents average value.

3.5A.5 C/N ratio

C/N ratio in the present study ranges from 6 to 50 with a mean of 23 for core S-10. The mean and standard deviation of C/N ratio in each zone is given in table 3.5a. In core S-10 C/N ratio showed large variations in zone 1, an overall decreasing trend in zone 2 while in zone 3 C/N ratio fluctuates at every depth interval (Figure 3.5a.4).

3.5A.6 pH

pH ranges from 6.8 to 7.55 with a mean of 7.21 for core S-7; 6.72 to 7.48 with a mean of 7.13 for core S-10 and 6.77 to 7.43 with a mean of 7.10 for core S-16. The mean and standard deviation of pH in each zone is given in table 3.5a. pH decreases from zone 1 to zone 3 in all the three cores (S-7, S-10 and S-16) (Figure 3.5a.5).

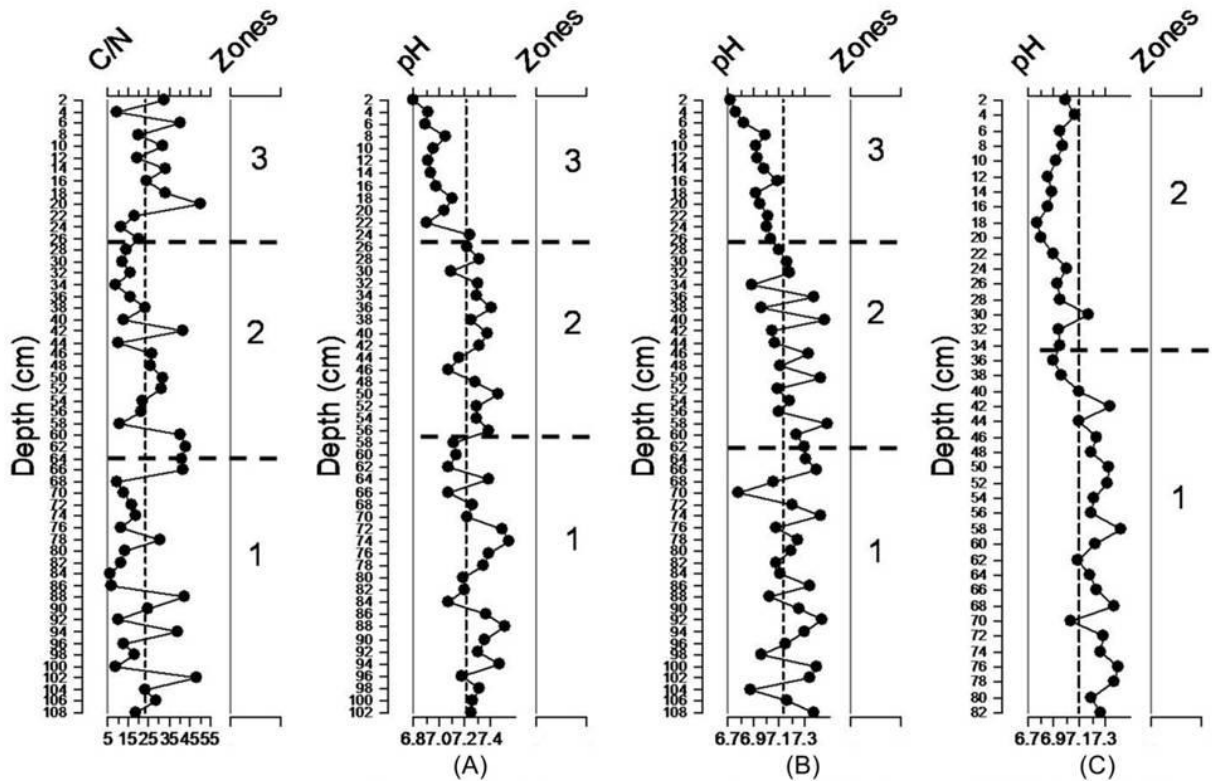


Figure 3.5A.4 Down-core variation of C/N ratio for core S-10

Figure 3.5A.5 Down-core variation of pH in for core S-7 (A), S-10 (B) and S-16 (C) in different zones with zone 1 representing bottom while zone 3 represents the top. The vertical line represents average value.

3.5A.7 Major elements (Fe, Mn and Al)

In core S-10, Fe ranges from 7.68 to 12.89% with a mean of 9.61%, Mn ranges from 1008 to 1963 ppm with a mean of 1418 ppm and Al concentration ranges from 7.21 to 15.52% with a mean of 10.43%. The mean and standard deviation of Fe, Mn and Al in each zone is given in table 3.5a. Fe, Mn and Al vary around average line in zone 1. In zone 2 Fe and Mn shows an overall decreasing trend, Al shows an overall increasing trend while in zone 3 Fe and Mn show an overall increasing trend, Al shows an overall decreasing trend (Figure 3.5a.6).

3.5A.8 Trace elements (Ni, Cr, Co, Zn and Pb)

In core S-10 Ni ranges from 102.33 to 145 with a mean of 120.87 ppm, Cr ranges from 157 to 253.67 with a mean of 190.31 ppm, Co ranges from 62.67 to 94.33 ppm with a mean of 80.21 ppm, Zn ranges from 116.63 to 183.47 ppm with a mean of 145.71 and Pb ranges from 32 to 72.33 ppm with a mean of 47.12 ppm. The mean and standard deviation of Ni, Cr, Co, Zn

and Pb in each zone is given in table 3.5a. Cr, Zn and Pb concentration increases from zone 1 to zone 3. Co concentration decreases from zone 1 to zone 3. Ni showed relatively higher concentration in zone 2 and 3 (Figure 3.5a.6).

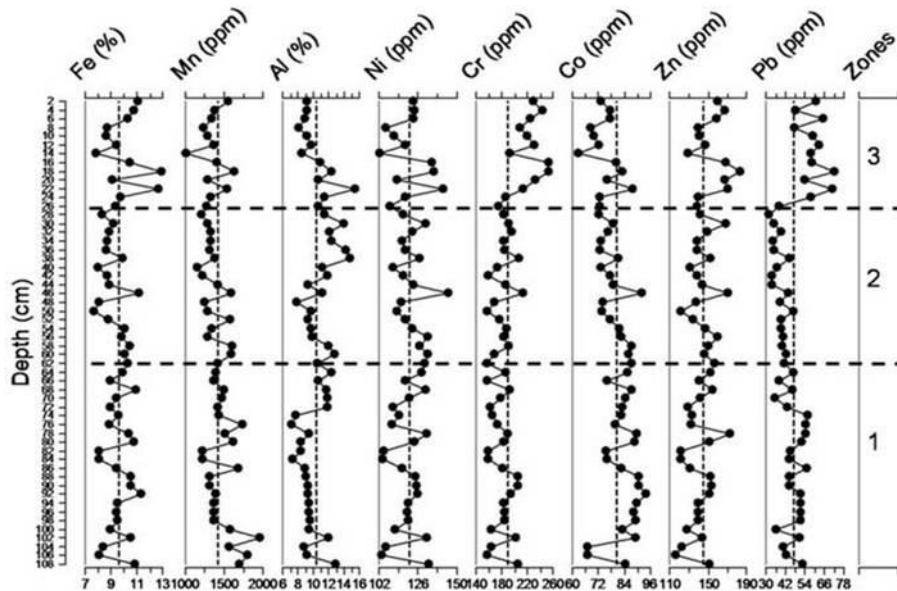


Figure 3.5a.6 Down-core variation of major (Fe, Mn and Al) and trace (Ni, Cr, Co, Zn and Pb) elements in different zones with zone 1 representing bottom while zone 3 represents the top for core S-10. The vertical line represents average value.

3.5A.9 Correlation

Fe showed significant positive correlation with Mn (0.44), Al (0.327), Ni (0.819), Cr (0.597), Co (0.667), Zn (0.792) and Pb (0.516) (Table 3.5A.1). Mn showed significant positive correlation with Ni (0.356) and Co (0.391). Al showed significant positive correlation with Ni (0.535) and Zn (0.394). Among the sediment grain size and organic elements sand showed significant positive correlation with Co (0.474), silt showed significant positive correlation with Cr (0.322) and Zn (0.284) and TP showed significant relation with Cr, thus indicating the role of sediment grain size and organic elements as carriers of trace metals. Interrelationship among trace metals suggests a common source (Table 3.5a.1).

Table 3.5a.1 Pearson correlation for core S-10

	Sand	Silt	Clay	TOC	TN	TP	C/N	pH	Fe	Mn	Al	Ni	Cr	Co	Zn	Pb
Sand	1															
Silt	-0.247	1														
Clay	-.484**	-.729**	1													
TOC	-.337*	-0.14	.364**	1												
TN	-.322*	-0.055	.277*	0.122	1											
TP	-.336*	0.183	0.072	0.137	0.206	1										
C/N	.301*	-0.01	-0.204	0.164	-.859**	-.284*	1									
pH	.431**	-.481**	0.13	-0.232	-0.062	-0.113	-0.015	1								
Fe	0.042	0.233	-0.24	-0.114	-0.16	0.031	0.101	-0.051	1							
Mn	-0.042	-0.113	0.132	-0.214	-0.086	-0.199	0.048	0.187	.440**	1						
Al	0.012	0.063	-0.066	0.198	0.019	0.187	0.044	0.085	.327*	0.099	1					
Ni	0.163	0.096	-0.202	-0.087	-0.201	0.078	0.16	0.123	.819**	.356**	.535**	1				
Cr	-.359**	.322*	-0.037	0.253	-0.079	.272*	0.132	-.434**	.597**	0.054	0.174	.463**	1			
Co	.474**	-0.063	-.278*	-.357**	-0.114	-0.209	0.041	.380**	.667**	.391**	0.172	.692**	0.082	1		
Zn	-0.026	.284*	-0.238	0.093	-0.206	0.229	0.223	-0.187	.792**	0.107	.394**	.824**	.735**	.448**	1	
Pb	-0.257	0.129	0.065	0.109	-0.199	0.17	0.185	-0.259	.516**	0.216	-0.111	0.21	.601**	0.105	.359**	1

** Correlation is significant at the 0.01 level (2-tailed). * Correlation is significant at the 0.05 level (2-tailed).

3.5A.10 Factor analysis

In core S-10 (Table 3.5a.2), the five factors (F1, F2, F3, F4 and F5) correspond to 75.52% of the total variance. F1, F2, F3, F4 and F5 accounted for 21.33%, 15.71%, 13.39%, 13.15% and 11.73% respectively. F1 showed positive loadings on Fe (0.74), Al (0.74), Ni (0.91), Co (0.58) and Zn (0.82). F2 showed significant positive loadings on Cr (0.75) and Pb (0.82). F3 showed significant loadings on Mn (0.64) and Co (0.70). F4 showed significant positive loadings on clay (0.93) and F5 showed positive loadings on sand (0.60) and C/N ratio (0.78).

Table 3.5a.2 R-mode factor analysis for core S-10

Rotated Component Matrix					
	Component				
	1	2	3	4	5
Variance (%)	21.33	15.71	13.59	13.15	11.73
Sand	0.12	-0.50	0.34	-0.12	0.60
Silt	0.13	0.19	-0.07	-0.92	-0.13
Clay	-0.18	0.08	-0.11	0.93	-0.19
pH	0.18	-0.61	0.33	0.37	0.16
TOC	0.14	0.19	-0.69	0.31	-0.09
TN	-0.07	-0.23	-0.09	0.09	-0.78
TP	0.24	0.11	-0.42	-0.12	-0.41
CN	0.01	-0.15	-0.14	0.05	0.78
Fe	0.74	0.43	0.40	-0.10	0.02
Mn	0.23	0.16	0.64	0.21	-0.09
Al	0.74	-0.27	-0.28	-0.15	-0.08
Ni	0.91	0.12	0.27	-0.04	0.07
Cr	0.48	0.75	-0.16	-0.11	-0.08
Co	0.58	-0.11	0.70	-0.03	0.09
Zn	0.82	0.42	-0.01	-0.13	0.09
Pb	0.14	0.82	0.14	0.07	0.04

Positive loadings marked in Bold are >0.5 significant at p<0.05

3.5B Mangroves

3.5B.1 Collection of sediment cores

Amongst the two cores, S-20 was collected from lower middle estuary while S-15 was collected from upper middle estuary. The core length varied from 78 cm for core S-20 to 80 cm for core S-15. The cores were analyzed for sediment grain size and TOC. S-20 was further analyzed for metals.

3.5B.2 Colour

The colour variations between brown and mixed black-brown were seen visually. The sediment was uniform brown from 0 to 78 cm in core S-20 and 0 to 5 cm in core S-15. The remaining part of core S-15 was mixed black-brown.

3.5B.3 Sediment grain size

The data showed a range of 0.49 to 5.46% with a mean of 1.89% sand, 30.87 to 63.1% with a mean of 44.22% silt and 33.16 to 68.4% with a mean of 53.91% clay for core S-20 and 0.96 to 41.41% with a mean of 9.97% sand, 28.63 to 71.03% with a mean of 49.92% silt and 27.52 to 56.36% with a mean of 40.11% clay for core S-15. The core has been divided into different zones depending upon the distribution pattern of sediment components. The mean and standard deviation of sediment grain size in each zone is given in table 3.5b.

Table 3.5b Mean and standard deviation of different parameters in each zone for core S-20 and S-15
 p-value denotes results of one-way ANOVA statistically significant at $p < 0.05$.
 N = number of samples

Core S-20							
	Zone 1 (78-52 cm)		Zone 2 (52-8 cm)		Zone 3 (8-0 cm)		p-value
	N	Mean	N	Mean	N	Mean	
Sand (%)	14	2.96±1.05	23	1.11±0.59	4	2.77±0.84	*0.00
Silt (%)	14	47.35±3.68	23	40.79±4.67	4	53.66±9.22	*0.00
Clay (%)	14	49.74±3.96	23	58.10±5.07	4	43.57±10.04	*0.00
TOC (%)	14	2.90±0.29	23	2.85±0.34	4	3.36±0.14	*0.02
Fe (%)	14	10.14±0.85	23	9.43±0.70	4	9.05±0.55	*0.01
Mn (ppm)	14	1378±114.09	23	1243.70±91.11	4	1353.40±208.63	*0.00
Al (%)	14	9.51±0.88	23	8.92±0.78	4	8.88±0.73	0.10
Ni (ppm)	14	125.38±8.49	23	118.45±6.83	4	111.67±3.16	*0.00
Cr (ppm)	14	237.05±20.76	23	240.48±13.51	4	238.25±9.78	0.82
Co (ppm)	14	77.07±4.48	23	73.75±4.21	4	70.42±2.60	*0.01
Zn (ppm)	14	98.99±6.28	23	102.89±24.94	4	106.16±12.53	0.76
Pb (ppm)	14	56.90±5.87	23	47.35±7.48	4	48.92±5.32	*0.00

Core S-15						
	Zone 1 (80-54 cm)		Zone 2 (54-28 cm)		Zone 3 (28-0 cm)	
	N	Mean (Standard deviation)	N	Mean (Standard deviation)	N	Mean (Standard deviation)
Sand (%)	14	6.15±2.06	14	20.07±11.02	14	3.37±2.66
Silt (%)	14	51.67±4.35	14	41.83±7.74	14	55.28±9.95
Clay (%)	14	42.17±3.36	14	38.10±8.46	14	41.35±9.33
TOC (%)	14	2.48±0.61	14	2.26±0.39	14	2.38±0.20

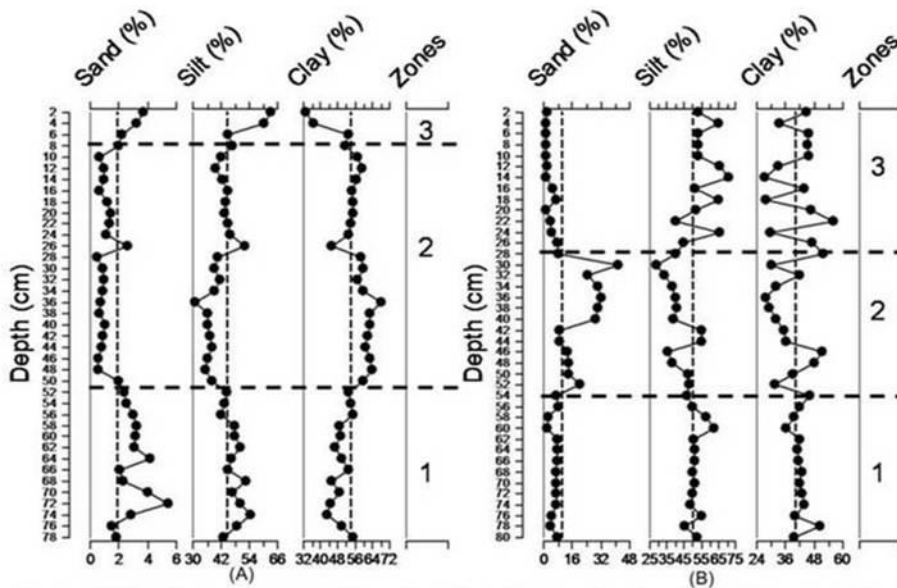


Figure 3.5b.1 Down-core variation of sediment grain size in different zones with zone 1 representing bottom while zone 3 represents the top for core S-20 (A) and S-15 (B). The vertical line represents average value.

In zone 1 and 3 of core S-20 sand and silt is higher than average while clay is less than average (Figure 3.5b.1). However, in zone 2 major portion of sand and silt falls below average line while clay falls above average line. In zone 1 and 3 of core S-15 major portion of silt and clay falls above average

line while sand falls below average line. Silt and clay were relatively constant in zone 1 but showed large variations in zone 3 compensating each other. Sand is nearly constant in zone 1 and 3. In zone 2, sand increases with values falling above average line while silt and clay decreases with major portion falling below average line (Figure 3.5b.1).

Ternary diagram (Pejrup 1988) reveals that the core S-20 and S-15 collected from lower middle and upper middle estuary fall within section III and II indicating that sediments must have deposited under relatively violent to less violent hydrodynamic conditions (Figure 3.5b.2). However, core collected from lower middle estuary (S-20) falls within “D type” indicating presence of poor sand and high concentration of silt and clay components while some samples of core S-15 collected from upper middle estuary fall within “C type” indicating the presence of slightly sand dominated sediment.

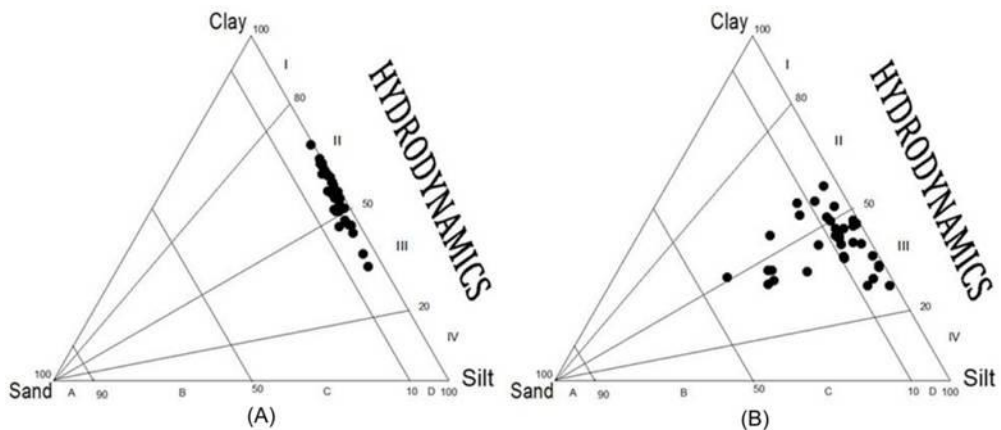


Figure 3.5b.2 Ternary diagram for the classification of hydrodynamic condition after Pejrup (1988) for core S-20 (A) and S-15 (B)

3.5B.4 Nutrients (TOC)

The data showed a range of 2.04 to 3.52% with a mean of 2.92% TOC for core S-20 and 1.03 to 3.13% with a mean of 2.37% TOC for core S-15. The mean and standard deviation of TOC in each zone is given in table 3.5b.

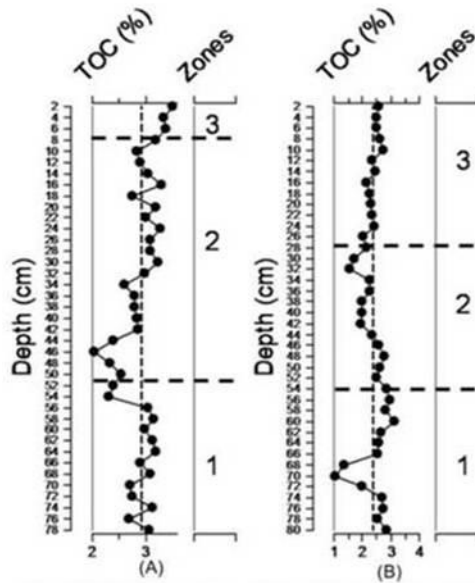


Figure 3.5b.3 Down-core variation of total organic carbon (TOC) in different zones with zone 1 representing bottom while zone 3 represents the top for core S-20 (A) and S-15 (B). The vertical line represents average value.

In core S-20 TOC generally falls above average line in zone 1 and 3 while TOC increases gradually in zone 2. In core S-15 TOC showed negative peak in zone 1, decreases in zone 2 and increases in zone 3 (Figure 3.5b.3).

3.5B.5 Metals (*Fe, Mn, Al, Ni, Cr, Co, Zn and Pb*)

In core S-20, Fe ranges from 8.27 to 11.6% with a mean of 9.64%, Mn 1099.67 to 1624 ppm with a mean of 1304.5 ppm, Al 7.31 to 10.95% with a mean of 9.11%, Ni 104.67 to 137 ppm with a mean of 120.26 ppm, Cr 198.33 to 268.33 ppm with a mean of 238.97 ppm, Co 65.67 to 86 ppm with a mean of 74.54 ppm, Zn 87.88 to 125 ppm with a mean of 99.20 ppm and Pb 37 to 66.67 with a mean of 50.79 ppm. The mean and standard deviation of metals in each zone is given in table 3.5b. The major and trace elements fluctuate around average line in zone 1 and 2 with values generally falling above line and with increasing trend in zone 1 and below average line and with decreasing trend in zone 2. In zone 3 Ni, Cr, Co, Pb decreases while Mn and Zn increases (Figure 3.5b.4).

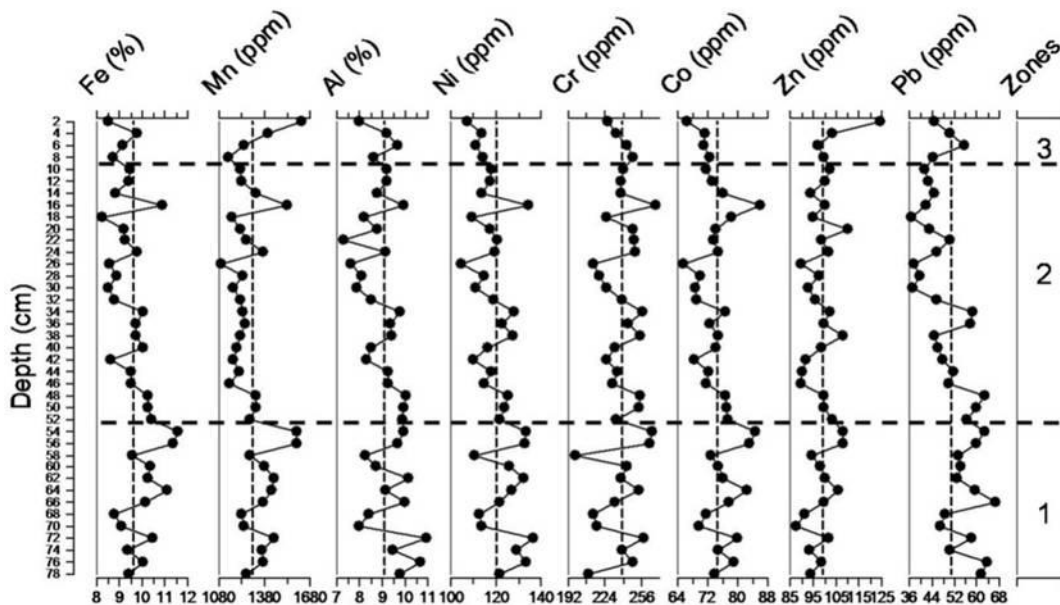


Figure 3.5b.4 Down-core variation of major (Fe, Mn and Al) and trace (Ni, Cr, Co, Zn and Pb) elements for core S-20.

3.5B.6 Correlation

In core S-20 the significant positive correlation of Fe and Mn with trace metals suggest that trace metals are associated with Fe-Mn oxyhydroxides (Chatterjee et al 2007) (Table 3.5b.1). The strong correlation of trace metals (except Zn) with Al indicate that metals are bound to aluminosilicates and have common terrigenous origin (Windom et al 1989). The significant positive association between sand and Mn ($r=0.49$) is attributed to Mn oxide coating on the sand grains (Badr et al 2009). Interrelationship among metals indicated a similar source or a similar enrichment mechanism.

Table 3.5b.1 Pearson correlation for core S-20												
	Sand	Silt	Clay	TOC	Fe	Mn	Al	Ni	Cr	Co	Zn	Pb
Sand	1											
Silt	.687**	1										
Clay	-.764**	-.994**	1									
TOC	0.241	.540**	-.518**	1								
Fe	0.266	-0.113	0.059	-0.298	1							
Mn	.488**	.426**	-.454**	0.182	.650**	1						
Al	0.123	-0.098	0.071	-.342*	.686**	.435**	1					
Ni	0.169	-0.103	0.068	-0.256	.817**	.574**	.763**	1				
Cr	-0.058	-0.213	0.2	-0.173	.648**	.460**	.551**	.730**	1			
Co	0.143	-0.108	0.075	-0.226	.818**	.587**	.645**	.792**	.678**	1		
Zn	-0.095	0.085	-0.06	0.277	.317*	.429**	0.195	.320*	.447**	.445**	1	
Pb	0.312	-0.065	0.009	-.362*	.664**	.432**	.679**	.585**	0.314	.492**	-0.148	1

** . Correlation is significant at the 0.01 level (2-tailed).
 * . Correlation is significant at the 0.05 level (2-tailed).

3.5B.7 Factor analysis

In core S-20 (Table 3.5b.2), the three factors (F1, F2 and F3) correspond to 82.17%. F1, F2 and F3 account for 41.90%, 26.67% and 13.60% respectively. F1 showed significant loadings on Fe (0.93), Mn (0.67), Al (0.83), Ni (0.92), Cr (0.77), Co (0.88) and Pb (0.72). F2 showed significant loadings on sand (0.86), silt (0.95), TOC (0.54) and Mn (0.53). F3 showed significant loadings on TOC (0.56) and Zn (0.85).

Fe and Al are the major components of silica minerals that are the products of rock and soil weathering on land (Zhou et al 2004). F1 can be associated as a lithogenic group, since the variability of trace metals (except Zn) appears to be controlled by terrestrial and natural sources. Similarly, F3 can be associated as organic matter controlled factor. The significant association of Zn with TOC may suggest possible anthropogenic source such as industrial and agricultural activities (Badr et al 2009).

Factor	F1	F2	F3
Variance (%)	41.90	26.67	13.60
Sand (%)	0.21	0.86	-0.23
Silt (%)	-0.11	0.95	0.13
Clay (%)	0.07	-0.97	-0.07
TOC (%)	-0.33	0.54	0.56
Fe (%)	0.93	0.03	-0.02
Mn (ppm)	0.67	0.53	0.25
Al (%)	0.83	-0.03	-0.17
Ni (ppm)	0.92	-0.02	0.05
Cr (ppm)	0.77	-0.20	0.34
Co (ppm)	0.88	-0.03	0.18
Zn (ppm)	0.36	0.01	0.85
Pb (ppm)	0.72	0.11	-0.54

Values highlighted in bold are >0.5 significant at $p < 0.05$
number of samples = 39

3.5B.8 Isocon and enrichment factor (EF)

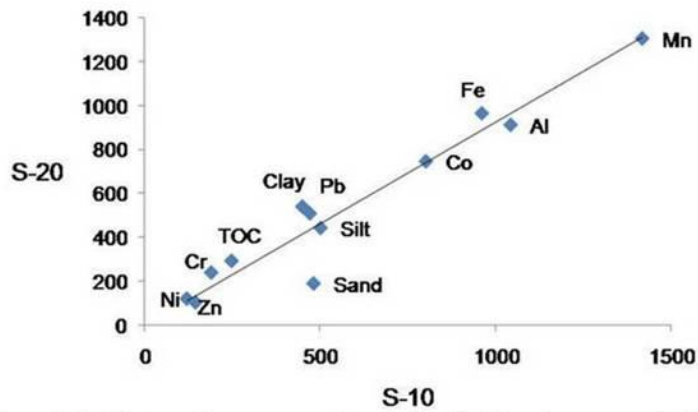


Figure 3.5b.5 Isocon diagram comparing mudflat (S-10) and mangrove (S-20)

Table 3.5b.3 Mean value of EF for mudflat (S-10) and mangroves (S-20)

	S-10	S-20
Fe	1.60	1.80
Mn	1.32	1.35
Ni	1.40	1.56
Cr	1.67	2.34
Co	3.33	3.46
Zn	1.20	0.96
Pb	1.87	2.23

When the mudflat (S-10) and mangrove (S-20) are compared, clay and TOC is higher in mangroves (S-20) while sand and silt is higher in mudflats (S-10) (Figure 3.5b.5). The data computed showed relatively higher EF value for all the elements in mangroves (S-20) when compared to mudflats (S-10) (Table 3.5b.3).

The mangrove vegetation is associated with a unique horizontal root network (Kumaran et al 2004) that enhances the deposition of fine grained suspended sediments and prevents re-suspension and erosion of fine sediments (Soto-Jimenez and Paez-Osuna 2001). Mangrove environments are highly productive and are sources of organic matter which may be transferred to adjacent coastal (Robertson and Duke 1990). Further, mangrove sediments are capable of trapping large quantities of pollutants, particularly trace metals (Delacerd 1983).

3.6 Comparison of different estuaries (mudflats) along central west coast of India

3.6.1 Rivers and catchment area

The Dharamtar, Kundalika, Rajapuri, Savitri and Vashishti are either major estuaries or creeks along central west coast of India which differs from one another with respect to catchment area (Table 3.6).

Rivers/Creek	Length (km)	Basin Perimeter (km)	Basin Area (km ²)
Dharamtar	69.99	164.96	570.58
Kundalika	69.99	166.96	489.44
Rajapuri	24.99	92.69	166.92
Savitri	97.47	267.44	1445.91
Vashishti	87.41	254.94	1393.62

3.6.2 Sediment grain size

The study of sediment grain size distribution is essential for understanding the source, transport and energy conditions and their variations are affected by physical and hydrodynamic processes (Folk and Ward 1957; Friedman 1961). The sediment grain size i.e. sand, silt and clay had shown significant difference ($p < 0.05$) along lower and middle estuary (Table 3.6.1). The relatively low average sand content (average 1%, Table 3.6.1) near the

mouth of Dharamtar creek is mainly attributed to manmade structure (jetty) which reduced the tidal flow resulting in the deposition of fine sediments (average 99%, Table 3.6.1). However, in Rajapuri creek, the relatively low average sand content (average ~5%, Table 3.6.1) near the mouth is mainly attributed to reduced transport processes in the main channel as being sheltered area which acts as natural physical barrier that lessens the energy levels facilitating the deposition of fine sediments (average 96%, Table 3.1.6). Here, the fine sediments i.e. silt and clay had also shown maximum variations and may therefore be attributed to regular resuspension by changing freshwater interaction with tidal currents which are more likely to affect fine (<63 μ m) rather than coarse particles in a protected sheltered environment (Zhang et al 1988; Stephens et al 1992). The lower portion of Vashishti, Savitri and Kundalika estuary on the contrary had shown higher average sand content (Table 3.6.1). Chauhan et al (2004) studied the tidal range along the Indian coast. They reported that tidal range vary from 3.70 m in Shrivardhan located near the mouth of Savitri estuary to 4.12 m in Revdanda located near the mouth of Kundalika estuary. As the core locations of lower Vashishti, Savitri and Kundalika estuary are under the direct influence of tides therefore variations in tidal range might be one of the factors controlling the distribution of average sand content (Feng 1985). On the other hand, in the middle estuary, the average sand content increased from Vashishti to Dharamtar (Table 3.6.1). Sand is mainly transported as bed load during spring tides or during high river discharge (Walsh and Nittrouer 2004). Additionally, agricultural practices/anthropogenic activities, including sand mining, may also contribute to increased sand content (Dandekar 2010). The cores collected from lower estuary contained higher sand content in the middle section (varying from 20 cm to about 50 cm depths) and higher percentage of fine sediments in the bottom section (below 50 cm depth).

Table 3.6.1 Mean and standard deviation of sediment grain size for lower (A) and middle (B) estuary
 * p value denotes results of one-way ANOVA significant at $p < 0.05$
 n denotes number of samples

(A) Lower Estuary				
Rivers/Creek	Sand (%)	Silt (%)	Clay (%)	p value
Dharamtar	1.01±0.55 (n=23)	52.39±5.67 (n=23)	46.53±6.02 (n=23)	*0.00
Kundalika	11.52±5.10 (n=33)	49.58±10.84 (n=33)	38.90±11.69 (n=33)	*0.00
Rajapuri	4.96±7.89 (n=49)	43.60±22.08 (n=49)	51.41±20.70 (n=49)	*0.00
Savitri	29.8±11.16 (n=50)	40.30±6.02 (n=50)	29.90±7.22 (n=50)	*0.00
Vashishti	13.66±3.94 (n=51)	47.73±3.39 (n=51)	38.61±3.64 (n=51)	*0.00
(B) Middle Estuary				
Dharamtar	7.87±6.65 (n=41)	34.09±5.15 (n=41)	58.04±6.86 (n=41)	*0.00
Kundalika	3.46±2.36 (n=33)	46.57±16.58 (n=33)	49.97±16.48 (n=33)	*0.00
Savitri	5.1±2.51 (n=39)	42.2±7.08 (n=39)	52.8±7.33 (n=39)	*0.00
Vashishti	4.51±3.70 (n=54)	55.73±13.88 (n=54)	39.75±12.67 (n=54)	*0.00

When the distribution of sediment grain size along lower and middle estuary is compared (Table 3.6.1), it is observed that maximum average sand content is noted in lower estuary (except near mouth of Dharamtar creek), indicating increased energy conditions from middle to lower estuary (Lorenzo et al 2007). The relatively high tidal energy in lower estuary results in higher hydro dynamics near the mouth which facilitates the deposition of coarser sediments as fine sediments are more mobile and are carried to the middle estuary where tidal currents are weaker resulting in the deposition of mud (Manning et al 2010). Hydrodynamic conditions on Ternary plots (Pejrup 1988) also revealed that sediment deposition took under relatively violent conditions in lower estuary while under less violent conditions in middle estuary (Figure 3.6).

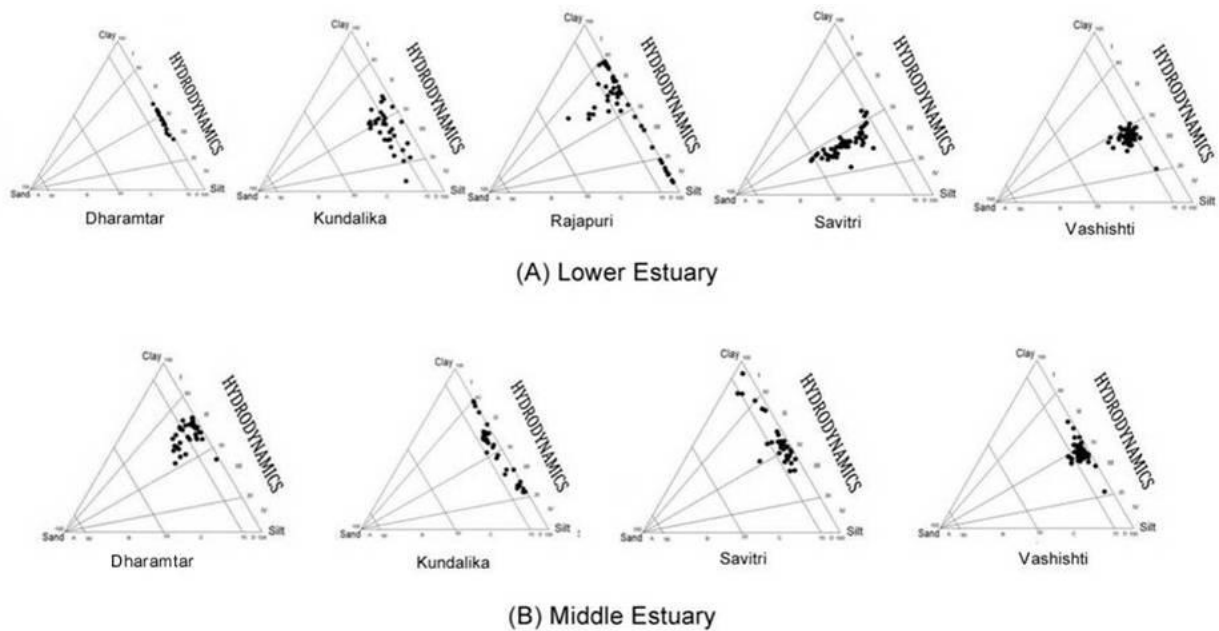


Figure 3.6 Ternary diagram for the classification of hydrodynamic conditions after Pejrup (1988) for lower (A) and middle (B) estuary

3.6.3 Nutrients (TN, TP and TOC)

Nutrients are mainly derived either through river input or from diffuse sources such as sewers and canals, intense agricultural and industrial activities most of which eventually settle to the bottom and are incorporated into the sediment (Ghosh and Choudhury 1989; Zedler 2000; Michaels et al 2001; Hansson et al 2005). The distribution of nutrients i.e. carbon, nitrogen and phosphorous had shown significant difference ($p < 0.05$) along lower and middle estuary (Table 3.6.2). When the distribution of average TOC content along lower and middle estuary is compared it is observed that in Kundalika and Savitri estuary average TOC content is higher in the middle estuary while in Dharamtar and Vashishti estuary average TOC content is higher in lower estuary (Table 3.6.2). The average TN concentration is relatively higher in the middle estuary while average TP concentration is relatively higher in the lower estuary (Table 3.6.2). The variations in TOC concentrations are probably related to differences in the primary productivity, bioturbation, decomposition and sedimentation rates (Kuwae et al 2006). The relatively higher average TOC content is the middle portion of Savitri and Kundalika estuary where the sediments are muddy (95 % mud) and relatively low average TOC content near the mouth where sediments are

slightly sandy (75–95 % mud) to sandy mud (50-75% mud) (Flemming 2000) is therefore attributed to relatively high adsorptive capacity of fine particles for organic matter (Cotano and Villate 2006; Ramaswamy et al 2008, Gireeshkumar et al 2013) (Table 3.6.1, Table 3.6.2). The concentrations of TOC, TN and TP had also shown significant positive correlation with fine grained sediment (Table 3.6.3). Sediment grain size is therefore the main factor influencing the distribution of TN, TP and TOC concentration both in lower and middle estuary. The terrestrial input from the adjacent land masses (Jonathan et al 2004), surrounding halophytic vegetation (mangroves) and anthropogenic such as industrial and agricultural activities in the catchment are other factors responsible for variations in TOC, TN and TP concentration.

Table 3.6.2 Mean and standard deviation of nutrients (TN, TP and TOC) for lower (A) and middle (B) estuary
*p value denotes results of one-way ANOVA significant at p<0.05
n denotes number of samples

Lower Estuary				
Rivers/Creek	TN (%)	TP (%)	TOC (%)	p-value
Dharamtar	0.04±0.02 (n=23)	0.04±0.01 (n=23)	1.63±0.32 (n=23)	*0.00
Kundalika	0.15±0.04 (n=33)	-	1.10±0.34 (n=33)	*0.00
Rajapuri	0.08±0.03 (n=22)	-	2.97±0.57 (n=49)	*0.00
Savitri	0.09±0.04 (n=25)	0.05±0.01 (n=25)	1.28±0.5 (n=50)	*0.00
Vashishti	-	-	3.09±0.47 (n=51)	*0.00
Middle Estuary				
Dharamtar	0.11±0.04 (n=41)	0.03±0.01 (n=41)	1.56±0.32 (n=41)	*0.00
Kundalika	-	0.03±0.01 (n=33)	1.35±0.38 (n=33)	*0.00
Savitri	0.16±0.03 (n=18)	0.04±0.01 (n=18)	1.92±0.36 (n=39)	*0.00
Vashishti	0.14±0.07 (n=54)	0.03±0.01 (n=54)	2.48±0.52 (n=54)	*0.00

Table 3.6.3 Relationship between nutrients (TOC, TN and TP) and fine sediments for lower (A) and middle (B) estuary

	(A) Lower Estuary			(B) Middle Estuary		
	TOC	TN	TP	TOC	TN	TP
Dharamtar (n=23)						
Silt	-0.208	-0.025	-0.188	0.195	.376*	.362*
Clay	0.219	0.026	0.198	0.267	-0.034	0.119
Mud	0.251	0.03	0.224	0.427**	0.256	.404**
Kundalika (n=33)						
Silt	0.323	-0.184	-	-0.124	-	0.158
Clay	-0.066	0.041	-	0.051	-	-0.197
Mud	.535**	-0.297	-	-.687**	-	-.363*
Rajapuri (n=22)						
Silt	0.308	-0.262	-			
Clay	-0.145	0.197	-			
Mud	.536*	-0.242	-			
Savitri (n=25)						
Silt	.478*	0.375	0.17	0.022	-0.221	0.058
Clay	.745**	.666**	.587**	0.26	0.282	0.017
Mud	.773**	.665**	.505**	.711**	0.155	0.189
Vashishti (n=51)						
Silt	-0.104	-	-	-0.14	-0.055	0.183
Clay	0.007	-	-	.364**	.277*	0.072
Mud	-0.083	-	-	.337*	.322*	.336*

**Correlation is significant at the 0.01 level
*Correlation is significant at the 0.05 level

3.6.4 C/N ratio

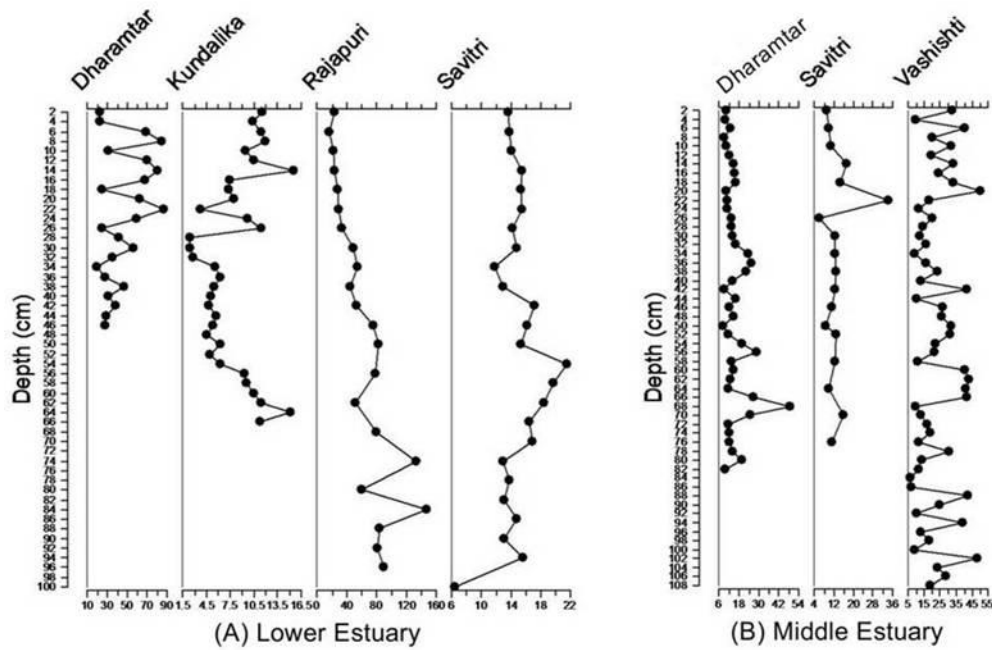


Figure 3.6.1 Down-core variation of C/N ratio for lower (A) and middle (B) estuary

Carbon/nitrogen (C/N) ratio is widely used to distinguish the source of organic matter. C/N ratio had shown significant difference along lower and middle estuary (Table 3.6.4). In general, C/N ratio showed a decreasing trend in the upper section of cores collected from lower and middle estuary reflecting increased marine processes in the recent years (Figure 3.6.1). Higher average C/N ratio near the mouth of Dharamtar and Rajapuri creek may indicate the enrichment of carbon over nitrogen (Table 3.6.4). The degradation of organic matter influences the distribution of C/N ratios suggesting diagenesis as nitrogen is generally remineralized faster than carbon, which serves to increase the C/N ratio (Tyson 1995; Lehmann et al 2002). Alternatively, elevated average C/N ratio may be explained by the increased input of organic matter from the surrounding mangrove vegetation and its high sedimentation rate (Lanza et al 2011). Magni et al (2008) suggested the role of hydrodynamics and geomorphology in the distribution and transportation of organic matter. Extremely small estuaries with weak hydrodynamics, such as Rajapuri creek, can have sediments with terrestrial sources because of the short transport distances involved (Matson and Brinson 1990). The low average C/N ratio ($C/N < 9$) in lower Kundalika estuary may indicate strong tidal based hydrodynamics and high microbial

activity and/or low primary production. On the other hand, the average C/N ratio in middle estuary ranged from 14 to 23 which indicate mainly terrestrial input (C/N>12) (Table 3.6.4) (Meyers 1994; Twichell et al 2002; Rumolo et al 2011). When the distribution of average C/N ratio along lower and middle estuary is compared (Table 3.6.4), it is observed that in Savitri estuary, relatively higher average C/N ratio is in lower estuary. The variations in C/N ratios are ascribed to differences in sediment grain size and anthropogenic activity. The results of sediment grain size analysis indicated that in lower estuary sediments are sandy mud (50-75% mud) while in the middle estuary sediments are muddy (95% mud) (Flemming 2000). The degradation rate of organic matter is higher in sandy than muddy sediments with high silt and clay content (Rasheed et al 2003). Additionally, anthropogenic activities such as the widespread use of organic chemicals may alter the C/N ratios (Gao et al 2012). The concentrations of carbon and nitrogen are highly correlated in Savitri estuary, indicating similar sources for carbon and nitrogen while in Dharamtar, Kundalika, Rajapuri and Vashishti estuary the weak correlation between carbon and nitrogen may suggest different sources (Figure 3.6.2).

Table 3.6.4 Mean and standard deviation of carbon/nitrogen ratio (C/N) for lower (A) and middle (B) estuary		
(A) Lower Estuary		
Rivers/Creek	C/N ratio	p value
Dharamtar (n=23)	46.19±22.08	0.00
Kundalika (n=33)	8.01±3.50	0.00
Rajapuri (n=22)	58.99±35.87	0.00
Savitri (n=25)	17.60±2.36	0.00
(B) Middle Estuary		
Dharamtar (n=41)	15.67±7.44	0.00
Savitri (n=18)	13.91±1.41	0.00
Vashishti (n=54)	23.22±12.10	0.00

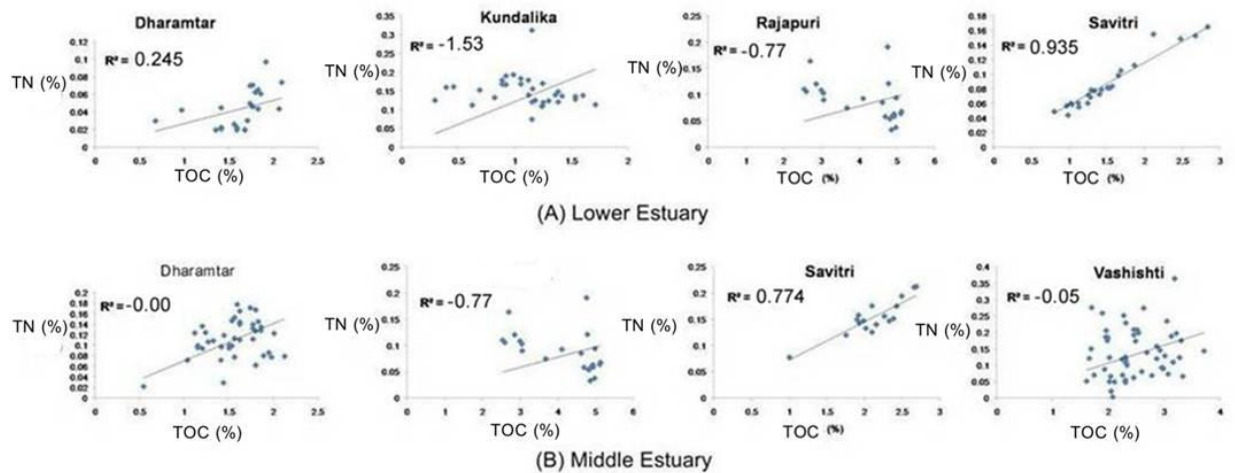


Figure 3.6.2 Scatter plot of C vs N for lower (A) and middle (B) estuary

3.6.5 Diatoms

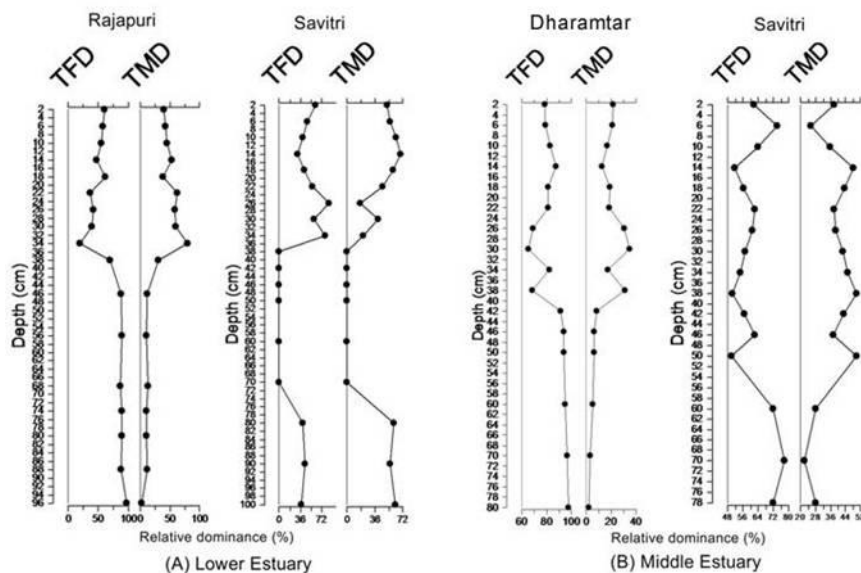


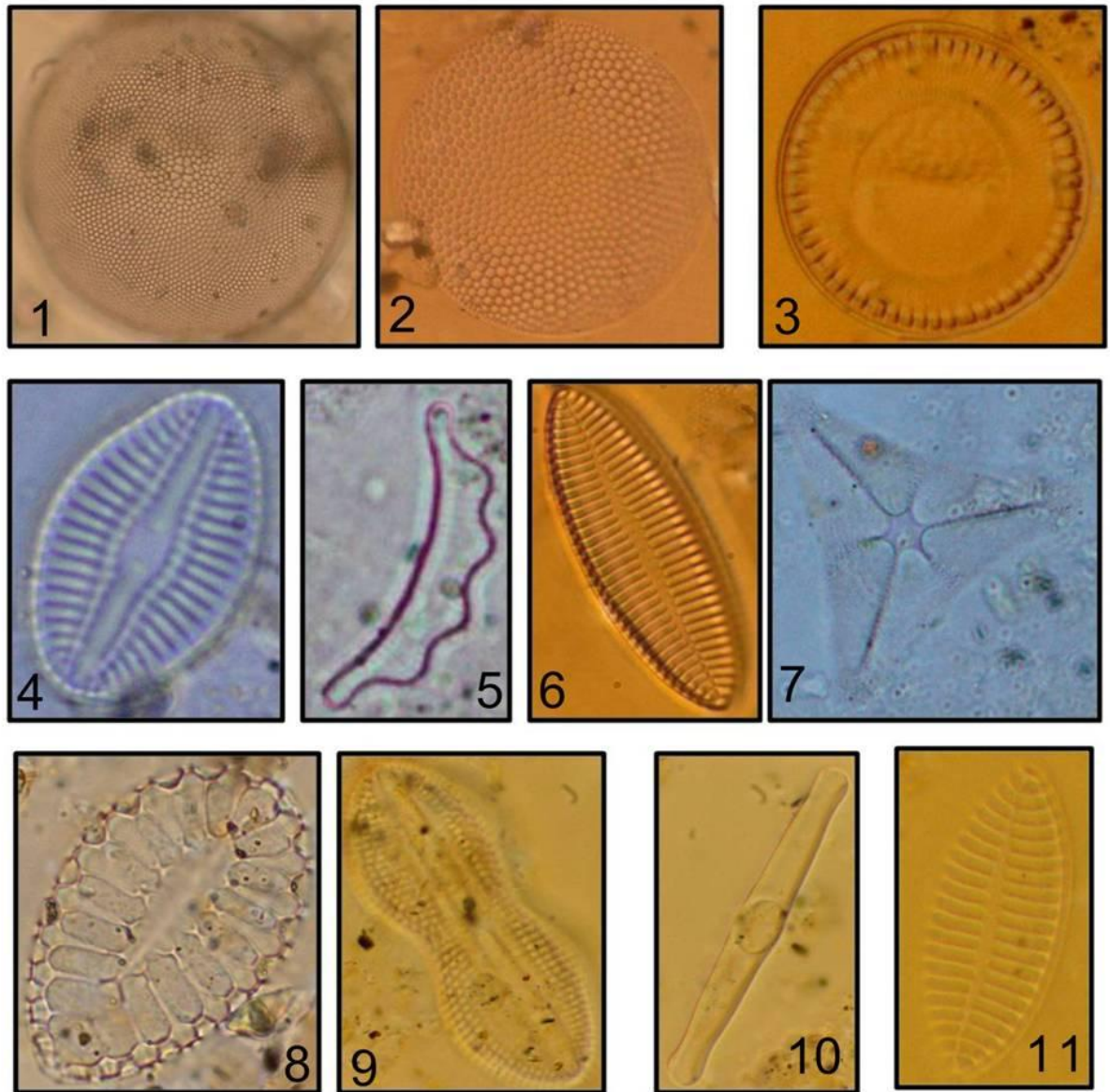
Figure 3.6.3 Down-core variation of diatoms for lower (A) and middle (B) estuary

TFD-Total Freshwater diatoms, TMD-Total Marine diatoms

The diatom assemblage revealed the dominance of freshwater diatoms in middle estuary and an increased proportion of marine diatoms in lower estuary (Table 3.6.5). Among the freshwater genera *Cyclotella*, *Nitzschia*, *Coscinodiscus*, *Synedra* and *Cymatotheca* (Figure 3.6.4) are the major component and they are consistently represented with average 57% to 84% whereas marine genera *Thalassiosira*, *Rhaphoneis*, *Diploneis*, *Thalassionema*, *Hyalodiscus* and *Chaetoceros* represented remaining 16%

to 43% (Table 3.6.5). The relatively higher diatom dominance in Savitri estuary and Rajapuri creek in comparison to Dharamtar creek is attributed to higher organic matter content resulting in increased primary productivity and phytoplankton production. Both in lower and middle estuary marine diatoms showed increasing proportion in the upper section of the cores reflecting increased marine processes in the recent years while freshwater diatoms were predominant in lower portion providing greater evidence of freshwater input in the past (Figure 3.6.3).

Table 3.6.5 Mean diatom assemblage for lower (A) and middle (B) estuary				
(A) Lower Estuary				
	Total Freshwater diatoms (%)	Total Marine Diatoms (%)	Predominant Freshwater genera	Predominant Marine genera
Rajapuri (n=17)	66	34	<i>Cyclotella sp.</i>	<i>Hyalodiscus sp.</i> , <i>Chaetoceros sp.</i>
Savitri (n=18)	57	43	<i>Cyclotella sp.</i> , <i>Cymatotheca sp.</i> , <i>Nitzschia sp.</i>	<i>Thalassiosira sp.</i> , <i>Rhaphoneis sp.</i> , <i>Diploneis sp.</i> , <i>Thalassionema sp.</i>
(B) Middle Estuary				
Dharamtar (n=16)	84	16	<i>Cyclotella sp.</i> , <i>Nitzschia sp.</i>	<i>Thalassiosira sp.</i> , <i>Triceratium sp.</i>
Savitri (n=16)	62	38	<i>Synedra ulna</i> , <i>Cyclotella sp.</i> , <i>Cymatotheca sp.</i> , <i>Nitzschia sp.</i> , <i>Coscinodiscus sp.</i>	<i>Rhaphoneis sp.</i> , <i>Hyalodiscus sp.</i> , <i>Thalassiosira sp.</i>



(A)

List of Diatom taxa (A)

- 1,2 *Coscinodiscus* sp.
- 3 *Cyclotella* sp.
- 8 *Surirella* sp.
- 9 *Diploneis* sp2
- 5 *Eunotia* sp.

- 10 *Grammatophora* sp.
- 6,11 *Nitzschia* sp
- 4 *Diploneis* sp1
- 7 *Schuetzia* sp.

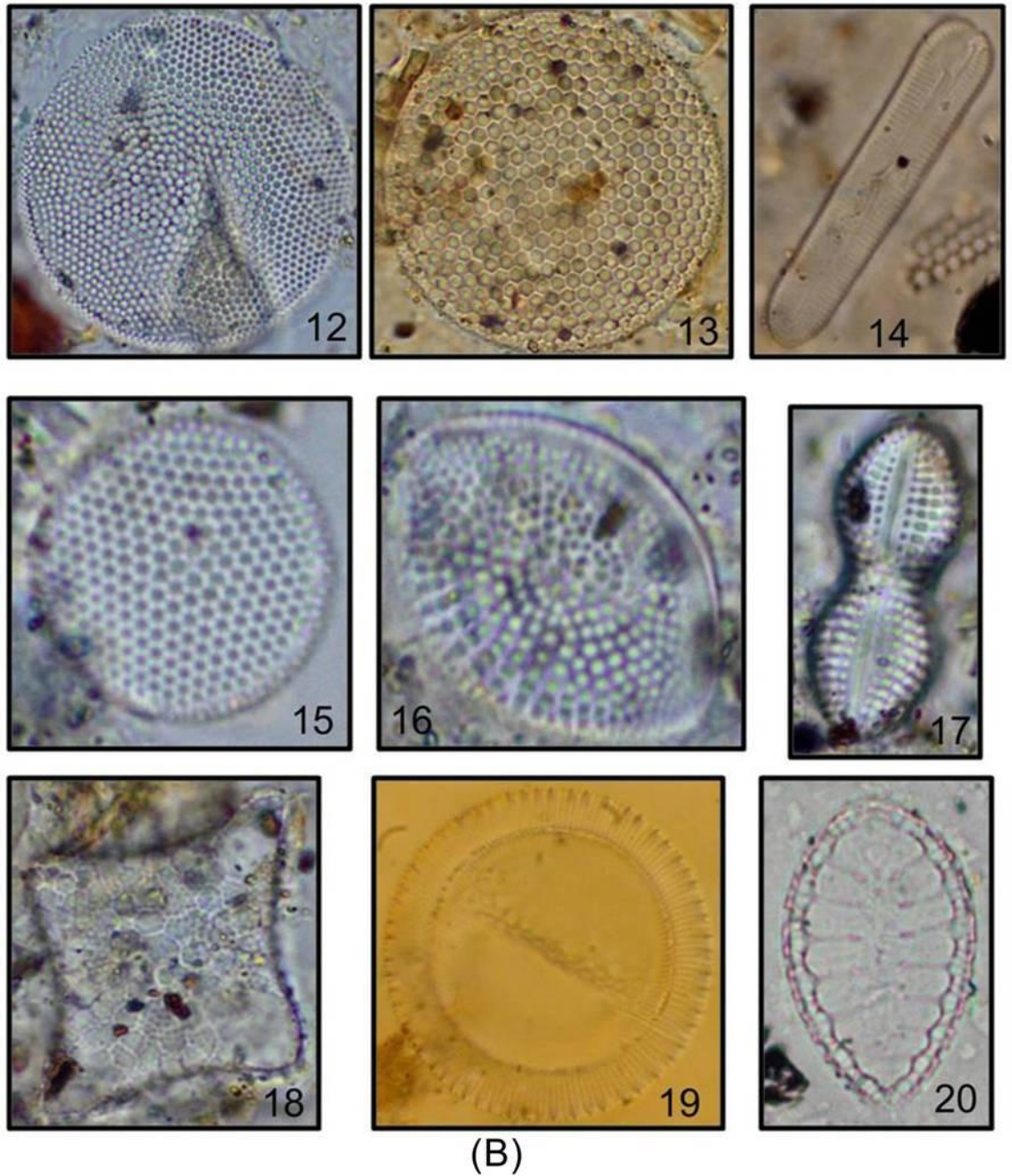


Figure 3.6.4 Diatom photographs (A and B) from studied estuaries along central west coast of India

List of Diatom taxa (B)

- | | |
|---------------------------------|---------------------------|
| 13 <i>Coscinodiscus</i> sp. | 14 <i>Pinnularia</i> sp. |
| 12, 15 <i>Thalassiosira</i> sp. | 17 <i>Diploneis</i> sp. |
| 20 <i>Surirella</i> sp. | 16 <i>Cymatotheca</i> sp. |
| 18. <i>Biddulphia</i> sp. | 19 <i>Cyclotella</i> sp. |

In general, the average concentration of Mn and Al is higher in the middle estuary while average Fe concentration is higher in the lower estuary (Table 3.6.6). Fe and Al are the major component of silica minerals and together with Mn are the products of rock and soil weathering on land (Zourarah et al 2009). These elements are controlled by sediment grain size to a large degree and fine sediments usually have higher contents (Zhou et al 2004). The result of sediment grain size analysis clearly indicated higher percentage of fine sediments in middle estuary when compared to lower estuary (Table 3.6.1). However, in Dharamtar creek higher percentage of fine sediments was found near the mouth. Therefore, the observed higher concentration of Al and Mn is attributed to higher percentage of fine sediments. On the other hand, elevated Fe content in lower estuary could be attributed to terrigenous supply of ferromagnesian minerals, industrial and municipal discharges (Sagheer 2004; Bhagure and Mirgane 2011) and greater recycling of Fe by resuspension of bottom sediments due to tidal mixing in lower estuarine region (Kumar and Edward 2009).

Table 3.6.3 Mean and standard deviation of metals for lower (A) and middle (B) estuary
* p value denotes results of one-way ANOVA significant at p<0.05
n denotes number of samples

Lower Estuary									
Rivers/Creek	Fe (%)	Mn (ppm)	Al (%)	Ni (ppm)	Cr (ppm)	Co (ppm)	Zn (ppm)	Pb (ppm)	p value
Dharamtar	8.44±0.46 (n=23)	726.88±60.03 (n=23)	9.43±0.47 (n=23)	102.91±10.23 (n=23)	238.93±12.44 (n=23)	54.62±4.10 (n=23)	133.30±4.79 (n=23)	69.57±25.54 (n=23)	*0.00
Kundalika	11.61±0.69 (n=33)	899.14±72.04 (n=33)	6.95±0.31 (n=33)	112.54±10.42 (n=33)	298.44±81.03 (n=33)	87.60±7.52 (n=33)	199.00±59.39 (n=33)	109.66±28.84 (n=33)	*0.00
Rajapuri	6.28±1.57 (n=49)	677.93±48.72 (n=49)	6.22±0.91 (n=49)	92.60±11.42 (n=49)	221.89±70.61 (n=49)	52.10±13.61 (n=49)	86.46±14.45 (n=49)	62.86±23.92 (n=49)	*0.00
Savitri	13.97±4.52 (n=50)	1969.60±465.59 (n=50)	9.08±1.27 (n=50)	150.53±15.85 (n=50)	239.86±42.14 (n=50)	93.49±13.10 (n=50)	169.40±21.77 (n=50)	53.67±16.75 (n=50)	*0.00
Middle Estuary									
Dharamtar	7.60±0.34 (n=41)	794.74±55.85 (n=41)	8.23±0.37 (n=41)	95.72±7.97 (n=41)	244.61±30.21 (n=41)	70.55±3.55 (n=41)	135.54±24.79 (n=41)	87.32±22.99 (n=41)	*0.00
Kundalika	8.61±0.67 (n=33)	954.05±96.22 (n=33)	8.10±0.60 (n=33)	94.64±11.65 (n=33)	340.81±37.42 (n=33)	71.19±7.36 (n=33)	140.67±10.26 (n=33)	118.64±30.72 (n=33)	*0.00
Savitri	11.01±2.05 (n=39)	1990.30±287.52 (n=39)	9.55±1.61 (n=39)	137.65±21.39 (n=39)	248.67±60.15 (n=39)	104.82±11.67 (n=39)	153.92±20.06 (n=39)	49.30±9.54 (n=39)	*0.00
Vashishti	9.61±1.15 (n=54)	1418.00±176.40 (n=54)	10.43±1.90 (n=54)	120.87±9.75 (n=54)	190.31±24.96 (n=54)	80.21±7.47 (n=54)	145.71±14.94 (n=54)	47.12±9.68 (n=54)	*0.00

3.6.7 Trace elements (Ni, Cr, Co, Zn and Pb)

In Dharamtar creek, average trace metals (except Ni) concentration is higher in middle portion (Table 3.6.6). In Kundalika estuary average Ni, Co and Zn concentration is higher in the lower estuary while Cr and Pb concentration is

higher in the middle (Table 3.6.6). In Savitri estuary Ni, Zn and Pb concentration is higher in the lower estuary while Cr and Co is higher in the middle estuary (Table 3.6.6). In Rajapuri creek trace metals showed relatively low concentration (Table 3.6.6). In Vashishti estuary concentration of Pb and Cr is relatively low (Table 3.6.6). The distribution of trace metals depends upon factors such as the distance of element sources to estuary, hydrodynamics, the chemical characteristics (e.g. sorption-adsorption capacity of trace metals, flocculation, etc.), and the chemical and biochemical condition of sedimentary environment (Willams et al 1994).

3.6.8 Normalization

Normalization is a common approach to assess whether anomalous metal concentration are present in the sediments and to compensate the spatial and temporal variations in trace metal distribution which may be related to variations in sediment grain size and mineralogy (Chatterjee et al 2007). To compensate for this effect, elements such as Al and Fe have been used in the past. The geochemical normalization was obtained using Al as the reference element for the following reasons: (1) Al is a major constituent of clay mineral and therefore is an indicator of clay fraction; (2) Al is regarded as conservative major element, which unlike Fe is not significantly affected by early diagenetic processes or strong redox effect such as are frequently observed in estuarine and coastal environments; (3) Al normalization is based on the fact that there is a natural relationship between trace metals and Al that exist in the absence of any human influence (since Al is the major component of clays, its concentration is always assumed to be a natural concentration) (Ebbing et al 2002).

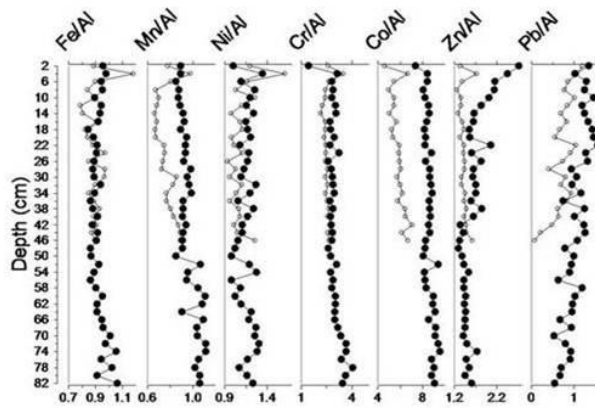


Figure 3.6.5 Down-core variation of metal/Al for Dharamtar creek. Note empty circles=lower estuary, filled circles=middle estuary

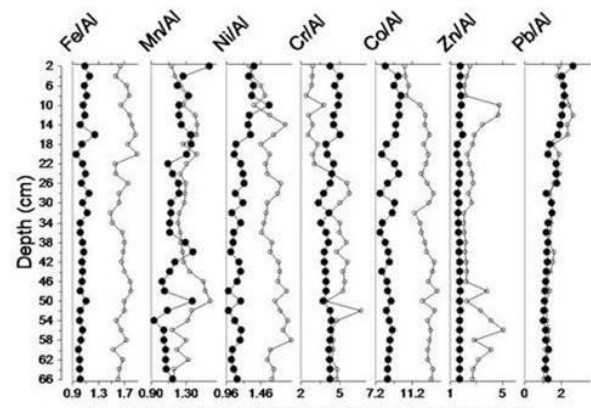


Figure 3.6.6 Down-core variation of metal/Al for Kundalika estuary. Note empty circles=lower estuary, filled circles=middle estuary

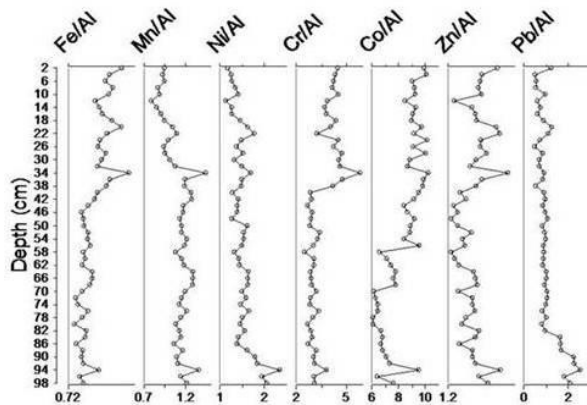


Figure 3.6.7 Down-core variation of metal/Al for Rajapuri creek.

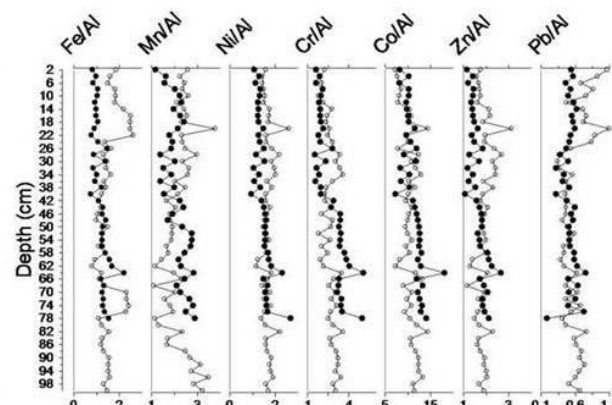


Figure 3.6.8 Down-core variation of metal/Al for Savitri estuary. Note empty circles=lower estuary, filled circles=middle estuary

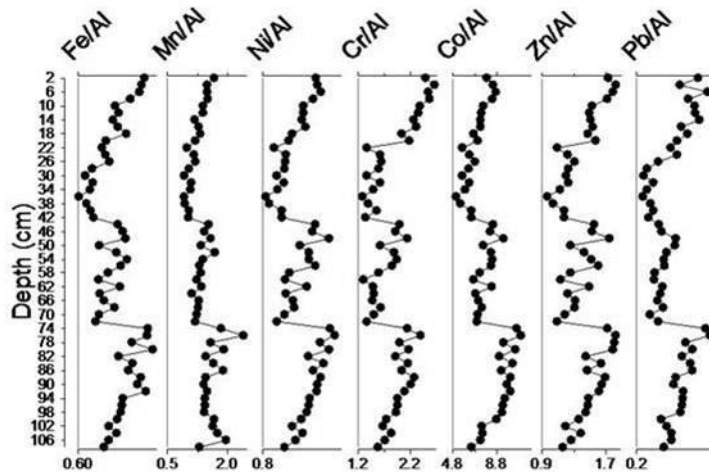


Figure 3.6.9 Down-core variation of metal/Al for Vashishti estuary.

Metals had shown significant difference along lower and middle estuary (Table 3.6.6). The normalized data showed higher metal/Al ratios for Cr and Co in all the cores (Figure 3.6.5 - 3.6.9). The metal/Al ratio for Zn, Pb and Fe is higher in Kundalika estuary while Ni/Al was higher in Savitri estuary (Figure 3.6.5 - 3.6.9). In Dharamtar creek, both in middle and lower portion, metal/Al ratio for Fe, Mn, Ni, Cr, Co and Zn showed almost uniform

distribution except slightly higher concentration in the bottom section. Zn/Al and Pb/Al in the upper section showed increasing trend (Figure 3.6.5). At surface, metal/Al ratio generally showed a sudden decrease (Figure 3.6.5). In Kundalika estuary, metal/Al ratio showed almost uniform distribution pattern in the middle estuary while in lower estuary they showed some variations (Figure 3.6.6). In middle estuary generally metal/Al showed an increasing trend from bottom to surface while in the lower estuary metal/Al showed a decreasing trend (Figure 3.6.6). In Rajapuri creek metal/Al ratio except for Mn/Al, Ni/Al and Pb/Al showed an increasing trend from bottom to surface (Figure 3.6.7). In Savitri estuary, metal/Al ratio showed large variations in lower estuary in comparison to middle estuary (Figure 3.6.8). In Vashishti estuary metal/Al ratio showed similar distribution pattern and increasing trend from bottom to surface (Figure 3.6.9).

3.6.9 Correlation

Fe and/or Mn generally showed significant positive correlation with trace metals suggesting the role of Fe-Mn oxyhydroxides as scavengers of trace metals (Table 3.6.7) (Chester and Hughes 1967; Loring 1991; Salomons and Förstner 1984). In lower Rajapuri creek and middle portion of Kundalika estuary trace metals generally showed significant positive correlation with Al which suggests their crustal origin while in lower Dharamtar creek and middle portion of Savitri estuary trace metals showed weak correlation with Al which suggests their different origin (Table 3.6.7). The significant positive correlation of Zn and Pb with TOC, TN and TP in the middle portion of Dharamtar creek, Pb with TOC and TP in middle portion of Kundalika estuary and Cr, Co and Zn with TN near the mouth of Rajapuri creek underlines an association in the form of organometallic complexes (Table 3.6.7) (Baptistaneto et al 2000; Marchand et al 2006). Metals like Cr, Co and Zn near the mouth of Rajapuri creek, Ni and Pb in middle Kundalika estuary, Cr in middle portion of Dharamtar creek, Zn in lower Savitri estuary and Cr and Zn in middle Vashishti estuary showed significant positive correlation with sand suggesting that these metals are preferably attached to the coarser grains and are deposited as coatings (Table 3.6.7) (Jonathan et al 2010). The significant association of metals with silt and clay may be due to

the fact that these metals tend to be adsorbed by clay minerals such as smectite and illite (Alloway 1995) (Table 3.6.7).

Table 3.6.6 Pearson's correlation coefficient between trace metals and sediment grain size, nutrients and major elements for lower (A) and middle (B) estuary
n=number of samples n.s.=not significant
**Correlation is significant at the 0.01 level (2-tailed) **Correlation is significant at the 0.05 level (2-tailed)

(A) Lower Estuary										(B) Middle Estuary									
	Sand	Silt	Clay	TOC	TN	TP	Fe	Mn	Al	Sand	Silt	Clay	TOC	TN	TP	Fe	Mn	Al	
Dharamtar (n=23)										Dharamtar (n=41)									
Ni	n.s.	n.s.	n.s.	n.s.	n.s.	n.s.	n.s.	n.s.	n.s.	n.s.	n.s.	n.s.	n.s.	n.s.	n.s.	0.429**	n.s.	0.347*	
Cr	n.s.	n.s.	n.s.	n.s.	n.s.	n.s.	0.567**	0.558**	n.s.	0.476**	n.s.	n.s.	n.s.	n.s.	n.s.	0.394*	0.498**	n.s.	
Co	n.s.	n.s.	n.s.	0.593**	0.503*	n.s.	n.s.	0.439*	n.s.	n.s.	n.s.	n.s.	n.s.	n.s.	n.s.	0.421**	0.587**	0.469**	
Zn	n.s.	n.s.	n.s.	n.s.	0.641**	n.s.	n.s.	n.s.	n.s.	n.s.	0.381*	n.s.	0.319*	0.564**	0.418**	n.s.	n.s.	n.s.	
Pb	n.s.	n.s.	n.s.	n.s.	n.s.	n.s.	n.s.	n.s.	n.s.	n.s.	n.s.	n.s.	0.349*	0.591**	0.370*	n.s.	n.s.	0.328*	
Kundalika (n=33)										Kundalika (n=33)									
Ni	n.s.	n.s.	n.s.	n.s.	n.s.	-	n.s.	0.395*	n.s.	0.372*	n.s.	n.s.	0.442**	-	n.s.	0.562**	0.411*	0.465**	
Cr	n.s.	n.s.	0.383*	n.s.	n.s.	-	n.s.	n.s.	0.469**	n.s.	n.s.	n.s.	n.s.	-	n.s.	0.586**	n.s.	0.534**	
Co	n.s.	n.s.	0.495**	n.s.	n.s.	-	0.383*	0.368*	0.523**	n.s.	n.s.	n.s.	n.s.	-	n.s.	0.748**	n.s.	0.708**	
Zn	n.s.	n.s.	n.s.	n.s.	n.s.	-	n.s.	n.s.	n.s.	n.s.	n.s.	n.s.	n.s.	-	n.s.	0.703**	0.400*	0.787**	
Pb	n.s.	n.s.	n.s.	n.s.	n.s.	-	n.s.	n.s.	n.s.	0.617*	n.s.	n.s.	0.856**	-	0.494**	n.s.	n.s.	n.s.	
Rajapuri (n=49)										Savitri (n=39)									
Ni	n.s.	n.s.	n.s.	n.s.	n.s.	-	0.463**	0.301*	0.454**	n.s.	n.s.	n.s.	n.s.	n.s.	n.s.	0.762**	0.460**	n.s.	
Cr	0.636**	n.s.	n.s.	n.s.	0.689**	-	0.934**	0.402**	0.832**	n.s.	n.s.	n.s.	n.s.	n.s.	n.s.	0.639**	0.318*	n.s.	
Co	0.450**	n.s.	0.314*	n.s.	0.715**	-	0.935**	0.523**	0.872**	n.s.	n.s.	n.s.	n.s.	n.s.	n.s.	0.871**	0.487**	n.s.	
Zn	0.436**	n.s.	n.s.	n.s.	0.675**	-	0.950**	0.393**	0.907**	n.s.	n.s.	n.s.	n.s.	n.s.	n.s.	0.919**	0.343*	n.s.	
Pb	n.s.	n.s.	n.s.	0.531**	n.s.	-	n.s.	n.s.	n.s.	n.s.	n.s.	n.s.	n.s.	n.s.	n.s.	n.s.	n.s.	0.373*	
Savitri (n=50)										Vashishti (n=54)									
Ni	n.s.	n.s.	n.s.	n.s.	n.s.	n.s.	0.450**	0.499**	0.350*	n.s.	n.s.	n.s.	n.s.	n.s.	n.s.	0.819**	0.356**	0.535**	
Cr	n.s.	n.s.	n.s.	n.s.	n.s.	n.s.	n.s.	n.s.	0.408**	n.s.	0.322*	n.s.	n.s.	n.s.	0.272*	0.597**	n.s.	n.s.	
Co	n.s.	n.s.	n.s.	n.s.	n.s.	n.s.	n.s.	n.s.	0.295*	0.474**	n.s.	n.s.	n.s.	n.s.	n.s.	0.667**	0.391**	n.s.	
Zn	0.473**	n.s.	n.s.	0.300*	n.s.	n.s.	0.356*	0.550**	n.s.	n.s.	0.284*	n.s.	n.s.	n.s.	n.s.	0.792**	n.s.	0.394**	
Pb	n.s.	n.s.	0.376**	n.s.	n.s.	n.s.	0.597**	0.521**	0.287*	n.s.	n.s.	n.s.	n.s.	n.s.	n.s.	0.516**	n.s.	n.s.	

3.6.10 Factor analysis

The distribution of metals in the middle portion of Savitri and Kundalika estuary is mainly controlled by Fe-Mn oxyhydroxides and/or aluminosilicates while in the lower estuary metals showed no significant association with Fe-Mn oxyhydroxides and/or aluminosilicate suggesting different process controlling metal distribution in lower and middle estuary (Table 3.6.8). On the other hand, in Rajapuri creek, Dharamtar and Vashishti estuary distribution of metals in lower as well as middle estuary is controlled by Fe-Mn oxyhydroxides and/or aluminosilicates (Table 3.6.8).

Table 3.6.8 Varimax R-mode factor analysis for cores collected from lower (A) and middle (B) estuary
 Values marked in bold are >0.5 significant at p<0.05

Note D=Dharamtar creek, K=Kundalika estuary, R=Rajapuri creek, S=Savitri estuary, V=Vashishti estuary

(A) Lower Estuary

Factor 1					Factor 2					Factor 3					Factor 4				
	D1	K1	R1	S1		D2	K2	R2	S2		D3	K3	R3	S3		D4	K4	S4	
Variance (%)	22.92	23.58	43.38	27.32	Variance (%)	22.37	21.45	16.79	20.74	Variance (%)	20.87	18.88	16.79	20.74	Variance (%)	13.56	15.77	11.33	
Sand	0.13	-0.09	0.49	-0.99	Sand	0.71	0.01	0.14	-0.03	Sand	0.58	0.39	-0.41	0.02	Sand	-0.04	-0.82	0.03	
Silt	-0.02	-0.26	-0.21	0.82	Silt	0.97	-0.91	-0.95	0.07	Silt	-0.02	0.09	0.07	0.13	Silt	-0.04	0.06	-0.26	
Clay	0.00	0.28	0.03	0.84	Clay	-0.98	0.83	0.96	-0.02	Clay	-0.04	-0.25	0.08	-0.14	Clay	0.04	0.30	0.16	
TOC	0.71	-0.42	-0.39	0.67	TOC	-0.19	-0.24	-0.16	0.14	TOC	-0.32	-0.20	0.72	-0.45	TOC	0.55	0.65	0.30	
Fe	-0.20	-0.04	0.93	0.01	Fe	0.05	0.08	0.17	0.72	Fe	0.79	0.89	-0.22	-0.01	Fe	-0.02	0.03	0.38	
Mn	0.48	0.23	0.35	0.12	Mn	0.308	-0.10	0.60	0.81	Mn	0.69	0.80	-0.30	0.20	Mn	-0.10	-0.24	-0.31	
Al	-0.29	0.09	0.89	0.02	Al	-0.15	0.74	0.11	0.11	Al	-0.06	0.35	-0.12	0.31	Al	0.82	-0.08	0.87	
Ni	-0.40	0.82	0.65	-0.26	Ni	-0.30	0.12	0.25	0.63	Ni	0.42	0.38	0.51	0.64	Ni	-0.59	0.17	0.12	
Cr	0.01	0.77	0.93	0.03	Cr	-0.02	0.41	0.11	0.04	Cr	0.77	0.07	-0.25	0.89	Cr	-0.48	-0.26	0.21	
Co	0.89	0.69	0.87	-0.08	Co	0.05	0.47	0.28	0.11	Co	0.06	0.42	-0.23	0.90	Co	0.03	0.12	0.04	
Zn	0.59	0.04	0.97	-0.53	Zn	-0.11	0.19	0.12	0.68	Zn	0.35	0.23	-0.03	0.31	Zn	-0.13	0.72	-0.17	
Pb	-0.76	-0.84	-0.07	0.34	Pb	-0.14	-0.11	-0.00	0.77	Pb	0.28	0.28	0.89	-0.11	Pb	0.20	0.07	0.31	

(B) Middle Estuary

Factor 1					Factor 2					Factor 3					Factor 4				
	D1	K1	S1	V1		D2	K2	S2	V2		D3	K3	S3	V3		D4	S4	V4	
Variance (%)	26.17	37.75	36.12	24.34	Variance (%)	19.03	26.28	17.62	19.8	Variance (%)	16.44	17.26	15.09	19.09	Variance (%)	13.57	14.94	16.61	
Sand	0.59	-0.02	0.13	0.13	Sand	0.02	0.82	0.13	-0.60	Sand	-0.55	-0.06	-0.84	0.53	Sand	0.25	-0.11	0.12	
Silt	-0.27	-0.04	-0.10	0.11	Silt	0.03	-0.07	-0.96	0.20	Silt	0.31	-0.99	0.08	-0.10	Silt	0.79	0.10	0.93	
Clay	-0.37	0.04	0.07	-0.17	Clay	-0.05	-0.02	0.97	0.12	Clay	0.30	1.00	0.14	-0.18	Clay	-0.84	-0.07	-0.94	
TOC	-0.18	-0.14	-0.23	0.28	TOC	-0.12	0.95	0.24	0.16	TOC	0.77	0.09	0.82	-0.73	TOC	-0.02	0.20	-0.28	
Fe	0.01	0.88	0.93	0.64	Fe	0.80	0.02	-0.01	0.51	Fe	-0.32	0.06	-0.22	0.49	Fe	0.30	0.08	0.11	
Mn	0.80	0.40	0.55	0.12	Mn	0.20	0.39	0.03	0.26	Mn	-0.09	-0.21	0.56	0.57	Mn	0.14	-0.13	-0.23	
Al	0.08	0.90	0.03	0.80	Al	0.52	-0.26	0.06	-0.19	Al	0.64	0.09	0.06	-0.20	Al	0.17	0.85	0.15	
Ni	0.02	0.69	0.89	0.85	Ni	0.83	0.56	0.26	0.20	Ni	0.15	0.14	0.07	0.41	Ni	-0.17	-0.05	0.04	
Cr	0.63	0.76	0.70	0.43	Cr	0.47	0.38	0.10	0.78	Cr	-0.31	0.03	-0.11	-0.12	Cr	-0.04	-0.61	0.16	
Co	0.69	0.90	0.94	0.48	Co	0.58	0.24	-0.01	-0.04	Co	0.21	0.01	-0.06	0.78	Co	0.14	0.17	0.02	
Zn	-0.87	0.91	0.94	0.77	Zn	0.25	-0.07	0.01	0.45	Zn	0.11	-0.07	-0.13	0.14	Zn	0.19	0.06	0.15	
Pb	-0.53	0.28	0.14	0.02	Pb	0.05	0.91	-0.22	0.85	Pb	0.45	0.07	0.13	0.16	Pb	0.06	0.75	-0.01	

3.6.11 Index of geoaccumulation (Igeo) and enrichment factor (EF)

The Index of geo-accumulation (Igeo) values computed for metals in Dharamtar, Kundalika and Savitri estuary fall mostly in igeo class 1 or 2 suggesting that sediments are unpolluted to moderately polluted (Table 3.6.9). Enrichment factor (EF) computed indicate minor enrichment (EF 1-3) for all metals (except Co) in Vashishti and Savitri estuary (Table 3.6.10). Rajapuri creek indicated moderate (EF 3-5) enrichment for Cr, Co and Pb and minor enrichment for Fe and Ni (Table 3.6.10). Kundalika estuary indicated minor enrichment (EF 1-3) for Fe, Mn, Ni and Zn, moderate enrichment (3-5) for Cr and moderately severe (EF 5-10) enrichment for Pb (Table 3.6.10). Dharamtar creek indicated minor enrichment (EF 1-3) for all the elements except Mn (Table 3.6.10). Thus amongst the five estuaries Kundalika estuary is most contaminated while Savitri, Vashthi, Rajapuri and Dharamtar are relatively less contaminated.

Table 3.6.9 Mean and standard deviation of index of geoaccumulation (Igeo) for lower (A) and middle (B) estuary

Note: UP-Unpolluted, MP-Moderately polluted, HP-Highly polluted

(A) Lower Estuary							
	Igeo (Fe)	Igeo (Mn)	Igeo (Ni)	Igeo (Cr)	Igeo (Co)	Igeo (Zn)	Igeo (Pb)
Dharamtar (n=23)	0.25±0.08 UP to MP	-0.81±0.12 UP	0.01±0.14 UP to MP	0.82±0.07 UP to MP	0.93±0.11 UP to MP	-0.01±0.05 UP	1.04±0.88 MP
Kundalika (n=33)	0.71±0.09 UP to MP	-0.51±0.11 UP	0.14±0.13 UP to MP	1.09±0.43 MP	1.61±0.13 MP	0.43±0.38 UP to MP	1.82±0.36 MP
Rajapuri (n=49)	-0.22±0.35 UP	-0.41±0.11 UP	-0.15±0.18 UP to MP	0.77±0.44 UP to MP	0.82±0.39 UP to MP	-0.74±0.24 UP	0.98±0.48 UP to MP
Savitri (n=50)	0.91±0.43 UP to MP	0.59±0.34 UP to MP	0.55±0.14 UP to MP	0.81±0.26 UP to MP	1.70±0.21 MP	0.24±0.17 UP to MP	0.77±0.43 UP to MP
(B) Middle Estuary							
	Igeo (Fe)	Igeo (Mn)	Igeo (Ni)	Igeo (Cr)	Igeo (Co)	Igeo (Zn)	Igeo (Pb)
Dharamtar (n=41)	0.10±0.06 UP to MP	-0.69±0.10 UP	-0.1±0.12 UP	0.84±0.21 UP to MP	1.31±0.07 MP	-0.09±0.24 UP	1.49±0.41 MP
Kundalika (n=33)	0.28±0.12 UP to MP	-0.43±0.15 UP	-0.12±0.17 UP	1.33±0.17 MP	1.31±0.16 MP	-0.02±0.12 UP	1.94±0.35 MP
Savitri (n=39)	0.61±0.25 UP to MP	0.63±0.22 UP to MP	0.42±0.20 UP to MP	0.84±0.33 UP to MP	1.87±0.15 MP	0.10±0.18 UP to MP	0.68±0.35 UP to MP
Vashishti (n=54)	1.36±0.16 MP	1.11±0.14 MP	1.19±0.10 MP	1.41±0.18 MP	2.81±0.26 MP to HP	1.02±0.10 MP	1.57±0.32 MP

Table 3.6.10 Mean and standard deviation of enrichment factor (EF) for lower (A) and middle (B) estuary

(A) Lower Estuary							
Rivers/Creek	EF (Fe)	EF (Mn)	EF (Ni)	EF (Cr)	EF (Co)	EF (Zn)	EF (Pb)
Dharamtar (n=23)	1.52±0.13 Minor Enrichment	0.73±0.08 No Enrichment	1.29±0.17 Minor Enrichment	2.26±0.22 Minor Enrichment	2.45±0.25 Minor Enrichment	1.19±0.08 Minor Enrichment	2.94±1.08 Minor Enrichment
Kundalika (n=33)	2.84±0.17 Minor Enrichment	1.22±0.10 Minor Enrichment	1.91±0.17 Minor Enrichment	3.81±0.98 Moderate Enrichment	5.31±0.39 Moderately Severe	2.42±0.72 Minor Enrichment	6.34±1.76 Moderately Severe
Rajapuri (n=49)	1.69±0.24 Minor Enrichment	1.04±0.13 Minor Enrichment	1.77±0.26 Minor Enrichment	3.12±0.67 Moderate Enrichment	3.49±0.55 Moderate Enrichment	1.17±0.08 Minor Enrichment	4.17±1.88 Moderate Enrichment
Savitri (n=50)	2.62±0.79 Minor Enrichment	2.08±0.54 Minor Enrichment	1.98±0.28 Minor Enrichment	2.37±0.43 Minor Enrichment	4.39±0.73 Moderate Enrichment	1.60±0.29 Minor Enrichment	2.37±0.71 Minor Enrichment
(B) Middle Estuary							
	EF (Fe)	EF (Mn)	EF (Ni)	EF (Cr)	EF (Co)	EF (Zn)	EF (Pb)
Dharamtar (n=41)	1.57±0.08 Minor Enrichment	0.91±0.07 No Enrichment	1.37±0.11 Minor Enrichment	2.65±0.36 Minor Enrichment	3.61±0.18 Moderate Enrichment	1.39±0.26 Minor Enrichment	4.23±1.07 Moderate Enrichment
Kundalika (n=33)	1.80±0.09 Minor Enrichment	1.1137 Minor Enrichment	1.38±0.15 Minor Enrichment	3.75±0.35 Moderate Enrichment	3.70±0.27 Moderate Enrichment	1.47±0.07 Minor Enrichment	5.91±1.68 Moderately Severe
Savitri (n=39)	2.00±0.48 Minor Enrichment	2.01±0.42 Minor Enrichment	1.74±0.38 Minor Enrichment	2.42±0.84 Minor Enrichment	4.73±0.85 Moderate Enrichment	1.39±0.28 Minor Enrichment	2.09±0.42 Minor Enrichment
Vasishthi (n=54)	1.60±0.28 Minor Enrichment	1.32±0.28 Minor Enrichment	1.40±0.21 Minor Enrichment	1.67±0.33 Minor Enrichment	3.33±0.61 Moderate Enrichment	1.20±0.20 Minor Enrichment	1.87±0.51 Minor Enrichment